UNIVERSITA' DEGLI STUDI DI PADOVA

Centro Interdipartimentale di Studi e Attività Spaziali (CISAS)

DOTTORATO DI RICERCA IN SCIENZE TECNOLOGIE E MISURE SPAZIALI
(XVIII Ciclo)
Sede Amministrativa: Università degli Studi di Padova

Indirizzo: Astronautica e Scienze da Satellite

Curriculum: Esplorazione del Sistema Solare

DETERMINATION OF THE ORBITS OF THE NATURAL SATELLITES OF SATURN FROM OPTICAL OBSERVATIONS

DETERMINAZIONE DELLE ORBITE DEI SATELLITI NATURALI DI SATURNO DA OSSERVAZIONI OTTICHE

Dottorando: Massimo Bardella

Supervisore: Prof. Stefano Casotto (Università degli Studi di Padova)

Coordinatore dell'Indirizzo: Prof. Pierluigi Bernacca

Direttore della Scuola: Prof. Pierluigi Bernacca

31 Dicembre 2007

Alla mia cara Patrizia
Ai miei genitori

Contents

List of Figures

List of Tables

Sintesi

La ricerca presentata in questo lavoro di tesi riguarda la determinazione delle orbite dei principali satelliti naturali del sistema di Saturno mediante l'uso di osservazioni ottiche effettuate da Terra. L'obiettivo principale di questo lavoro consiste quindi nello sviluppo di un software di calcolo per la determinazione numerica delle orbite dei satelliti naturali di Saturno, insieme alla stima dei parametri dinamici che caratterizzano il sistema quali, ad esempio, i parametri gravitazionali dei satellliti e dell'intero sistema e i coefficienti di Stokes zonali di Saturno, mediante l'uso di osservazioni ottiche effettuate da Terra.

Questo lavoro può essere diviso in 4 parti:

- Nella prima parte introduciamo i concetti fondamentali che riguardano la determinazione orbitale e sviluppiamo gli strumenti matematici necessari per il prosieguo del lavoro.
- Nella seconda parte diamo una descrizione dettagliata del modello dinamico che abbiamo utilizzato per descrivere realisticamente il moto dei satelliti naturali del sistema di Saturno. L'implementazione di questo modello in un codice di calcolo ci ha consentito di integrare numericamente le effemeridi dei satelliti di Saturno a partire da condizioni iniziali note e ci ha permesso di confrontarci con le effemeridi numeriche prodotte da JPL.
- Nella terza parte poi diamo una descrizione dettagliata degli effetti di cui è necessario tenere conto, nel caso di osservazioni ottiche da Terra, per poter confrontare le quantità calcolate con le quantità effettivamente misurate.
- Nella quarta parte infine diamo la nostra soluzione numerica ottenuta applicando le tecniche sviluppate nel corso del lavoro di tesi.

Determinazione orbitale

Il problema della determinazione orbitale consiste nel determinare la miglior stima dello stato dinamico (che comprende tutti gli stati dinamici, cioè posizione e velocità dei satelliti, e tutti i parametri dinamici relativi ai satelliti e non) le cui condizioni sono note con precisione finita, utilizzando osservazioni di un certo tipo e un modello dinamico che descriva il sistema con una accuratezza limitata.

Le orbite degli 8 satelliti principali di Saturno (Mimas, Encelado, Teti, Dione, Rea, Titano, Iperione e Giapeto) sono state ampiamente studiate nel corso degli anni sulla base del gran numero di osservazioni astrometriche effettuate da terra. Tuttavia, il maggior numero di studi recenti su questo argomento sono tutti basati su teorie analitiche. Tra i maggiori lavori ricordiamo quelli di Dourneau e di Harper & Taylor, entrambi del 1993, che hanno determinato gli elementi orbitali e le masse dei satelliti basandosi su teorie analitiche del moto dei satelliti. Duriez & Vienne (1991) and Vienne & Duriez (1991, 1992, 1995) hanno invece espresso analiticamente sia le perturbazioni a lungo periodo sia quelle a breve periodo e, mediante un processo di stima ai minimi quadrati, hanno risolto per i parametri dinamici dei satelliti "fittando" le osservazioni.

Tuttavia, pur essendo queste teorie molto eleganti, la loro precisione non è in ogni caso sufficiente a supportare i livelli di accuratezza raggiungibili dalla recente missione spaziale *Cassini*, che sta attualmente orbitando nel sistema di Saturno con lo scopo di studiarlo dettagliatamente. Per questo motivo il problema della determinazione orbitale può essere trattato solamente per via numerica mediante l'uso di teorie

statistiche. A questo proposito Jacobson sembra essere stato il primo ad aver adottato un approccio puramente numerico per la determinazione delle orbite dei satelliti naturali di Saturno. Jacobson (2004) ha integrato numericamente le equazioni del moto dei satelliti, aggiungendo agli otto citati in precedenza, i 4 satelliti Febe, Elene, Telesto e Calipso. Il set di osservazioni utilizzate da Jacobson nel processo di determinazione orbitale copre un arco che va 1966 al 2003 e le osservazioni sono di quattro tipi: osservazioni astrometriche effettuate dalla Terra e dall'HST (Hubble Space Telescope) e dati di telemetria e immagini provenienti da sonde interplanetarie.

Modello dinamico

Il modello dinamico che abbiamo adottato e sviluppato per descrivere il moto dei satelliti naturali di Saturno deriva essenzialmente da quello di Peters [48] ed è puramente classico. A differenza di Peters che calcola il potenziale dei corpi estesi in coordinate cartesiane, noi abbiamo preferito utilizzare l'usuale sviluppo in armoniche sferiche. Il modello di Peters è stato successivamente migliorato da Jacobson [24] che, oltre a calcolare il potenziale dei corpi estesi usando il metodo di Pines per il primario e la formula di MacCullagh per i satelliti, ha introdotto alcuni miglioramenti più sostanziali. Queste modifiche consistono nel considerare gli anelli di Saturno, nel tener conto delle maree sollevate dai satelliti su Saturno e infine nel considerare gli effetti relativistici dovuti a Saturno. Le modifiche introdotte da Jacobson sono state necessarie per soddisfare il requisito di accuratezza della missione Cassini. Nel nostro caso, limitando la nostra indagine a osservazioni ottiche da Terra, l'accuratezza richiesta è limitata dall'accuratezza intrinseca delle osservazioni ottiche e corrisponde, nei casi migliori, a $0''.08$, ovvero circa 500 km su Saturno. Quindi, per il nostro scopo, le modifiche introdotte da Jacobson non sono necessarie.

Il modello dinamico che abbiamo adottato è essenzialmente classico, basato cioè sulla dinamica newtoniana, e vale per qualsiasi sistema costituito da un pianeta centrale e dai suoi satelliti naturali. Tale modello tiene conto di

- un pianeta centrale non sferico;
- n satelliti estesi mutuamente interagenti;
- m pianeti puntiformi agenti da perturbatori.

Assumendo che il corpo centrale, cioè il primario, venga identificato dall'indice 0, le equazioni del moto degli n satelliti, espresse in un sistema di riferimento centrato nel baricentro del sistema di Saturno, sono

$$\ddot{\mathbf{R}}_i = \sum_{\substack{j=0 \\ j\neq i}}^{n} \mu_j \mathbf{Q}_{ji} + \Delta\ddot{\mathbf{R}}_i + \ddot{\mathbf{R}}_B \,, \qquad i = 1, ..., n \,, \tag{1}$$

dove

$$\mathbf{Q}_{ji} = \frac{\mathbf{R}_j - \mathbf{R}_i}{|\mathbf{R}_j - \mathbf{R}_i|^3} + \mathbf{G}_{ij} - \mathbf{G}_{ji} \,, \qquad \begin{cases} j = 0, ..., n+m \\ i = 0, ..., n \end{cases} \,, \tag{2}$$

$$\mathbf{Q}_{ii} = \mathbf{0} \,, \tag{3}$$

$$\Delta\ddot{\mathbf{R}}_i = \sum_{j=n+1}^{n+m} \mu_j \mathbf{Q}_{ji} \,, \qquad i = 0, ..., n \,, \tag{4}$$

$$\ddot{\mathbf{R}}_B = -\frac{1}{\mu_B} \sum_{k=0}^{n} \sum_{\substack{j=n+1 \\ j\neq k}}^{n+m} \mu_k \mu_j \mathbf{Q}_{jk} = -\frac{1}{\mu_B} \sum_{k=0}^{n} \mu_k \Delta\ddot{\mathbf{R}}_k \,, \tag{5}$$

dove i termini del tipo $\mu_j \mathbf{G}_{ij}$ e $\mu_j \mathbf{G}_{ji}$ rappresentano l'accelerazione dovuta alla non sfericità dei corpi, il termine $\Delta\ddot{\mathbf{R}}_i$ esprime l'accelerazione del corpo i-esimo dovuta all'azione degli m corpi perturbatori esterni al sistema satellitare, e $\ddot{\mathbf{R}}_B$ è l'accelerazione del baricentro del sistema dovuta all'azione degli m corpi perturbatori.

Il modello dinamico sviluppato è stato implementato nel software di calcolo SOSYA (SOlar SYstem Astrometry) codificato in Fortran95. La metodologia di programmazione che abbiamo scelto di adottare è orientata agli oggetti perché tale metodologia ha permesso, da una parte, di semplificare e migliorare la progettazione del software e, dall'altra, di fare uso delle nuove potenzialità introdotte dai linguaggi di programmazione ad oggetti, ovvero l'incapsulazione, l'ereditarietà e il polimorfismo. Il software creato è descritto in dettaglio nell'appendice D. L'integratore numerico che abbiamo scelto di usare è DIVA che è un integratore numerico a ordine e step variabile. DIVA è un integratore molto sofisticato ed è il medesimo utilizzato dal JPL per la produzione delle effemeridi dei corpi del sistema solare. La particolarità di DIVA è che permette di impostare tolleranze diverse per ciascuna equazione differenziale.

Utilizzando SOSYA abbiamo integrato numericamente le equazioni del moto (1) in un sistema di riferimento centrato nel baricentro del sistema di Saturno. I perturbatori sono Giove e il Sole. Abbiamo inoltre considerato Saturno esteso con i soli coefficienti zonali J_2, J_4, J_6, and J_8 diversi da zero. Abbiamo testato l'integrazione numerica confrontandoci con 8 differenti versioni delle effemeridi di JPL. Per effettuare il confronto, le condizioni iniziali all'epoca, i parametri gravitazionali del sistema, dei satelliti e dei perturbatori, i coefficienti di Stokes di Saturno e la direzione del polo e del meridiano primo di Saturno sono stati determinati accuratamente estraendoli direttamente dai file di effemeridi di JPL mediante un programma ausiliario dell'ODP, il programma di determinazione di orbite del JPL. Tali parametri vengono mostrati nelle tabelle 2.4, 2.5, 2.6 e 2.7 del capitolo 2, ad eccezione delle condizioni iniziali all'epoca.

I risultati che abbiamo ottenuto indicano che le orbite integrate su un periodo di 5 anni si discostano da quelle di JPL di pochi metri in rms (ad eccezione di Febe che si discosta di circa 300 metri ma solo nella versione **sat136** di JPL). I risultati che abbiamo ottenuto sono presentati nella tabelle 1 e 2. e nei grafici di figura 1 (attenzione alla scala logaritmica delle ordinate).

Per essere in grado di condurre una determinazione orbitale abbiamo dovuto anche sviluppare il calcolo delle equazioni variazionali che si ottengono direttamente differenziando l'equazione (1) rispetto allo stato (posizione e velocità) di ciascun satellite, ai parametri gravitazionali dei satelliti e dell'intero sistema e ai coefficienti di Stokes zonali di Saturno. Il calcolo delle derivate parziali variazionali non è stato semplice dal momento che il sistema satellitare è mutuamente interagente e le derivate parziali devono essere calcolate con attenzione seguendo la regola della catena. Lo sviluppo delle equazioni del moto e il calcolo di tutte le derivate parziali variazionali sono oggetto del capitolo 2. L'implementazione delle derivate parziali in SOSYA ci ha permesso di integrare le equazioni variazionali e ottenere la matrice di transizione di stato numerica. In merito a ciò abbiamo verificato che le derivate parziali mostrano lo stesso andamento descritto in Hadjifotinou & Harper [17], e in Hadjifotinou & Ichtiaroglou [16]. Ovvero alcune derivate parziali hanno una ampiezza di librazione che tende a crescere nel tempo mentre altre mostrano delle librazioni a lungo e a corto periodo causate dalla presenza sia di risonanze nel sistema di satelliti sia di perturbazioni dovute alla non sfericità dei corpi che costuituiscono il sistema.

Osservazioni ottiche

Le osservazioni ottiche sono una delle fonti più importanti dei dati astrometrici. L'astrometria è quella parte dell'astronomia che si occupa delle misurazioni delle posizioni, delle distanze e dei movimenti delle stelle e di altri corpi celesti. Essa include lo studio delle tecniche osservative e della strumentazione, l'analisi e il processamento dei dati osservativi, lo studio del moto dei corpi e la definizione dei sistemi di riferimento. Tuttavia, in generale, l'osservazione astrometrica non fornisce direttamente la direzione da cui la luce proviene, bensì una quantità direttamente collegata alla posizione geometrica dei corpi celesti all'istante di emissione. Infatti, quello che si osserva è la direzione tangente alla luce quando essa raggiunge l'osservatore.

Il percorso della luce quindi non è rettilineo e, per determinare la direzione effettiva da cui la luce proviene, è necessario applicare una serie di correzioni alla direzione osservata. Gli effetti principali, dipendenti dalla posizione dell'osservatore e non dallo strumento usato, sono:

	SAT132		SAT136		SAT143		SAT185	
	$\Delta\|\mathbf{r}\|\,(m)$	$\Delta\|\mathbf{v}\|\,(m/s)$	$\Delta\|\mathbf{r}\|\,(m)$	$\Delta\|\mathbf{v}\|\,(m/s)$	$\Delta\|\mathbf{r}\|\,(m)$	$\Delta\|\mathbf{v}\|\,(m/s)$	$\Delta\|\mathbf{r}\|\,(m)$	$\Delta\|\mathbf{v}\|\,(m/s)$
Mimas	23.1	$1.1 \cdot 10^{-2}$	21.8	$1.9 \cdot 10^{-2}$	48.6	$1.1 \cdot 10^{-2}$	51.9	$2.5 \cdot 10^{-2}$
Enceladus	1.9	$7.7 \cdot 10^{-4}$	1.9	$7.7 \cdot 10^{-4}$	2.1	$7.8 \cdot 10^{-4}$	64.5	$1.6 \cdot 10^{-2}$
Tethys	1.8	$4.5 \cdot 10^{-4}$	1.8	$4.5 \cdot 10^{-4}$	1.9	$4.7 \cdot 10^{-4}$	25.9	$4.3 \cdot 10^{-3}$
Dione	8.6	$1.4 \cdot 10^{-3}$	8.6	$1.4 \cdot 10^{-3}$	8.7	$1.4 \cdot 10^{-3}$	51.0	$6.3 \cdot 10^{-3}$
Rhea	6.9	$8.4 \cdot 10^{-4}$	6.9	$8.4 \cdot 10^{-4}$	6.9	$8.4 \cdot 10^{-4}$	57.2	$4.7 \cdot 10^{-3}$
Titan	2.0	$6.6 \cdot 10^{-5}$	2.2	$6.7 \cdot 10^{-5}$	0.8	$6.6 \cdot 10^{-5}$	24.4	$9.9 \cdot 10^{-4}$
Hyperion	4.9	$1.7 \cdot 10^{-4}$	5.0	$1.7 \cdot 10^{-4}$	4.0	$1.7 \cdot 10^{-4}$	61.3	$2.6 \cdot 10^{-3}$
Iapetus	19.2	$4.1 \cdot 10^{-5}$	21.0	$4.2 \cdot 10^{-5}$	1.7	$3.7 \cdot 10^{-5}$	29.2	$6.1 \cdot 10^{-4}$
Phoebe	—	—	306.9	$1.6 \cdot 10^{-4}$	23.8	$1.6 \cdot 10^{-4}$	23.8	$1.6 \cdot 10^{-4}$
Helene	—	—	9.5	$1.6 \cdot 10^{-3}$	9.5	$1.6 \cdot 10^{-3}$	212.6	$2.7 \cdot 10^{-2}$
Telesto	—	—	1.8	$4.5 \cdot 10^{-4}$	1.9	$4.7 \cdot 10^{-4}$	26.2	$4.4 \cdot 10^{-3}$
Calypso	—	—	1.8	$4.4 \cdot 10^{-4}$	1.9	$4.6 \cdot 10^{-4}$	30.0	$5.0 \cdot 10^{-3}$

Table 1: Valori in rms delle differenze tra le effemeridi **SAT132**, **SAT136**, **SAT143** e **SAT185** rispetto all'integrazione numerica. La durata dell'integrazione numerica è di 5 anni con un output ogni ora.

	SAT199		SAT207		SAT243		SAT252	
	$\Delta\|\mathbf{r}\|\,(m)$	$\Delta\|\mathbf{v}\|\,(m/s)$	$\Delta\|\mathbf{r}\|\,(m)$	$\Delta\|\mathbf{v}\|\,(m/s)$	$\Delta\|\mathbf{r}\|\,(m)$	$\Delta\|\mathbf{v}\|\,(m/s)$	$\Delta\|\mathbf{r}\|\,(m)$	$\Delta\|\mathbf{v}\|\,(m/s)$
Mimas	51.5	$2.5 \cdot 10^{-2}$	51.6	$2.5 \cdot 10^{-2}$	13.5	$5.3 \cdot 10^{-3}$	10.5	$5.2 \cdot 10^{-3}$
Enceladus	64.5	$1.6 \cdot 10^{-2}$	64.5	$1.6 \cdot 10^{-2}$	1.9	$7.9 \cdot 10^{-4}$	1.9	$7.9 \cdot 10^{-4}$
Tethys	25.7	$4.3 \cdot 10^{-3}$	25.7	$4.3 \cdot 10^{-3}$	1.5	$3.5 \cdot 10^{-4}$	1.5	$3.5 \cdot 10^{-4}$
Dione	50.9	$6.3 \cdot 10^{-3}$	50.9	$6.3 \cdot 10^{-3}$	2.0	$4.1 \cdot 10^{-4}$	2.0	$4.1 \cdot 10^{-4}$
Rhea	57.1	$4.7 \cdot 10^{-3}$	57.1	$4.7 \cdot 10^{-3}$	2.1	$2.8 \cdot 10^{-4}$	2.1	$2.8 \cdot 10^{-4}$
Titan	0.8	$6.7 \cdot 10^{-5}$	0.8	$6.7 \cdot 10^{-5}$	0.9	$6.1 \cdot 10^{-5}$	0.9	$6.1 \cdot 10^{-5}$
Hyperion	61.3	$2.6 \cdot 10^{-3}$	61.3	$2.6 \cdot 10^{-3}$	3.9	$1.7 \cdot 10^{-4}$	3.9	$1.7 \cdot 10^{-4}$
Iapetus	29.2	$6.1 \cdot 10^{-4}$	29.2	$6.1 \cdot 10^{-4}$	1.7	$3.6 \cdot 10^{-5}$	1.7	$3.6 \cdot 10^{-5}$
Phoebe	23.8	$1.6 \cdot 10^{-4}$	23.8	$1.6 \cdot 10^{-4}$	6.9	$6.5 \cdot 10^{-5}$	6.9	$6.5 \cdot 10^{-5}$
Helene	212.6	$2.7 \cdot 10^{-2}$	212.7	$2.7 \cdot 10^{-2}$	5.1	$1.1 \cdot 10^{-3}$	5.2	$1.1 \cdot 10^{-3}$
Telesto	26.5	$4.4 \cdot 10^{-3}$	26.6	$4.5 \cdot 10^{-3}$	1.9	$4.7 \cdot 10^{-4}$	1.9	$4.7 \cdot 10^{-4}$
Calypso	31.5	$5.3 \cdot 10^{-3}$	31.6	$5.3 \cdot 10^{-3}$	1.9	$4.7 \cdot 10^{-4}$	1.9	$4.7 \cdot 10^{-4}$
Methon	—	—	—	—	9.3	$1.2 \cdot 10^{-3}$	2.6	$1.0 \cdot 10^{-3}$

Table 2: Valori in rms delle differenze tra le effemeridi **SAT199**, **SAT207**, **SAT243** e **SAT252** rispetto all'integrazione numerica. La durata dell'integrazione numerica è di 5 anni con un output ogni ora.

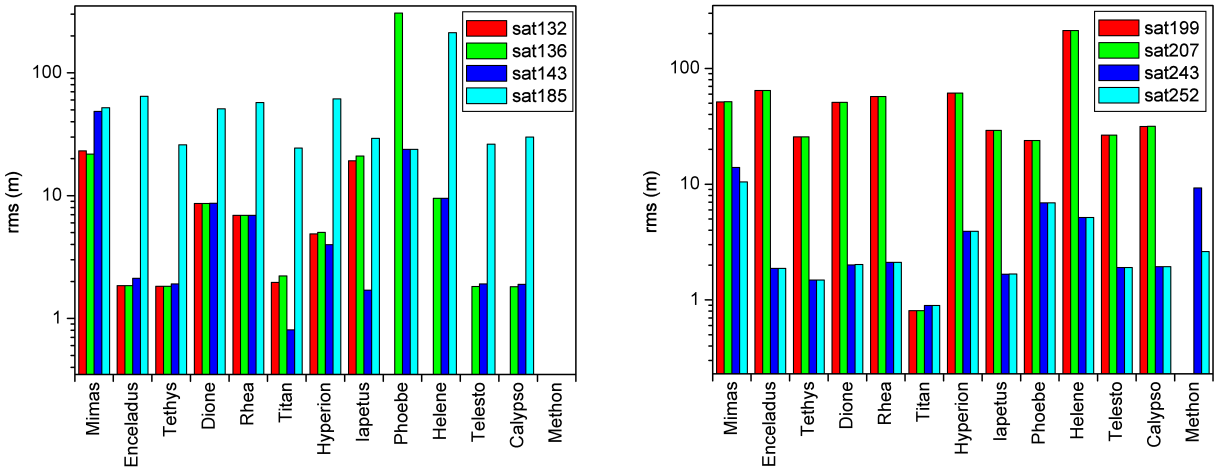

Figure 1: Valori in rms delle differenze tra le effemeridi di JPL e l'integrazione numerica. L'asse y ha scala logaritmica.

- La rifrazione atmosferica che è sempre presente per qualsiasi osservatore topocentrico ed è dovuta alla presenza dell'atmosfera. La rifrazione tende ad aumentare la distanza zenitale dell'oggetto osservato. L'effetto della rifrazione in generale viene corretto direttamente da chi effettua le osservazioni in fase di riduzione.
- L'aberrazione della luce che è dovuta alla composizione del moto dell'osservatore con la velocità finita della luce.
- Il tempo luce che si manifesta solo per oggetti nel Sistema Solare (e quindi per i satelliti di Saturno) e che è dovuto al moto dell'oggetto osservato. Infatti la posizione dell'oggetto nell'istante di osservazione è diversa da quella che aveva nell'istante di emissione della luce perché nell'intervallo di tempo in cui la luce copre la distanza oggetto-osservatore, l'oggetto si è mosso seguendo la sua traiettoria nello spazio.
- La deflessione gravitazionale della luce da parte del Sole. Tale effetto era stato predetto da Einstein e successivamente confermato nel 1919 dalle osservazioni effettuate durante una eclisse.

A dipendere dal tipo di osservazione e dalla riduzione che è stata eseguita dagli osservatori, gli effetti che abbiamo descritto possono essere o non essere applicati. Abbiamo quindi analizzato una serie di algoritmi per calcolare la posizione osservata nel caso di un osservatore geocentrico e topocentrico assumendo che la rifrazione atmosferica sia già stata corretta nelle osservazioni. La trattazione è vettoriale in modo da mantenere tutta l'informazione possibile contenuta nell'osservabile. Abbiamo anche considerato il caso di osservazioni differenziali e il caso di osservazioni da sonda spaziale.

Teoria numerica dei principali satelliti di Saturno

A questo punto siamo passati alla vera e propria determinazione delle orbite dei satelliti di Saturno. I dati osservativi dei satelliti naturali che abbiamo scelto di utilizzare sono tutti quelli disponibili acquisiti con il Flagstaff Astrometric Scanning Transit Telescope (FASTT) che è un telescopio rifrattore meridiano completamente automatizzato. Le osservazioni diponibili sono coordinate assolute (α, δ), nel sistema ICRF e riferite all'epoca J2000.0. Le osservazioni coprono un arco temporale che va dal 1998 al 2007 e sono state ridotte dagli osservatori utilizzando i cataloghi ACT (Astrographic Catalogue + Tycho) e Tycho-2. L'accuratezza di ciascuna misura va da $\pm 0''.08$ (corrispondente a un errore in posizione di circa 500 km su Saturno) a $\pm 0''.25$. Tutte le osservazioni sono già corrette per la rifrazione atmosferica e l'aberrazione diurna. L'aberrazione annua viene rimossa automaticamente usando i cataloghi stellari sopraccitati in fase di riduzione.

Il numero totale delle osservazioni è 3153 e i satelliti coinvolti sono Teti, Dione, Rhea, Titano, Giapeto, Iperione e Febe. Il numero di osservazioni per ciascun satellite viene dato in tabella 3.

Satellite	**numero di osservazioni**
Tethys	238
Dione	379
Rhea	621
Titan	615
Hyperion	434
Iapetus	654
Phobe	212
Total	3153

Table 3: Numero di osservazioni per ciascun satellite effettuate con il Flagstaff Astrometric Scanning Transit Telescope (FASTT) nel periodo 1998-2007.

L'algoritmo per il calcolo dell'osservabile nel caso delle osservazioni di Flagstaff è discusso nel capitolo 4 nel quale vengono anche calcolate le derivate parziali geometriche della relazione geometrica che lega il

vettore osservatore-satellite j-esimo $\mathbf{u}_j = (u_{jx}, u_{jy}, u_{jz})^T$ alle coordinate assolute (α_j, δ_j), ovvero

$$\begin{cases} \alpha_j = \arctan\left(\dfrac{u_{jy}}{u_{jx}}\right) \\ \delta_j = \arctan\left(\dfrac{u_{jz}}{w_j}\right) \end{cases}, \tag{6}$$

dove $w_j = \sqrt{u_{jx}^2 + u_{jy}^2}$. Utilizzando SOSYA nella modalità di determinazione orbitale abbiamo cercato di aggiustare il modello delle orbite dei satelliti di Saturno, mediante il metodo dei minimi quadrati, in modo da fittare le osservazioni. Il set di parametri stimabili è costituito dalla posizione e dalla velocità iniziale di ciascun satellite osservato, ovvero dalle posizioni e dalle velocità iniziali di Teti, Dione, Rhea, Titano, Iperione, Giapeto e Febe. Mima ed Encelado sono stati integrati numericamente insieme agli altri satelliti ma, non essendoci osservazioni, non sono stati stimati. È stato necessario integrare numericamente anche Mima ed Encelado insieme agli altri satelliti perché la loro interazione gravitazionale con gli altri satelliti non è trascurabile. Le tabelle 4 contengono i residui pre-fit (a sinistra) e post-fit (a destra) delle osservazioni per ciascun satellite in α e in δ. Nelle medesime tabelle vengono presentate anche la media e la deviazione standard dei residui.

first	$\boldsymbol{\alpha}$ (arcsec)			$\boldsymbol{\delta}$ (arcsec)		
iteration	**mean**	$\boldsymbol{\sigma}$	**rms**	**mean**	$\boldsymbol{\sigma}$	**rms**
Tethys	0.041	0.218	0.222	-0.017	0.207	0.207
Dione	0.074	0.151	0.168	-0.033	0.168	0.171
Rhea	0.070	0.121	0.140	-0.050	0.122	0.132
Titan	0.084	0.130	0.155	-0.052	0.131	0.141
Hyperion	0.085	0.204	0.221	-0.030	0.214	0.216
Iapetus	0.074	0.115	0.137	-0.059	0.112	0.127
Phoebe	0.034	0.292	0.294	-0.053	0.334	0.338
Total	0.072	0.164	0.179	-0.045	0.172	0.177

last	$\boldsymbol{\alpha}$ (arcsec)			$\boldsymbol{\delta}$ (arcsec)		
iteration	**mean**	$\boldsymbol{\sigma}$	**rms**	**mean**	$\boldsymbol{\sigma}$	**rms**
Tethys	0.040	0.216	0.220	-0.016	0.202	0.203
Dione	0.026	0.146	0.148	-0.013	0.172	0.173
Rhea	0.004	0.125	0.125	-0.036	0.122	0.127
Titan	0.013	0.126	0.127	-0.059	0.130	0.143
Hyperion	0.008	0.190	0.190	-0.040	0.213	0.216
Iapetus	0.024	0.110	0.112	-0.077	0.110	0.134
Phoebe	0.017	0.291	0.291	-0.026	0.329	0.329
Total	0.017	0.160	0.161	-0.045	0.171	0.177

Table 4: Rms, media e deviazione standard dei residui relativi alla prima iterazione (a sinistra) e all'ultima iterazione (a destra)

Come si può notare dalle tabelle 4 l'rms dei residui post-fit è la media tra la migliore e la peggiore accuratezza delle osservazioni di Flagstaff e la soluzione che abbiamo trovato è quindi limitata dalla accuratezza intrinseca delle osservazioni. Inoltre è presente un bias in entrambe le coordinate che sarà oggetto di indagine futura. I residui post-fit in α e δ per i Teti, Dione, Rhea, Titano, Iperione, Giapeto e Phoebe sono presentati nelle figure 4.1, 4.2, 4.3, 4.4, 4.5, 4.6 e 4.7 del capitolo 4.

Sviluppi futuri

La formulazione analitica e gli strumenti numerici sviluppati nel corso di questo lavoro sono assolutamente generali e possono essere applicati facilmente ad altri sistemi costituiti da un primario a dai suoi satelliti naturali.

La direzione verso cui muoversi nel prossimo futuro per migliorare la teoria numerica dei satelliti di Saturno è sicuramente quella di aumentare il periodo temporale delle osservazioni e disporre anche di osservazioni da altri osservatori. Idealmente sarebbe auspicabile spingersi indietro fino a considerare tutte le osservazioni disponibili dal 1874, periodo nel quale sono state effettuate le prime osservazioni visuali micrometriche con accuratezza inferiore a $0''.5$. In aggiunta a ciò sarebbe utile utilizzare nuovi tipi di dati quali ad esempio le misure differenziali, le distanze reciproche tra satelliti e le osservazioni fotometriche. Inoltre, dal momento che le osservazioni ottiche effettuate da terra raramente hanno un'accuratezza migliore di $0''.08$, per migliorare l'accuratezza delle teorie numeriche sarà assolutamente necessario usare le ben più accurate osservazioni spaziali, quali ad esempio le osservazioni HST e le osservazioni di Cassini. Per quanto riguarda l'accuratezza delle osservazioni HST essa varia tra $0''.014$ e $0''.02$, cioè tra circa

80 km e 120 km alla distanza di Saturno. Tale accuratezza è la migliore ottenibile da osservazioni ottiche effettuate dalla Terra. Per quanto riguarda le osservazioni di Cassini invece la loro accuratezza è compresa tra i 5 e i 200 km a dipendere dalla distanza che intercorre tra la sonda e il satellite naturale.

L'utilizzo di un maggior numero di osservazioni e di nuovi tipi di dati sicuramente potrà esserci di aiuto per rimuovere il bias sia che esso sia dovuto ad errori nelle osservazioni sia che esso sia dovuto ad errori nel modello. Inoltre aumentare il periodo temporale delle osservazioni potrà permetterci di stimare oltre che gli stati iniziali dei satelliti, anche i loro parametri gravitazionali.

Summary

The research presented in this thesis concerns the determination of the orbits of the main satellites of the Saturnian system by means of optical, Earth-based observations. The purpose of this work is the development of a software tool for numerical orbit determination and estimation of the parameters that characterize the dynamical environment of the Saturnian system, such as the gravitational parameters and the planetary zonal gravity harmonics. This thesis can ideally be diveded into four parts.

The first part is concerned with the fundamentals of orbit determination. Statistical orbit determination is the set of techniques that allows the estimation of the orbital parameters of a spacecraft or a celestial body during its motion around the Earth, or more generally in the Solar System. More precisely, the problem of determining the best estimate of the dynamical state of a body, from observations influenced by random and systematic errors, using a mathematical model that is not exact, is referred to as the problem of state estimation.

The second part part of this work gives a detailed description of the physical model that will be used to represent the dynamics of the Saturnian satellite system. We adopt essentially the model developed by Peters with the difference that we compute the gravitational potential of extended bodies using a spherical harmonics expansion. Our adopted dynamical model is general and can be applied to any system formed by a central, massive planet and its satellites. This model is based on Newtonian dynamics and contains the effects of an extended central planet, n mutually interacting extended satellites and m point-mass perturbing bodies external to the system. This model has been implemented in a software tool, named SOSYA (SOlar SYstem Astrometry) and coded in Fortran95. The adopted programming method is object-oriented because this allows for better and safer programming design. The developed software is described in detail in Appendix D. By means of the *Orbit Simulation* capability of SOSYA, we have numerically integrated the equations of motion and the variational equations of the main natural satellites of Saturn, in a reference frame centered in the barycenter of the Saturnian system. The perturbers are the Sun and Jupiter. We have also considered the zonal Stokes coefficients J_2, J_4, J_6, and J_8 of Saturn. We have used the numerical integrator DIVA [28], which is a variable order and variable step integrator for q-th order and mixed order problems. This integrator is the same used by JPL to produce the ephemerides of Solar System objects. The initial conditions of the satellites and the epoch of the initial conditions as well as the parameters of the Saturnian system have been accurately determined using a utility application of JPL's *Orbit Determination Program* (ODP), which allows to extract these pieces of information directly from the JPL ephemeris files. The comparison between our numerically integrated ephemeris and eight different versions of the JPL ephemeris is good, particularly with respect to the latest versions of the JPL ephemerides. In fact, in this case the rms over a period of 5 years is on the order of 10 meters and 7 meters respectively for Mimas and Phoebe and on the order of 2-3 meters for the other satellites. As regards the integration of the variational equations we have verified that the partial derivatives ehibit the behaviour described by Hadjifotinou and Harper [17] and Hadjifotinou and Ichtiaroglou [16]. Some partials librate with an amplitude that increases linearly with time, while some other show long-period and short period-librations due to the oblateness perturbations and to the presence of resonances in the system of satellites. The state transition matrix obtained by numerical integration shows a linear growth with time due to the linear increase of the partials with time.

In the third part of this work we describe the corrections that have to be applied to Earth-based observations. In fact the apparent direction in the sky at which the celestial object appears is not the true direction from which the light was emitted. What is observed is the tangent direction of the light when it reaches the observer. For this reason the light path is not rectilinear and several corrections describing the effects of bending, or shift in direction, are to be applied to the direction from which the light is observed to determine the actual direction of the emission. The main effects, related to the observer position and not to the instrument used, are

- the atmospheric refraction which increase the zenith distance of the observed object;
- the aberration due to the composition of the observer velocity with the speed of light;
- the light time correction due to the motion of the observed object; this effect is taken into account only for Solar System object;
- the gravitational light deflection due to the Sun.

Additionally, algorithm for the computation of the apparent place for Earth-based observations and for spacecraft-based observations, and for the computation of the topocentric and the apparent places in the case of differential astrometric observations has been given.

Finally in the last part we give our solution for the orbits of the main natural satellites of Saturn. The correct development and implementation both of the equations of motion and of the variational equations, in conjunction with the study of the algorithm for computing the ground-based observables have been the key for this result. By means of the *Orbit Determination* capability of the SOSYA program we have tried to adjust the models of the orbits of the satellites of Saturn using a weighted least squares fit to the observational data. The set of adjustable dynamical parameters contains only position and velocity at epoch of the observed satellites Tethys, Dione, Rhea, Titan, Hyperion, Iapetus and Phoebe. Our model has been adjusted to a total of 3153 observations covering a period between 1998 and 2007 and acquired with the Flagstaff Astrometric Scanning Transit Telescope (FASTT). The observation are in the form of absolute coordinates (α, δ) in the International Celestial Reference Frame (ICRF) with no correction for light time. All the observations were pre-corrected for atmospheric refraction and diurnal aberration. The annual aberration is automatically corrected using the ACT catalogue for reduction. The accuracy for single observation ranging from $\pm 0''.08$ (about 500 km at Saturn's distance) to $\pm 0''.25$. Mimas and Enceladus have been included in the numerical integration, but their states have not been estimated because no observational data were available for these two satellites. The rms of the post-fit residuals we obtained are $0''.161$ and $0''.177$ respectively in α and δ. The accuracy of our solution is limited by the intrinsic accuracy of the observational data and by the relatively short period of time covered by the observations.

Our research can be further extended in several ways to reach a better accuracy in the numerical theory of the orbits of the main Saturnian satellites. Among several possible lines of work we can point to an increase in the number of data and to an extension of the time period covered by observations. Moreover new data types could be included, particularly HST data and spacecraft-based observations, as well as photometric observations, which are all more accurate of ground-based observations.

Introduction

The research presented in this work concerns the orbit determination of the main satellites of the Saturnian system by means of optical, Earth-based observations. The purpose of this work is the development of a software tool for numerical orbit determination and the estimation of the parameters that characterize the dynamical environment of the Saturnian system, such as the gravitational parameters and the planetary zonal gravity harmonics.

The orbits of the main satellites of Saturn have been extensively studied, based on fits to a great number of ground-based astrometric observations starting from 1874 [20]. Ephemerides of the Saturnian system have been traditionally based on analytical theories. Among the recent major works are the analytical theories of Dourneau (1993), Harper & Taylor (1993) and Vienne & Duriez (1995). The precision of these theories, however, is insufficient to support the needs of the scientific operations of a spacecraft orbiting the Saturnian system such as *Cassini*. For this reason numerical integration is currently the preferred approach for the generation of highly accurate satellite ephemerides. Jacobson [24], [25] appears to have been the first to produce numerically integrated ephemerides of the eight major satellites of Saturn, as well as of Phoebe, Helene, Telesto e Calypso. These ephemerides were obtained by fitting a combination of ground-based and HST astrometric observations, spacecraft tracking and spacecraft satellites imaging over the period 1966 to 2003.

Orbit determination of natural satellites of the Saturnian system is a task performed by only few research groups. One of these is at the Jet Propolsion Laboratory, led by Robert Jacobson, to support NASA's Solar System exploration missions. Another group is at the Bureau des Longitudes of Paris where the main concern is the development of analytical and semianalytical theories. Concerning the determination of planetary orbits the major past effort is the work of Oesterwinter and Cohen [46] who, in 1971, found new orbital elements of Moon and planets by a least-squares fit to about 40,000 optical Earth-based observations of planets and Moon taken since 1913.

The basic requirement of the present work is the development of a general and accurate model of the Saturnian system describing the mutual gravitational interactions between the satellites and the perturbing effects of the planets and the Sun. The implementation of a complete model allows to obtain, by numerical integration, ephemerides significantly more accurate than those provided by current analytical theories, thus allowing for a more accurate propagation and determination of the motion of an exploration spacecraft, both for planning and data reduction purposes [63].

With this goal in mind the major part of this work is focused on the derivation of an accurate dynamical model of the Saturnian system for application to ephemeris propagation and observational data reduction and its implementation in a SW tool. We adopt essentially the model developed by Peters [48] and later improved by Jacobson [24]. Unlike Peters who computes the gravitational potential of extended bodies in cartesian coordinates, we adopted a spherical harmonics expansion approach. An alternative choice is that of Jacobson who uses Pine's method for the extended primary and the MacCullagh expansion for the extended satellites. The improvement introduced by Jacobson concernig the planetary rings, the planetary tides raised by the satellites and the effect of general relativity, are needed in order to achieve the accuracy required by the *Cassini* mission. Since, in our case, we limit our investigation to ground-based observations, the effects introduced by Jacobson are not necessary given the accuracy of the data

type considered, which is of the order of $0''.08$ at best, this correspondig to about 500 km at Saturn.

Although our work is limited to Earth-based observations, the correct implementation of the equations of motion and the variational equations is the starting point for future extensions to new data types, such as HST and spacecraft-based observations.

In Chapter 1 we give some generalities on the theory of statistical orbit determination. We present the mathematical tools necessary for the subsequent developments of this investigation.

In Chapter 2 we derive the dynamical model suitable for the numerical integration of the satellites of Saturn. Our adopted dynamical model is general and can be applied to any system formed by a central, massive planet and its satellites. This model is based on Newtonian dynamics and contains the effects of an extended central planet, n mutually interacting extended satellites and m point-mass perturbing bodies external to the system. The equations of motion and the variational partials have been implemented in a software tool named SOSYA, which has been coded in Fortran 95. Additionally, our numerically integrated ephemerides have been compared with the JPL ephemerides and the numerical results of the comparison are given in this chapter.

In Chapter 3 we describe the corrections that must be applied to the Earth-based observations. These corrections list includes atmospheric refraction, aberration, light-time and gravitational light deflection corrections. Additionally, we give the computational algorithms necessary to compute the position of a Solar System object as viewed by an observer. In particular we give the algorithm for the computation of the apparent place for Earth-based observations and for spacecraft-based observations, the topocentric place and the apparent place in the case of differential astrometric observations. Finally we give the observation equations for obsolute, differential and tangential coordinates.

Chapter 4 is entirely devoted to the determination of the orbits of the main satellites of Saturn obtained by applying the metholodogy developed in the previous chapters.

In Chapter 5 we give conclusions and suggestions for future work.

Appendix A presents some backgroung material on the coordinate systems and on the time systems used in this work and implemented in the software developed.

Appendix C gives the procedure to compute the topocentric right ascension and declination from the geocentric right ascension and declination and the geocentric parallax.

Appendix D presents a description of the software tool SOSYA.

Chapter 1

Fundamentals of Statistical Orbit Determination

1.1 Introduction

Statistical Orbit Determination is the set of techniques that allows the estimate of the orbital parameters of a spacecraft or a celestial body during its motion around the Earth or more generally in the Solar System.

Because the knowledge of the true state (position, velocity and several other parameters) of the considered body will never be absolute, we have to find a workaround that overcomes our simplified modeling of the orbital motion. This is done through extensive use of statistical techniques. In particular, we will use a least squares approach to minimize the differences between observations and a model of them, computed through a set of parameters that form the *dynamic* and *kinematic* models and propagated in time through a set of differential equations (equations of motion). This requires a parametrization of the problem and it depends on the physics of the problem itself.

The classical orbit determination problem is characterized by the assumption that the bodies move under the influence of a central force. For the satellite orbit determination problem the minimal set of parameters will be the position and velocity vectors at some given epoch. This minimal set will be expanded to include dynamic and measurement model parameters, which may be needed to improve the prediction accuracy. If we indicate the general state vector at a time t as $\mathbf{X}(t)$, the general orbit determination problem can be posed as follow.

If at some initial time, t_0, the state $\mathbf{X}_0$ of a vehicle following a ballistic trajectory is given and if the differential equations that govern the motion are known, then the equations of motion can be integrated to determine the state of the vehicle at any time. However, during an actual flight, the initial state is never known exactly. Moreover, certain physical constants as well as the mathematical specification of the forces required to define the differential equations of motion are known only approximately. Such errors will cause the actual motion to deviate from the predicted motion. Consequently, in order to determine the position of the spacecraft at some time $t > t_0$, it must be tracked or observed from tracking stations whose positions are known precisely. With the observations of the spacecraft motion, a better estimate of the trajectory can be determined. The estimate of the trajectory will not be exact because the observations will be subject to both random and systematic errors.

The problem of determining the best estimate of the state of a body, whose initial state is unknown, from observations influenced by random and systematic errors, using a mathematical model that is not exact, is referred to as the problem of state estimation.

When an estimate of the trajectory has been made, the subsequent motion and values for the observations can be predicted.

The predicted values will differ from the true values due to the following effects:

- inaccuracies in the estimated state vector caused by errors in the orbit determination process, such as:
  1. approximations involved in the method of orbit improvement and in the mathematical model;
  2. errors in the observations;
  3. errors in the computational procedure used in the solution process;
- errors in the numerical integration procedure caused by errors in the dynamical model and computer truncation and roundoff errors.

Consequently, the process of observation and estimation must be repeated continually as the vehicle's motion evolves. To obtain a better orbit estimate, a sufficient number of observations must be available covering the time span of interest.

In general, rather than being directly observable, the measurements are non-linear functions of the state vector parameters. Also, the differential equations that describe the motion are strongly non linear. This leads to the conclusion that multiple solutions can be found, but only one is optimal.

Once an optimal estimate of the orbital parameters is obtained, a set of ephemerides of the satellite can be obtained by simply integrating the equations of motion using the parameters just determined. The accuracy of the obtained ephemerides or orbit, is strictly connected with the precision and accuracy of the models and the measurements errors. The process of orbit estimation is not only related with orbital parameters, but any parameter that affects the orbital motion of the satellite can be, at least in theory, estimated.

To illustrates some of the basic ideas involved in the orbit determination process, consider the flight of a vehicle moving under the influence of a uniform gravitational field, as shown in Figure 1.1. Assume that the range (linear distance along the line of sight), ρ, and the elevation, θ, of the line of sight to satellite can be measured. In the preliminary design of the trajectory, an initial state $\mathbf{X}_0^*$ (i.e., the initial position and the initial velocity vectors), is selected in such a way that the vehicle will follow a desired nominal (design) trajectory. In practice, however, the design conditions are never realized. Hence, the *true initial state*, $\mathbf{X}_0$, will differ from the *nominal initial state*, $\mathbf{X}_0^*$, and consequently, the true trajectory followed by the vehicle will differ from the nominal trajectory. An indication of these two trajectories is given in Figure 1.1. Here the true trajectory is denoted as $\mathbf{X}$, the nominal trajectory as $\mathbf{X}^*$, and the *best estimate* of the true trajectory is indicated by $\hat{\mathbf{X}}$. To determine an estimate, $\hat{\mathbf{X}}$, of the true trajectory of the vehicle, tracking information must be used. It is clear that even the simple case of estimating only the position and velocity vectors of the satellite requires more than one observation in time.

The most common method of state parameters estimation is the *least-squares* approach. The goal is to minimize the *observation residuals* (difference between the true measurements and their computed values). There are essentially two ways to update the state vector: if a new estimate is obtained after each observation we talk about *sequential* or *recursive* estimation. If all the measurements are collected and then processed to obtain an estimate of the state vector at a specified initial epoch (*batch epoch*) we are talking about *batch* estimation.

Generally speaking, a sequential estimator (filter) will be more sensitive to the goodness of the individual points than a batch filter. Also, a sequential algorithm will converge faster to the right solution (if it is properly tuned) than a batch algorithm. The last one may require several iterations before converging. The method as it is presented here was first developed and applied for satellite precise orbit determination by Tapley, [61].

The outlined procedure, as we have seen at the beginning of the chapter, can be can be adopted also in our case, that is in the determination of orbits of natural satellites of Saturn from optical observations. As approach for the estimation procedure we adopt a least square batch filter.

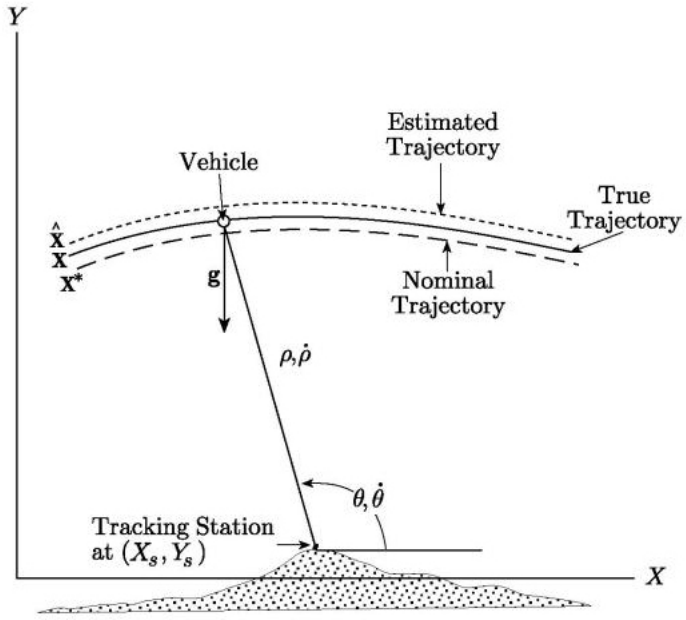

Figure 1.1: Uniform gravity field trajectory [61].

1.2 Linearization of the orbit determination process

In the general orbit determination problem, both the dynamics and the measurements involve significant nonlinear relationships. For the general case, the governing relations involve the nonlinear expression

$$\dot{\mathbf{X}} = \mathbf{F}(\mathbf{X}, t)\,, \qquad \mathbf{X}(t_k) \equiv \mathbf{X}_k\,, \tag{1.1}$$

$$\mathbf{Y}_i = \mathbf{G}(\mathbf{X}_i, t_i) + \boldsymbol{\varepsilon}_i\,, \qquad i = 1, ..., l\,, \tag{1.2}$$

where $\mathbf{X}_k$ is the unknown n-dimensional state vector at the time t_k, and $\mathbf{Y}_i$ for $i = 1, ..., l$, is a p-dimensional set of observations that are to be used to obtain a best estimate of the unknown value of $\mathbf{X}_k$, i.e. $\hat{\mathbf{X}}_k$. In general, $p < n$ and $m = p \times l \gg n$.

The formulation represented by equations (1.1) and (1.2) is characterized by:

- the inability to observe the state directly;
- nonlinear relations between the observations and the state;
- fewer observations at any time epoch than there are state vector components ($p < n$);
- errors in the observations represented by $\boldsymbol{\varepsilon}_i$.

The problem of determining the trajectory of a space vehicle in the presence of these effects is referred to as the nonlinear estimation or orbit determination problem. If the state vector and the observation vector can be related in a linear manner, then several powerful techniques from the field of linear estimation theory can be applied to the orbit determination problem.

If a reasonable reference trajectory is available and if $\mathbf{X}$, the true trajectory, and $\mathbf{X}^*$, the reference trajectory, remain sufficiently close throughout the time interval of interest, then the trajectory for the actual motion can be expanded in a Taylor's series about the reference trajectory at each point in time. If this expansion is truncated to eliminate higher order terms, then the deviation in the state from the reference trajectory can be described by a set of linear differential equations with time-dependent coefficients. A linear relation between the observation deviation and the state deviation can be obtained by

a similar expansion procedure. Then, the nonlinear orbit determination problem in which the complete state vector is to be estimated can be replaced by a linear orbit determination problem in which the deviation from some reference solution is to be determined.

To carry out this linearization procedure, let the $n \times 1$ state deviation vector, $\mathbf{x}$, and the $p \times 1$ observation deviation vector, $\mathbf{y}$, be defined as follows:

$$\begin{aligned} \mathbf{x}(t) &= \mathbf{X}(t) - \mathbf{X}^*(t)\,, \\ \mathbf{y}(t) &= \mathbf{Y}(t) - \mathbf{Y}^*(t)\,. \end{aligned} \tag{1.3}$$

It follow that

$$\dot{\mathbf{x}}(t) = \dot{\mathbf{X}}(t) - \dot{\mathbf{X}}^*(t)\,. \tag{1.4}$$

Expanding equations (1.1) and (1.2) in a Taylor's series about the reference trajectory leads to

$$\begin{aligned} \dot{\mathbf{X}}(t) &= \mathbf{F}(\mathbf{X},t) = \mathbf{F}(\mathbf{X}^*,t) + \left[\frac{\partial \mathbf{F}(t)}{\partial \mathbf{X}(t)}\right]^* \mathbf{x}(t) + \dots\,, \\ \mathbf{Y}_i(t) &= \mathbf{G}(\mathbf{X}_i,t_i) + \boldsymbol{\varepsilon}_i = \mathbf{G}(\mathbf{X}_i^*,t_i) + \left[\frac{\partial \mathbf{G}}{\partial \mathbf{X}}\right]_i^* \mathbf{x}_i + \dots + \boldsymbol{\varepsilon}_i\,, \end{aligned} \tag{1.5}$$

where $[\,]^*$ indicates that the partial derivative matrix is evaluated on the reference solution, $\mathbf{X}^*(t)$, which is obtained by integrating equation (1.1) with the specified initial conditions, $\mathbf{X}^*(t_0)$. If the terms of order higher than the first in equations (1.5) are neglected, under the assumption that the higher order products are small compared to the first order terms, and if the condition $\dot{\mathbf{X}}^* = \mathbf{F}(\mathbf{X}^*,t)$ and $\mathbf{Y}_i^* = \mathbf{G}(\mathbf{X}_i^*,t_i)$ are used, equations (1.5) can be written as

$$\begin{aligned} \dot{\mathbf{x}}(t) &= \mathbf{A}(t)\mathbf{x}(t)\,, \\ \mathbf{y}_i &= \tilde{\mathbf{H}}_i\mathbf{x}_i + \boldsymbol{\varepsilon}_i\,, \qquad i = 1, ..., l\,, \end{aligned} \tag{1.6}$$

where

$$\mathbf{A}(t) = \left[\frac{\partial \mathbf{F}(t)}{\partial \mathbf{X}(t)}\right]^*, \qquad \tilde{\mathbf{H}}_i = \left[\frac{\partial \mathbf{G}}{\partial \mathbf{X}}\right]_i^*. \tag{1.7}$$

Hence, the original nonlinear estimation problem is replaced by the linear estimation problem described by equations (1.6), where

$$\begin{aligned} \mathbf{x}(t) &= \mathbf{X}(t) - \mathbf{X}^*(t)\,, \\ \mathbf{x}_i &= \mathbf{X}(t_i) - \mathbf{X}^*(t_i)\,, \\ \mathbf{y}_i &= \mathbf{Y}_i - \mathbf{G}(\mathbf{X}_i^*,t_i)\,. \end{aligned} \tag{1.8}$$

Notice that if the original system of differential equations $\dot{\mathbf{X}} = F(\mathbf{X},t)$ is linear, the second and higher order partial derivatives of $\mathbf{F}(\mathbf{X},t)$ are zero. The same statements apply to $\mathbf{G}(\mathbf{X}_i,t_i)$. Hence, for a linear system there is no need to deal with a state or observational deviation vector or a reference solution. However, for the orbit determination problem, $\mathbf{F}(\mathbf{X},t)$ and $\mathbf{G}(\mathbf{X}_i,t_i)$ will always be nonlinear in $\mathbf{X}(t)$, thus requiring that we deal with deviation vectors and a reference trajectory in order to linearize the system.

1.2.1 The state transition matrix

The first of equations (1.6) represents a system of linear differential equations with time-dependents coefficients. The symbol $[\,]^*$ indicates that the values of $\mathbf{X}$ are derived from a particular solution to the equations $\dot{\mathbf{X}} = \mathbf{F}(\mathbf{X},t)$ which is generated with the initial conditions $\mathbf{X}(t_0) = \mathbf{X}_0^*$. The general solution for this system, $\dot{\mathbf{x}}(t) = \mathbf{A}(t)\mathbf{x}(t)$, can be expressed as

$$\mathbf{x}(t) = \boldsymbol{\Phi}(t,t_k)\mathbf{x}_k\,, \tag{1.9}$$

where $\mathbf{x}_k$ is the value of $\mathbf{x}$ at t_k, that is, $\mathbf{x}_k = \mathbf{x}(t_k)$. The matrix $\mathbf{\Phi}(t_i, t_k)$ is called the *state transition matrix*. The state transition matrix has the following useful properties:

$$\begin{aligned} \mathbf{\Phi}(t_i, t_i) &= \mathbf{I}\,, \\ \mathbf{\Phi}(t_i, t_k) &= \mathbf{\Phi}(t_i, t_j)\mathbf{\Phi}(t_j, t_k)\,, \\ \mathbf{\Phi}(t_i, t_k) &= \mathbf{\Phi}^{-1}(t_k, t_i)\,. \end{aligned} \tag{1.10}$$

The differential equation for $\mathbf{\Phi}(t_i, t_k)$ can be obtained by differentiating equation (1.9) (noting that $\mathbf{x}_k$ is a constant). This yields

$$\dot{\mathbf{x}}(t) = \dot{\mathbf{\Phi}}(t, t_k)\mathbf{x}_k\,. \tag{1.11}$$

Substituting equation (1.11) into the first of equations (1.6) and using equation (1.9) yields

$$\dot{\mathbf{\Phi}}(t, t_k)\mathbf{x}_k = \mathbf{A}(t)\mathbf{\Phi}(t, t_k)\mathbf{x}_k\,. \tag{1.12}$$

Since this condition must be satisfied for all $\mathbf{x}_k$, it follows that

$$\dot{\mathbf{\Phi}}(t, t_k) = \mathbf{A}(t)\mathbf{\Phi}(t, t_k)\,, \tag{1.13}$$

with initial conditions

$$\mathbf{\Phi}(t_k, t_k) = \mathbf{I}\,. \tag{1.14}$$

Under certain conditions on $\mathbf{A}(t)$, the state transition matrix may be inverted analytically.

1.2.2 Solution for the state transition matrix

A linear differential equation of the type $\dot{\mathbf{x}}(t) = \mathbf{A}(t)\mathbf{x}(t)$ or $\dot{\mathbf{\Phi}}(t, t_0) = \mathbf{A}(t)\mathbf{\Phi}(t, t_0)$ has an infinite number of solutions in terms of arbitrary constants. However, when initial conditions, $\mathbf{x}(t_0)$ and $\mathbf{\Phi}(t_0, t_0)$, are specified and the elements of $\mathbf{A}(t)$ are continuous functions of time, the solution becomes unique.

The solution for $\mathbf{\Phi}(t, t_0)$ is facilitated by noting that the individual columns of the differential equation for $\dot{\mathbf{\Phi}}(t, t_0)$ are uncoupled and independent. To illustrate this, consider a one-dimensional case where the state vector is given by

$$\mathbf{X}(t) = [\mathbf{r}, \mathbf{v}, \boldsymbol{\beta}]^T\,. \tag{1.15}$$

$\mathbf{X}$ is the state vector containing six position and velocity elements and $\boldsymbol{\beta}$, an m-vector, represents all constants parameters that are to be solved for. Hence, $\mathbf{X}$ is a vector of dimension $n = m + 6$. Equation (1.13) can be written in terms of the individual elements of the state transition matrix as follows:

$$\dot{\mathbf{\Phi}}(t, t_0) = \begin{bmatrix} \dot{\Phi}_{11} & \dot{\Phi}_{12} & \dot{\Phi}_{13} \\ \dot{\Phi}_{21} & \dot{\Phi}_{22} & \dot{\Phi}_{23} \\ \dot{\Phi}_{31} & \dot{\Phi}_{32} & \dot{\Phi}_{33} \end{bmatrix} = \begin{bmatrix} A_{11} & A_{12} & A_{13} \\ A_{21} & A_{22} & A_{23} \\ A_{31} & A_{32} & A_{33} \end{bmatrix} \begin{bmatrix} \Phi_{11} & \Phi_{12} & \Phi_{13} \\ \Phi_{21} & \Phi_{22} & \Phi_{23} \\ \Phi_{31} & \Phi_{32} & \Phi_{33} \end{bmatrix}, \tag{1.16}$$

subject to the following initial conditions at t_0

$$\begin{bmatrix} \Phi_{11} & \Phi_{12} & \Phi_{13} \\ \Phi_{21} & \Phi_{22} & \Phi_{23} \\ \Phi_{31} & \Phi_{32} & \Phi_{33} \end{bmatrix} = \begin{bmatrix} \mathbf{I} & \mathbf{0} & \mathbf{0} \\ \mathbf{0} & \mathbf{I} & \mathbf{0} \\ \mathbf{0} & \mathbf{0} & \mathbf{I} \end{bmatrix} = \mathbf{I}\,. \tag{1.17}$$

Equation (1.16) expands to

$$\begin{bmatrix} \dot{\Phi}_{11} & \dot{\Phi}_{12} & \dot{\Phi}_{13} \\ \dot{\Phi}_{21} & \dot{\Phi}_{22} & \dot{\Phi}_{23} \\ \dot{\Phi}_{31} & \dot{\Phi}_{32} & \dot{\Phi}_{33} \end{bmatrix} = \begin{bmatrix} A_{11}\Phi_{11} + A_{12}\Phi_{21} + A_{13}\Phi_{31} & A_{11}\Phi_{12} + A_{12}\Phi_{22} + A_{13}\Phi_{32} & A_{11}\Phi_{13} + A_{12}\Phi_{23} + A_{13}\Phi_{33} \\ A_{21}\Phi_{11} + A_{22}\Phi_{21} + A_{23}\Phi_{31} & A_{21}\Phi_{12} + A_{22}\Phi_{22} + A_{23}\Phi_{32} & A_{21}\Phi_{13} + A_{22}\Phi_{23} + A_{23}\Phi_{33} \\ A_{31}\Phi_{11} + A_{32}\Phi_{21} + A_{33}\Phi_{31} & A_{31}\Phi_{12} + A_{32}\Phi_{22} + A_{33}\Phi_{32} & A_{31}\Phi_{13} + A_{32}\Phi_{23} + A_{23}\Phi_{33} \end{bmatrix}. \tag{1.18}$$

Recall that the A_{ij} are known quantities obtained by evaluating

$$A_{ij}(t) = \left[\frac{\partial \mathbf{F}_i(t)}{\partial \mathbf{X}_j(t)}\right]^* , \tag{1.19}$$

on the reference trajectory. From equation (1.18) we see that the columns of $\dot{\mathbf{\Phi}}(t, t_0)$ are independent. Hence, we can solve for $\mathbf{\Phi}(t, t_0)$ by integrating independently two 3×1 vector differential equations. For any practical orbit determination application, the solution for $\mathbf{\Phi}(t, t_0)$ will be obtained via numerical integration. Hence, we can supply a vector of derivative values for the differential equation of the nominal state vector and $\dot{\mathbf{\Phi}}(t, t_0)$ to the numerical integration routine. For this one-dimensional case we would supply the integrator with the following vector at each time point:

$$\left[\begin{array}{cccccccccc} \dot{\mathbf{r}} & \dot{\mathbf{v}} & \dot{\Phi}_{11} & \dot{\Phi}_{21} & \dot{\Phi}_{31} & \dot{\Phi}_{12} & \dot{\Phi}_{22} & \dot{\Phi}_{32} & \dot{\Phi}_{13} & \dot{\Phi}_{23} & \dot{\Phi}_{33} \end{array}\right]^T . \tag{1.20}$$

The first two elements would provide the reference orbit, $\mathbf{X}^*(t)$, and the next nine would yield the elements of $\mathbf{\Phi}(t, t_0)$. The reference orbit is used to evaluate $\mathbf{A}(t)$, which is needed to evaluate $\dot{\mathbf{\Phi}}(t, t_0)$ in equation (1.18).

1.2.3 Relating the observations to an epoch state

Using equation (1.9), the second of equations (1.6) may be written in terms of the state at t_k as

$$\begin{aligned} \mathbf{y}_1 &= \tilde{\mathbf{H}}_1 \mathbf{\Phi}(t_1, t_k)\mathbf{x}_k + \boldsymbol{\varepsilon}_1 , \\ \mathbf{y}_2 &= \tilde{\mathbf{H}}_2 \mathbf{\Phi}(t_2, t_k)\mathbf{x}_k + \boldsymbol{\varepsilon}_2 , \\ &\vdots \\ \mathbf{y}_l &= \tilde{\mathbf{H}}_l \mathbf{\Phi}(t_l, t_k)\mathbf{x}_k + \boldsymbol{\varepsilon}_l . \end{aligned} \tag{1.21}$$

Equations (1.21) now contain $m = p \times l$ observations and only n unknown components of the state. If $\boldsymbol{\varepsilon}_i$ (with $i = 1, ..., l$) is zero, any linearly independent n of equations (1.21) can be used to determine $\mathbf{x}_k$.

If the following definitions are used

$$\mathbf{y} = \left[\begin{array}{c} \mathbf{y}_1 \\ \vdots \\ \mathbf{y}_l \end{array}\right] , \qquad \mathbf{H} = \left[\begin{array}{c} \tilde{\mathbf{H}}_1 \mathbf{\Phi}(t_1, t_k) \\ \vdots \\ \tilde{\mathbf{H}}_l \mathbf{\Phi}(t_l, t_k) \end{array}\right] , \qquad \boldsymbol{\varepsilon} = \left[\begin{array}{c} \boldsymbol{\varepsilon}_1 \\ \vdots \\ \boldsymbol{\varepsilon}_l \end{array}\right] , \tag{1.22}$$

and if the subscript on $\mathbf{x}_k$ is dropped for convenience, then equations (1.21) can be expressed as follows:

$$\mathbf{y} = \mathbf{H}\mathbf{x} + \boldsymbol{\varepsilon} , \tag{1.23}$$

where $\mathbf{y}$ is an $m \times 1$ vector, $\mathbf{x}$ is an $n \times 1$ vector, $\boldsymbol{\varepsilon}$ is an $m \times 1$ vector, $\mathbf{H}$ is an $m \times n$ mapping matrix, where $m = p \times l$ is the total number of observations. If p or l is sufficiently large, the essential condition $m > n$ is satisfied.

1.3 Least squares estimate

The least squares solution selects the estimate of $\mathbf{x}$ as that value that minimizes the sum of the squares of the calculated observation residuals. That is, $\mathbf{x}$ is selected to minimize the following *performance index*:

$$J(\mathbf{x}) = \frac{1}{2}\boldsymbol{\varepsilon}^T \boldsymbol{\varepsilon} . \tag{1.24}$$

The sum of the squares of the calculated observation errors is a logical choice for the performance index. A criterion defined, for example, by the sum of calculated observation errors could be identically zero

with very large observation errors having plus and minus signs that cancel each other. Whether the observation error is positive or negative, its square will be positive and the performance index defined by equation (1.24) can vanish only if each of the observation errors is identically zero. If $\boldsymbol{\varepsilon}$, as defined by equation (1.23), is substituted into equation (1.24), the following expression is obtained:

$$J(\mathbf{x}) = \frac{1}{2}\boldsymbol{\varepsilon}^T\boldsymbol{\varepsilon} = \sum_{i=1}^{l} \frac{1}{2}\boldsymbol{\varepsilon}_i^T\boldsymbol{\varepsilon}_i = \frac{1}{2}(\mathbf{y}-\mathbf{H}\mathbf{x})^T(\mathbf{y}-\mathbf{H}\mathbf{x})\,. \tag{1.25}$$

Note that equation (1.25) is a quadratic function of $\mathbf{x}$, and as a consequence the expression will have a unique minima when

$$\frac{\partial J}{\partial \mathbf{x}} = \mathbf{0}\,, \qquad \text{and} \qquad \delta\mathbf{x}^T\frac{\partial^2 J}{\partial \mathbf{x}^2}\delta\mathbf{x} > \mathbf{0}\,, \tag{1.26}$$

for all $\delta\mathbf{x} \neq 0$. The second condition implies that the symmetric matrix $\frac{\partial^2 J}{\partial \mathbf{x}^2}$ is positive definite.

Carrying out the first operation on equation (1.25) yields

$$\frac{\partial J}{\partial \mathbf{x}} = \mathbf{0} = -(\mathbf{y}-\mathbf{H}\mathbf{x})^T\mathbf{H} = -\mathbf{H}^T(\mathbf{y}-\mathbf{H}\mathbf{x})\,. \tag{1.27}$$

The value of $\mathbf{x}$ that satisfies equation (1.27) will be the best estimate of $\mathbf{x}$, which we will call $\hat{\mathbf{x}}$. Hence,

$$(\mathbf{H}^T\mathbf{H})\hat{\mathbf{x}} = \mathbf{H}^T\mathbf{y}\,. \tag{1.28}$$

Also

$$\frac{\partial^2 J}{\partial \mathbf{x}^2} = \mathbf{H}^T\mathbf{H}\,, \tag{1.29}$$

which will be positive definite if $\mathbf{H}$ is full rank.

Three major shortcomings of the simple least square solution are:

1. each observation error is weighted equally even though the accuracy of observations may differ;
2. the observation errors may be correlated (not independent), and the simple least squares solution makes no allowance for this;
3. the method does not consider that the errors are samples from a random process and makes no attempt to utilize any statistical information.

1.3.1 Weighted least squares solution

Given a vector sequence of observations $\mathbf{y}_1$, $\mathbf{y}_2$, ..., $\mathbf{y}_l$ related through the state transition matrix to the state at some epoch time, $\mathbf{x}_k$, and an associated weighting matrix, $\mathbf{w}_i$, for each of the observations vectors, one can write

$$\begin{aligned} \mathbf{y}_1 &= \mathbf{H}_1\mathbf{x}_k + \boldsymbol{\varepsilon}_1\,, & \mathbf{w}_1;\\ \mathbf{y}_2 &= \mathbf{H}_2\mathbf{x}_k + \boldsymbol{\varepsilon}_2\,, & \mathbf{w}_2;\\ &\vdots & \\ \mathbf{y}_l &= \mathbf{H}_l\mathbf{x}_k + \boldsymbol{\varepsilon}_l\,, & \mathbf{w}_l; \end{aligned} \tag{1.30}$$

where $\mathbf{H}_i$ is the matrix $\tilde{\mathbf{H}}_i$ propagated at the time t_i:

$$\mathbf{H}_i = \tilde{\mathbf{H}}_i\boldsymbol{\Phi}(t_i, t_k)\,. \tag{1.31}$$

In equations (1.30) the weighting matrices, $\mathbf{w}_i$, are assumed to be diagonal with their elements normalized to a range between zero and one. Observations weighted with a one would be given the highest possible

weight and those weighted with zero would be neglected. The following definitions can be used

$$\mathbf{y} = \begin{bmatrix} \mathbf{y}_1 \\ \mathbf{y}_2 \\ \vdots \\ \mathbf{y}_l \end{bmatrix}, \qquad \mathbf{H} = \begin{bmatrix} \mathbf{H}_1 \\ \mathbf{H}_2 \\ \vdots \\ \mathbf{H}_l \end{bmatrix}, \qquad \boldsymbol{\varepsilon} = \begin{bmatrix} \boldsymbol{\varepsilon}_1 \\ \boldsymbol{\varepsilon}_2 \\ \vdots \\ \boldsymbol{\varepsilon}_l \end{bmatrix}, \qquad \mathbf{W} = \begin{bmatrix} \mathbf{w}_1 & 0 & ... & 0 \\ 0 & \mathbf{w}_2 & ... & 0 \\ \vdots & \vdots & ... & \vdots \\ 0 & 0 & ... & \mathbf{w}_l \end{bmatrix}. \tag{1.32}$$

Each observation $\mathbf{y}_i$ is assumed to be a p-vector and $\mathbf{x}_k$ is a n-vector. Equations (1.30) now can be expressed as

$$\mathbf{y} = \mathbf{H}\mathbf{x}_k + \boldsymbol{\varepsilon}\,, \qquad \mathbf{W}\,. \tag{1.33}$$

The weighted least square problem can then be posed as follows: given the linear observation state relationship expressed by (1.33), find the estimate of $\mathbf{x}_k$ to minimize the weighted sum of the squares of the calculated observation errors.

The performance index is

$$J(\mathbf{x}_k) = \frac{1}{2}\boldsymbol{\varepsilon}^T\mathbf{W}\boldsymbol{\varepsilon} = \sum_{i=1}^{l}\frac{1}{2}\boldsymbol{\varepsilon}_i^T\mathbf{W}\boldsymbol{\varepsilon}_i\,. \tag{1.34}$$

Using equation (1.33), $J(\mathbf{x}_k)$ can be expressed as

$$J(\mathbf{x}_k) = \frac{1}{2}(\mathbf{y} - \mathbf{H}\mathbf{x}_k)^T\mathbf{W}(\mathbf{y} - \mathbf{H}\mathbf{x}_k)\,. \tag{1.35}$$

A necessary condition for a minimum of $J(\mathbf{x}_k)$ is that its first derivative with respect to $\mathbf{x}_k$ vanishes

$$\frac{\partial J}{\partial \mathbf{x}_k} = \mathbf{0} = -(\mathbf{y} - \mathbf{H}\mathbf{x}_k)^T\mathbf{W}\mathbf{H} = -\mathbf{H}^T\mathbf{W}(\mathbf{y} - \mathbf{H}\mathbf{x}_k)\,. \tag{1.36}$$

This expression can be rearranged to obtain the normal equations in the least squares formulation as

$$(\mathbf{H}^T\mathbf{W}\mathbf{H})\mathbf{x}_k = \mathbf{H}^T\mathbf{W}\mathbf{y}\,. \tag{1.37}$$

If the normal matrix $\mathbf{H}^T\mathbf{W}\mathbf{H}$ is positive definite, it will have an inverse and the solution to (1.37) is

$$\hat{\mathbf{x}}_k = (\mathbf{H}^T\mathbf{W}\mathbf{H})^{-1}\mathbf{H}^T\mathbf{W}\mathbf{y}\,. \tag{1.38}$$

The value of $\hat{\mathbf{x}}_k$ given by equation (1.38) is the weighted least squares estimate and is the estimate that minimizes the sum of squares of the weighted observation errors. Note that equation (1.38) can be expressed as

$$\hat{\mathbf{x}}_k = \mathbf{P}_k\mathbf{H}^T\mathbf{W}\mathbf{y}\,, \tag{1.39}$$

where

$$\mathbf{P}_k = (\mathbf{H}^T\mathbf{W}\mathbf{H})^{-1}\,. \tag{1.40}$$

The $n \times n$ matrix $\mathbf{P}_k$ is symmetric. Furthermore, if it exists, it must be positive definite, since it is computed as the inverse of the positive definite matrix, $\mathbf{H}^T\mathbf{W}\mathbf{H}$. The parameter observability is related to the rank of this matrix. If all parameters in $\mathbf{x}_k$ are observable (i.e., can be uniquely determined with the observation set $\mathbf{y}$), then $\mathbf{P}_k$ will be full rank and $\mathbf{P}_k$ will have an inverse. The number of independent observations must be greater than or equal to the number of parameters being estimated if $\mathbf{P}_k$ is to be invertible. Furthermore, $\mathbf{P}_k$ is related to the accuracy of the estimate, $\hat{\mathbf{x}}_k$. In general, the larger the magnitude of the elements of the matrix, $\mathbf{P}_k$, the less accurate the estimate.

If an a priori value, $\bar{\mathbf{x}}_k$, is available for $\mathbf{x}_k$ and an associated weighting matrix, $\bar{\mathbf{W}}_k$, is given, the weighted least square estimate for $\mathbf{x}_k$ can be obtained by choosing for $\hat{\mathbf{x}}_k$ the value of $\mathbf{x}_k$, which minimizes the performance index

$$J(\mathbf{x}_k) = \frac{1}{2}(\mathbf{y} - \mathbf{H}\mathbf{x}_k)^T\mathbf{W}(\mathbf{y} - \mathbf{H}\mathbf{x}_k) + \frac{1}{2}(\bar{\mathbf{x}}_k - \mathbf{x}_k)^T\bar{\mathbf{W}}_k(\bar{\mathbf{x}}_k - \mathbf{x}_k)\,. \tag{1.41}$$

This results in

$$\hat{\mathbf{x}}_k = (\mathbf{H}^T\mathbf{W}\mathbf{H} + \bar{\mathbf{W}}_k)^{-1}\left(\mathbf{H}^T\mathbf{W}\mathbf{y} + \bar{\mathbf{W}}_k\bar{\mathbf{x}}_k\right)\,, \tag{1.42}$$

where $\bar{\mathbf{x}}_k$ represents an a priori estimate of $\mathbf{x}_k$ and $\bar{\mathbf{W}}_k$ represents a weighting matrix for the a priori estimate of $\mathbf{x}_k$.

1.3.2 The minimum variance estimate

The least squares and weighted least squares methods do not include any information on the statistical characteristics of the measurement errors or the a priori errors in the values of the parameters to be estimated. The minimum variance approach is one method for removing this limitation. The minimum variance criterion is used widely in developing solutions to estimation problems because of the simplicity in its use. It has the advantage that the complete statistical description of the random errors in the problem is not required. Rather, only the first and second moments of the probability density function of the observation errors are required. This information is expressed in the mean and covariance matrix associated with the random error.

If it is assumed that the observation error $\boldsymbol{\varepsilon}_i$ is random with zero mean and specified covariance, the state estimation problem can be formulated as follows.

Given the system of state-propagation equations and observation state equations

$$\mathbf{x}_i = \boldsymbol{\Phi}(t_i, t_k)\mathbf{x}_k\,, \tag{1.43}$$

$$\mathbf{y}_i = \tilde{\mathbf{H}}_i\mathbf{x}_i + \boldsymbol{\varepsilon}_i\,, \qquad i = 1, ..., l\,, \tag{1.44}$$

find the linear, unbiased, minimum variance estimate, $\hat{\mathbf{x}}_k$, of the state $\mathbf{x}_k$.

Using the state transition matrix and the definitions of equations (1.30), it is possible to reduce equation (1.43) to the following form

$$\mathbf{y} = \mathbf{H}\mathbf{x}_k + \boldsymbol{\varepsilon}\,, \tag{1.45}$$

where

$$E[\boldsymbol{\varepsilon}] = \begin{bmatrix} E[\boldsymbol{\varepsilon}_1] \\ E[\boldsymbol{\varepsilon}_2] \\ \vdots \\ E[\boldsymbol{\varepsilon}_l] \end{bmatrix} = \begin{bmatrix} \mathbf{0} \\ \mathbf{0} \\ \vdots \\ \mathbf{0} \end{bmatrix}\,, \qquad E[\boldsymbol{\varepsilon}\boldsymbol{\varepsilon}^T] = \begin{bmatrix} \mathbf{R}_{11} & \mathbf{R}_{12} & ... & \mathbf{R}_{1l} \\ \mathbf{R}_{12}^T & \mathbf{R}_{22} & ... & \mathbf{R}_{2l} \\ \vdots & ... & ... & \vdots \\ \mathbf{R}_{1l}^T & ... & ... & \mathbf{R}_{ll} \end{bmatrix} = \mathbf{R}\,.$$

Generally, $\mathbf{R}_{11} = \mathbf{R}_{22} = ... = \mathbf{R}_{ll}$ and $\mathbf{R}_{ij} = \mathbf{0}$ $(i \neq j)$, but this is not a necessary restriction. $\mathbf{R}_{ij} \neq \mathbf{0}$ $(i \neq j)$ corresponds to the more general case of time-correlated observation errors.

From the problem statement, the estimate is to be the best linear, unbiased, minimum variance estimate. The consequences of each of these requirements are addressed in the following steps.

1. *Linear*: the requirement of a linear estimate implies that the estimate is to be made up of a linear combination of the observations:

   $$\mathbf{x}_k = \mathbf{M}\mathbf{y}\,. \tag{1.46}$$

   The $n \times m$ matrix $\mathbf{M}$ is unspecified and is to be selected to obtain the best estimate.

2. *Unbiased*: if the estimate is unbiased, then by definition

   $$E[\hat{\mathbf{x}}] = \mathbf{x}\,. \tag{1.47}$$

   Substituting equations (1.46) and (1.43) into equation (1.47) leads to the following requirement

   $$E[\hat{\mathbf{x}}_k] = E[\mathbf{M}\mathbf{y}] = E[\mathbf{M}\mathbf{H}\mathbf{x}_k + \mathbf{M}\boldsymbol{\varepsilon}] = \mathbf{x}_k\,. \tag{1.48}$$

   But, since $E[\boldsymbol{\varepsilon}] = \mathbf{0}$, this reduces to

   $$\mathbf{M}\mathbf{H}\mathbf{x}_k = \mathbf{x}_k\,, \tag{1.49}$$

from which the following constraint on $\mathbf{M}$ is obtained

$$\mathbf{MH} = \mathbf{I}\,. \tag{1.50}$$

That is, if the estimate is to be unbiased, the linear mapping matrix $\mathbf{M}$ must satisfy equation (1.50). This condition requires the rows of $\mathbf{M}$ to be orthogonal to the columns of $\mathbf{H}$.

3. *Minimum Variance*: if the estimate is unbiased, then the estimation error covariance matrix can be expressed as

$$\mathbf{P}_k = E\{[(\hat{\mathbf{x}}_k - \mathbf{x}_k) - E(\hat{\mathbf{x}}_k - \mathbf{x}_k)][(\hat{\mathbf{x}}_k - \mathbf{x}_k) - E(\hat{\mathbf{x}}_k - \mathbf{x}_k)]^T\} = E[(\hat{\mathbf{x}}_k - \mathbf{x}_k)(\hat{\mathbf{x}}_k - \mathbf{x}_k)^T]\,. \tag{1.51}$$

The strategy is to minimize the last expression satisfying the two constraints 1) and 2) at the same time. It can be shown (see [61]) that this leads to the following formulas:

$$\mathbf{P}_k = \left(\mathbf{H}^T\mathbf{R}^{-1}\mathbf{H}\right)^{-1}\,, \tag{1.52}$$

$$\hat{\mathbf{x}}_k = \left(\mathbf{H}^T\mathbf{R}^{-1}\mathbf{H}\right)^{-1}\mathbf{H}^T\mathbf{R}^{-1}\mathbf{y}\,. \tag{1.53}$$

Note that computation of the estimate, $\hat{\mathbf{x}}_k$, requires inverting the $n \times n$ normal matrix $\mathbf{H}^T\mathbf{R}^{-1}\mathbf{H}$. For a large dimension system the computation of this inverse may be difficult. For this reason, alternative techniques have been employed (Cholesky decomposition, Householder transformations and Given's rotations, see [61] [50]). The solution given by equations (1.53) will agree with the weighted least square solution if the weighting matrix, $\mathbf{W}$, used in the least square approach is equal to the inverse of the observation noise covariance matrix; that is if $\mathbf{W} = \mathbf{R}^{-1}$.

1.3.3 Propagation of the estimate and covariance matrix

If an estimate at a time t_j is obtained by using equation (1.53), the estimate may be mapped to any later time by using the state transition matrix $\mathbf{\Phi}$

$$\bar{\mathbf{x}}_k = \mathbf{\Phi}\left(t_k, t_j\right)\hat{\mathbf{x}}_j\,, \tag{1.54}$$

where $\bar{\mathbf{x}}_k$ is the best estimate of $\mathbf{x}_k$ at time $t_k > t_j$ based on the observations collected up to t_j. The expression for propagating the covariance matrix $\bar{\mathbf{P}}_k$ is the following:

$$\bar{\mathbf{P}}_k = \mathbf{\Phi}\left(t_k, t_j\right)\mathbf{P}_j\mathbf{\Phi}^T\left(t_k, t_j\right)\,, \tag{1.55}$$

where $\mathbf{P}_j = E[(\hat{\mathbf{x}}_j - \mathbf{x}_j)(\hat{\mathbf{x}}_j - \mathbf{x}_j)^T|\mathbf{y}_1, ..., \mathbf{y}_j]$ is the covariance matrix at time t_j provided the observations up to t_j.

1.3.4 Minimum variance estimate with a priori information

If an estimate $\hat{\mathbf{x}}_j$ and the associated covariance matrix $\mathbf{P}_j$ are obtained at a time t_j, and an additional observation or observation sequence is obtained at time t_k, the estimate and the observation can be combined in a straightforward manner to obtain the new estimate $\hat{\mathbf{x}}_k$. The problem can be stated as follows: given the propagated estimates of the state vector $\bar{\mathbf{x}}_k$ and the covariance matrix $\bar{\mathbf{P}}_k$ and a new observation $\mathbf{y}_k$ at time t_k

$$\mathbf{y}_k = \tilde{\mathbf{H}}_k\mathbf{x}_k + \boldsymbol{\varepsilon}_k, \tag{1.56}$$

where $E\left[\boldsymbol{\varepsilon}_k\right] = \mathbf{0}$, $E[\boldsymbol{\varepsilon}_k\boldsymbol{\varepsilon}_j^T] = \mathbf{R}_k\delta_{kj}$, and $E[(\mathbf{x}_j - \hat{\mathbf{x}}_j)\boldsymbol{\varepsilon}_k^T] = \mathbf{0}$, find the linear, minimum variance, unbiased estimate of $\mathbf{x}_k$.

The solution to this problem can be obtained easily in the case that $\bar{\mathbf{x}}_k$ can be interpreted as an observation. In this case, we can prove [61] that the new optimal estimate is:

$$\hat{\mathbf{x}}_k = (\mathbf{H}_k^T\mathbf{R}_k^{-1}\mathbf{H}_k + \overline{\mathbf{P}}_k^{-1})^{-1}(\mathbf{H}_k^T\mathbf{R}_k^{-1}\mathbf{y}_k + \overline{\mathbf{P}}_k^{-1}\bar{\mathbf{x}}_k)\,, \tag{1.57}$$

and the associated covariance is:

$$\mathbf{P}_k = E[(\hat{\mathbf{x}}_k - E[\hat{\mathbf{x}}_k])(\hat{\mathbf{x}}_k - E[\hat{\mathbf{x}}_k])^T] = (\mathbf{H}_k^T \mathbf{R}_k^{-1} \mathbf{H}_k + \overline{\mathbf{P}}_k^{-1})^{-1}. \tag{1.58}$$

It has to be pointed out that:

- the array $\mathbf{y}_k$ can be a single observation or it may include a batch of observations mapped to t_k;
- the a-priori estimate $\bar{\mathbf{x}}_k$ may represent the estimate based on a priori initial conditions or the estimate based upon a set of previously reduced observations;
- the $n \times n$ normal matrix of (1.57) must be inverted and if the dimension n is large, this inversion can lead to computational problems.

The algorithm that uses equations (1.57) and (1.58) is called **batch processor** or **batch filter**. An in depth discussion on the algorithm can be found in Tapley, [61].

1.4 Computational algorithm for the batch processor

Assume that we wish to estimate the state deviation vector $\mathbf{x}_0$ at a reference time, t_0. Given a set of initial conditions $\mathbf{X}^*(t_0)$, an a priori estimate $\bar{\mathbf{x}}_0$ and the associated error covariance matrix, $\bar{\mathbf{P}}_0$, the computational algorithm for the batch processor generally uses the normal equation form for $\hat{\mathbf{x}}_0$. Writing equation (1.42) in normal equations form for a batch of observations and recognizing that $\mathbf{W} = \mathbf{R}^{-1}$ and $\bar{\mathbf{W}} = \bar{\mathbf{P}}_0^{-1}$ yields

$$(\mathbf{H}^T \mathbf{R}^{-1} \mathbf{H} + \bar{\mathbf{P}}_0^{-1}) \hat{\mathbf{x}}_0 = \mathbf{H}^T \mathbf{R}^{-1} \mathbf{y} + \bar{\mathbf{P}}_0^{-1} \bar{\mathbf{x}}_0 \,. \tag{1.59}$$

Here t_0 is an arbitrary epoch and all quantities in equation (1.59) are assumed to have been mapped to this epoch using the appropriate state transition matrices as illustrated in equations (1.30) and (1.32).

If $\mathbf{R}$ is a block diagonal matrix, that is the observations are uncorrelated in time although correlations between the observations at any given time may exist, these matrices simply may be accumulated as follows:

$$\mathbf{H}^T \mathbf{R}^{-1} \mathbf{H} = \sum_{i=1}^{l} [\tilde{\mathbf{H}}_i \mathbf{\Phi}(t_i, t_0)]^T \mathbf{R}_i^{-1} \tilde{\mathbf{H}}_i \mathbf{\Phi}(t_i, t_0) \,, \tag{1.60}$$

$$\mathbf{H}^T \mathbf{R}^{-1} \mathbf{y} = \sum_{i=1}^{l} [\tilde{\mathbf{H}}_i \mathbf{\Phi}(t_i, t_0)]^T \mathbf{R}_i^{-1} \mathbf{y}_i \,. \tag{1.61}$$

In general $\mathbf{X}^*(t_0)$ would be chosen so that $\bar{\mathbf{x}}_0 = \mathbf{0}$, and $\bar{\mathbf{P}}_0$ would reflect the relative accuracy of the elements of the initial conditions vector $\mathbf{X}^*(t_0)$. In theory $\bar{\mathbf{x}}_0$ and $\bar{\mathbf{P}}_0$ represent information and should be treated as data that are merged with the observation data, as indicated by equation (1.59). Consequently, the value of $\mathbf{X}_0^* + \bar{\mathbf{x}}_0$ should be held constant for the beginning of each iteration. Since the initial condition vector $\mathbf{X}_0^*$ is augmented by the value of $\hat{\mathbf{x}}_0$ after each iteration, that is, $(\mathbf{X}_0^*)_n = (\mathbf{X}_0^*)_{n-1} + (\hat{\mathbf{x}}_0)_{n-1}$, holding $\mathbf{X}_0^* + \bar{\mathbf{x}}_0$ constant results in the following expression for $(\bar{\mathbf{x}}_0)_n$

$$(\bar{\mathbf{x}}_0)_n = (\bar{\mathbf{x}}_0)_{n-1} - (\hat{\mathbf{x}}_0)_{n-1} \,. \tag{1.62}$$

Recall that the state transition matrix is obtained by integrating

$$\dot{\mathbf{\Phi}}(t, t_k) = \mathbf{A}(t) \mathbf{\Phi}(t, t_k) \,, \tag{1.63}$$

subject to the initial conditions $\mathbf{\Phi}(t_k, t_k) = \mathbf{I}$ along with the nonlinear equations, $\dot{\mathbf{X}}^* = \mathbf{F}(\mathbf{X}^*, t)$, which define the nominal trajectory, $\dot{\mathbf{X}}^*(t)$. The matrix $\mathbf{A}(t)$ is evaluated on the reference trajectory,

$$\mathbf{A}(t) = \frac{\partial \mathbf{F}(\mathbf{X}^*, t)}{\partial \mathbf{X}} \,, \tag{1.64}$$

where $\mathbf{F}(\mathbf{X}^*, t)$ is the time derivative of the state vector in the differential equations governing the time evolution of the system. The observation-state mapping matrix is given by

$$\tilde{\mathbf{H}}_i = \frac{\partial \mathbf{G}(\mathbf{X}_i^*, t_i)}{\partial \mathbf{X}} , \tag{1.65}$$

where $\mathbf{G}(\mathbf{X}_i^*, t_i)$ are the observation-state relationships evaluated on the nominal or reference trajectory.

Notice that the solution for $\hat{\mathbf{x}}_0$ involved inversion of the information matrix, $\mathbf{\Lambda}_0$, where

$$\mathbf{\Lambda}_0 = \mathbf{H}^T \mathbf{R}^{-1} \mathbf{H} + \bar{\mathbf{P}}_0^{-1} . \tag{1.66}$$

Generally the normal equations would not be solved by a direct inversion of $\mathbf{\Lambda}_0$ but rather would be solved by an indirect but more accurate technique, such as the Cholesky decomposition. The sequence of operations required to implement the batch estimation process is outlined in Figure 1.2, where we assume that there are no observations at t_0. If observations exist at t_0, set $\mathbf{\Lambda} = \bar{\mathbf{P}}_0^{-1} + \mathbf{H}_0^T \mathbf{R}_0^{-1} \mathbf{H}_0$ and $\mathbf{N} = \mathbf{H}_0^T \mathbf{R}_0^{-1} \mathbf{y}_0$ in the initialization. As previously stated, the entire sequence of computations are repeated until the estimation process has converged. If there are observations at t_0, the state transition matrix for processing these observations is the identity matrix.

This procedure yields a minimum value of the performance index

$$J(\mathbf{x}) = (\hat{\mathbf{x}}_0 - \bar{\mathbf{x}}_0)^T \bar{\mathbf{P}}_0^{-1} + \sum_{i=1}^{l} \hat{\boldsymbol{\varepsilon}}_i^T \mathbf{R}_i^{-1} \hat{\boldsymbol{\varepsilon}}_i , \tag{1.67}$$

where

$$\hat{\boldsymbol{\varepsilon}}_i = \mathbf{y}_i - \mathbf{H}_i \hat{\mathbf{x}}_0 , \tag{1.68}$$

and $\hat{\boldsymbol{\varepsilon}}_i$ is the best estimate of the observation error.

In practice, $\bar{\mathbf{P}}_0$ is generally not a realistic representation of the accuracy of $\bar{\mathbf{x}}_0$ and it is used only to better condition to estimation error covariance matrix, $\mathbf{P}$. In this case, $\bar{\mathbf{x}}_0$ usually is set to zero for each iteration and $\bar{\mathbf{P}}_0$ is chosen to be a diagonal matrix with large diagonal values. Hence, the first term in equation (1.67) will be very small and the tracking data residuals will determine the value of $J(\mathbf{x})$. The rms (root mean square) of the observation residuals generally is computed and may be used as a measure of convergence; when the rms no larger changes the solution is assumed to be converged. The rms is computed from

$$rms = \left\{ \frac{\sum_{i=1}^{l} \hat{\boldsymbol{\varepsilon}}_i^T \mathbf{R}_i^{-1} \hat{\boldsymbol{\varepsilon}}_i}{m} \right\}^{\frac{1}{2}} , \tag{1.69}$$

where $\hat{\boldsymbol{\varepsilon}}_i$ is a p-vector and $m = l \times p$. Hence, m is the total number of observations. The equation (1.69) is referred to as the weighted rms. If the rms is computed without including the weighting matrix, $\mathbf{R}_i^{-1}$, it may be referred to as the unweighted rms or just the rms.

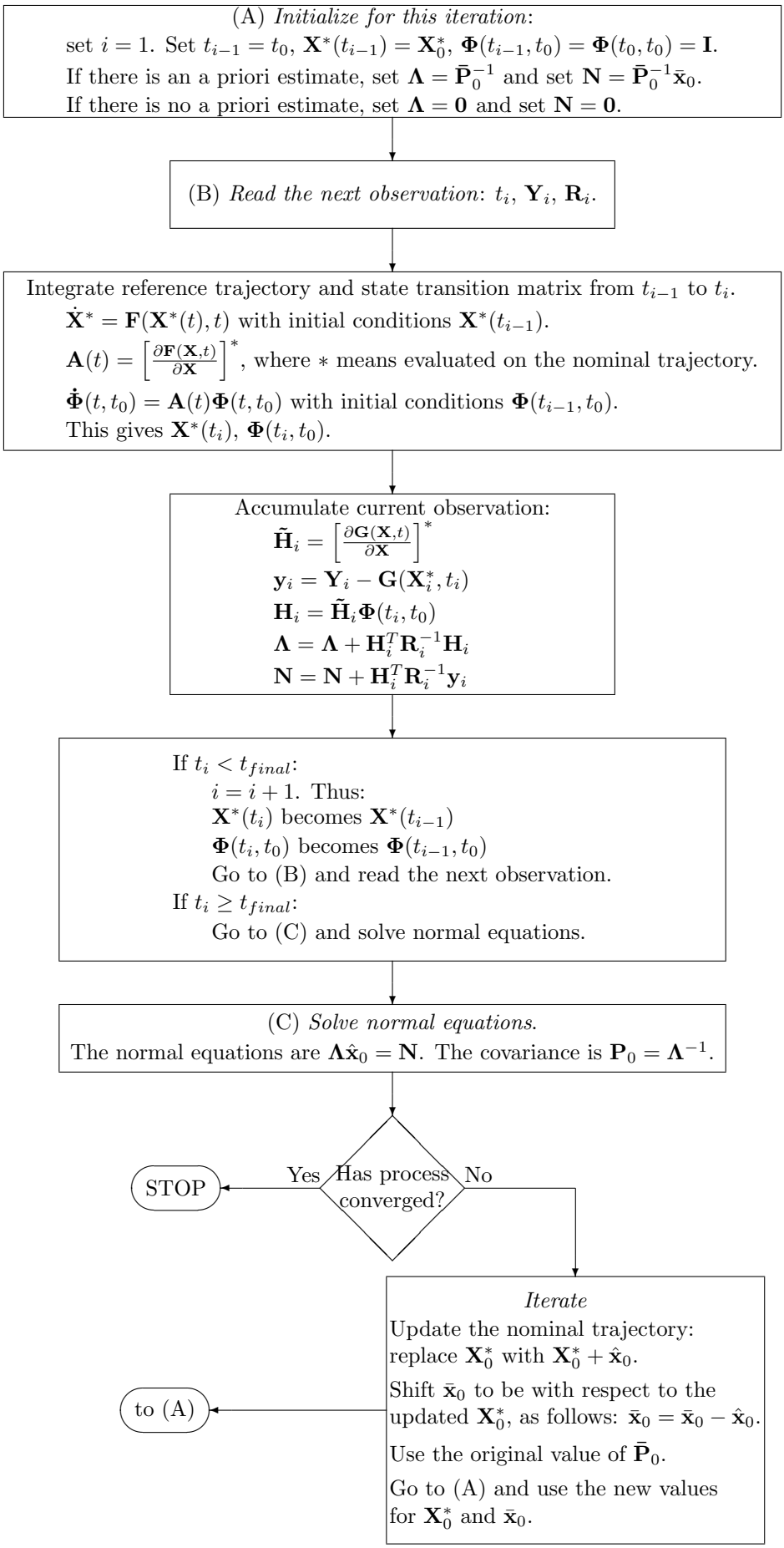

Figure 1.2: Batch processing algorithm flow chart.

Chapter 2

Dynamical model of the satellites of the Saturnian System

2.1 Introduction

In this chapter we derive the dynamical model suitable for the numerical integration of the orbits of the natural satellites of Saturn. The dynamical model is general and can be applied to any system formed by a central, massive planets and its satellite. The force model includes n oblate integrated satellites and m external perturbing planets. We include the variational equations for initial state, gravitational parameters, oblateness and pole parameters. The model is taken from [48], [24] with some adaptations. We implement this dynamical model in a software tool (see Appendix D) which allows to numerically integrate the equations of motion and variational equations. At the end of chapter we give the results of our integration comparing it with the ephemerides delivered by JPL.

2.2 Equations of motion for a system of N point masses

Given an inertial reference systems $O\,[x, y, z]$, consider a system of N point mass particles P_i with masses m_i and coordinates (x_i, y_i, z_i) , $i = 1, ..., N$, mutually interacting (see Figure 2.1).

Indicate the position of P_j with respect to P_i with the vector

$$\mathbf{r}_{ij} = \mathbf{r}_j - \mathbf{r}_i \,. \tag{2.1}$$

Each particle P_i is attracted by the $N - 1$ particles P_j with $j = 1, ..., N$ and $j \neq i$. So, each particle P_j exerts on particle P_i an attractive gravitational force $\mathbf{f}_{ij}$ given by

$$\mathbf{f}_{ij} = G\frac{m_i m_j}{r_{ij}^3}\mathbf{r}_{ij} \,, \qquad i \neq j \,, \tag{2.2}$$

with the direction of the vector $\mathbf{r}_{ij}$, where G indicates the gravitational constant. The previous equation represents the force by which the particle P_j attracts the particle P_i. As required by Newton's third law of motion we have

$$\mathbf{f}_{ji} = -\mathbf{f}_{ij}. \tag{2.3}$$

The total force $\mathbf{F}_{ij}$ acting on particle i due to the $N - 1$ particles is given by the summation

$$\mathbf{F}_{ij} = m_i\frac{d^2\mathbf{r}_i}{dt^2} = G\sum_{\substack{j=1\\ j\neq i}}^{N}\frac{m_i m_j}{r_{ij}^3}\mathbf{r}_{ij} \,, \qquad i = 1, ..., N \,. \tag{2.4}$$

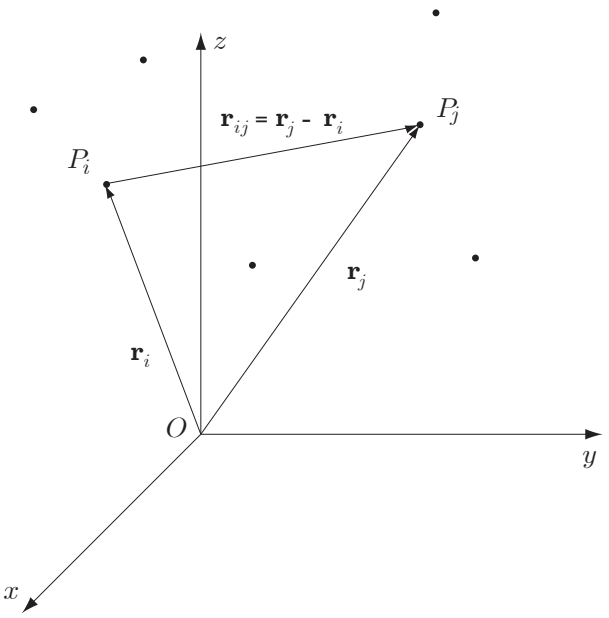

Figure 2.1: System of N point masses

Introducing the gravitational parameter $\mu = Gm$ we can rewrite the previous equation as

$$\mu_i \frac{d^2\mathbf{r}_i}{dt^2} = \sum_{\substack{j=1 \\ j\neq i}}^{N} \frac{\mu_i \mu_j}{r_{ij}^3} \mathbf{r}_{ij} \,, \qquad i = 1, ..., N \,, \tag{2.5}$$

and, simplifing for μ_i we have

$$\frac{d^2\mathbf{r}_i}{dt^2} = \sum_{\substack{j=1 \\ j\neq i}}^{N} \frac{\mu_j}{r_{ij}^3} \mathbf{r}_{ij} \,, \qquad i = 1, ..., N \,, \tag{2.6}$$

which represents the complete set of differential equations necessary to describe the motion of the N point masses.

2.3 Equations of motion for a system of two extended bodies

Consider two extended bodies P_i and P_j. The force of attraction between the two bodies consists of [33] [40] [41]:

1. The force of attraction between the point mass P_i and the point mass P_j.
2. The force of attraction between the non-spherical part of P_i and the point mass P_j.
3. The force of attraction between the non-spherical part of P_j and the point mass P_i.
4. The force of attraction between the non-spherical part of P_i and the non-spherical part of P_j.

The force given in point 1. is accounted for in Section 2.2. The formulation of this section will account for the forces in point 2. and 3. We will ignore the force given in point 4. which is negligible.

2.3.1 Direct acceleration of a point mass P_i due to non sphericity of body P_j

The force of attraction between the non-spherical (oblateness) part of body P_j and the point mass P_i in the body j fixed reference frame is that due to the gravitational potential expressed in spherical

harmonics expansion. In polar coordinates $(r_{ji}, \varphi_i, \lambda_i)$, where r_{ji} is the distance of the point mass P_i from the barycenter of the body P_j, φ_i is the latitude of the point mass P_i and λ_i is the longitude of the point mass P_i, the potential is given by [44] [8]

$$\mathcal{V}_j\left(r_{ji}, \varphi_i, \lambda_i\right) = \frac{\mu_j}{r_{ji}}\left[1 + \sum_{l=2}^{\infty}\sum_{m=0}^{l}\left(\frac{R_e^j}{r_{ji}}\right)^l\left[\mathcal{C}_{lm}^j \cos m\lambda_i + \mathcal{S}_{lm}^j \sin m\lambda_i\right] P_l^m\left(\sin\varphi_i\right)\right], \tag{2.7}$$

where P_l^m are the associated Legendre functions, R_e^j the equatorial radius of the body P_j, $\mu_j = Gm_j$ the gravitational parameter of the body P_j and $\mathcal{C}_{lm}^j$ and $\mathcal{S}_{lm}^j$ the Stokes coefficients of the gravitational potential of body P_j. The transformation from cartesian coordinates to polar coordinates (omitting the index i and j) is given by

$$\begin{cases} r = \sqrt{x^2 + y^2 + z^2} \\ \varphi = \sin^{-1}\left(\frac{z}{r}\right) \\ \lambda = \tan^{-1}\left(\frac{y}{x}\right) \end{cases}, \tag{2.8}$$

and the inverse is

$$\begin{cases} x = r\cos\varphi\cos\lambda \\ y = r\cos\varphi\sin\lambda \\ z = r\sin\varphi \end{cases}. \tag{2.9}$$

The first term of the equation (2.7) is due to the mass of the body P_j and is already included in the equation (2.6) so we considere only the last part of the (2.7) due to the non sphericity of the body that is

$$\mathcal{U}_j\left(r_{ji}, \varphi_i, \lambda_i\right) = \frac{\mu_j}{r_{ji}}\sum_{l=2}^{\infty}\sum_{m=0}^{l}\left(\frac{R_e^j}{r_{ji}}\right)^l\left[\mathcal{C}_{lm}^j \cos m\lambda_i + \mathcal{S}_{lm}^j \sin m\lambda_i\right] P_l^m\left(\sin\varphi_i\right), \tag{2.10}$$

so that

$$\mathcal{V}_j\left(r_{ji}, \varphi_i, \lambda_i\right) = \frac{\mu_j}{r_{ji}} + \mathcal{U}_j\left(r_{ji}, \varphi_i, \lambda_i\right). \tag{2.11}$$

The acceleration of the point mass P_i due to the non-sphericity of the body P_j is obtained computing the gradient of (2.10) with respect to the vector $\mathbf{r}_{ji}$. For simplicity of notation in the following we omit the index i and j so $\mathbf{r}_{ji} \to \mathbf{r}$, $r_{ji} \to r$, $\varphi_i \to \varphi$, $\lambda_i \to \lambda$, $\mu_j \to \mu$, $\mathcal{C}_{lm}^j \to \mathcal{C}_{lm}$, $\mathcal{S}_{lm}^j \to \mathcal{S}_{lm}$, $R_e^j \to R_e$ and $\mathcal{U}_j \to \mathcal{U}$. Since $\mathcal{U}_j$ is expressed in polar coordinates, applying the chain rule we have

$$\frac{\partial \mathcal{U}_j}{\partial \mathbf{r}_{ji}} = \frac{\partial \mathcal{U}}{\partial r}\frac{\partial r}{\partial \mathbf{r}} + \frac{\partial \mathcal{U}}{\partial \varphi}\frac{\partial \varphi}{\partial \mathbf{r}} + \frac{\partial \mathcal{U}}{\partial \lambda}\frac{\partial \lambda}{\partial \mathbf{r}}, \tag{2.12}$$

so the acceleration of the point mass P_i in the extended body P_j fixed reference frame is given by

$$\begin{aligned}\left(\frac{\partial \mathcal{U}_j}{\partial \mathbf{r}_{ji}}\right)^T &= \boldsymbol{\nabla}_{\mathbf{r}_{ji}}\mathcal{U}_j = \left[\frac{\partial \mathcal{U}}{\partial r}\frac{\partial r}{\partial \mathbf{r}} + \frac{\partial \mathcal{U}}{\partial \varphi}\frac{\partial \varphi}{\partial \mathbf{r}} + \frac{\partial \mathcal{U}}{\partial \lambda}\frac{\partial \lambda}{\partial \mathbf{r}}\right]^T \\ &= \left(\frac{\partial r}{\partial \mathbf{r}}\right)^T\frac{\partial \mathcal{U}}{\partial r} + \left(\frac{\partial \varphi}{\partial \mathbf{r}}\right)^T\frac{\partial \mathcal{U}}{\partial \varphi} + \left(\frac{\partial \lambda}{\partial \mathbf{r}}\right)^T\frac{\partial \mathcal{U}}{\partial \lambda}.\end{aligned} \tag{2.13}$$

Computing the involved partials we have

$$\frac{\partial \mathcal{U}}{\partial r} = -\frac{\mu}{r^2}\sum_{l=2}^{\infty}\sum_{m=0}^{l}(l+1)\left(\frac{R_e}{r}\right)^l\left[\mathcal{C}_{lm}\cos m\lambda + \mathcal{S}_{lm}\sin m\lambda\right] P_l^m\left(\sin\varphi\right), \tag{2.14}$$

$$\begin{aligned}\frac{\partial \mathcal{U}}{\partial \varphi} &= \frac{\mu}{r}\sum_{l=2}^{\infty}\sum_{m=0}^{l}\left(\frac{R_e}{r}\right)^l\left[\mathcal{C}_{lm}\cos m\lambda + \mathcal{S}_{lm}\sin m\lambda\right]\frac{\partial}{\partial \varphi}\left[P_l^m\left(\sin\varphi\right)\right] \\ &= \frac{\mu}{r}\sum_{l=2}^{\infty}\sum_{m=0}^{l}\left(\frac{R_e}{r}\right)^l\left\{\begin{array}{c}\left[\mathcal{C}_{lm}\cos m\lambda + \mathcal{S}_{lm}\sin m\lambda\right]\times \\ \left[-m\tan\varphi P_l^m\left(\sin\varphi\right) + P_l^{m+1}\left(\sin\varphi\right)\right]\end{array}\right\},\end{aligned} \tag{2.15}$$

$$\frac{\partial \mathcal{U}}{\partial \lambda} = \frac{\mu}{r} \sum_{l=2}^{\infty} \sum_{m=0}^{l} m \left(\frac{R_e}{r} \right)^l \left[-\mathcal{C}_{lm} \sin m\lambda + \mathcal{S}_{lm} \cos m\lambda \right] P_l^m \left(\sin \varphi \right) . \tag{2.16}$$

For the Jacobian we have from the equations (2.8)

$$\left(\frac{\partial r}{\partial \mathbf{r}} \right)^T = \begin{pmatrix} \frac{\partial r}{\partial x} \\ \frac{\partial r}{\partial y} \\ \frac{\partial r}{\partial z} \end{pmatrix} = \begin{pmatrix} \frac{x}{r} \\ \frac{y}{r} \\ \frac{z}{r} \end{pmatrix} = \frac{\mathbf{r}}{r} . \tag{2.17}$$

$$\frac{\partial \varphi}{\partial x} = \frac{\partial}{\partial x} \sin^{-1} \left(\frac{z}{r} \right) = \frac{1}{\sqrt{1 - \left(\frac{z}{r} \right)^2}} \frac{\partial}{\partial x} \left(\frac{z}{r} \right) = \frac{r}{\sqrt{x^2 + y^2}} \left(-\frac{z}{r^3} x \right) = \frac{1}{\sqrt{x^2 + y^2}} \left(-\frac{z}{r^2} x \right) , \tag{2.18}$$

$$\frac{\partial \varphi}{\partial y} = \frac{\partial}{\partial y} \sin^{-1} \left(\frac{z}{r} \right) = \frac{r}{\sqrt{x^2 + y^2}} \left(-\frac{z}{r^3} y \right) = \frac{1}{\sqrt{x^2 + y^2}} \left(-\frac{z}{r^2} y \right) , \tag{2.19}$$

$$\frac{\partial \varphi}{\partial z} = \frac{\partial}{\partial z} \sin^{-1} \left(\frac{z}{r} \right) = \frac{r}{\sqrt{x^2 + y^2}} \left(\frac{r - z\frac{z}{r}}{r^2} \right) = \frac{1}{\sqrt{x^2 + y^2}} \left(1 - \frac{z}{r^2} z \right) = \frac{\sqrt{x^2 + y^2}}{r^2} , \tag{2.20}$$

and in compact form

$$\left(\frac{\partial \varphi}{\partial \mathbf{r}} \right)^T = \frac{1}{(x^2 + y^2)^{1/2}} \left(\left(\frac{\partial z}{\partial \mathbf{r}} \right)^T - \frac{z}{r^2} \mathbf{r} \right) . \tag{2.21}$$

Finally

$$\frac{\partial \lambda}{\partial x} = \frac{1}{1 + \left(\frac{y}{x} \right)^2} \frac{\partial}{\partial x} \left(\frac{y}{x} \right) = \frac{x^2}{x^2 + y^2} \left(-\frac{y}{x^2} \right) = -\frac{y}{x^2 + y^2} , \tag{2.22}$$

$$\frac{\partial \lambda}{\partial y} = \frac{1}{1 + \left(\frac{y}{x} \right)^2} \frac{\partial}{\partial y} \left(\frac{y}{x} \right) = \frac{x^2}{x^2 + y^2} \left(\frac{x}{x^2} \right) = \frac{x}{x^2 + y^2} , \tag{2.23}$$

$$\frac{\partial \lambda}{\partial z} = 0 , \tag{2.24}$$

and in compact form

$$\begin{aligned} \left(\frac{\partial \lambda}{\partial \mathbf{r}} \right)^T &= \frac{1}{1 + \left(\frac{y}{x} \right)^2} \left[\frac{\partial}{\partial \mathbf{r}} \frac{y}{x} \right] \\ &= \frac{1}{x^2 + y^2} \left[x \left(\frac{\partial y}{\partial \mathbf{r}} \right)^T - y \left(\frac{\partial x}{\partial \mathbf{r}} \right)^T \right] . \end{aligned} \tag{2.25}$$

2.3.2 Rotation from inertial barycentric frame to body fixed frame

The computation of the acceleration of a point mass due to the oblateness of an extended body given in section 2.3.1 is performed in the body fixed reference frame of the extended body. So it is necessary to introduce the rotation matrix from inertial to body fixed reference frame. This matrix is given in this section.

Planetary coordinate systems are defined relatively to their mean axis of rotation. The direction of the north pole is specified by the value of its right ascension α_0 and declination δ_0 whereas the location of the prime meridian is specified by the angle that is measured along the planet's equator in an easterly direction with respect to the planet north pole from the node Q (located at right ascension $90° + \alpha_0$) at the planet's equator on the standard equator to the point B where the prime meridian crosses the

planet's equator (see Figure 2.2). The right ascension of the point Q is $90^\circ + \alpha_0$ and the inclination of the planet's equator to the standard equator is $90^\circ - \delta_0$. Because the prime meridian is assumed to rotate uniformly with the planet, the angle W that defines the direction of the prime meridian, accordingly varies linearly with time. The rotation matrix $\mathbf{C}$ from inertial barycentric frame to body fixed frame is given by

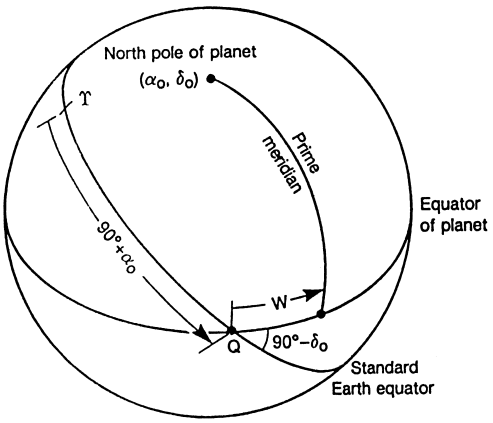

Figure 2.2: Reference system used to define orientation of a planet [53]

$$\mathbf{C}\left(\alpha + 90^\circ, 90^\circ - \delta, w\right) = \mathbf{R}_z\left(W\right)\mathbf{R}_x\left(90^\circ - \delta\right)\mathbf{R}_z\left(\alpha + 90^\circ\right) , \tag{2.26}$$

that is

$$\begin{aligned}
\mathbf{C} &= \begin{pmatrix} \cos W & \sin W & 0 \\ -\sin W & \cos W & 0 \\ 0 & 0 & 1 \end{pmatrix} \begin{pmatrix} 1 & 0 & 0 \\ 0 & \sin\delta & \cos\delta \\ 0 & -\cos\delta & \sin\delta \end{pmatrix} \begin{pmatrix} -\sin\alpha & \cos\alpha & 0 \\ -\cos\alpha & -\sin\alpha & 0 \\ 0 & 0 & 1 \end{pmatrix} \\
&= \begin{pmatrix} -\cos W\sin\alpha - \sin W\cos\alpha\sin\delta & \cos W\cos\alpha - \sin W\sin\alpha\sin\delta & \sin W\cos\delta \\ \sin W\sin\alpha - \cos W\cos\alpha\sin\delta & -\sin W\cos\alpha - \cos W\sin\alpha\sin\delta & \cos W\cos\delta \\ \cos\alpha\cos\delta & \cos\delta\sin\alpha & \sin\delta \end{pmatrix}
\end{aligned} \tag{2.27}$$

where the pole orientation angles α, δ and the direction of the prime meridian W are specified as linear function of time t measured from some epoch t_{p0} [53], so

$$\begin{cases} \alpha &= \alpha_0 + \dot{\alpha}\left(t - t_{p0}\right) , \\ \delta &= \delta_0 + \dot{\delta}\left(t - t_{p0}\right) , \\ W &= W_0 + \dot{W}\left(t - t_{p0}\right) . \end{cases} \tag{2.28}$$

Usually $\dot{\alpha}$ and $\dot{\delta}$ are measured in degrees per Julian Century so the term $(t - t_{p0})$ in the first two equations of (2.28) represents an interval in Julian Century of 36525 day from the standard epoch. On the contrary the term $(t - t_{p0})$ in the equations (2.28) involving W represents a time interval measured in days from the standard epoch.

2.3.3 Indirect acceleration of an extended body P_j due to the acceleration between the non sphericity of body P_j and the point mass P_i

Let $\mathbf{a}_{P_i}(P_j)$ be the acceleration of point mass P_i due to the oblateness part of P_j. As we have seen in section 2.3.1, this acceleration is given from (2.13) that is

$$\mathbf{a}_{P_i}(P_j) = \boldsymbol{\nabla}_{\mathbf{r}_{ji}}\mathcal{U}_j . \tag{2.29}$$

Consider the force of attraction between the oblateness part of body P_j and the point mass P_i. This force produce the acceleration $\mathbf{a}_{P_i}(P_j)$ given by (2.29) and also $\mathbf{a}_{P_j}(P_j)$ that is the acceleration of the extended body P_j due to the force of attraction between the non-spherical part of body P_j and the point mass P_i. Since these two accelerations, $\mathbf{a}_{P_i}(P_j)$ and $\mathbf{a}_{P_j}(P_j)$, are derived from equal and opposite forces, we have

$$\mu_j \mathbf{a}_{P_j}(P_j) = -\mu_i \mathbf{a}_{P_i}(P_j)\,, \tag{2.30}$$

that is

$$\mathbf{a}_{P_j}(P_j) = -\frac{\mu_i}{\mu_j}\mathbf{a}_{P_i}(P_j)\,, \tag{2.31}$$

where μ_j and μ_i are the gravitational parameters of extended body P_j and point mass P_i respectively.

The situation is similar in the case that P_i is extended and P_j is a point mass. Let $\mathbf{a}_{P_j}(P_i)$ be the acceleration of point mass P_j due to the oblateness part of P_i, that is

$$\mathbf{a}_{P_j}(P_i) = \boldsymbol{\nabla}_{\mathbf{r}_{ij}}\mathcal{U}_i\,. \tag{2.32}$$

Consider the force of attraction between the oblateness part of body P_i and the point mass P_j. This force produce the acceleration $\mathbf{a}_{P_j}(P_i)$ given by (2.32) and also $\mathbf{a}_{P_i}(P_i)$ that is the acceleration of the extended body P_i due to the force of attraction between the non-spherical part of body P_i and the point mass P_j. Since these two accelerations, $\mathbf{a}_{P_j}(P_i)$ and $\mathbf{a}_{P_i}(P_i)$, are derived from equal and opposite forces, we have

$$\mu_i \mathbf{a}_{P_i}(P_i) = -\mu_j \mathbf{a}_{P_j}(P_i)\,, \tag{2.33}$$

that is

$$\mathbf{a}_{P_i}(P_i) = -\frac{\mu_j}{\mu_i}\mathbf{a}_{P_j}(P_i)\,. \tag{2.34}$$

By the previous considerations we have that in a system of two extended bodies P_i and P_j:

- the acceleration of an extended body P_j due to the oblateness of body P_j attracting the point mass P_i and due to the oblateness of body P_i attracting the point mass P_j is given by

$$\mathbf{a}_{P_j} = \mathbf{a}_{P_j}(P_i) + \mathbf{a}_{P_j}(P_j) = \mathbf{a}_{P_j}(P_i) - -\frac{\mu_i}{\mu_j}\mathbf{a}_{P_i}(P_j)\,; \tag{2.35}$$

- the acceleration of an extended body P_i due to the oblateness of body P_i attracting the point mass P_j and due to the oblateness of body P_j attracting the point mass P_i is given by

$$\mathbf{a}_{P_i} = \mathbf{a}_{P_i}(P_j) + \mathbf{a}_{P_i}(P_i) = \mathbf{a}_{P_i}(P_j) - \frac{\mu_j}{\mu_i}\mathbf{a}_{P_j}(P_i)\,. \tag{2.36}$$

2.3.4 Equations of motion of two extended bodies

On the basis of that we have previously derived (see sections 2.2, 2.3.1 and 2.3.3) we can derive the equation of motion for two extended bodies P_i and P_j in the framework given at the begin of section 2.3.

The quantity $\mathbf{a}_{P_i}(P_j)$ (see 2.29) represents the acceleration of point mass P_i due to the oblateness part of P_j computed in body P_j fixed reference frame. Now we introduce for convenience the function $\mathbf{G}_{ij}^{BF}$ computed in the body P_j fixed reference frame

$$\mathbf{G}_{ij}^{BF} = \frac{1}{\mu_j}\boldsymbol{\nabla}_{\mathbf{r}_{ji}^{BF}}\mathcal{U}_j = \frac{1}{\mu_j}\mathbf{a}_{P_i}^{BF}(P_j)\,, \tag{2.37}$$

where $\mathbf{a}_{P_i}^{BF}(P_j) = \mathbf{a}_{P_i}(P_j)$ and the index BF is introduced to make clear that the quantity is computed in the body fixed frame. So that

$$\mathbf{a}_{P_i}^{BF}(P_j) = \mu_j \mathbf{G}_{ij}^{BF}\,, \tag{2.38}$$

is just the acceleration of body i due to the asphericity of body j in the body P_j fixed reference frame.

In the inertial reference frame introduced in section 2.2 we can define an analogous quantity $\mathbf{G}_{ij}$, computed just in an inertial reference frame, which is related to $\mathbf{G}_{ij}^{BF}$ by means of

$$\mathbf{G}_{ij} = \mathbf{C}_j^T \mathbf{G}_{ij}^{BF} \,, \tag{2.39}$$

where $\mathbf{C}_j^T$ is the transpose of the rotation matrix $\mathbf{C}_j$ that rotates from inertial barycentric to body j fixed frame (see section 2.3.2). So we have that $\mu_j \mathbf{G}_{ij}$ is the acceleration of body i due to the asphericity of body j in the inertial reference frame, that is

$$\mathbf{a}_{P_i}^I(P_j) = \mathbf{C}_j^T \mathbf{a}_{P_i}^{BF}(P_j) = \mathbf{C}_j^T \mu_j \mathbf{G}_{ij}^{BF} = \mu_j \mathbf{G}_{ij} \,, \tag{2.40}$$

where the index I indicates that $\mathbf{a}_{P_i}^I(P_j)$ is computed in the inertial reference frame.

Putting together the equations (2.6), (2.35) and (2.36) the accelerations acting on bodies P_i and P_j in the inertial reference frame are respectively:

$$\frac{d^2\mathbf{r}_i}{dt^2} = \frac{\mu_j}{r_{ij}^3}\mathbf{r}_{ij} + \mathbf{a}_{P_i}^I(P_j) - \frac{\mu_j}{\mu_i}\mathbf{a}_{P_j}^I(P_i) \,, \tag{2.41}$$

$$\frac{d^2\mathbf{r}_j}{dt^2} = \frac{\mu_i}{r_{ji}^3}\mathbf{r}_{ji} + \mathbf{a}_{P_j}^I(P_i) - \frac{\mu_i}{\mu_j}\mathbf{a}_{P_i}^I(P_j) \,. \tag{2.42}$$

Using the equations (2.38) and (2.40) we have that

$$\mathbf{a}_{P_i}^I(P_j) = \mu_j \mathbf{G}_{ij} \,, \tag{2.43}$$

$$\mathbf{a}_{P_j}^I(P_i) = \mu_i \mathbf{G}_{ji} \,, \tag{2.44}$$

so we can rewrite the equations (2.41) and (2.42) as

$$\frac{d^2\mathbf{r}_i}{dt^2} = \frac{\mu_j}{r_{ij}^3}\mathbf{r}_{ij} + \mu_j \mathbf{G}_{ij} - \mu_j \mathbf{G}_{ji} = \mu_j \left(\frac{\mathbf{r}_{ij}}{r_{ij}^3} + \mathbf{G}_{ij} - \mathbf{G}_{ji} \right) \,, \tag{2.45}$$

$$\frac{d^2\mathbf{r}_j}{dt^2} = \frac{\mu_i}{r_{ji}^3}\mathbf{r}_{ji} + \mu_i \mathbf{G}_{ji} - \mu_i \mathbf{G}_{ij} = \mu_i \left(\frac{\mathbf{r}_{ji}}{r_{ji}^3} + \mathbf{G}_{ji} - \mathbf{G}_{ij} \right) \,, \tag{2.46}$$

which represent the two differential equations necessary to describe the motion of the two extended bodies. We can easily demonstrate that the sum of the forces acting on the system is zero, in fact

$$\begin{aligned} \mu_i \frac{d^2\mathbf{r}_i}{dt^2} + \mu_j \frac{d^2\mathbf{r}_j}{dt^2} &= \mu_i\mu_j \left(\frac{\mathbf{r}_{ij}}{r_{ij}^3} + \mathbf{G}_{ij} - \mathbf{G}_{ji} \right) + \mu_j\mu_i \left(\frac{\mathbf{r}_{ji}}{r_{ji}^3} + \mathbf{G}_{ji} - \mathbf{G}_{ij} \right) \\ &= \mu_i\mu_j \left(\frac{\mathbf{r}_{ij}}{r_{ij}^3} + \frac{\mathbf{r}_{ji}}{r_{ji}^3} + \mathbf{G}_{ij} - \mathbf{G}_{ji} + \mathbf{G}_{ji} - \mathbf{G}_{ij} \right) = \mathbf{0} \,, \end{aligned} \tag{2.47}$$

since $\mathbf{r}_{ij} = -\mathbf{r}_{ji}$. So we can recognize that the terms $\mathbf{H}_{ij} = \mathbf{G}_{ij} - \mathbf{G}_{ji}$ present in (2.45) is antisymmetric that is

$$\mathbf{H}_{ij} = \mathbf{G}_{ij} - \mathbf{G}_{ji} = \mathbf{G}_{ji} - \mathbf{G}_{ij} = -\mathbf{H}_{ji} \,. \tag{2.48}$$

The equations (2.45) and (2.46) can be generalized to a system of N extended bodies by means of summation sign as

$$\frac{d^2\mathbf{r}_i}{dt^2} = \sum_{\substack{j=1 \\ j\neq i}}^{N} \mu_j \left(\frac{\mathbf{r}_{ij}}{r_{ij}^3} + \mathbf{G}_{ij} - \mathbf{G}_{ji} \right) \,, \qquad i = 1, ..., N \,, \tag{2.49}$$

where the first term is the the interaction between the point masses (see equation (2.6)) and the last two terms are due to the asphericity of the bodies. Equation (2.49) represents the complete set of differential equations of motion necessary to describe the motion of the system of N extended bodies [48], [24].

2.3.5 Case of an oblate body

In the case of an oblate body we have rotational symmetry and so there is no dependency of the potential on the longitude. In this case the rotation matrix $\mathbf{C}$ given by (2.27) can be simplified because $W = 0$ so

$$\mathbf{C}_{obl} = \begin{pmatrix} -\sin\alpha & \cos\alpha & 0 \\ -\cos\alpha\sin\delta & -\sin\alpha\sin\delta & \cos\delta \\ \cos\alpha\cos\delta & \cos\delta\sin\alpha & \sin\delta \end{pmatrix} . \tag{2.50}$$

Also the expression of the potential and its partials given in section 2.3.1 can be simplified. Setting

$$J_n = -\mathcal{C}_{n0} , \tag{2.51}$$

and remembering that in this case $m = 0$ and $\mathcal{U}_{obl} = \mathcal{U}_{obl}(r, \varphi)$ we can write

$$\begin{aligned} \mathcal{U}_{obl}(r,\varphi) &= \frac{\mu}{r}\sum_{l=2}^{\infty}\left(\frac{R_e}{r}\right)^l \mathcal{C}_{l0} P_l^0(\sin\varphi) \\ &= -\frac{\mu}{r}\sum_{l=2}^{\infty}\left(\frac{R_e}{r}\right)^l J_l P_l^0(\sin\varphi) , \end{aligned} \tag{2.52}$$

$$\begin{aligned} \left(\frac{\partial \mathcal{U}_{obl}}{\partial \mathbf{r}}\right)^T &= \boldsymbol{\nabla}_{\mathbf{r}}\mathcal{U}_{obl} = \left[\frac{\partial \mathcal{U}_{obl}}{\partial r}\frac{\partial r}{\partial \mathbf{r}} + \frac{\partial \mathcal{U}_{obl}}{\partial \varphi}\frac{\partial \varphi}{\partial \mathbf{r}}\right]^T \\ &= \left(\frac{\partial r}{\partial \mathbf{r}}\right)^T \frac{\partial \mathcal{U}_{obl}}{\partial r} + \left(\frac{\partial \varphi}{\partial \mathbf{r}}\right)^T \frac{\partial \mathcal{U}_{obl}}{\partial \varphi} , \end{aligned} \tag{2.53}$$

$$\begin{aligned} \frac{\partial \mathcal{U}_{obl}}{\partial r} &= -\frac{\mu}{r^2}\sum_{l=2}^{\infty}(l+1)\left(\frac{R_e}{r}\right)^l \mathcal{C}_{l0} P_l^0(\sin\varphi) \\ &= \frac{\mu}{r^2}\sum_{l=2}^{\infty}(l+1)\left(\frac{R_e}{r}\right)^l J_l P_l^0(\sin\varphi) , \end{aligned} \tag{2.54}$$

$$\begin{aligned} \frac{\partial \mathcal{U}_{obl}}{\partial \varphi} &= \frac{\mu}{r}\sum_{l=2}^{\infty}\left(\frac{R_e}{r}\right)^l \mathcal{C}_{l0} P_l^1(\sin\varphi) \\ &= -\frac{\mu}{r}\sum_{l=2}^{\infty}\left(\frac{R_e}{r}\right)^l J_l P_l^1(\sin\varphi) , \end{aligned} \tag{2.55}$$

$$\frac{\partial \mathcal{U}_{obl}}{\partial \lambda} = 0 . \tag{2.56}$$

For the Jacobian of the coordinates we have the same expression of the general case given in Section 2.3.1 except for the the element $\left(\frac{\partial \lambda}{\partial \mathbf{r}}\right)^T$ that becomes

$$\left(\frac{\partial \lambda}{\partial \mathbf{r}}\right)^T = \mathbf{0} . \tag{2.57}$$

2.4 Equations of motion of a system of extended bodies

Given a system of $n + m + 1$ bodies we adopt the following convention concerning the enumeration of the bodies [48] [24]:

1. body 0 is the non-spherical primary;

2. bodies from 1 to n are the oblate satellites;
3. bodies from $n+1$ to $n+m$ are the point masses planets acting as perturbers.

If we choose a reference frame centered in the barycenter of a system formed by the primary and its satellites, in the equations of motion of one of the satellites there will be 3 terms:

1. a term that describes the acceleration due to the other n extended bodies (satellites) plus the primary;
2. a term describing the acceleration due to the m point mass planets (perturbers);
3. a term describing the acceleration of the barycenter due to the m point mass planets (perturbers).

In an inertial frame the force $\mathbf{F}_{ij}$ acting on body i due to body j is given by (see equation (2.45))

$$\mathbf{F}_{ij} = \mu_i \frac{d^2\mathbf{r}_i}{dt^2} = \mu_i\mu_j \left(\frac{\mathbf{r}_j - \mathbf{r}_i}{|\mathbf{r}_j - \mathbf{r}_i|^3} + \mathbf{G}_{ij} - \mathbf{G}_{ji} \right) , \tag{2.58}$$

where i and j ranging from 0 to $n+m$, $\mathbf{r}$ represents the position vector of the body and the functions $\mu_j\mathbf{G}_{ij}$ and $\mu_j\mathbf{G}_{ji}$ are the accelerations due to the non-sphericity of the bodies (see section 2.3.4). More precisely the quantity $\mu_j\mathbf{G}_{ij}$ is the acceleration of body i due to the oblateness of body j.

The equations of motion in an inertial system are derived from (2.49) that is

$$\frac{d^2\mathbf{r}_i}{dt^2} = \sum_{\substack{j=0 \\ j\neq i}}^{n+m} \mu_j \left(\frac{\mathbf{r}_j - \mathbf{r}_i}{|\mathbf{r}_j - \mathbf{r}_i|^3} + \mathbf{G}_{ij} - \mathbf{G}_{ji} \right) , \qquad i = 0, ..., n+m. \tag{2.59}$$

If we set, as a notational convenience

$$\mathbf{Q}_{ji} = \frac{\mathbf{r}_j - \mathbf{r}_i}{|\mathbf{r}_j - \mathbf{r}_i|^3} + \mathbf{G}_{ij} - \mathbf{G}_{ji} , \qquad i \neq j , \tag{2.60}$$

$$\mathbf{Q}_{ii} = \mathbf{0} , \tag{2.61}$$

the equations of motion (2.59) become

$$\frac{d^2\mathbf{r}_i}{dt^2} = \sum_{\substack{j=0 \\ j\neq i}}^{n+m} \mu_j \mathbf{Q}_{ji} , \qquad i = 0, ..., n+m . \tag{2.62}$$

The equations of motion (2.62) can be referred to the center of mass of the system $\mathbf{r}_B$ as defined by

$$\mathbf{r}_B = \frac{1}{\mu_B} \sum_{i=0}^{n} \mu_i \mathbf{r}_i , \tag{2.63}$$

where μ_B is the total GM for the planetary system that is

$$\mu_B = \sum_{i=0}^{n} \mu_i . \tag{2.64}$$

The inertial acceleration of the center of mass is found by differentiating equation (2.63) and substituting from (2.62) so that

$$\frac{d^2\mathbf{r}_B}{dt^2} = \frac{1}{\mu_B} \sum_{i=0}^{n} \mu_i \frac{d^2\mathbf{r}_i}{dt^2} = \frac{1}{\mu_B} \sum_{i=0}^{n} \sum_{j=0}^{n+m} \mu_i\mu_j \mathbf{Q}_{ji} , \tag{2.65}$$

and, since

$$\sum_{i=0}^{n} \sum_{j=0}^{n} \mu_i\mu_j \mathbf{Q}_{ji} = \mathbf{0} , \qquad \text{and} \qquad \mathbf{Q}_{ji} = -\mathbf{Q}_{ij} , \tag{2.66}$$

that is the sum of the internal forces is zero, the (2.65) reduces to

$$\frac{d^2\mathbf{r}_B}{dt^2} = \frac{1}{\mu_B}\sum_{i=0}^{n}\sum_{j=n+1}^{n+m}\mu_i\mu_j\mathbf{Q}_{ji}\,. \tag{2.67}$$

The positions $\mathbf{R}_i$ of the bodies relative to the center of mass are

$$\mathbf{R}_i = \mathbf{r}_i - \mathbf{r}_B\,, \qquad i = 0, ..., n+m\,. \tag{2.68}$$

To obtain the equations in the barycenter of the first $n+1$ bodies (the primary and its satellites) we have to differentiate the previous equation (2.68) so

$$\frac{d^2\mathbf{R}_i}{dt^2} = \frac{d^2\mathbf{r}_i}{dt^2} - \frac{d^2\mathbf{r}_B}{dt^2}\,, \tag{2.69}$$

and using (2.62) and (2.65) we obtain

$$\frac{d^2\mathbf{R}_i}{dt^2} = \sum_{\substack{j=0\\ j\neq i}}^{n+m}\mu_j\mathbf{Q}_{ji} - \frac{1}{\mu_B}\sum_{i=0}^{n}\sum_{j=n+1}^{n+m}\mu_i\mu_j\mathbf{Q}_{ji}\,, \qquad i = 1, ..., n\,. \tag{2.70}$$

Isolating the terms pertaining the primary and its satellites we can write the previous equation (2.70) as

$$\frac{d^2\mathbf{R}_i}{dt^2} = \sum_{\substack{j=0\\ j\neq i}}^{n}\mu_j\mathbf{Q}_{ji} + \sum_{\substack{j=n+1\\ j\neq i}}^{n+m}\mu_j\mathbf{Q}_{ji} - \frac{1}{\mu_B}\sum_{i=0}^{n}\sum_{\substack{j=n+1\\ j\neq i}}^{n+m}\mu_i\mu_j\mathbf{Q}_{ji}\,, \qquad i = 1, ..., n\,, \tag{2.71}$$

that is, in a more compact form [48], [24]

$$\ddot{\mathbf{R}}_i = \sum_{\substack{j=0\\ j\neq i}}^{n}\mu_j\mathbf{Q}_{ji} + \Delta\ddot{\mathbf{R}}_i + \ddot{\mathbf{R}}_B\,, \qquad i = 1, ..., n\,, \tag{2.72}$$

where

$$\mathbf{Q}_{ji} = \frac{\mathbf{R}_j - \mathbf{R}_i}{|\mathbf{R}_j - \mathbf{R}_i|^3} + \mathbf{G}_{ij} - \mathbf{G}_{ji}\,, \qquad \begin{cases} j = 0, ..., n+m \\ i = 0, ..., n \end{cases}\,, \tag{2.73}$$

$$\mathbf{Q}_{ii} = \mathbf{0}\,, \tag{2.74}$$

$$\Delta\ddot{\mathbf{R}}_i = \sum_{j=n+1}^{n+m}\mu_j\mathbf{Q}_{ji}\,, \qquad i = 0, ..., n\,, \tag{2.75}$$

$$\ddot{\mathbf{R}}_B = -\frac{1}{\mu_B}\sum_{k=0}^{n}\sum_{\substack{j=n+1\\ j\neq k}}^{n+m}\mu_k\mu_j\mathbf{Q}_{jk} = -\frac{1}{\mu_B}\sum_{k=0}^{n}\mu_k\Delta\ddot{\mathbf{R}}_k\,, \tag{2.76}$$

The term $\Delta\ddot{\mathbf{R}}_i$ represents the acceleration of the i^{th} body due to the m external perturbing bodies and $\ddot{\mathbf{R}}_B$ is the acceleration of the barycenter due to the m perturbing bodies. For the limiting case in which the m perturbing bodies are so far away that

$$\frac{\mathbf{R}_j - \mathbf{R}_i}{|\mathbf{R}_j - \mathbf{R}_i|^3} \to \frac{\mathbf{R}_j}{|\mathbf{R}_j|^3}\,, \qquad (i \leq n, j > n) \tag{2.77}$$

than $\Delta\ddot{\mathbf{R}}_i + \ddot{\mathbf{R}}_B \to \mathbf{0}$. Note that equations of motion for the planet are not included in (2.72). Instead, from the center of mass relation

$$\sum_{i=0}^{n}\mu_i\mathbf{R}_i = \mathbf{0}\,, \tag{2.78}$$

the position of the primary $\mathbf{R}_0$ is a dependent quantity, that is

$$\mathbf{R}_0 = -\frac{1}{\mu_0}\sum_{i=1}^{n}\mu_i\mathbf{R}_i\,. \tag{2.79}$$

In practice, the system $GM = \mu_B$ is taken to be fundamental, and μ_0, the gravitational parameter of planet, is computed from it by means

$$\mu_0 = \mu_B - \sum_{i=1}^{n}\mu_i\,. \tag{2.80}$$

The equations of motion (2.72) were first derived by Peters in 1971 [48]. Unlike Peters who computes the gravitational potential of extended bodies in cartesian coordinates, we prefer to compute it using a classical spherical harmonic expansion. Jacobson in 1999 [24] improved Peters' formulations. First of all, for the computation of the gravitational potential of extended bodies, Jacobson uses Pine's method [49] for the extend primary and the MacCullagh expansion [5] for the extended satellites. Then he added three new terms to the equations of motion which regard the contribution of the planetary rings, the planetary tides raised by the satellites and the effects of general relativity. The addition of these effects was needed as a consequence of the study of the effects of several perturbations acting on the natural satellites of Saturn carried out by Tragesser and Longuski in 1997 [63] in order to achieve the ephemeris accuracy required by the *Cassini* mission. Since we here use ground-based observations, the effects introduced by Jacobson are not necessary given the accuracy of this data type, which is on the order of $0''.08$ (in the best case) correspondig to about 500 km at Saturn.

2.4.1 Computation of $\mathbf{G}_{ij}$

For clarity we give here the algorithm for the computation of the functions $\mathbf{G}_{ij}$. As we have told in section 2.3.4 $\mu_j\mathbf{G}_{ij}$ is the acceleration of body i due to the asphericity of body j in the inertial reference frame and therefore also in the sytem centered in the barycenter of the firsts $n+1$ bodies. To compute the functions $\mathbf{G}_{ij}$ we have to:

1. rotate the vector $\mathbf{R}_i - \mathbf{R}_j$ from the inertial barycentric into body j fixed reference frame corotating with body j via the rotation matrix $\mathbf{C}_j$ (see section 2.3.2 equation (2.27))
$$\mathbf{r}_{ji}^{BF} = \mathbf{C}_j\left(\mathbf{R}_i - \mathbf{R}_j\right)\,; \tag{2.81}$$
2. compute the acceleration of body i due to the asphericity of body j in the body j fixed reference frame as described in section 2.3.1 and 2.3.4
$$\mathbf{G}_{ij}^{BF} = \frac{1}{\mu_j}\left(\frac{\partial\mathcal{U}_j}{\partial\mathbf{r}_{ji}^{BF}}\right)^T\,; \tag{2.82}$$
3. rotate the resulting function $\mathbf{G}_{ij}^{BF}$ from body j fixed frame to barycentric frame via (see section 2.3.4)
$$\mathbf{G}_{ij} = \mathbf{C}_j^T\mathbf{G}_{ij}^{BF}\,. \tag{2.83}$$

2.5 Structure of the matrix A and Φ

Following the scheme outlined in Chapter 1, the state vector $\mathbf{X}$ is formed by all the variables and the constant parameters which are required to describe the time variation of our dynamical system: from this definition the state vector, of dimension N can be represented as [61]

$$\mathbf{X}(t) = \begin{pmatrix}\mathbf{X}_{ss}\\ \boldsymbol{\alpha}\end{pmatrix}, \tag{2.84}$$

where $\mathbf{X}_{ss}$ is the state of natural satellites with n_{ss} components and $\boldsymbol{\alpha} = \mathbf{p} + \mathbf{q}$ represents the $s = p + q$ parameters respectively of the dynamical and observation model. We remark that $N = n_{ss} + p + q$. As we have seen in Chapter 1, to solve the linearized problem and compute the solution, it is necessary to compute the state transition matrix $\boldsymbol{\Phi}$**:** this matrix is computed by numerical integration of the system of differential equations

$$\dot{\boldsymbol{\Phi}}(t, t_0) = \mathbf{A}(t)\,\boldsymbol{\Phi}(t, t_0)\ , \tag{2.85}$$

with the initial conditions

$$\boldsymbol{\Phi}(t_0, t_0) = \mathbf{I}\,, \tag{2.86}$$

where the matrix $\mathbf{A}$ is given by

$$\mathbf{A}(t) = \frac{\partial \mathbf{F}}{\partial \mathbf{X}}(\mathbf{X}^*, t)\ , \tag{2.87}$$

that is, the partials of $\mathbf{F}$ with respect to the state vector $\mathbf{X}$ are computed on the nominal trajectory defined by the nominal state vector $\mathbf{X}^*$. We assume that the dimension of the state vector $\mathbf{X}$ be N. Since the dimension of the state transition matrix is $N \times N$, in theory it should be integrated integrate N^2 differential equations; however the matrix $\mathbf{A}$ is a pseudo-sparse matrix that is it has not all the elements different from zero. It is so possible to reduce the number of equations that have to be integrated.

Before all we can immediately reduce the dimension of the original state vector $\mathbf{X}$ from N to $N - q$ eliminating the kinematic parameters $\mathbf{q}$ linked only to the observation model: this simplification is justified by the fact that the differential equations to which the state transition matrix satisfies are dependent only by the dynamical model represented by $\mathbf{F}$ (as it is possible to deduce from (2.85) and from (2.87)) and they are uncorrelated from the observation model.

Given the state vector of dimension $N - q = n_{ss} + p$

$$\mathbf{X}(t) = \begin{pmatrix} \mathbf{X}_{ss} \\ \mathbf{p} \end{pmatrix}\ , \tag{2.88}$$

where $\mathbf{X}_{ss}$ is the state of natural satellites with n_{ss} components while $\mathbf{p}$ represents the set of dynamical parameters that enter in the force model and such that $\dot{\mathbf{p}} = 0$. If we consider n satellites the state vector will be

$$\mathbf{X}_{ss} = \begin{pmatrix} \mathbf{r}_1 \\ \vdots \\ \mathbf{r}_n \\ \mathbf{v}_1 \\ \vdots \\ \mathbf{v}_n \end{pmatrix}\ , \tag{2.89}$$

where $\mathbf{r}_i$ and $\mathbf{v}_i$ represent the position and velocity vectors of the i-th satellite respectively. The differential equations of the state are

$$\dot{\mathbf{X}}(t) = \mathbf{F}(\mathbf{X}(t), t) = \begin{pmatrix} \dot{\mathbf{X}}_{ss} \\ \mathbf{0} \end{pmatrix}\ , \qquad \mathbf{X}(t_0) = \mathbf{X}_0\,, \tag{2.90}$$

where $\dot{\mathbf{X}}_{ss}$ is

$$\dot{\mathbf{X}}_{ss} = \begin{pmatrix} \mathbf{v}_1 \\ \vdots \\ \mathbf{v}_n \\ \mathbf{a}_1 \\ \vdots \\ \mathbf{a}_n \end{pmatrix}\ , \tag{2.91}$$

and $\mathbf{a}_i$ is the gravitational acceleration acting on the i-th satellite. The equations (2.90) represent a system of N non linear differential equations of the first order (N is the total number of the components of the state vector $\mathbf{X}$) containing the $n_{ss} = 6n$ components of the equations (2.91). The matrix $\mathbf{A}$, explicitly, is

$$\mathbf{A} = \begin{pmatrix} \frac{\partial \mathbf{v}_1}{\partial \mathbf{r}_1} & \frac{\partial \mathbf{v}_1}{\partial \mathbf{r}_2} & \cdots & \frac{\partial \mathbf{v}_1}{\partial \mathbf{r}_n} & \frac{\partial \mathbf{v}_1}{\partial \mathbf{v}_1} & \frac{\partial \mathbf{v}_1}{\partial \mathbf{v}_2} & \cdots & \frac{\partial \mathbf{v}_1}{\partial \mathbf{v}_n} & \frac{\partial \mathbf{v}_1}{\partial \mathbf{p}} \\ \frac{\partial \mathbf{v}_2}{\partial \mathbf{r}_1} & \frac{\partial \mathbf{v}_2}{\partial \mathbf{r}_2} & \cdots & \frac{\partial \mathbf{v}_2}{\partial \mathbf{r}_n} & \frac{\partial \mathbf{v}_2}{\partial \mathbf{v}_1} & \frac{\partial \mathbf{v}_2}{\partial \mathbf{v}_2} & \cdots & \frac{\partial \mathbf{v}_1}{\partial \mathbf{v}_n} & \frac{\partial \mathbf{v}_2}{\partial \mathbf{p}} \\ \vdots & \vdots & \ddots & \vdots & \vdots & \vdots & \ddots & \vdots & \vdots \\ \frac{\partial \mathbf{v}_n}{\partial \mathbf{r}_1} & \frac{\partial \mathbf{v}_n}{\partial \mathbf{r}_2} & \cdots & \frac{\partial \mathbf{v}_n}{\partial \mathbf{r}_n} & \frac{\partial \mathbf{v}_n}{\partial \mathbf{v}_1} & \frac{\partial \mathbf{v}_n}{\partial \mathbf{v}_2} & \cdots & \frac{\partial \mathbf{v}_n}{\partial \mathbf{v}_n} & \frac{\partial \mathbf{v}_n}{\partial \mathbf{p}} \\ \frac{\partial \mathbf{a}_1}{\partial \mathbf{r}_1} & \frac{\partial \mathbf{a}_1}{\partial \mathbf{r}_2} & \cdots & \frac{\partial \mathbf{a}_1}{\partial \mathbf{r}_n} & \frac{\partial \mathbf{a}_1}{\partial \mathbf{v}_1} & \frac{\partial \mathbf{a}_1}{\partial \mathbf{v}_2} & \cdots & \frac{\partial \mathbf{a}_1}{\partial \mathbf{v}_n} & \frac{\partial \mathbf{a}_1}{\partial \mathbf{p}} \\ \frac{\partial \mathbf{a}_2}{\partial \mathbf{r}_1} & \frac{\partial \mathbf{a}_2}{\partial \mathbf{r}_2} & \cdots & \frac{\partial \mathbf{a}_2}{\partial \mathbf{r}_n} & \frac{\partial \mathbf{a}_2}{\partial \mathbf{v}_1} & \frac{\partial \mathbf{a}_2}{\partial \mathbf{v}_2} & \cdots & \frac{\partial \mathbf{a}_2}{\partial \mathbf{v}_n} & \frac{\partial \mathbf{a}_2}{\partial \mathbf{p}} \\ \vdots & \vdots & \ddots & \vdots & \vdots & \vdots & \ddots & \vdots & \vdots \\ \frac{\partial \mathbf{a}_n}{\partial \mathbf{r}_1} & \frac{\partial \mathbf{a}_n}{\partial \mathbf{r}_2} & \cdots & \frac{\partial \mathbf{a}_n}{\partial \mathbf{r}_n} & \frac{\partial \mathbf{a}_n}{\partial \mathbf{v}_1} & \frac{\partial \mathbf{a}_n}{\partial \mathbf{v}_2} & \cdots & \frac{\partial \mathbf{a}_n}{\partial \mathbf{v}_n} & \frac{\partial \mathbf{a}_n}{\partial \mathbf{p}} \\ \mathbf{0}_{p\times 3} & \mathbf{0}_{p\times 3} & \cdots & \mathbf{0}_{p\times 3} & \mathbf{0}_{p\times 3} & \mathbf{0}_{p\times 3} & \cdots & \mathbf{0}_{p\times 3} & \mathbf{0}_{p\times p} \end{pmatrix}, \tag{2.92}$$

or in compact form

$$\mathbf{A} = \begin{pmatrix} \mathbf{A}_{11} & \mathbf{A}_{12} & \mathbf{A}_{13} \\ \mathbf{A}_{21} & \mathbf{A}_{22} & \mathbf{A}_{23} \\ \mathbf{0}_{p\times 3n} & \mathbf{0}_{p\times 3n} & \mathbf{0}_{p\times p} \end{pmatrix}, \tag{2.93}$$

where

$$\mathbf{A}_{11} = \begin{pmatrix} \frac{\partial \mathbf{v}_1}{\partial \mathbf{r}_1} & \frac{\partial \mathbf{v}_1}{\partial \mathbf{r}_2} & \cdots & \frac{\partial \mathbf{v}_1}{\partial \mathbf{r}_n} \\ \frac{\partial \mathbf{v}_2}{\partial \mathbf{r}_1} & \frac{\partial \mathbf{v}_2}{\partial \mathbf{r}_2} & \cdots & \frac{\partial \mathbf{v}_2}{\partial \mathbf{r}_n} \\ \vdots & \vdots & \ddots & \vdots \\ \frac{\partial \mathbf{v}_n}{\partial \mathbf{r}_1} & \frac{\partial \mathbf{v}_n}{\partial \mathbf{r}_2} & \cdots & \frac{\partial \mathbf{v}_n}{\partial \mathbf{r}_n} \end{pmatrix}, \quad \mathbf{A}_{12} = \begin{pmatrix} \frac{\partial \mathbf{v}_1}{\partial \mathbf{v}_1} & \frac{\partial \mathbf{v}_1}{\partial \mathbf{v}_2} & \cdots & \frac{\partial \mathbf{v}_1}{\partial \mathbf{v}_n} \\ \frac{\partial \mathbf{v}_2}{\partial \mathbf{v}_1} & \frac{\partial \mathbf{v}_2}{\partial \mathbf{v}_2} & \cdots & \frac{\partial \mathbf{v}_1}{\partial \mathbf{v}_n} \\ \vdots & \vdots & \ddots & \vdots \\ \frac{\partial \mathbf{v}_n}{\partial \mathbf{v}_1} & \frac{\partial \mathbf{v}_n}{\partial \mathbf{v}_2} & \cdots & \frac{\partial \mathbf{v}_n}{\partial \mathbf{v}_n} \end{pmatrix}, \tag{2.94}$$

$$\mathbf{A}_{21} = \begin{pmatrix} \frac{\partial \mathbf{a}_1}{\partial \mathbf{r}_1} & \frac{\partial \mathbf{a}_1}{\partial \mathbf{r}_2} & \cdots & \frac{\partial \mathbf{a}_1}{\partial \mathbf{r}_n} \\ \frac{\partial \mathbf{a}_2}{\partial \mathbf{r}_1} & \frac{\partial \mathbf{a}_2}{\partial \mathbf{r}_2} & \cdots & \frac{\partial \mathbf{a}_2}{\partial \mathbf{r}_n} \\ \vdots & \vdots & \ddots & \vdots \\ \frac{\partial \mathbf{a}_n}{\partial \mathbf{r}_1} & \frac{\partial \mathbf{a}_n}{\partial \mathbf{r}_2} & \cdots & \frac{\partial \mathbf{a}_n}{\partial \mathbf{r}_n} \end{pmatrix}, \quad \mathbf{A}_{22} = \begin{pmatrix} \frac{\partial \mathbf{a}_1}{\partial \mathbf{v}_1} & \frac{\partial \mathbf{a}_1}{\partial \mathbf{v}_2} & \cdots & \frac{\partial \mathbf{a}_1}{\partial \mathbf{v}_n} \\ \frac{\partial \mathbf{a}_2}{\partial \mathbf{v}_1} & \frac{\partial \mathbf{a}_2}{\partial \mathbf{v}_2} & \cdots & \frac{\partial \mathbf{a}_2}{\partial \mathbf{v}_n} \\ \vdots & \vdots & \ddots & \vdots \\ \frac{\partial \mathbf{a}_n}{\partial \mathbf{v}_1} & \frac{\partial \mathbf{a}_n}{\partial \mathbf{v}_2} & \cdots & \frac{\partial \mathbf{a}_n}{\partial \mathbf{v}_n} \end{pmatrix}, \tag{2.95}$$

$$\mathbf{A}_{13} = \begin{pmatrix} \frac{\partial \mathbf{v}_1}{\partial \mathbf{p}} \\ \frac{\partial \mathbf{v}_2}{\partial \mathbf{p}} \\ \vdots \\ \frac{\partial \mathbf{v}_n}{\partial \mathbf{p}} \end{pmatrix}, \quad \mathbf{A}_{23} = \begin{pmatrix} \frac{\partial \mathbf{a}_1}{\partial \mathbf{p}} \\ \frac{\partial \mathbf{a}_2}{\partial \mathbf{p}} \\ \vdots \\ \frac{\partial \mathbf{a}_n}{\partial \mathbf{p}} \end{pmatrix}. \tag{2.96}$$

Since

$$\frac{\partial \mathbf{v}_i}{\partial \mathbf{r}_j} = \mathbf{0}_{3n\times 3n}\,, \qquad \frac{\partial \mathbf{v}_i}{\partial \mathbf{p}} = \mathbf{0}_{3n\times p}\,, \qquad i,j = 1,..,n\,, \tag{2.97}$$

and

$$\mathbf{A}_{12} = \begin{pmatrix} \frac{\partial \mathbf{v}_1}{\partial \mathbf{v}_1} & \frac{\partial \mathbf{v}_1}{\partial \mathbf{v}_2} & \cdots & \frac{\partial \mathbf{v}_1}{\partial \mathbf{v}_n} \\ \frac{\partial \mathbf{v}_2}{\partial \mathbf{v}_1} & \frac{\partial \mathbf{v}_2}{\partial \mathbf{v}_2} & \cdots & \frac{\partial \mathbf{v}_1}{\partial \mathbf{v}_n} \\ \vdots & \vdots & \ddots & \vdots \\ \frac{\partial \mathbf{v}_n}{\partial \mathbf{v}_1} & \frac{\partial \mathbf{v}_n}{\partial \mathbf{v}_2} & \cdots & \frac{\partial \mathbf{v}_n}{\partial \mathbf{v}_n} \end{pmatrix} = \begin{pmatrix} \mathbf{I}_{3\times 3} & \mathbf{0}_{3\times 3} & \cdots & \mathbf{0}_{3\times 3} \\ \mathbf{0}_{3\times 3} & \mathbf{I}_{3\times 3} & \cdots & \mathbf{0}_{3\times 3} \\ \vdots & \vdots & \ddots & \vdots \\ \mathbf{0}_{3\times 3} & \mathbf{0}_{3\times 3} & \cdots & \mathbf{I}_{3\times 3} \end{pmatrix} = \mathbf{I}_{3n\times 3n}\,, \tag{2.98}$$

the matrix $\mathbf{A}$ can be simplified as

$$\mathbf{A} = \begin{pmatrix} \mathbf{0}_{3n\times 3n} & \mathbf{I}_{3n\times 3n} & \mathbf{0}_{3n\times p} \\ \mathbf{A}_{21} & \mathbf{A}_{22} & \mathbf{A}_{23} \\ \mathbf{0}_{p\times 3n} & \mathbf{0}_{p\times 3n} & \mathbf{0}_{p\times p} \end{pmatrix}, \tag{2.99}$$

where $\mathbf{A}_{21}, \mathbf{A}_{22}$ are $[3n \times 3n]$ matrices and $\mathbf{A}_{23}$ is a $[3n \times p]$ matrix. We remark that the partials $\frac{\partial \mathbf{v}_i}{\partial \mathbf{p}}$ are zero because $\mathbf{v}_i$ are not explicitly dependent from parameters $\mathbf{p}$.

So, assuming for $\mathbf{\Phi}$ a general structure as

$$\mathbf{\Phi} = \frac{\partial \mathbf{X}}{\partial \mathbf{X}_0} = \begin{pmatrix} \mathbf{\Phi}_{11} & \mathbf{\Phi}_{12} & \mathbf{\Phi}_{13} \\ \mathbf{\Phi}_{21} & \mathbf{\Phi}_{22} & \mathbf{\Phi}_{23} \\ \mathbf{\Phi}_{31} & \mathbf{\Phi}_{32} & \mathbf{\Phi}_{33} \end{pmatrix}, \tag{2.100}$$

where

$$\mathbf{\Phi}_{11} = \begin{pmatrix} \frac{\partial \mathbf{r}_1}{\partial \mathbf{r}_{01}} & \frac{\partial \mathbf{r}_1}{\partial \mathbf{r}_{02}} & \cdots & \frac{\partial \mathbf{r}_1}{\partial \mathbf{r}_{0n}} \\ \frac{\partial \mathbf{r}_2}{\partial \mathbf{r}_{01}} & \frac{\partial \mathbf{r}_2}{\partial \mathbf{r}_{02}} & \cdots & \frac{\partial \mathbf{r}_2}{\partial \mathbf{r}_{0n}} \\ \vdots & \vdots & \ddots & \vdots \\ \frac{\partial \mathbf{r}_n}{\partial \mathbf{r}_{01}} & \frac{\partial \mathbf{r}_n}{\partial \mathbf{r}_{02}} & \cdots & \frac{\partial \mathbf{r}_n}{\partial \mathbf{r}_{0n}} \end{pmatrix}, \qquad \mathbf{\Phi}_{12} = \begin{pmatrix} \frac{\partial \mathbf{r}_1}{\partial \mathbf{v}_{01}} & \frac{\partial \mathbf{r}_1}{\partial \mathbf{v}_{02}} & \cdots & \frac{\partial \mathbf{r}_1}{\partial \mathbf{v}_{0n}} \\ \frac{\partial \mathbf{r}_2}{\partial \mathbf{v}_{01}} & \frac{\partial \mathbf{r}_2}{\partial \mathbf{v}_{02}} & \cdots & \frac{\partial \mathbf{r}_2}{\partial \mathbf{v}_{0n}} \\ \vdots & \vdots & \ddots & \vdots \\ \frac{\partial \mathbf{r}_n}{\partial \mathbf{v}_{01}} & \frac{\partial \mathbf{r}_n}{\partial \mathbf{v}_{02}} & \cdots & \frac{\partial \mathbf{r}_n}{\partial \mathbf{v}_{0n}} \end{pmatrix}, \tag{2.101}$$

$$\mathbf{\Phi}_{21} = \begin{pmatrix} \frac{\partial \mathbf{v}_1}{\partial \mathbf{r}_{01}} & \frac{\partial \mathbf{v}_1}{\partial \mathbf{r}_{02}} & \cdots & \frac{\partial \mathbf{v}_1}{\partial \mathbf{r}_{0n}} \\ \frac{\partial \mathbf{v}_2}{\partial \mathbf{r}_{01}} & \frac{\partial \mathbf{v}_2}{\partial \mathbf{r}_{02}} & \cdots & \frac{\partial \mathbf{v}_2}{\partial \mathbf{r}_{0n}} \\ \vdots & \vdots & \ddots & \vdots \\ \frac{\partial \mathbf{v}_n}{\partial \mathbf{r}_{01}} & \frac{\partial \mathbf{v}_n}{\partial \mathbf{r}_{02}} & \cdots & \frac{\partial \mathbf{v}_n}{\partial \mathbf{r}_{0n}} \end{pmatrix}, \qquad \mathbf{\Phi}_{22} = \begin{pmatrix} \frac{\partial \mathbf{v}_1}{\partial \mathbf{v}_{01}} & \frac{\partial \mathbf{v}_1}{\partial \mathbf{v}_{02}} & \cdots & \frac{\partial \mathbf{v}_1}{\partial \mathbf{v}_{0n}} \\ \frac{\partial \mathbf{v}_2}{\partial \mathbf{v}_{01}} & \frac{\partial \mathbf{v}_2}{\partial \mathbf{v}_{02}} & \cdots & \frac{\partial \mathbf{v}_2}{\partial \mathbf{v}_{0n}} \\ \vdots & \vdots & \ddots & \vdots \\ \frac{\partial \mathbf{v}_n}{\partial \mathbf{v}_{01}} & \frac{\partial \mathbf{v}_n}{\partial \mathbf{v}_{02}} & \cdots & \frac{\partial \mathbf{v}_n}{\partial \mathbf{v}_{0n}} \end{pmatrix}, \tag{2.102}$$

$$\mathbf{\Phi}_{13} = \begin{pmatrix} \frac{\partial \mathbf{r}_1}{\partial \mathbf{p}_0} \\ \frac{\partial \mathbf{r}_2}{\partial \mathbf{p}_0} \\ \vdots \\ \frac{\partial \mathbf{r}_n}{\partial \mathbf{p}_0} \end{pmatrix}, \qquad \mathbf{\Phi}_{23} = \begin{pmatrix} \frac{\partial \mathbf{v}_1}{\partial \mathbf{p}_0} \\ \frac{\partial \mathbf{v}_2}{\partial \mathbf{p}_0} \\ \vdots \\ \frac{\partial \mathbf{v}_n}{\partial \mathbf{p}_0} \end{pmatrix}, \tag{2.103}$$

$$\mathbf{\Phi}_{31} = \begin{pmatrix} \frac{\partial \mathbf{p}}{\partial \mathbf{r}_{01}} & \frac{\partial \mathbf{p}}{\partial \mathbf{r}_{02}} & \cdots & \frac{\partial \mathbf{p}}{\partial \mathbf{r}_{0n}} \end{pmatrix} = \mathbf{0}_{p\times 3n}, \tag{2.104}$$

$$\mathbf{\Phi}_{32} = \begin{pmatrix} \frac{\partial \mathbf{p}}{\partial \mathbf{v}_{01}} & \frac{\partial \mathbf{p}}{\partial \mathbf{v}_{02}} & \cdots & \frac{\partial \mathbf{p}}{\partial \mathbf{v}_{0n}} \end{pmatrix} = \mathbf{0}_{p\times 3n}, \tag{2.105}$$

$$\mathbf{\Phi}_{33} = \begin{pmatrix} \frac{\partial \mathbf{p}}{\partial \mathbf{p}_0} \end{pmatrix} = \mathbf{I}_{p\times p}, \tag{2.106}$$

then, performing matrices multiplication, the differential equations for $\mathbf{\Phi}$ become

$$\dot{\mathbf{\Phi}} = \mathbf{A}(t)\,\mathbf{\Phi} = \begin{pmatrix} \mathbf{\Phi}_{21} & \mathbf{\Phi}_{22} & \mathbf{\Phi}_{23} \\ \mathbf{B}_{11} & \mathbf{B}_{12} & \mathbf{B}_{13} \\ \mathbf{0}_{p\times 3n} & \mathbf{0}_{p\times 3n} & \mathbf{0}_{p\times p} \end{pmatrix}, \tag{2.107}$$

where

$$\begin{aligned} \mathbf{B}_{11} &= \mathbf{A}_{21}\mathbf{\Phi}_{11} + \mathbf{A}_{22}\mathbf{\Phi}_{21} + \mathbf{A}_{23}\mathbf{\Phi}_{31}, \\ \mathbf{B}_{12} &= \mathbf{A}_{21}\mathbf{\Phi}_{12} + \mathbf{A}_{22}\mathbf{\Phi}_{22} + \mathbf{A}_{23}\mathbf{\Phi}_{32}, \\ \mathbf{B}_{13} &= \mathbf{A}_{21}\mathbf{\Phi}_{13} + \mathbf{A}_{22}\mathbf{\Phi}_{23} + \mathbf{A}_{23}\mathbf{\Phi}_{33}. \end{aligned} \tag{2.108}$$

By integration of the last raw of $\dot{\mathbf{\Phi}}$ given by (2.107) with the initial conditions $\mathbf{\Phi}(t_0, t_0) = \mathbf{I}_{N\times N}$ we obtain

$$\mathbf{\Phi}_{31} = \mathbf{\Phi}_{32} = \mathbf{0}_{p\times 3n}, \qquad \mathbf{\Phi}_{33} = \mathbf{I}_{p\times p}. \tag{2.109}$$

So the set of equations (2.108) reduce to

$$\begin{aligned} \mathbf{B}_{11} &= \mathbf{A}_{21}\mathbf{\Phi}_{11} + \mathbf{A}_{22}\mathbf{\Phi}_{21}, \\ \mathbf{B}_{12} &= \mathbf{A}_{21}\mathbf{\Phi}_{12} + \mathbf{A}_{22}\mathbf{\Phi}_{22}, \\ \mathbf{B}_{13} &= \mathbf{A}_{21}\mathbf{\Phi}_{13} + \mathbf{A}_{22}\mathbf{\Phi}_{23} + \mathbf{A}_{23}. \end{aligned} \tag{2.110}$$

In general, the not trivial differential equations for $\dot{\mathbf{\Phi}}$ that have to be integrated are the following

$$\begin{aligned} \dot{\mathbf{\Phi}}_{11} &= \mathbf{\Phi}_{21}\,, \\ \dot{\mathbf{\Phi}}_{12} &= \mathbf{\Phi}_{22}\,, \\ \dot{\mathbf{\Phi}}_{13} &= \mathbf{\Phi}_{23}\,, \end{aligned} \tag{2.111}$$

with

$$\begin{aligned} \dot{\mathbf{\Phi}}_{21} &= \mathbf{A}_{21}\mathbf{\Phi}_{11} + \mathbf{A}_{22}\mathbf{\Phi}_{21}\,, \\ \dot{\mathbf{\Phi}}_{22} &= \mathbf{A}_{21}\mathbf{\Phi}_{12} + \mathbf{A}_{22}\mathbf{\Phi}_{22}\,, \\ \dot{\mathbf{\Phi}}_{23} &= \mathbf{A}_{21}\mathbf{\Phi}_{13} + \mathbf{A}_{22}\mathbf{\Phi}_{23} + \mathbf{A}_{23}\,. \end{aligned} \tag{2.112}$$

We remark here that as already told in chapter 1 the individual columns of the differential equations for $\mathbf{\Phi}$ are uncoupled and independent. So if we have a system with n_s satellites and we want to integrate the state transition matrix for n_l satellites, with $n_l \leq n_s$, it is sufficient to integrate the $6 \times n_l$ columns of $\mathbf{\Phi}$ referred to the n_l satellites.

2.6 Partial derivatives

Remembering the equations (2.95) and (2.96) now we have to compute the partial derivatives [48], [24]

$$\frac{\partial \ddot{\mathbf{R}}_i}{\partial \mathbf{R}_j}\,, \qquad \frac{\partial \ddot{\mathbf{R}}_i}{\partial \dot{\mathbf{R}}_j}\,, \qquad \frac{\partial \ddot{\mathbf{R}}_i}{\partial \mathbf{p}}\,, \qquad i,j = 1,...,n\,. \tag{2.113}$$

Since the acceleration comes from a conservative potential then $\frac{\partial \ddot{\mathbf{R}}_i}{\partial \dot{\mathbf{R}}_j} = \mathbf{0}, \forall\, i,j = 1,...,n$, so $\mathbf{A}_{22} = \mathbf{0}_{3n\times 3n}$ and the only matrices to be computed are

$$\mathbf{A}_{21} = \begin{pmatrix} \frac{\partial \mathbf{a}_1}{\partial \mathbf{r}_1} & \frac{\partial \mathbf{a}_1}{\partial \mathbf{r}_2} & \cdots & \frac{\partial \mathbf{a}_1}{\partial \mathbf{r}_n} \\ \frac{\partial \mathbf{a}_2}{\partial \mathbf{r}_1} & \frac{\partial \mathbf{a}_2}{\partial \mathbf{r}_2} & \cdots & \frac{\partial \mathbf{a}_2}{\partial \mathbf{r}_n} \\ \vdots & \vdots & \ddots & \vdots \\ \frac{\partial \mathbf{a}_n}{\partial \mathbf{r}_1} & \frac{\partial \mathbf{a}_n}{\partial \mathbf{r}_2} & \cdots & \frac{\partial \mathbf{a}_n}{\partial \mathbf{r}_n} \end{pmatrix}\,, \qquad \mathbf{A}_{23} = \begin{pmatrix} \frac{\partial \mathbf{a}_1}{\partial \mathbf{p}} \\ \frac{\partial \mathbf{a}_2}{\partial \mathbf{p}} \\ \vdots \\ \frac{\partial \mathbf{a}_n}{\partial \mathbf{p}} \end{pmatrix}\,. \tag{2.114}$$

2.6.1 Partials with respect to the satellites positions

Differentiating the equations (2.72) with respect to $\mathbf{R}_l$, $l = 1,...,n$, we have

$$\frac{\partial \ddot{\mathbf{R}}_i}{\partial \mathbf{R}_l} = \sum_{\substack{j=0 \\ j\neq i}}^{n} \left(\mathbf{Q}_{ji} \frac{\partial \mu_j}{\partial \mathbf{R}_l} + \mu_j \frac{\partial \mathbf{Q}_{ji}}{\partial \mathbf{R}_l} \right) + \frac{\partial \Delta \ddot{\mathbf{R}}_i}{\partial \mathbf{R}_l} + \frac{\partial \ddot{\mathbf{R}}_B}{\partial \mathbf{R}_l}\,, \qquad \begin{cases} i = 1,...,n \\ l = 1,...,n \end{cases}\,. \tag{2.115}$$

Isolating the term $j = 0$ we have

$$\frac{\partial \ddot{\mathbf{R}}_i}{\partial \mathbf{R}_l} = \mathbf{Q}_{0i} \frac{\partial \mu_0}{\partial \mathbf{R}_l} + \mu_0 \frac{\partial \mathbf{Q}_{0i}}{\partial \mathbf{R}_l} + \sum_{\substack{j=1 \\ j\neq i}}^{n} \left(\mathbf{Q}_{ji} \frac{\partial \mu_j}{\partial \mathbf{R}_l} + \mu_j \frac{\partial \mathbf{Q}_{ji}}{\partial \mathbf{R}_l} \right) + \frac{\partial \Delta \ddot{\mathbf{R}}_i}{\partial \mathbf{R}_l} + \frac{\partial \ddot{\mathbf{R}}_B}{\partial \mathbf{R}_l}\,, \qquad \begin{cases} i = 1,...,n \\ l = 1,...,n \end{cases}\,, \tag{2.116}$$

where each term on the right side are computed in the following pages. Since $\mu_0 = \mu_0\left(\mu_i, \mu_B\right)$, $i = 1,...,n$ we have that

$$\frac{\partial \mu_0}{\partial \mathbf{R}_l} = \mathbf{0}_{1\times 3}\,, \qquad l = 1,...,n\,, \tag{2.117}$$

$$\frac{\partial \mu_j}{\partial \mathbf{R}_l} = \mathbf{0}_{1\times 3}\,, \qquad l = 1,...,n\,, \tag{2.118}$$

so we can simplify (2.116) into

$$\frac{\partial \ddot{\mathbf{R}}_i}{\partial \mathbf{R}_l} = \mu_0 \frac{\partial \mathbf{Q}_{0i}}{\partial \mathbf{R}_l} + \sum_{\substack{j=1 \\ j\neq i}}^{n} \mu_j \frac{\partial \mathbf{Q}_{ji}}{\partial \mathbf{R}_l} + \frac{\partial \Delta\ddot{\mathbf{R}}_i}{\partial \mathbf{R}_l} + \frac{\partial \ddot{\mathbf{R}}_B}{\partial \mathbf{R}_l}\,, \qquad \left\{ \begin{array}{l} i = 1, ..., n \\ l = 1, ..., n \end{array} \right. , \tag{2.119}$$

which is equivalent to

$$\frac{\partial \ddot{\mathbf{R}}_i}{\partial \mathbf{R}_l} = \sum_{\substack{j=0 \\ j\neq i}}^{n} \mu_j \frac{\partial \mathbf{Q}_{ji}}{\partial \mathbf{R}_l} + \frac{\partial \Delta\ddot{\mathbf{R}}_i}{\partial \mathbf{R}_l} + \frac{\partial \ddot{\mathbf{R}}_B}{\partial \mathbf{R}_l}\,, \qquad \left\{ \begin{array}{l} i = 1, ..., n \\ l = 1, ..., n \end{array} \right. . \tag{2.120}$$

Computation of $\frac{\partial \mathbf{Q}_{ji}}{\partial \mathbf{R}_l}$

The terms $\frac{\partial \mathbf{Q}_{ji}}{\partial \mathbf{R}_l}$ are computed differentiating the equations (2.73) that is

$$\frac{\partial \mathbf{Q}_{ji}}{\partial \mathbf{R}_l} = \frac{\partial}{\partial \mathbf{R}_l}\left(\frac{\mathbf{R}_{ij}}{R_{ij}^3}\right) + \frac{\partial \mathbf{G}_{ij}}{\partial \mathbf{R}_l} - \frac{\partial \mathbf{G}_{ji}}{\partial \mathbf{R}_l}\,. \tag{2.121}$$

where $\mathbf{R}_{ij} = \mathbf{R}_j - \mathbf{R}_i$ and $R_{ij} = |\mathbf{R}_j - \mathbf{R}_i|$. First of all we treat the first term of the right member of the previous equation.

Because the position of the primary is a dependent quantity derived from the center of mass relation (see equations (2.78) and (2.79)), we have to separate the terms containing the primary (that is $j = 0$ or $i = 0$) from the other terms.

Computation of $\frac{\partial}{\partial \mathbf{R}_l}\left(\frac{\mathbf{R}_{ij}}{R_{ij}^3}\right)$: case $i, j \neq 0$.

It is easy to see that,

$$\frac{\partial}{\partial \mathbf{R}_l}\left(\frac{\mathbf{R}_{ij}}{R_{ij}^3}\right) = \mathbf{0}_{3\times 3}\,, \qquad l \neq i, j\,, \tag{2.122}$$

because of there is no direct dependence by the $\mathbf{R}_l$ term.

Case $l = j$

$$\begin{aligned} \frac{\partial}{\partial \mathbf{R}_j}\left(\frac{\mathbf{R}_{ij}}{R_{ij}^3}\right) &= \frac{1}{R_{ij}^6}\left[R_{ij}^3 \frac{\partial \mathbf{R}_{ij}}{\partial \mathbf{R}_j} - \mathbf{R}_{ij}\frac{\partial R_{ij}^3}{\partial \mathbf{R}_j}\right] \\ &= \frac{1}{R_{ij}^3}\frac{\partial \mathbf{R}_{ij}}{\partial \mathbf{R}_j} - \frac{3}{R_{ij}^4}\mathbf{R}_{ij}\frac{\partial R_{ij}}{\partial \mathbf{R}_j} \\ &= \frac{1}{R_{ij}^3}\mathbf{I}_{3\times 3} - \frac{3}{R_{ij}^4}\mathbf{R}_{ij}\frac{\partial R_{ij}}{\partial \mathbf{R}_j}\,. \end{aligned} \tag{2.123}$$

Since $R_{ij} = \sqrt{\mathbf{R}_{ij}\cdot\mathbf{R}_{ij}}$ then

$$\begin{aligned} \frac{\partial R_{ij}}{\partial \mathbf{R}_j} &= \frac{\partial}{\partial \mathbf{R}_j}\left(\sqrt{\mathbf{R}_{ij}\cdot\mathbf{R}_{ij}}\right) \\ &= \frac{1}{2\sqrt{\mathbf{R}_{ij}\cdot\mathbf{R}_{ij}}}\left[2\frac{\partial \mathbf{R}_{ij}}{\partial \mathbf{R}_j}\mathbf{R}_{ij}^T\right] \\ &= \frac{\mathbf{R}_{ij}^T}{R_{ij}}\,, \end{aligned} \tag{2.124}$$

so equation (2.123) becomes

$$\begin{aligned}\frac{\partial}{\partial \mathbf{R}_j}\left(\frac{\mathbf{R}_{ij}}{R_{ij}^3}\right) &= \frac{1}{R_{ij}^3}\mathbf{I}_{3\times 3} - \frac{3}{R_{ij}^4}\mathbf{R}_{ij}\frac{\mathbf{R}_{ij}^T}{R_{ij}} \\ &= \frac{1}{R_{ij}^3}\mathbf{I}_{3\times 3} - 3\frac{\mathbf{R}_{ij}\mathbf{R}_{ij}^T}{R_{ij}^5}\,. \end{aligned} \tag{2.125}$$

Case $l = i$

$$\frac{\partial}{\partial \mathbf{R}_i}\left(\frac{\mathbf{R}_{ij}}{R_{ij}^3}\right) = -\frac{\partial}{\partial \mathbf{R}_i}\left(\frac{\mathbf{R}_{ji}}{R_{ij}^3}\right) = -\frac{\partial}{\partial \mathbf{R}_j}\left(\frac{\mathbf{R}_{ij}}{R_{ij}^3}\right)\,, \tag{2.126}$$

that is the opposite sign of the case $l = j$.

General case

Summarizing the two previous cases we have that in the case $i, j \neq 0$

$$\frac{\partial}{\partial \mathbf{R}_j}\left(\frac{\mathbf{R}_{ij}}{R_{ij}^3}\right) = -\frac{\partial}{\partial \mathbf{R}_i}\left(\frac{\mathbf{R}_{ij}}{R_{ij}^3}\right) = \frac{1}{R_{ij}^3}\mathbf{I}_{3\times 3} - 3\frac{\mathbf{R}_{ij}\mathbf{R}_{ij}^T}{R_{ij}^5}\,, \tag{2.127}$$

and, more generally

$$\frac{\partial}{\partial \mathbf{R}_l}\left(\frac{\mathbf{R}_{ij}}{R_{ij}^3}\right) = \delta_l^{ji}\left(\frac{1}{R_{ij}^3}\mathbf{I}_{3\times 3} - 3\frac{\mathbf{R}_{ij}\mathbf{R}_{ij}^T}{R_{ij}^5}\right)\,, \tag{2.128}$$

where

$$\delta_l^{ji} = \begin{cases} 1 & \text{for } l = j \\ -1 & \text{for } l = i \\ 0 & \text{otherwise} \end{cases}\,, \quad \text{and} \quad \begin{cases} i = 1, ..., n \\ j = 1, ..., n+m \\ l = 1, ..., n \end{cases}\,. \tag{2.129}$$

Computation of $\frac{\partial}{\partial \mathbf{R}_l}\left(\frac{\mathbf{R}_{ij}}{R_{ij}^3}\right)$**: case** $i = 0$ **or** $j = 0$.

Case $j = 0,\ i \neq 0,\ l \neq 0$

$$\begin{aligned}\frac{\partial}{\partial \mathbf{R}_l}\left(\frac{\mathbf{R}_{i0}}{R_{i0}^3}\right) &= \frac{1}{R_{i0}^6}\left(R_{i0}^3\frac{\partial \mathbf{R}_{i0}}{\partial \mathbf{R}_l} - \mathbf{R}_{i0}\frac{\partial R_{i0}^3}{\partial \mathbf{R}_l}\right) \\ &= \frac{1}{R_{i0}^3}\frac{\partial \mathbf{R}_{i0}}{\partial \mathbf{R}_l} - \frac{3}{R_{i0}^4}\mathbf{R}_{i0}\frac{\partial R_{i0}}{\partial \mathbf{R}_l}\,. \end{aligned} \tag{2.130}$$

So we have to compute $\frac{\partial \mathbf{R}_{i0}}{\partial \mathbf{R}_l}$ and $\frac{\partial R_{i0}}{\partial \mathbf{R}_l}$. Explicitly we have

$$\frac{\partial \mathbf{R}_{i0}}{\partial \mathbf{R}_l} = \frac{\partial\left(\mathbf{R}_0 - \mathbf{R}_i\right)}{\partial \mathbf{R}_l} = \frac{\partial \mathbf{R}_0}{\partial \mathbf{R}_l} - \frac{\partial \mathbf{R}_i}{\partial \mathbf{R}_l} = \frac{\partial \mathbf{R}_0}{\partial \mathbf{R}_l} - \delta_l^i\,\mathbf{I}_{3\times 3}\,. \tag{2.131}$$

Because $\mathbf{R}_0 = \mathbf{R}_0\left(\mu_0, \mu_i, \mathbf{R}_i\right)$ (see equation (2.79)) then

$$\frac{\partial \mathbf{R}_0}{\partial \mathbf{R}_l} = \frac{\partial}{\partial \mathbf{R}_l}\left(-\frac{1}{\mu_0}\sum_{i=1}^{n}\mu_i\mathbf{R}_i\right) = -\frac{1}{\mu_0}\sum_{i=1}^{n}\mu_i\frac{\partial \mathbf{R}_i}{\partial \mathbf{R}_l} = -\frac{\mu_l}{\mu_0}\mathbf{I}_{3\times 3}\,, \tag{2.132}$$

and finally

$$\frac{\partial \mathbf{R}_{i0}}{\partial \mathbf{R}_l} = \left(-\frac{\mu_l}{\mu_0} - \delta_l^i\right)\mathbf{I}_{3\times 3}\,. \tag{2.133}$$

For the term $\frac{\partial R_{i0}}{\partial \mathbf{R}_l}$, since $R_{i0} = \sqrt{\mathbf{R}_{i0} \cdot \mathbf{R}_{i0}}$ then

$$\begin{aligned}\frac{\partial R_{i0}}{\partial \mathbf{R}_l} &= \frac{\partial \left(|\mathbf{R}_0 - \mathbf{R}_i|\right)}{\partial \mathbf{R}_l} = \frac{\partial}{\partial \mathbf{R}_l}\left(\sqrt{\mathbf{R}_{i0} \cdot \mathbf{R}_{i0}}\right) \\ &= \frac{1}{2\sqrt{\mathbf{R}_{i0} \cdot \mathbf{R}_{i0}}}\left[2\frac{\partial \mathbf{R}_{i0}}{\partial \mathbf{R}_l}\mathbf{R}_{i0}^T\right] \\ &= \left(-\frac{\mu_l}{\mu_0} - \delta_l^i\right)\frac{\mathbf{R}_{i0}^T}{R_{i0}}\,. \end{aligned} \tag{2.134}$$

Finally, summarizing the results we have

$$\frac{\partial}{\partial \mathbf{R}_l}\left(\frac{\mathbf{R}_{i0}}{R_{i0}^3}\right) = -\left(\frac{\mu_l}{\mu_0} + \delta_l^i\right)\left[\frac{1}{R_{i0}^3}\mathbf{I}_{3\times 3} - 3\frac{\mathbf{R}_{i0}\mathbf{R}_{i0}^T}{R_{i0}^5}\right]\,. \tag{2.135}$$

Case $j = 0,\ i \neq 0,\ l = 0$

$$\frac{\partial}{\partial \mathbf{R}_0}\left(\frac{\mathbf{R}_{i0}}{R_{i0}^3}\right) = \frac{1}{R_{i0}^3}\frac{\partial \mathbf{R}_{i0}}{\partial \mathbf{R}_0} - \frac{3}{R_{i0}^4}\mathbf{R}_{i0}\frac{\partial R_{i0}}{\partial \mathbf{R}_0}\,. \tag{2.136}$$

But

$$\frac{\partial \mathbf{R}_{i0}}{\partial \mathbf{R}_0} = \frac{\partial \left(\mathbf{R}_0 - \mathbf{R}_i\right)}{\partial \mathbf{R}_0} = \mathbf{I}_{3\times 3}\,, \tag{2.137}$$

and

$$\begin{aligned}\frac{\partial R_{i0}}{\partial \mathbf{R}_0} &= \frac{\partial \left(|\mathbf{R}_0 - \mathbf{R}_i|\right)}{\partial \mathbf{R}_0} = \frac{\partial}{\partial \mathbf{R}_0}\left(\sqrt{\mathbf{R}_{i0} \cdot \mathbf{R}_{i0}}\right) \\ &= \frac{1}{2\sqrt{\mathbf{R}_{i0} \cdot \mathbf{R}_{i0}}}2\mathbf{R}_{i0}^T \\ &= \frac{\mathbf{R}_{i0}^T}{R_{i0}}\,, \end{aligned} \tag{2.138}$$

so finally

$$\frac{\partial}{\partial \mathbf{R}_0}\left(\frac{\mathbf{R}_{i0}}{R_{i0}^3}\right) = \frac{1}{R_{i0}^3}\mathbf{I}_{3\times 3} - 3\frac{\mathbf{R}_{i0}\mathbf{R}_{i0}^T}{R_{i0}^5}\,. \tag{2.139}$$

Case $i = 0,\ j \neq 0,\ l \neq 0$

Using the results already obtained (see equation (2.135)) we have

$$\begin{aligned}\frac{\partial}{\partial \mathbf{R}_l}\left(\frac{\mathbf{R}_{0j}}{R_{0j}^3}\right) &= -\frac{\partial}{\partial \mathbf{R}_l}\left(\frac{\mathbf{R}_{j0}}{R_{j0}^3}\right) \\ &= \left(\frac{\mu_l}{\mu_0} + \delta_l^j\right)\left[\frac{1}{R_{0j}^3}\mathbf{I}_{3\times 3} - 3\frac{\mathbf{R}_{j0}\mathbf{R}_{j0}^T}{R_{0j}^5}\right]\,. \end{aligned} \tag{2.140}$$

Case $i = 0,\ j \neq 0,\ l = 0$

Using the results already obtained (see equation (2.139)) we have

$$\begin{aligned}\frac{\partial}{\partial \mathbf{R}_0}\left(\frac{\mathbf{R}_{0j}}{R_{0j}^3}\right) &= -\frac{\partial}{\partial \mathbf{R}_0}\left(\frac{\mathbf{R}_{j0}}{R_{j0}^3}\right) \\ &= -\left[\frac{1}{R_{j0}^3}\mathbf{I}_{3\times 3} - 3\frac{\mathbf{R}_{j0}\mathbf{R}_{j0}^T}{R_{j0}^5}\right]\,. \end{aligned} \tag{2.141}$$

Computation of $\frac{\partial \mathbf{G}_{ij}}{\partial \mathbf{R}_l}$: case $i, j \neq 0$.

First of all we can say that, if $l \neq i, j$ then $\frac{\partial \mathbf{G}_{ij}}{\partial \mathbf{R}_l} = \mathbf{0}_{3\times 3}$ because of, from its definition, there is no direct dependence of the functions $\mathbf{G}_{ij}$ from the $\mathbf{R}_l$ term.

The partial derivatives of $\mathbf{G}_{ij}$ with respect to $\mathbf{R}_i$ and $\mathbf{R}_j$ are obtained using equation (2.83) which we take back here

$$\mathbf{G}_{ij} = \mathbf{C}_j^T \mathbf{G}_{ij}^{BF} \,, \tag{2.142}$$

so

$$\frac{\partial \mathbf{G}_{ij}}{\partial \mathbf{R}_j} = \mathbf{C}_j^T \frac{\partial \mathbf{G}_{ij}^{BF}}{\partial \mathbf{R}_j} \,, \tag{2.143}$$

$$\frac{\partial \mathbf{G}_{ij}}{\partial \mathbf{R}_i} = \mathbf{C}_j^T \frac{\partial \mathbf{G}_{ij}^{BF}}{\partial \mathbf{R}_i} \,. \tag{2.144}$$

But (see equation (2.82)) $\mathbf{G}_{ij}^{BF} = \frac{1}{\mu_j}\left(\frac{\partial \mathcal{U}_j}{\partial \mathbf{r}_{ji}^{BF}}\right)^T$ is a function referred to the body fixed frame centered on body j. Applying the chain rule we have

$$\frac{\partial \mathbf{G}_{ij}}{\partial \mathbf{R}_j} = \mathbf{C}_j^T \frac{\partial \mathbf{G}_{ij}^{BF}}{\partial \mathbf{r}_{ji}^{BF}} \frac{\partial \mathbf{r}_{ji}^{BF}}{\partial \mathbf{R}_j} \,, \tag{2.145}$$

$$\frac{\partial \mathbf{G}_{ij}}{\partial \mathbf{R}_i} = \mathbf{C}_j^T \frac{\partial \mathbf{G}_{ij}^{BF}}{\partial \mathbf{r}_{ji}^{BF}} \frac{\partial \mathbf{r}_{ji}^{BF}}{\partial \mathbf{R}_i} \,, \tag{2.146}$$

and using the equation (2.81) $\mathbf{r}_{ji}^{BF} = \mathbf{C}_j \left(\mathbf{R}_i - \mathbf{R}_j\right)$ we have

$$\frac{\mathbf{r}_{ji}^{BF}}{\partial \mathbf{R}_j} = -\mathbf{C}_j \,, \qquad \frac{\partial \mathbf{r}_{ji}}{\partial \mathbf{R}_i} = \mathbf{C}_j \,, \tag{2.147}$$

so at last we have

$$\frac{\partial \mathbf{G}_{ij}}{\partial \mathbf{R}_j} = -\mathbf{C}_j^T \frac{\partial \mathbf{G}_{ij}^{BF}}{\partial \mathbf{r}_{ji}^{BF}} \mathbf{C}_j \,, \tag{2.148}$$

$$\frac{\partial \mathbf{G}_{ij}}{\partial \mathbf{R}_i} = \mathbf{C}_j^T \frac{\partial \mathbf{G}_{ij}^{BF}}{\partial \mathbf{r}_{ji}^{BF}} \mathbf{C}_j \,, \tag{2.149}$$

where the derivatives $\frac{\partial \mathbf{G}_{ij}^{BF}}{\partial \mathbf{r}_{ji}^{BF}}$ will be computed in section 2.6.4. Coming back to equations (2.121) we can say that:

1. In the case that $l = j$, the last two terms of (2.121) are

$$+ \frac{\partial \mathbf{G}_{ij}}{\partial \mathbf{R}_j} - \frac{\partial \mathbf{G}_{ji}}{\partial \mathbf{R}_j} \,. \tag{2.150}$$

2. In the case that $l = i$ instead, the last two terms of (2.121) are

$$\frac{\partial \mathbf{G}_{ij}}{\partial \mathbf{R}_i} - \frac{\partial \mathbf{G}_{ji}}{\partial \mathbf{R}_i} = -\left(\frac{\partial \mathbf{G}_{ji}}{\partial \mathbf{R}_i} - \frac{\partial \mathbf{G}_{ij}}{\partial \mathbf{R}_i}\right) \,, \tag{2.151}$$

that is the opposite sign of the case $l = j$.

Computation of $\frac{\partial \mathbf{G}_{ij}}{\partial \mathbf{R}_l}$: case $i=0$ or $j=0$.

Case $i=0$

$$\frac{\partial \mathbf{G}_{0j}}{\partial \mathbf{R}_l} = \mathbf{C}_j^T \frac{\partial \mathbf{G}_{0j}^{BF}}{\partial \mathbf{R}_l} = \mathbf{C}_j^T \frac{\partial \mathbf{G}_{0j}^{BF}}{\partial \mathbf{r}_{j0}^{BF}} \frac{\partial \mathbf{r}_{j0}^{BF}}{\partial \mathbf{R}_l}\,, \tag{2.152}$$

where $\mathbf{r}_{j0}^{BF} = \mathbf{C}_j\,(\mathbf{R}_0 - \mathbf{R}_j)$. Differentiating and using the center of mass relation (2.79) and (2.133) we have three subcases

$$\begin{cases} \frac{\partial \mathbf{r}_{j0}^{BF}}{\partial \mathbf{R}_j} = \mathbf{C}_j \frac{\partial}{\partial \mathbf{R}_j}(\mathbf{R}_0 - \mathbf{R}_j) = \mathbf{C}_j \left(-\frac{\mu_j}{\mu_0} - 1\right), & l = j \neq 0\,, \\ \frac{\partial \mathbf{r}_{j0}^{BF}}{\partial \mathbf{R}_l} = \mathbf{C}_j \left(-\frac{\mu_l}{\mu_0}\right), & l \neq j \neq 0\,, \\ \frac{\partial \mathbf{r}_{j0}^{BF}}{\partial \mathbf{R}_0} = \mathbf{C}_j\,, \end{cases} \tag{2.153}$$

so (2.152) becomes

$$\begin{cases} \frac{\partial \mathbf{G}_{0j}}{\partial \mathbf{R}_l} = -\left(\frac{\mu_l}{\mu_0} + \delta_l^j\right) \mathbf{C}_j^T \frac{\partial \mathbf{G}_{0j}^{BF}}{\partial \mathbf{r}_{j0}^{BF}} \mathbf{C}_j\,, & l \neq 0\,, \\ \frac{\partial \mathbf{G}_{0j}}{\partial \mathbf{R}_l} = \mathbf{C}_j^T \frac{\partial \mathbf{G}_{0j}^{BF}}{\partial \mathbf{r}_{j0}^{BF}} \mathbf{C}_j\,, & l = 0\,, \end{cases} \tag{2.154}$$

where the derivatives $\frac{\partial \mathbf{G}_{0j}^{BF}}{\partial \mathbf{r}_{j0}^{BF}}$ will be computed in section 2.6.4.

Case $j=0$

$$\frac{\partial \mathbf{G}_{i0}}{\partial \mathbf{R}_l} = \mathbf{C}_0^T \frac{\partial \mathbf{G}_{i0}^{BF}}{\partial \mathbf{R}_l} = \mathbf{C}_0^T \frac{\partial \mathbf{G}_{i0}^{BF}}{\partial \mathbf{r}_{0i}^{BF}} \frac{\partial \mathbf{r}_{0i}^{BF}}{\partial \mathbf{R}_l}\,, \tag{2.155}$$

where $\mathbf{r}_{0i}^{BF} = \mathbf{C}_0\,(\mathbf{R}_i - \mathbf{R}_0)$. Differentiating and using the center of mass relation (2.79) and (2.133) we have three subcases

$$\begin{cases} \frac{\partial \mathbf{r}_{0i}^{BF}}{\partial \mathbf{R}_i} = \mathbf{C}_0 \frac{\partial}{\partial \mathbf{R}_i}(\mathbf{R}_i - \mathbf{R}_0) = \mathbf{C}_0 \left(1 + \frac{\mu_i}{\mu_0}\right), & l = i \neq 0\,, \\ \frac{\partial \mathbf{r}_{0i}^{BF}}{\partial \mathbf{R}_l} = \mathbf{C}_0 \frac{\mu_l}{\mu_0}\,, & l \neq i \neq 0\,, \\ \frac{\partial \mathbf{r}_{0i}^{BF}}{\partial \mathbf{R}_0} = -\mathbf{C}_0\,, \end{cases} \tag{2.156}$$

so (2.155) becomes

$$\begin{cases} \frac{\partial \mathbf{G}_{i0}}{\partial \mathbf{R}_l} = \left(\frac{\mu_l}{\mu_0} + \delta_l^i\right) \mathbf{C}_0^T \frac{\partial \mathbf{G}_{i0}^{BF}}{\partial \mathbf{r}_{0i}^{BF}} \mathbf{C}_0\,, & l \neq 0\,, \\ \frac{\partial \mathbf{G}_{i0}}{\partial \mathbf{R}_l} = -\mathbf{C}_0^T \frac{\partial \mathbf{G}_{i0}^{BF}}{\partial \mathbf{r}_{0i}^{BF}} \mathbf{C}_0\,, & l = 0\,, \end{cases} \tag{2.157}$$

where the derivatives $\frac{\partial \mathbf{G}_{i0}^{BF}}{\partial \mathbf{r}_{0i}^{BF}}$ will be computed in section 2.6.4.

Computation of $\frac{\partial \Delta \ddot{\mathbf{R}}_i}{\partial \mathbf{R}_l}$

By differentiation of equations (2.75) we have

$$\frac{\partial \Delta \ddot{\mathbf{R}}_i}{\partial \mathbf{R}_l} = \sum_{j=n+1}^{n+m} \mu_j \frac{\partial \mathbf{Q}_{ji}}{\partial \mathbf{R}_l}\,, \tag{2.158}$$

but, because $\frac{\partial \mathbf{Q}_{ji}}{\partial \mathbf{R}_l} = \mathbf{0}$ if $l \neq 0$ and $j \neq i \neq 0$, then expression of $\frac{\partial \Delta \ddot{\mathbf{R}}_i}{\partial \mathbf{R}_l}$ can be simplified into

$$\frac{\partial \Delta \ddot{\mathbf{R}}_i}{\partial \mathbf{R}_l} = \delta_l^i \sum_{j=n+1}^{n+m} \mu_j \frac{\partial \mathbf{Q}_{ji}}{\partial \mathbf{R}_l}\,, \qquad \begin{cases} l \neq 0 \\ i \neq 0 \end{cases}\,, \tag{2.159}$$

while

$$\frac{\partial \Delta \ddot{\mathbf{R}}_0}{\partial \mathbf{R}_l} = \sum_{j=n+1}^{n+m} \mu_j \frac{\partial \mathbf{Q}_{j0}}{\partial \mathbf{R}_l}\,, \tag{2.160}$$

$$\frac{\partial \Delta \ddot{\mathbf{R}}_0}{\partial \mathbf{R}_0} = \sum_{j=n+1}^{n+m} \mu_j \frac{\partial \mathbf{Q}_{j0}}{\partial \mathbf{R}_0}\,, \tag{2.161}$$

where $\frac{\partial \mathbf{Q}_{j0}}{\partial \mathbf{R}_l}$ and $\frac{\partial \mathbf{Q}_{j0}}{\partial \mathbf{R}_0}$ are already been computed in (2.135), (2.139), (2.157) and (2.154).

Computation of $\frac{\partial \ddot{\mathbf{R}}_B}{\partial \mathbf{R}_l}$

From equations (2.76), isolating the term with $k = 0$ and differentiating we have

$$\frac{\partial \ddot{\mathbf{R}}_B}{\partial \mathbf{R}_l} = -\frac{1}{\mu_B}\left(\mu_0 \frac{\partial \Delta \ddot{\mathbf{R}}_0}{\partial \mathbf{R}_l} + \sum_{k=1}^{n} \mu_k \frac{\partial \Delta \ddot{\mathbf{R}}_k}{\partial \mathbf{R}_l}\right)\,, \tag{2.162}$$

where $\frac{\partial \Delta \ddot{\mathbf{R}}_0}{\partial \mathbf{R}_l}$ and $\frac{\partial \Delta \ddot{\mathbf{R}}_k}{\partial \mathbf{R}_l}$ are given by (2.160) and (2.159) respectively.

2.6.2 Partials involving the vector to the primary

The derivatives of the vector to the primary with respect to satellites' positions are obtained by differentiation of equation (2.79). So, because $\mathbf{R}_0\left(\mu_0, \mu_i, \mathbf{R}_i\right)$, for the partials with respect to the initial states of the satellites we have, as we have seen repeatedly in the previous sections

$$\begin{aligned} \frac{\partial \mathbf{R}_0}{\partial \mathbf{R}_k} &= -\frac{1}{\mu_0}\sum_{j=1}^{n} \mu_j \frac{\partial \mathbf{R}_j}{\partial \mathbf{R}_k} \\ &= -\frac{\mu_k}{\mu_0}\mathbf{I}_{3\times 3}\,. \end{aligned} \tag{2.163}$$

For the gravitational parameters of the satellites μ_k, $k = 1, ..., n$, because of the system $GM = \mu_B$ is taken to be fundamental, and $\mu_0 = \mu_0\left(\mu_B, \mu_i\right)$ is computed from it (see equation (2.80)), deriving (2.79) we have

$$\begin{aligned} \frac{\partial \mathbf{R}_0}{\partial \mu_k} &= \frac{\partial}{\partial \mu_k}\left[-\frac{1}{\mu_0}\sum_{j=1}^{n} \mu_j \mathbf{R}_j\right] \\ &= \sum_{j=1}^{n} \mu_j \mathbf{R}_j \frac{\partial}{\partial \mu_k}\left(-\frac{1}{\mu_0}\right) - \frac{1}{\mu_0}\frac{\partial}{\partial \mu_k}\sum_{j=1}^{n} \mu_j \mathbf{R}_j\,. \end{aligned} \tag{2.164}$$

Now, using (2.80) we have

$$\frac{\partial}{\partial \mu_k}\left(-\frac{1}{\mu_0}\right) = \frac{1}{\mu_0^2}\frac{\partial \mu_0}{\partial \mu_k}\,, \tag{2.165}$$

and

$$\frac{\partial \mu_0}{\partial \mu_k} = \frac{\partial}{\partial \mu_k}\left(\mu_B - \sum_{i=1}^{n} \mu_i\right) = -1\,, \tag{2.166}$$

so

$$\begin{aligned}\frac{\partial \mathbf{R}_0}{\partial \mu_k} &= -\frac{1}{\mu_0^2}\sum_{j=1}^{n}\mu_j\mathbf{R}_j - \frac{1}{\mu_0}\sum_{j=1}^{n}\left[\frac{\partial \mu_j}{\partial \mu_k}\mathbf{R}_j + \mu_j\frac{\partial \mathbf{R}_j}{\partial \mu_k}\right] \\ &= \frac{1}{\mu_0}\left(-\frac{1}{\mu_0}\sum_{j=1}^{n}\mu_j\mathbf{R}_j\right) - \frac{1}{\mu_0}\mathbf{R}_k \\ &= -\frac{1}{\mu_0}\left(\mathbf{R}_k - \mathbf{R}_0\right) . \end{aligned} \tag{2.167}$$

For the gravitational parameter of the planet-satellites system μ_B we have

$$\begin{aligned}\frac{\partial \mathbf{R}_0}{\partial \mu_B} &= \frac{\partial}{\partial \mu_B}\left[-\frac{1}{\mu_0}\sum_{j=1}^{n}\mu_j\mathbf{R}_j\right] \\ &= \sum_{j=1}^{n}\mu_j\mathbf{R}_j\frac{\partial}{\partial \mu_B}\left(-\frac{1}{\mu_0}\right) - \frac{1}{\mu_0}\frac{\partial}{\partial \mu_B}\sum_{j=1}^{n}\mu_j\mathbf{R}_j \\ &= \frac{1}{\mu_0^2}\frac{\partial \mu_0}{\partial \mu_B}\sum_{j=1}^{n}\mu_j\mathbf{R}_j , \end{aligned} \tag{2.168}$$

and, since the partial derivative of μ_0 with respect to μ_B is (see equation (2.80))

$$\frac{\partial \mu_0}{\partial \mu_B} = \frac{\partial}{\partial \mu_B}\left(\mu_B - \sum_{i=1}^{n}\mu_i\right) = 1 , \tag{2.169}$$

$\frac{\partial \mathbf{R}_0}{\partial \mu_B}$ becomes

$$\frac{\partial \mathbf{R}_0}{\partial \mu_B} = \frac{1}{\mu_0^2}\sum_{j=1}^{n}\mu_j\mathbf{R}_j = -\frac{1}{\mu_0}\mathbf{R}_0 . \tag{2.170}$$

2.6.3 Partials with respect to the mass

As we have repeatedly told, instead of solving for the gravitational parameter of the primary μ_0 we solve for the gravitational parameter of the planetary system μ_B. Therefore we must treat $\mu_0\left(\mu_B, \mu_i\right)$ as a function of the other gravitational parameters of the system by means of the (2.80).

Computation of $\frac{\partial \ddot{\mathbf{R}}_i}{\partial \mu_k}$ in the case $k = 1, ..., n$

By differentiation of the equations of motion (2.72) with respect to the gravitational parameters of the satellites μ_k we have

$$\frac{\partial \ddot{\mathbf{R}}_i}{\partial \mu_k} = \frac{\partial}{\partial \mu_k}\sum_{\substack{j=0\\ j\neq i}}^{n}\mu_j\mathbf{Q}_{ji} + \frac{\partial \Delta\ddot{\mathbf{R}}_i}{\partial \mu_k} + \frac{\partial \ddot{\mathbf{R}}_B}{\partial \mu_k} , \qquad \begin{cases} k = 1, ..., n \\ i = 1, ..., n \end{cases} . \tag{2.171}$$

Treating term by term we have

$$\begin{aligned}\frac{\partial}{\partial \mu_k}\sum_{\substack{j=0\\ j\neq i}}^{n}\mu_j\mathbf{Q}_{ji} &= \frac{\partial}{\partial \mu_k}\left(\mu_0\mathbf{Q}_{0i}\right) + \frac{\partial}{\partial \mu_k}\sum_{\substack{j=1\\ j\neq i}}^{n}\mu_j\mathbf{Q}_{ji} \\ &= \frac{\partial \mu_0}{\partial \mu_k}\mathbf{Q}_{0i} + \mu_0\frac{\partial \mathbf{Q}_{0i}}{\partial \mu_k} + \sum_{\substack{j=1\\ j\neq i}}^{n}\left(\frac{\partial \mu_j}{\partial \mu_k}\mathbf{Q}_{ji} + \mu_j\frac{\partial \mathbf{Q}_{ji}}{\partial \mu_k}\right) . \end{aligned} \tag{2.172}$$

Since because by definition $\mathbf{Q}_{ji}$ (see equations (2.73), (2.83), (2.82), and (2.10)) are independent from any μ_k, $k = 1, ..., n$, $\frac{\partial \mu_j}{\partial \mu_k} = \delta_k^j$ for $j \neq 0$ and $\frac{\partial \mu_0}{\partial \mu_k}$ is given by (2.166), we have

$$\begin{aligned} \frac{\partial}{\partial \mu_k} \sum_{\substack{j=0 \\ j \neq i}}^{n} \mu_j \mathbf{Q}_{ji} &= \frac{\partial \mu_0}{\partial \mu_k} \mathbf{Q}_{0i} + \mu_0 \frac{\partial \mathbf{Q}_{0i}}{\partial \mu_k} + \mathbf{Q}_{ki} \\ &= \mathbf{Q}_{ki} - \mathbf{Q}_{0i} + \mu_0 \frac{\partial \mathbf{Q}_{0i}}{\partial \mu_k} \,. \end{aligned} \tag{2.173}$$

Then

$$\frac{\partial \Delta \ddot{\mathbf{R}}_i}{\partial \mu_k} = \frac{\partial}{\partial \mu_k} \left[\sum_{j=n+1}^{n+m} \mu_j \mathbf{Q}_{ji} \right] = \mathbf{0}_{3\times 1} \,, \qquad i = 1, ..., n \,, \tag{2.174}$$

$$\frac{\partial \Delta \ddot{\mathbf{R}}_0}{\partial \mu_k} = \sum_{j=n+1}^{n+m} \mu_j \frac{\partial \mathbf{Q}_{j0}}{\partial \mu_k} = \frac{\partial \Delta \ddot{\mathbf{R}}_0}{\partial \mathbf{R}_0} \frac{\partial \mathbf{R}_0}{\partial \mu_k} \,, \tag{2.175}$$

where $\frac{\partial \Delta \ddot{\mathbf{R}}_0}{\partial \mathbf{R}_0}$ and $\frac{\partial \mathbf{R}_0}{\partial \mu_k}$ are given by (2.161) and (2.167) respectively.

Then

$$\begin{aligned} \frac{\partial \ddot{\mathbf{R}}_B}{\partial \mu_k} &= \frac{\partial}{\partial \mu_k} \left[-\frac{1}{\mu_B} \sum_{j=0}^{n} \mu_j \Delta \ddot{\mathbf{R}}_j \right] = -\frac{1}{\mu_B} \frac{\partial}{\partial \mu_k} \left[\mu_0 \Delta \ddot{\mathbf{R}}_0 + \sum_{j=1}^{n} \mu_j \Delta \ddot{\mathbf{R}}_j \right] \\ &= -\frac{1}{\mu_B} \left[\frac{\partial \mu_0}{\partial \mu_k} \Delta \ddot{\mathbf{R}}_0 + \mu_0 \frac{\partial \Delta \ddot{\mathbf{R}}_0}{\partial \mu_k} + \sum_{j=1}^{n} \left(\frac{\partial \mu_j}{\partial \mu_k} \Delta \ddot{\mathbf{R}}_j + \mu_j \frac{\partial \Delta \ddot{\mathbf{R}}_j}{\partial \mu_k} \right) \right] \\ &= -\frac{1}{\mu_B} \left(-\Delta \ddot{\mathbf{R}}_0 + \mu_0 \frac{\partial \Delta \ddot{\mathbf{R}}_0}{\partial \mu_k} + \Delta \ddot{\mathbf{R}}_k \right) \,, \end{aligned} \tag{2.176}$$

where the partials $\frac{\partial \Delta \ddot{\mathbf{R}}_0}{\partial \mu_k}$ are given in (2.175) and for $\frac{\partial \Delta \ddot{\mathbf{R}}_j}{\partial \mu_k}$ and $\frac{\partial \mu_0}{\partial \mu_k}$ we have used (2.174) and (2.166) respectively. Remain to compute $\frac{\partial \mathbf{Q}_{0i}}{\partial \mu_k}$ and $\frac{\partial \mathbf{Q}_{j0}}{\partial \mu_k}$. Using the chain rule we have

$$\frac{\partial \mathbf{Q}_{0i}}{\partial \mu_k} = \frac{\partial \mathbf{Q}_{0i}}{\partial \mathbf{R}_0} \frac{\partial \mathbf{R}_0}{\partial \mu_k} = -\frac{1}{\mu_0} \frac{\partial \mathbf{Q}_{0i}}{\partial \mathbf{R}_0} (\mathbf{R}_k - \mathbf{R}_0) \,, \tag{2.177}$$

$$\frac{\partial \mathbf{Q}_{j0}}{\partial \mu_k} = \frac{\partial \mathbf{Q}_{j0}}{\partial \mathbf{R}_0} \frac{\partial \mathbf{R}_0}{\partial \mu_k} = -\frac{1}{\mu_0} \frac{\partial \mathbf{Q}_{j0}}{\partial \mathbf{R}_0} (\mathbf{R}_k - \mathbf{R}_0) \,, \tag{2.178}$$

where we have used (2.167) and the partials $\frac{\partial \mathbf{Q}_{0i}}{\partial \mathbf{R}_0}$ and $\frac{\partial \mathbf{Q}_{j0}}{\partial \mathbf{R}_0}$ are been already computed in section 2.6.1.

So at last, putting the (2.173), (2.174), (2.175) into (2.171) and using (2.177) and (2.178) with (2.167) we have

$$\begin{aligned} \frac{\partial \ddot{\mathbf{R}}_i}{\partial \mu_k} &= \mathbf{Q}_{ki} - \mathbf{Q}_{0i} + \mu_0 \frac{\partial \mathbf{Q}_{0i}}{\partial \mu_k} - \frac{1}{\mu_B} \left(-\Delta \ddot{\mathbf{R}}_0 + \mu_0 \frac{\partial \Delta \ddot{\mathbf{R}}_0}{\partial \mu_k} + \Delta \ddot{\mathbf{R}}_k \right) \\ &= \mathbf{Q}_{ki} - \mathbf{Q}_{0i} - \frac{1}{\mu_B} \left(\Delta \ddot{\mathbf{R}}_k - \Delta \ddot{\mathbf{R}}_0 \right) + \mu_0 \frac{\partial \mathbf{Q}_{0i}}{\partial \mu_k} - \frac{1}{\mu_B} \mu_0 \frac{\partial \Delta \ddot{\mathbf{R}}_0}{\partial \mathbf{R}_0} \frac{\partial \mathbf{R}_0}{\partial \mu_k} \\ &= \mathbf{Q}_{ki} - \mathbf{Q}_{0i} - \frac{1}{\mu_B} \left(\Delta \ddot{\mathbf{R}}_k - \Delta \ddot{\mathbf{R}}_0 \right) - \frac{\partial \mathbf{Q}_{0i}}{\partial \mathbf{R}_0} (\mathbf{R}_k - \mathbf{R}_0) + \frac{1}{\mu_B} \frac{\partial \Delta \ddot{\mathbf{R}}_0}{\partial \mathbf{R}_0} (\mathbf{R}_k - \mathbf{R}_0) \\ &= \mathbf{Q}_{ki} - \mathbf{Q}_{0i} - \frac{1}{\mu_B} \left(\Delta \ddot{\mathbf{R}}_k - \Delta \ddot{\mathbf{R}}_0 \right) + \left[\frac{1}{\mu_B} \frac{\partial \Delta \ddot{\mathbf{R}}_0}{\partial \mathbf{R}_0} - \frac{\partial \mathbf{Q}_{0i}}{\partial \mathbf{R}_0} \right] (\mathbf{R}_k - \mathbf{R}_0) \,, \end{aligned} \tag{2.179}$$

where $\frac{\partial \Delta \ddot{\mathbf{R}}_0}{\partial \mathbf{R}_0}$ are given by (2.161) and $\frac{\partial \mathbf{Q}_{0i}}{\partial \mathbf{R}_0}$ are given in section 2.6.1.

Computation of $\frac{\partial \ddot{\mathbf{R}}_i}{\partial \mu_k}$ in the case $k = n+1, ..., m$

By differentiation of the equations of motion (2.72) with respect to the gravitational parameters of the perturbers μ_k, $k = n+1, ..., m$, we have

$$\frac{\partial \ddot{\mathbf{R}}_i}{\partial \mu_k} = \frac{\partial}{\partial \mu_k} \sum_{\substack{j=0 \\ j \neq i}}^{n} \mu_j \mathbf{Q}_{ji} + \frac{\partial \Delta \ddot{\mathbf{R}}_i}{\partial \mu_k} + \frac{\partial \ddot{\mathbf{R}}_B}{\partial \mu_k} , \qquad \left\{ \begin{array}{l} k = n+1, ..., m \\ i = 1, ..., n \end{array} \right. . \tag{2.180}$$

Treating term by term we have

$$\frac{\partial}{\partial \mu_k} \sum_{\substack{j=0 \\ j \neq i}}^{n} \mu_j \mathbf{Q}_{ji} = \mathbf{0}_{3\times 1} . \tag{2.181}$$

For $\frac{\partial \Delta \ddot{\mathbf{R}}_i}{\partial \mu_k}$

$$\frac{\partial \Delta \ddot{\mathbf{R}}_i}{\partial \mu_k} = \frac{\partial}{\partial \mu_k} \left[\sum_{j=n+1}^{n+m} \mu_j \mathbf{Q}_{ji} \right] = \mathbf{Q}_{ki} , \tag{2.182}$$

and finally for $\frac{\partial \ddot{\mathbf{R}}_B}{\partial \mu_k}$

$$\begin{aligned} \frac{\partial \ddot{\mathbf{R}}_B}{\partial \mu_k} &= \frac{\partial}{\partial \mu_k} \left[-\frac{1}{\mu_B} \sum_{j=0}^{n} \mu_j \Delta \ddot{\mathbf{R}}_j \right] \\ &= -\frac{1}{\mu_B} \sum_{j=0}^{n} \mu_j \frac{\partial \Delta \ddot{\mathbf{R}}_j}{\partial \mu_k} = -\frac{1}{\mu_B} \sum_{j=0}^{n} \mu_j \mathbf{Q}_{kj} . \end{aligned} \tag{2.183}$$

So equations (2.180) become

$$\frac{\partial \ddot{\mathbf{R}}_i}{\partial \mu_k} = \mathbf{Q}_{ki} - \frac{1}{\mu_B} \sum_{j=0}^{n} \mu_j \mathbf{Q}_{kj} , \qquad \left\{ \begin{array}{l} k = n+1, ..., m \\ i = 1, ..., n \end{array} \right. . \tag{2.184}$$

Computation of $\frac{\partial \ddot{\mathbf{R}}_i}{\partial \mu_B}$

By differentiation of the equations of motion (2.72) with respect to the gravitational parameters μ_B of the planet-satellites system we have

$$\frac{\partial \ddot{\mathbf{R}}_i}{\partial \mu_B} = \frac{\partial}{\partial \mu_B} \sum_{\substack{j=0 \\ j \neq i}}^{n} \mu_j \mathbf{Q}_{ji} + \frac{\partial \Delta \ddot{\mathbf{R}}_i}{\partial \mu_B} + \frac{\partial \ddot{\mathbf{R}}_B}{\partial \mu_B} , \qquad i = 1, ..., n . \tag{2.185}$$

As in the previous computations, treating term by term we have

$$\begin{aligned} \frac{\partial}{\partial \mu_B} \sum_{\substack{j=0 \\ j \neq i}}^{n} \mu_j \mathbf{Q}_{ji} &= \frac{\partial \mu_0}{\partial \mu_B} \mathbf{Q}_{0i} + \mu_0 \frac{\partial \mathbf{Q}_{0i}}{\partial \mu_B} + \sum_{\substack{j=1 \\ j \neq i}}^{n} \frac{\partial \mu_j}{\partial \mu_B} \mathbf{Q}_{ji} + \sum_{\substack{j=1 \\ j \neq i}}^{n} \mu_j \frac{\partial \mathbf{Q}_{ji}}{\partial \mu_B} \\ &= \mathbf{Q}_{0i} + \mu_0 \frac{\partial \mathbf{Q}_{0i}}{\partial \mu_B} , \end{aligned} \tag{2.186}$$

because of

$$\frac{\partial \mu_0}{\partial \mu_B} = 1 , \tag{2.187}$$

$$\frac{\partial \mu_j}{\partial \mu_B} = 0 , \tag{2.188}$$

and $\frac{\partial \mathbf{Q}_{ji}}{\partial \mu_B} = \mathbf{0}$ (because of the quantity $\mathbf{Q}_{ji}$, by definition, are indipendet from any μ_k and also from μ_B) for $j = 1, ..., n$. Then

$$\frac{\partial \Delta\ddot{\mathbf{R}}_i}{\partial \mu_B} = \frac{\partial}{\partial \mu_B}\left(\sum_{j=n+1}^{n+m} \mu_j \mathbf{Q}_{ji}\right) = \mathbf{0}_{3\times 1}\,, \tag{2.189}$$

$$\frac{\partial \Delta\ddot{\mathbf{R}}_0}{\partial \mu_B} = \sum_{j=n+1}^{n+m} \mu_j \frac{\partial \mathbf{Q}_{j0}}{\partial \mu_B} = \frac{\partial \Delta\ddot{\mathbf{R}}_0}{\partial \mathbf{R}_0}\frac{\partial \mathbf{R}_0}{\partial \mu_B}\,, \tag{2.190}$$

and then

$$\begin{aligned}\frac{\partial \ddot{\mathbf{R}}_B}{\partial \mu_B} &= \frac{\partial}{\partial \mu_B}\left[-\frac{1}{\mu_B}\sum_{k=0}^{n} \mu_k \Delta\ddot{\mathbf{R}}_k\right] \\ &= \sum_{k=0}^{n} \mu_k \Delta\ddot{\mathbf{R}}_k \frac{\partial}{\partial \mu_B}\left(-\frac{1}{\mu_B}\right) - \frac{1}{\mu_B}\frac{\partial}{\partial \mu_B}\left(\sum_{k=0}^{n} \mu_k \Delta\ddot{\mathbf{R}}_k\right)\,. \end{aligned} \tag{2.191}$$

Developing the terms we have

$$\frac{\partial}{\partial \mu_B}\left(-\frac{1}{\mu_B}\right) = \frac{1}{\mu_B^2}\,, \tag{2.192}$$

and

$$\begin{aligned}\frac{\partial}{\partial \mu_B}\left(\sum_{k=0}^{n} \mu_k \Delta\ddot{\mathbf{R}}_k\right) &= \frac{\partial}{\partial \mu_B}\left(\mu_0 \Delta\ddot{\mathbf{R}}_0\right) + \frac{\partial}{\partial \mu_B}\sum_{k=1}^{n} \mu_k \Delta\ddot{\mathbf{R}}_k \\ &= \frac{\partial \mu_0}{\partial \mu_B}\Delta\ddot{\mathbf{R}}_0 + \mu_0 \frac{\partial \Delta\ddot{\mathbf{R}}_0}{\partial \mu_B} + \sum_{k=1}^{n}\left(\frac{\partial \mu_k}{\partial \mu_B}\Delta\ddot{\mathbf{R}}_k + \mu_k \frac{\partial \Delta\ddot{\mathbf{R}}_k}{\partial \mu_B}\right) \qquad (2.193) \\ &= \Delta\ddot{\mathbf{R}}_0 + \mu_0 \frac{\partial \Delta\ddot{\mathbf{R}}_0}{\partial \mu_B}\,, \qquad (2.194)\end{aligned}$$

where we have used (2.187), (2.188) and (2.189).

So $\frac{\partial \ddot{\mathbf{R}}_B}{\partial \mu_B}$ becomes

$$\begin{aligned}\frac{\partial \ddot{\mathbf{R}}_B}{\partial \mu_B} &= \frac{1}{\mu_B^2}\sum_{k=0}^{n} \mu_k \Delta\ddot{\mathbf{R}}_k - \frac{1}{\mu_B}\left(\Delta\ddot{\mathbf{R}}_0 + \mu_0 \frac{\partial \Delta\ddot{\mathbf{R}}_0}{\partial \mu_B}\right) \\ &= -\frac{1}{\mu_B}\ddot{\mathbf{R}}_B - \frac{1}{\mu_B}\Delta\ddot{\mathbf{R}}_0 - \frac{\mu_0}{\mu_B}\frac{\partial \Delta\ddot{\mathbf{R}}_0}{\partial \mu_B} \\ &= -\frac{\ddot{\mathbf{R}}_B + \Delta\ddot{\mathbf{R}}_0}{\mu_B} - \frac{\mu_0}{\mu_B}\frac{\partial \Delta\ddot{\mathbf{R}}_0}{\partial \mu_B}\,, \end{aligned} \tag{2.195}$$

where we have used (2.76) and the partials $\frac{\partial \Delta\ddot{\mathbf{R}}_0}{\partial \mu_B}$ are given by (2.190). Remain to develop the terms $\frac{\partial \mathbf{Q}_{0i}}{\partial \mu_B}$ and $\frac{\partial \mathbf{Q}_{j0}}{\partial \mu_B}$. Using the chain rule we have

$$\frac{\partial \mathbf{Q}_{0i}}{\partial \mu_B} = \frac{\partial \mathbf{Q}_{0i}}{\partial \mathbf{R}_0}\frac{\partial \mathbf{R}_0}{\partial \mu_B} = -\frac{1}{\mu_0}\frac{\partial \mathbf{Q}_{0i}}{\partial \mathbf{R}_0}\mathbf{R}_0\,, \tag{2.196}$$

$$\frac{\partial \mathbf{Q}_{j0}}{\partial \mu_B} = \frac{\partial \mathbf{Q}_{j0}}{\partial \mathbf{R}_0}\frac{\partial \mathbf{R}_0}{\partial \mu_B} = -\frac{1}{\mu_0}\frac{\partial \mathbf{Q}_{j0}}{\partial \mathbf{R}_0}\mathbf{R}_0\,, \tag{2.197}$$

So at last, putting the (2.186), (2.189), (2.195) into (2.185) and using (2.196) and (2.170) we have

$$\begin{aligned}
\frac{\partial \ddot{\mathbf{R}}_i}{\partial \mu_B} &= \mathbf{Q}_{0i} + \mu_0 \frac{\partial \mathbf{Q}_{0i}}{\partial \mu_B} - \frac{\ddot{\mathbf{R}}_B + \Delta\ddot{\mathbf{R}}_0}{\mu_B} - \frac{\mu_0}{\mu_B}\frac{\partial \Delta\ddot{\mathbf{R}}_0}{\partial \mu_B} \\
&= \mathbf{Q}_{0i} - \frac{\partial \mathbf{Q}_{0i}}{\partial \mathbf{R}_0}\mathbf{R}_0 - \frac{\ddot{\mathbf{R}}_B + \Delta\ddot{\mathbf{R}}_0}{\mu_B} - \frac{\mu_0}{\mu_B}\frac{\partial \Delta\ddot{\mathbf{R}}_0}{\partial \mathbf{R}_0}\frac{\partial \mathbf{R}_0}{\partial \mu_B} \\
&= \mathbf{Q}_{0i} - \frac{\partial \mathbf{Q}_{0i}}{\partial \mathbf{R}_0}\mathbf{R}_0 - \frac{\ddot{\mathbf{R}}_B + \Delta\ddot{\mathbf{R}}_0}{\mu_B} + \frac{1}{\mu_B}\frac{\partial \Delta\ddot{\mathbf{R}}_0}{\partial \mathbf{R}_0}\mathbf{R}_0 \\
&= \mathbf{Q}_{0i} - \frac{\ddot{\mathbf{R}}_B + \Delta\ddot{\mathbf{R}}_0}{\mu_B} - \left(\frac{\partial \mathbf{Q}_{0i}}{\partial \mathbf{R}_0} - \frac{1}{\mu_B}\frac{\partial \Delta\ddot{\mathbf{R}}_0}{\partial \mathbf{R}_0}\right)\mathbf{R}_0 \,, \qquad (2.198)
\end{aligned}$$

where $\frac{\partial \Delta\ddot{\mathbf{R}}_0}{\partial \mathbf{R}_0}$ are given by (2.161) and $\frac{\partial \mathbf{Q}_{0i}}{\partial \mathbf{R}_0}$ are given in section 2.6.1.

2.6.4 Computation of $\frac{\partial \mathbf{G}_{ij}^{BF}}{\partial \mathbf{r}_{ji}^{BF}}$ partials

It is necessary now to compute the partials $\frac{\partial \mathbf{G}_{ij}^{BF}}{\partial \mathbf{r}_{ji}^{BF}}$ which we have met in sections 2.6.1. Recalling that (see equation (2.82))

$$\mathbf{G}_{ij}^{BF} = \frac{1}{\mu_j}\left(\frac{\partial \mathcal{U}_j}{\partial \mathbf{r}_{ji}^{BF}}\right)^T \,, \qquad (2.199)$$

we have that

$$\frac{\partial \mathbf{G}_{ij}^{BF}}{\partial \mathbf{r}_{ji}^{BF}} = \frac{1}{\mu_j}\frac{\partial}{\partial \mathbf{r}_{ji}^{BF}}\left(\frac{\partial \mathcal{U}_j}{\partial \mathbf{r}_{ji}^{BF}}\right)^T \,, \qquad (2.200)$$

where $\mathcal{U}_j$ is given by (2.10) that is

$$\mathcal{U}_j\left(r_{ji}, \varphi_i, \lambda_i\right) = \frac{\mu_j}{r_{ji}}\sum_{l=2}^{\infty}\sum_{m=0}^{l}\left(\frac{R_e^j}{r_{ji}}\right)^l \left[\mathcal{C}_{lm}^j \cos m\lambda_i + \mathcal{S}_{lm}^j \sin m\lambda_i\right] P_l^m\left(\sin\varphi_i\right) \,. \qquad (2.201)$$

As in section 2.3.1, for simplicity of notation in the following we omit the index i and j so $\mathbf{r}_{ji} \to \mathbf{r}$, $r_{ji} \to r$, $\varphi_i \to \varphi$, $\lambda_i \to \lambda$, $\mu_j \to \mu$, $\mathcal{C}_{lm}^j \to \mathcal{C}_{lm}$, $\mathcal{S}_{lm}^j \to \mathcal{S}_{lm}$, $R_e^j \to R_e$ and $\mathcal{U}_j \to \mathcal{U}$. Since $\mathcal{U}_j$ is expressed in polar coordinates, applying the chain rule to (2.13) we have [8]

$$\begin{aligned}
\frac{\partial}{\partial \mathbf{r}}\left(\frac{\partial \mathcal{U}}{\partial \mathbf{r}}\right)^T &= \frac{\partial}{\partial \mathbf{r}}\left[\left(\frac{\partial r}{\partial \mathbf{r}}\right)^T \frac{\partial \mathcal{U}}{\partial r} + \left(\frac{\partial \varphi}{\partial \mathbf{r}}\right)^T \frac{\partial \mathcal{U}}{\partial \varphi} + \left(\frac{\partial \lambda}{\partial \mathbf{r}}\right)^T \frac{\partial \mathcal{U}}{\partial \lambda}\right] \\
&= \frac{\partial}{\partial \mathbf{r}}\left(\frac{\partial r}{\partial \mathbf{r}}\right)^T \frac{\partial \mathcal{U}}{\partial r} + \frac{\partial}{\partial \mathbf{r}}\left(\frac{\partial \varphi}{\partial \mathbf{r}}\right)^T \frac{\partial \mathcal{U}}{\partial \varphi} + \frac{\partial}{\partial \mathbf{r}}\left(\frac{\partial \lambda}{\partial \mathbf{r}}\right)^T \frac{\partial \mathcal{U}}{\partial \lambda} \\
&\quad + \left(\frac{\partial r}{\partial \mathbf{r}}\right)^T \frac{\partial}{\partial \mathbf{r}}\frac{\partial \mathcal{U}}{\partial r} + \left(\frac{\partial \varphi}{\partial \mathbf{r}}\right)^T \frac{\partial}{\partial \mathbf{r}}\frac{\partial \mathcal{U}}{\partial \varphi} + \left(\frac{\partial \lambda}{\partial \mathbf{r}}\right)^T \frac{\partial}{\partial \mathbf{r}}\frac{\partial \mathcal{U}}{\partial \lambda} \,, \qquad (2.202)
\end{aligned}$$

which can be rewrite in a simpler form as

$$\begin{aligned}
\frac{\partial}{\partial \mathbf{r}}\left(\frac{\partial \mathcal{U}}{\partial \mathbf{r}}\right)^T &= \frac{\partial}{\partial \mathbf{r}}\left(\frac{\partial r}{\partial \mathbf{r}}\right)^T \frac{\partial \mathcal{U}}{\partial r} + \frac{\partial}{\partial \mathbf{r}}\left(\frac{\partial \varphi}{\partial \mathbf{r}}\right)^T \frac{\partial \mathcal{U}}{\partial \varphi} + \frac{\partial}{\partial \mathbf{r}}\left(\frac{\partial \lambda}{\partial \mathbf{r}}\right)^T \frac{\partial \mathcal{U}}{\partial \lambda} \\
&\quad + \left(\frac{\partial r}{\partial \mathbf{r}}\right)^T \left[\frac{\partial^2 \mathcal{U}}{\partial r^2}\frac{\partial r}{\partial \mathbf{r}} + \frac{\partial^2 \mathcal{U}}{\partial r\,\partial \varphi}\frac{\partial \varphi}{\partial \mathbf{r}} + \frac{\partial^2 \mathcal{U}}{\partial r\,\partial \lambda}\frac{\partial \lambda}{\partial \mathbf{r}}\right] \\
&\quad + \left(\frac{\partial \varphi}{\partial \mathbf{r}}\right)^T \left[\frac{\partial^2 \mathcal{U}}{\partial \varphi\,\partial r}\frac{\partial r}{\partial \mathbf{r}} + \frac{\partial^2 \mathcal{U}}{\partial \varphi^2}\frac{\partial \varphi}{\partial \mathbf{r}} + \frac{\partial^2 \mathcal{U}}{\partial \varphi\,\partial \lambda}\frac{\partial \lambda}{\partial \mathbf{r}}\right] \\
&\quad + \left(\frac{\partial \lambda}{\partial \mathbf{r}}\right)^T \left[\frac{\partial^2 \mathcal{U}}{\partial \lambda\,\partial r}\frac{\partial r}{\partial \mathbf{r}} + \frac{\partial^2 \mathcal{U}}{\partial \lambda\,\partial \varphi}\frac{\partial \varphi}{\partial \mathbf{r}} + \frac{\partial^2 \mathcal{U}}{\partial \lambda^2}\frac{\partial \lambda}{\partial \mathbf{r}}\right] \,. \qquad (2.203)
\end{aligned}$$

If we define the matrix $\mathbf{F}$ as

$$\mathbf{F} = \begin{pmatrix} \frac{\partial r}{\partial \mathbf{r}} \\ \frac{\partial \varphi}{\partial \mathbf{r}} \\ \frac{\partial \lambda}{\partial \mathbf{r}} \end{pmatrix} = \begin{pmatrix} \frac{\partial r}{\partial x} & \frac{\partial r}{\partial y} & \frac{\partial r}{\partial z} \\ \frac{\partial \varphi}{\partial x} & \frac{\partial \varphi}{\partial y} & \frac{\partial \varphi}{\partial z} \\ \frac{\partial \lambda}{\partial x} & \frac{\partial \lambda}{\partial y} & \frac{\partial \lambda}{\partial z} \end{pmatrix}, \tag{2.204}$$

equivalent to the Jacobian matrix of transformation from polar coordinates to cartesian coordinates and define the matrix $\mathbf{E}$

$$\mathbf{E} = \begin{pmatrix} \frac{\partial^2 \mathcal{U}}{\partial r^2} & \frac{\partial^2 \mathcal{U}}{\partial r \, \partial \varphi} & \frac{\partial^2 \mathcal{U}}{\partial r \, \partial \lambda} \\ \frac{\partial^2 \mathcal{U}}{\partial \varphi \, \partial r} & \frac{\partial^2 \mathcal{U}}{\partial \varphi^2} & \frac{\partial^2 \mathcal{U}}{\partial \varphi \, \partial \lambda} \\ \frac{\partial^2 \mathcal{U}}{\partial \lambda \, \partial r} & \frac{\partial^2 \mathcal{U}}{\partial \lambda \, \partial \varphi} & \frac{\partial^2 \mathcal{U}}{\partial \lambda^2} \end{pmatrix}, \tag{2.205}$$

equivalent to the Hessian matrix of the potential in polar coordinates, we can rewrite the equation (2.203) in compact notation as

$$\frac{\partial}{\partial \mathbf{r}} \left(\frac{\partial \mathcal{U}}{\partial \mathbf{r}} \right)^T = \frac{\partial}{\partial \mathbf{r}} \left(\frac{\partial r}{\partial \mathbf{r}} \right)^T \frac{\partial \mathcal{U}}{\partial r} + \frac{\partial}{\partial \mathbf{r}} \left(\frac{\partial \varphi}{\partial \mathbf{r}} \right)^T \frac{\partial \mathcal{U}}{\partial \varphi} + \frac{\partial}{\partial \mathbf{r}} \left(\frac{\partial \lambda}{\partial \mathbf{r}} \right)^T \frac{\partial \mathcal{U}}{\partial \lambda} + \mathbf{F}^T \, \mathbf{E} \, \mathbf{F} \, . \tag{2.206}$$

We make clear that the partials just obtained are computed in the body fixed reference frame. The partials of the gravitational potential that we have not still computed are then

$$\frac{\partial^2 \mathcal{U}}{\partial r^2} = \frac{\mu}{r^3} \sum_{l=2}^{\infty} \sum_{m=0}^{l} (l+1)(l+2) \left(\frac{R_e}{r} \right)^l \left[\mathcal{C}_{lm} \cos m\lambda + \mathcal{S}_{lm} \sin m\lambda \right] P_l^m (\sin \varphi) \, , \tag{2.207}$$

$$\frac{\partial^2 \mathcal{U}}{\partial \lambda^2} = -\frac{\mu}{r} \sum_{l=2}^{\infty} \sum_{m=0}^{l} m^2 \left(\frac{R_e}{r} \right)^l \left[\mathcal{C}_{lm} \cos m\lambda + \mathcal{S}_{lm} \sin m\lambda \right] P_l^m (\sin \varphi) \, , \tag{2.208}$$

$$\begin{aligned} \frac{\partial^2 \mathcal{U}}{\partial \varphi^2} &= \frac{\mu}{r} \sum_{l=2}^{\infty} \sum_{m=0}^{l} \left(\frac{R_e}{r} \right)^l \left[\mathcal{C}_{lm} \cos m\lambda + \mathcal{S}_{lm} \sin m\lambda \right] \frac{\partial^2}{\partial \varphi^2} \left[P_l^m (\sin \varphi) \right] \\ &= \frac{\mu}{r} \sum_{l=2}^{\infty} \sum_{m=0}^{l} \left(\frac{R_e}{r} \right)^l \left\{ \begin{array}{c} \left[\mathcal{C}_{lm} \cos m\lambda + \mathcal{S}_{lm} \sin m\lambda \right] \times \\ \left\{ \begin{array}{c} -\frac{m}{\cos^2 \varphi} P_l^m (\sin \varphi) + m^2 \tan^2 \varphi P_l^m (\sin \varphi) \\ -(2m+1) \tan \varphi P_l^{m+1} (\sin \varphi) + P_l^{m+2} (\sin \varphi) \end{array} \right\} \end{array} \right\} , \end{aligned} \tag{2.209}$$

$$\begin{aligned} \frac{\partial^2 \mathcal{U}}{\partial r \partial \varphi} &= -\frac{\mu}{r^2} \sum_{l=2}^{\infty} \sum_{m=0}^{l} (l+1) \left(\frac{R_e}{r} \right)^l \left[\mathcal{C}_{lm} \cos m\lambda + \mathcal{S}_{lm} \sin m\lambda \right] \frac{\partial}{\partial \varphi} P_l^m (\sin \varphi) \\ &= -\frac{\mu}{r^2} \sum_{l=2}^{\infty} \sum_{m=0}^{l} (l+1) \left(\frac{R_e}{r} \right)^l \left\{ \begin{array}{c} \left[\mathcal{C}_{lm} \cos m\lambda + \mathcal{S}_{lm} \sin m\lambda \right] \times \\ \left[-m \tan \varphi P_l^m (\sin \varphi) + P_l^{m+1} (\sin \varphi) \right] \end{array} \right\} , \end{aligned} \tag{2.210}$$

$$\frac{\partial^2 \mathcal{U}}{\partial r \partial \lambda} = -\frac{\mu}{r^2} \sum_{l=2}^{\infty} \sum_{m=0}^{l} m \, (l+1) \left(\frac{R_e}{r} \right)^l \left[-\mathcal{C}_{lm} \sin m\lambda + \mathcal{S}_{lm} \cos m\lambda \right] P_l^m (\sin \varphi) \, , \tag{2.211}$$

$$\frac{\partial^2 \mathcal{U}}{\partial \varphi \partial \lambda} = \frac{\mu}{r} \sum_{l=2}^{\infty} \sum_{m=0}^{l} \left(\frac{R_e}{r} \right)^l \left\{ \begin{array}{c} m \left[-\mathcal{C}_{lm} \sin m\lambda + \mathcal{S}_{lm} \cos m\lambda \right] \times \\ \left[-m \tan \varphi P_l^m (\sin \varphi) + P_l^{m+1} (\sin \varphi) \right] \end{array} \right\} , \tag{2.212}$$

whereas for the partials with respect to the coordinates we have

$$\begin{aligned} \frac{\partial}{\partial \mathbf{r}} \left(\frac{\partial r}{\partial \mathbf{r}} \right)^T &= \frac{\partial}{\partial \mathbf{r}} \left(\frac{\mathbf{r}}{r} \right) = \frac{1}{r^2} \left[\frac{\partial \mathbf{r}}{\partial \mathbf{r}} \, r - \mathbf{r} \frac{\partial r}{\partial \mathbf{r}} \right] \\ &= \frac{1}{r^2} \left[\mathbf{I} \, r - \mathbf{r} \left(\frac{\mathbf{r}}{r} \right)^T \right] \\ &= \frac{1}{r} \left[\mathbf{I} - \frac{\mathbf{r} \, \mathbf{r}^T}{r^2} \right] , \end{aligned} \tag{2.213}$$

$$\frac{\partial}{\partial \mathbf{r}}\left(\frac{\partial \varphi}{\partial \mathbf{r}}\right)^T = -\frac{1}{r^2}\frac{1}{(x^2+y^2)^{1/2}}\left[\mathbf{I}\, z + \mathbf{r}\frac{\partial z}{\partial \mathbf{r}} - 2\frac{z}{r^2}\mathbf{r}\,\mathbf{r}^T\right] - \frac{1}{(x^2+y^2)^{3/2}}\left[\left(\frac{\partial z}{\partial \mathbf{r}}\right)^T - \mathbf{r}\frac{z}{r^2}\right]\left[x\frac{\partial x}{\partial \mathbf{r}} + y\frac{\partial y}{\partial \mathbf{r}}\right], \tag{2.214}$$

$$\frac{\partial}{\partial \mathbf{r}}\left(\frac{\partial \lambda}{\partial \mathbf{r}}\right)^T = \frac{1}{(x^2+y^2)}\left[\left(\frac{\partial y}{\partial \mathbf{r}}\right)^T\frac{\partial x}{\partial \mathbf{r}} - \left(\frac{\partial x}{\partial \mathbf{r}}\right)^T\frac{\partial y}{\partial \mathbf{r}}\right] - \frac{2}{(x^2+y^2)^2}\left[\left(\frac{\partial y}{\partial \mathbf{r}}\right)^T x - \left(\frac{\partial x}{\partial \mathbf{r}}\right)^T y\right]\left[x\frac{\partial x}{\partial \mathbf{r}} + y\frac{\partial y}{\partial \mathbf{r}}\right]. \tag{2.215}$$

The matrices, in explicit form are

$$\frac{\partial}{\partial \mathbf{r}}\left(\frac{\partial r}{\partial \mathbf{r}}\right)^T = \frac{\partial}{\partial \mathbf{r}}\begin{pmatrix} \frac{\partial r}{\partial x} \\ \frac{\partial r}{\partial y} \\ \frac{\partial r}{\partial z} \end{pmatrix} = \begin{pmatrix} \frac{\partial^2 r}{\partial x^2} & \frac{\partial^2 r}{\partial y \partial x} & \frac{\partial^2 r}{\partial z \partial x} \\ \frac{\partial^2 r}{\partial x \partial y} & \frac{\partial^2 r}{\partial y^2} & \frac{\partial^2 r}{\partial z \partial y} \\ \frac{\partial^2 r}{\partial x \partial z} & \frac{\partial^2 r}{\partial y \partial z} & \frac{\partial^2 r}{\partial z^2} \end{pmatrix}, \tag{2.216}$$

$$\frac{\partial}{\partial \mathbf{r}}\left(\frac{\partial \varphi}{\partial \mathbf{r}}\right)^T = \frac{\partial}{\partial \mathbf{r}}\begin{pmatrix} \frac{\partial \varphi}{\partial x} \\ \frac{\partial \varphi}{\partial y} \\ \frac{\partial \varphi}{\partial z} \end{pmatrix} = \begin{pmatrix} \frac{\partial^2 \varphi}{\partial x^2} & \frac{\partial^2 \varphi}{\partial y \partial x} & \frac{\partial^2 \varphi}{\partial z \partial x} \\ \frac{\partial^2 \varphi}{\partial x \partial y} & \frac{\partial^2 \varphi}{\partial y^2} & \frac{\partial^2 \varphi}{\partial z \partial y} \\ \frac{\partial^2 \varphi}{\partial x \partial z} & \frac{\partial^2 \varphi}{\partial y \partial z} & \frac{\partial^2 \varphi}{\partial z^2} \end{pmatrix}, \tag{2.217}$$

$$\frac{\partial}{\partial \mathbf{r}}\left(\frac{\partial \lambda}{\partial \mathbf{r}}\right)^T = \frac{\partial}{\partial \mathbf{r}}\begin{pmatrix} \frac{\partial \lambda}{\partial x} \\ \frac{\partial \lambda}{\partial y} \\ \frac{\partial \lambda}{\partial z} \end{pmatrix} = \begin{pmatrix} \frac{\partial^2 \lambda}{\partial x^2} & \frac{\partial^2 \lambda}{\partial y \partial x} & \frac{\partial^2 \lambda}{\partial z \partial x} \\ \frac{\partial^2 \lambda}{\partial x \partial y} & \frac{\partial^2 \lambda}{\partial y^2} & \frac{\partial^2 \lambda}{\partial z \partial y} \\ \frac{\partial^2 \lambda}{\partial x \partial z} & \frac{\partial^2 \lambda}{\partial y \partial z} & \frac{\partial^2 \lambda}{\partial z^2} \end{pmatrix}, \tag{2.218}$$

and the partials are

$$\frac{\partial^2 r}{\partial x^2} = \frac{1}{r}\left(1 - \frac{x^2}{r^2}\right), \qquad \frac{\partial^2 r}{\partial y^2} = \frac{1}{r}\left(1 - \frac{y^2}{r^2}\right), \qquad \frac{\partial^2 r}{\partial z^2} = \frac{1}{r}\left(1 - \frac{z^2}{r^2}\right), \tag{2.219}$$

$$\frac{\partial^2 r}{\partial x \partial y} = \frac{\partial^2 r}{\partial y \partial x} = -\frac{xy}{r^3}, \qquad \frac{\partial^2 r}{\partial z \partial y} = \frac{\partial^2 r}{\partial y \partial z} = -\frac{yz}{r^3}, \qquad \frac{\partial^2 r}{\partial z \partial x} = \frac{\partial^2 r}{\partial x \partial z} = -\frac{xz}{r^3}, \tag{2.220}$$

$$\frac{\partial^2 \varphi}{\partial x^2} = -\frac{1}{r^2}\left[\frac{1}{(x^2+y^2)^{1/2}}\left(z - 2\frac{z}{r^2}x^2\right) - \frac{zx^2}{(x^2+y^2)^{3/2}}\right], \tag{2.221}$$

$$\frac{\partial^2 \varphi}{\partial y^2} = -\frac{1}{r^2}\left[\frac{1}{(x^2+y^2)^{1/2}}\left(z - 2\frac{z}{r^2}y^2\right) - \frac{zy^2}{(x^2+y^2)^{3/2}}\right], \tag{2.222}$$

$$\frac{\partial^2 \varphi}{\partial x \partial y} = \frac{\partial^2 \varphi}{\partial y \partial x} = \frac{zxy}{r^2}\left[\frac{2}{r^2}\frac{1}{(x^2+y^2)^{1/2}} + \frac{1}{(x^2+y^2)^{3/2}}\right], \tag{2.223}$$

$$\frac{\partial^2 \varphi}{\partial z^2} = -\frac{1}{r^2}\frac{1}{(x^2+y^2)^{1/2}}\left(2z - 2\frac{z^3}{r^2}\right), \tag{2.224}$$

$$\frac{\partial^2 \varphi}{\partial x \partial z} = \frac{\partial^2 \varphi}{\partial z \partial x} = -\frac{1}{r^2}\frac{x}{(x^2+y^2)^{1/2}}\left(1 - 2\frac{z^2}{r^2}\right), \tag{2.225}$$

$$\frac{\partial^2 \varphi}{\partial y \partial z} = \frac{\partial^2 \varphi}{\partial z \partial y} = -\frac{1}{r^2}\frac{y}{(x^2+y^2)^{1/2}}\left(1 - 2\frac{z^2}{r^2}\right), \tag{2.226}$$

$$\frac{\partial^2 \lambda}{\partial x^2} = \frac{2}{(x^2+y^2)^2}yx, \qquad \frac{\partial^2 \lambda}{\partial y^2} = -\frac{2}{(x^2+y^2)^2}yx, \tag{2.227}$$

$$\frac{\partial^2\lambda}{\partial x\partial y} = \frac{\partial^2\lambda}{\partial y\partial x} = -\frac{1}{x^2+y^2} + \frac{2}{\left(x^2+y^2\right)^2}y^2\,, \tag{2.228}$$

$$\frac{\partial^2\lambda}{\partial z^2} = \frac{\partial^2\lambda}{\partial z\partial y} = \frac{\partial^2\lambda}{\partial y\partial z} = \frac{\partial^2\lambda}{\partial x\partial z} = \frac{\partial^2\lambda}{\partial z\partial x} = 0\,. \tag{2.229}$$

Case of an oblate body

As for the equations of motion, in the case of an oblate body we have rotational simmetry ($m = 0$ and no dependence of the potential from λ, that is $\mathcal{U}_{obl} = \mathcal{U}_{obl}\left(r,\varphi\right)$) and so we can simplify the expression of the partials so that

$$\begin{aligned}\frac{\partial}{\partial\mathbf{r}}\left(\frac{\partial\mathcal{U}_{obl}\left(r,\varphi\right)}{\partial\mathbf{r}}\right)^T &= \frac{\partial}{\partial\mathbf{r}}\left[\left(\frac{\partial r}{\partial\mathbf{r}}\right)^T\frac{\partial\mathcal{U}_{obl}}{\partial r} + \left(\frac{\partial\varphi}{\partial\mathbf{r}}\right)^T\frac{\partial\mathcal{U}_{obl}}{\partial\varphi}\right]\\ &= \frac{\partial}{\partial\mathbf{r}}\left(\frac{\partial r}{\partial\mathbf{r}}\right)^T\frac{\partial\mathcal{U}_{obl}}{\partial r} + \frac{\partial}{\partial\mathbf{r}}\left(\frac{\partial\varphi}{\partial\mathbf{r}}\right)^T\frac{\partial\mathcal{U}_{obl}}{\partial\varphi}\\ &\quad + \left(\frac{\partial r}{\partial\mathbf{r}}\right)^T\frac{\partial}{\partial\mathbf{r}}\frac{\partial\mathcal{U}_{obl}}{\partial r} + \left(\frac{\partial\varphi}{\partial\mathbf{r}}\right)^T\frac{\partial}{\partial\mathbf{r}}\frac{\partial\mathcal{U}_{obl}}{\partial\varphi}\,,\end{aligned} \tag{2.230}$$

which can be rewrite in a simpler form as

$$\begin{aligned}\frac{\partial}{\partial\mathbf{r}}\left(\frac{\partial\mathcal{U}_{obl}}{\partial\mathbf{r}}\right)^T &= \frac{\partial}{\partial\mathbf{r}}\left(\frac{\partial r}{\partial\mathbf{r}}\right)^T\frac{\partial\mathcal{U}_{obl}}{\partial r} + \frac{\partial}{\partial\mathbf{r}}\left(\frac{\partial\varphi}{\partial\mathbf{r}}\right)^T\frac{\partial\mathcal{U}_{obl}}{\partial\varphi}\\ &\quad + \left(\frac{\partial r}{\partial\mathbf{r}}\right)^T\left[\frac{\partial^2\mathcal{U}_{obl}}{\partial r^2}\frac{\partial r}{\partial\mathbf{r}} + \frac{\partial^2\mathcal{U}_{obl}}{\partial r\,\partial\varphi}\frac{\partial\varphi}{\partial\mathbf{r}}\right]\\ &\quad + \left(\frac{\partial\varphi}{\partial\mathbf{r}}\right)^T\left[\frac{\partial^2\mathcal{U}_{obl}}{\partial\varphi\,\partial r}\frac{\partial r}{\partial\mathbf{r}} + \frac{\partial^2\mathcal{U}_{obl}}{\partial\varphi^2}\frac{\partial\varphi}{\partial\mathbf{r}}\right]\,.\end{aligned} \tag{2.231}$$

If we define the matrix $\mathbf{F}_{obl}$ as

$$\mathbf{F}_{obl} = \begin{pmatrix}\frac{\partial r}{\partial\mathbf{r}}\\ \frac{\partial\varphi}{\partial\mathbf{r}}\end{pmatrix} = \begin{pmatrix}\frac{\partial r}{\partial x} & \frac{\partial r}{\partial y} & \frac{\partial r}{\partial z}\\ \frac{\partial\varphi}{\partial x} & \frac{\partial\varphi}{\partial y} & \frac{\partial\varphi}{\partial z}\end{pmatrix}\,, \tag{2.232}$$

equivalent to the Jacobian matrix of transformation from polar coordinates to cartesian coordinates and define the matrix $\mathbf{E}_{obl}$

$$\mathbf{E}_{obl} = \begin{pmatrix}\frac{\partial^2\mathcal{U}_{obl}}{\partial r^2} & \frac{\partial^2\mathcal{U}_{obl}}{\partial r\,\partial\varphi}\\ \frac{\partial^2\mathcal{U}_{obl}}{\partial\varphi\,\partial r} & \frac{\partial^2\mathcal{U}_{obl}}{\partial\varphi^2}\end{pmatrix}\,, \tag{2.233}$$

equivalent to the Hessian matrix of the potential in polar coordinates, we can rewrite the equation (2.231) in compact notation as

$$\frac{\partial}{\partial\mathbf{r}}\left(\frac{\partial\mathcal{U}_{obl}}{\partial\mathbf{r}}\right)^T = \frac{\partial}{\partial\mathbf{r}}\left(\frac{\partial r}{\partial\mathbf{r}}\right)^T\frac{\partial\mathcal{U}_{obl}}{\partial r} + \frac{\partial}{\partial\mathbf{r}}\left(\frac{\partial\varphi}{\partial\mathbf{r}}\right)^T\frac{\partial\mathcal{U}_{obl}}{\partial\varphi} + \mathbf{F}_{obl}^T\,\mathbf{E}_{obl}\mathbf{F}_{obl}\,. \tag{2.234}$$

We make clear that the partials only just obtained are computed in the body fixed reference frame. The partials of the gravitational potential are then

$$\begin{aligned}
\frac{\partial^2 \mathcal{U}_{obl}}{\partial r^2} &= \frac{\mu}{r^3}\sum_{l=2}^{\infty}(l+1)(l+2)\left(\frac{R_e}{r}\right)^l \mathcal{C}_{l0}P_l^0(\sin\varphi) \\
&= -\frac{\mu}{r^3}\sum_{l=2}^{\infty}(l+1)(l+2)\left(\frac{R_e}{r}\right)^l J_l P_l^0(\sin\varphi)\,, \qquad (2.235)\\
\frac{\partial^2 \mathcal{U}_{obl}}{\partial \varphi^2} &= \frac{\mu}{r}\sum_{l=2}^{\infty}\left(\frac{R_e}{r}\right)^l \mathcal{C}_{l0}\left[-\tan\varphi P_l^1(\sin\varphi)+P_l^2(\sin\varphi)\right] \\
&= -\frac{\mu}{r}\sum_{l=2}^{\infty}\left(\frac{R_e}{r}\right)^l J_l\left[-\tan\varphi P_l^1(\sin\varphi)+P_l^2(\sin\varphi)\right]\,, \qquad (2.236)\\
\frac{\partial^2 \mathcal{U}}{\partial r\partial \varphi} &= -\frac{\mu}{r^2}\sum_{l=2}^{\infty}(l+1)\left(\frac{R_e}{r}\right)^l \mathcal{C}_{l0}P_l^1(\sin\varphi) \\
&= \frac{\mu}{r^2}\sum_{l=2}^{\infty}(l+1)\left(\frac{R_e}{r}\right)^l J_l P_l^1(\sin\varphi)\,, \qquad (2.237)
\end{aligned}$$

whereas for the partials with respect to the coordinates we have

$$\begin{aligned}
\frac{\partial}{\partial \mathbf{r}}\left(\frac{\partial r}{\partial \mathbf{r}}\right)^T &= \frac{\partial}{\partial \mathbf{r}}\left(\frac{\mathbf{r}}{r}\right) = \frac{1}{r^2}\left[\frac{\partial \mathbf{r}}{\partial \mathbf{r}}\,r - \mathbf{r}\frac{\partial r}{\partial \mathbf{r}}\right] \\
&= \frac{1}{r^2}\left[\mathbf{I}\,r - \mathbf{r}\left(\frac{\mathbf{r}}{r}\right)^T\right] \\
&= \frac{1}{r}\left[\mathbf{I} - \frac{\mathbf{r}\,\mathbf{r}^T}{r^2}\right]\,, \qquad (2.238)\\
\frac{\partial}{\partial \mathbf{r}}\left(\frac{\partial \varphi}{\partial \mathbf{r}}\right)^T &= -\frac{1}{r^2}\frac{1}{(x^2+y^2)^{1/2}}\left[\mathbf{I}\,z + \mathbf{r}\frac{\partial z}{\partial \mathbf{r}} - 2\frac{z}{r^2}\mathbf{r}\,\mathbf{r}^T\right] \\
&\quad -\frac{1}{(x^2+y^2)^{3/2}}\left[\left(\frac{\partial z}{\partial \mathbf{r}}\right)^T - \mathbf{r}\frac{z}{r^2}\right]\left[x\frac{\partial x}{\partial \mathbf{r}} + y\frac{\partial y}{\partial \mathbf{r}}\right]\,. \qquad (2.239)
\end{aligned}$$

2.6.5 Partials with respect to $\mathcal{C}_{lm}, \mathcal{S}_{lm}, J_l$

If we set $\mathbf{p}_k = \left(\mathcal{C}_{lm}^k, \mathcal{S}_{lm}^k, J_l^k\right)$, $k = 0, ..., n$, where k indicates the non-spherical body that generates the gravitational field, differentiating the equations (2.72) with respect to $\mathbf{p}_k$ we have

$$\frac{\partial \ddot{\mathbf{R}}_i}{\partial \mathbf{p}_k} = \sum_{\substack{j=0\\ j\neq i}}^{n}\mu_j\frac{\partial \mathbf{Q}_{ji}}{\partial \mathbf{p}_k} + \frac{\partial \Delta\ddot{\mathbf{R}}_i}{\partial \mathbf{p}_k} + \frac{\partial \ddot{\mathbf{R}}_B}{\partial \mathbf{p}_k}\,, \qquad \left\{\begin{array}{l} i = 1, ..., n \\ k = 0, ..., n \end{array}\right. \,. \qquad (2.240)$$

Since, from equation (2.73), only $\mathbf{Q}_{ji}$ can depend on $\mathbf{p}_k$ throughout the functions $\mathbf{G}_{ij}$, we have that $\frac{\partial \mathbf{Q}_{ji}}{\partial \mathbf{p}_k}$ can be simplified as

$$\begin{aligned}
\frac{\partial \mathbf{Q}_{ji}}{\partial \mathbf{p}_k} &= \frac{\partial}{\partial \mathbf{p}_k}\left(\frac{\mathbf{R}_j - \mathbf{R}_i}{|\mathbf{R}_j - \mathbf{R}_i|^3} + \mathbf{G}_{ij} - \mathbf{G}_{ji}\right) \\
&= \delta_k^j\frac{\partial \mathbf{G}_{ij}}{\partial \mathbf{p}_k} - \delta_k^i\frac{\partial \mathbf{G}_{ji}}{\partial \mathbf{p}_k}\,, \qquad (2.241)
\end{aligned}$$

so, treating term by term the (2.240) and using (2.241) we have

$$\sum_{\substack{j=0\\ j\neq i}}^{n}\mu_j\frac{\partial \mathbf{Q}_{ji}}{\partial \mathbf{p}_k} = \sum_{\substack{j=0\\ j\neq i}}^{n}\mu_j\left(\delta_k^j\frac{\partial \mathbf{G}_{ij}}{\partial \mathbf{p}_k} - \delta_k^i\frac{\partial \mathbf{G}_{ji}}{\partial \mathbf{p}_k}\right) = \mu_k\frac{\partial \mathbf{G}_{ik}}{\partial \mathbf{p}_k} - \delta_k^i\sum_{\substack{j=0\\ j\neq i}}^{n}\mu_j\frac{\partial \mathbf{G}_{ji}}{\partial \mathbf{p}_k}\,. \qquad (2.242)$$

For $\frac{\partial \Delta \ddot{\mathbf{R}}_i}{\partial \mathbf{p}_k}$ we have

$$\frac{\partial \Delta \ddot{\mathbf{R}}_i}{\partial \mathbf{p}_k} = \sum_{j=n+1}^{n+m} \mu_j \frac{\partial \mathbf{Q}_{ji}}{\partial \mathbf{p}_k} = -\delta_k^i \sum_{j=n+1}^{n+m} \mu_j \frac{\partial \mathbf{G}_{ji}}{\partial \mathbf{p}_k}\,, \tag{2.243}$$

because $\frac{\partial \mathbf{G}_{ij}}{\partial \mathbf{p}_k} = \mathbf{0}$ if $j = n+1, ..., n+m$ (the perturbers are point masses). Finally for $\frac{\partial \ddot{\mathbf{R}}_B}{\partial \mathbf{p}_k}$ we have

$$\begin{aligned} \frac{\partial \ddot{\mathbf{R}}_B}{\partial \mathbf{p}_k} &= -\frac{1}{\mu_B} \sum_{l=0}^{n} \mu_l \frac{\partial \Delta \ddot{\mathbf{R}}_l}{\partial \mathbf{p}_k} = \frac{1}{\mu_B} \sum_{l=0}^{n} \mu_l \delta_k^l \sum_{j=n+1}^{n+m} \mu_j \frac{\partial \mathbf{G}_{jl}}{\partial \mathbf{p}_k} \\ &= \frac{\mu_k}{\mu_B} \sum_{j=n+1}^{n+m} \mu_j \frac{\partial \mathbf{G}_{jk}}{\partial \mathbf{p}_k}\,. \end{aligned} \tag{2.244}$$

Then the (2.240) becomes

$$\frac{\partial \ddot{\mathbf{R}}_i}{\partial \mathbf{p}_k} = \mu_k \frac{\partial \mathbf{G}_{ik}}{\partial \mathbf{p}_k} - \delta_k^i \sum_{\substack{j=0 \\ j\neq i}}^{n} \mu_j \frac{\partial \mathbf{G}_{ji}}{\partial \mathbf{p}_k} - \delta_k^i \sum_{j=n+1}^{n+m} \mu_j \frac{\partial \mathbf{G}_{ji}}{\partial \mathbf{p}_k} + \frac{\mu_k}{\mu_B} \sum_{j=n+1}^{n+m} \mu_j \frac{\partial \mathbf{G}_{jk}}{\partial \mathbf{p}_k}\,, \tag{2.245}$$

which can be splitted into two equation as

$$\begin{cases} \dfrac{\partial \ddot{\mathbf{R}}_i}{\partial \mathbf{p}_i} = -\sum\limits_{\substack{j=0 \\ j\neq i}}^{n} \mu_j \dfrac{\partial \mathbf{G}_{ji}}{\partial \mathbf{p}_i} + \left(\dfrac{\mu_i}{\mu_B} - 1\right) \sum\limits_{j=n+1}^{n+m} \mu_j \dfrac{\partial \mathbf{G}_{ji}}{\partial \mathbf{p}_i}\,, & k = i\,, \\ \dfrac{\partial \ddot{\mathbf{R}}_i}{\partial \mathbf{p}_k} = \mu_k \dfrac{\partial \mathbf{G}_{ik}}{\partial \mathbf{p}_k} + \dfrac{\mu_k}{\mu_B} \sum\limits_{j=n+1}^{n+m} \mu_j \dfrac{\partial \mathbf{G}_{jk}}{\partial \mathbf{p}_k}\,, & k \neq i\,, \end{cases} \tag{2.246}$$

Remain to compute the partials $\frac{\partial \mathbf{G}_{ij}}{\partial \mathbf{p}_j}$. Recalling equations (2.83) we have that

$$\frac{\partial \mathbf{G}_{ij}}{\partial \mathbf{p}_j} = \mathbf{C}_j^T \frac{\partial \mathbf{G}_{ij}^{BF}}{\partial \mathbf{p}_j}\,. \tag{2.247}$$

Recalling equations (2.82) we have for $\frac{\partial \mathbf{G}_{ij}^{BF}}{\partial \mathbf{p}_j}$

$$\frac{\partial \mathbf{G}_{ij}^{BF}}{\partial \mathbf{p}_j} = \frac{1}{\mu_j} \frac{\partial}{\partial \mathbf{p}_j} \left(\frac{\partial \mathcal{U}_j}{\partial \mathbf{r}_{ji}^{BF}}\right)^T\,, \tag{2.248}$$

where $\mathcal{U}_j$ is given by (2.10). As in section 2.3.1, for simplicity of notation in the following we omit the index i and j so $\mathbf{r}_{ji} \to \mathbf{r}$, $r_{ji} \to r$, $\varphi_i \to \varphi$, $\lambda_i \to \lambda$, $\mu_j \to \mu$, $\mathcal{C}_{lm}^j \to \mathcal{C}_{lm}$, $\mathcal{S}_{lm}^j \to \mathcal{S}_{lm}$, $R_e^j \to R_e$ and $\mathcal{U}_j \to \mathcal{U}$. So explicitly the partials are

$$\frac{\partial^2 \mathcal{U}}{\partial \mathcal{C}_{lm} \partial r} = -\frac{\mu}{r^2} (l+1) \left(\frac{R_e}{r}\right)^l \cos m\lambda P_l^m (\sin\varphi)\,, \tag{2.249}$$

$$\frac{\partial^2 \mathcal{U}}{\partial \mathcal{S}_{lm} \partial r} = -\frac{\mu}{r^2} (l+1) \left(\frac{R_e}{r}\right)^l \sin m\lambda P_l^m (\sin\varphi)\,, \tag{2.250}$$

$$\frac{\partial^2 \mathcal{U}}{\partial \mathcal{C}_{lm} \partial \lambda} = -\frac{\mu}{r} m \left(\frac{R_e}{r}\right)^l \sin m\lambda P_l^m (\sin\varphi)\,, \tag{2.251}$$

$$\frac{\partial^2 \mathcal{U}}{\partial \mathcal{S}_{lm} \partial \lambda} = \frac{\mu}{r} m \left(\frac{R_e}{r}\right)^l \cos m\lambda P_l^m (\sin\varphi)\,, \tag{2.252}$$

$$\begin{aligned}\frac{\partial^2 \mathcal{U}}{\partial \mathcal{C}_{lm}\partial\varphi} &= \frac{\mu}{r}\left(\frac{R_e}{r}\right)^l \cos m\lambda \frac{\partial}{\partial\varphi}\left[P_l^m(\sin\varphi)\right] \\ &= \frac{\mu}{r}\left(\frac{R_e}{r}\right)^l \cos m\lambda \left[-m\tan\varphi P_l^m(\sin\varphi) + P_l^{m+1}(\sin\varphi)\right], \qquad (2.253)\\ \frac{\partial^2 \mathcal{U}}{\partial \mathcal{S}_{lm}\partial\varphi} &= \frac{\mu}{r}\left(\frac{R_e}{r}\right)^l \sin m\lambda \left[-m\tan\varphi P_l^m(\sin\varphi) + P_l^{m+1}(\sin\varphi)\right]. \qquad (2.254)\end{aligned}$$

If the exended body is oblate instead we have

$$\begin{aligned}\frac{\partial^2 \mathcal{U}_{obl}}{\partial J_l \partial r} &= \frac{\mu}{r^2}(l+1)\left(\frac{R_e}{r}\right)^l P_l^0(\sin\varphi), \qquad (2.255)\\ \frac{\partial^2 \mathcal{U}_{obl}}{\partial J_l \partial \varphi} &= -\frac{\mu}{r}\left(\frac{R_e}{r}\right)^l P_l^1(\sin\varphi). \qquad (2.256)\end{aligned}$$

2.6.6 Partials with respect to the pole

The pole parameters enter the problem only through the rotation matrix in the functions $\mathbf{G}_{ij}$. The partials are analogous to the partial computed in section 2.6.5. So, if we indicate with $\mathbf{s}_k = (\alpha_k, \delta_k, W_k)$, $k = 0, ..., n$ the pole parameters, we have

$$\begin{cases} \dfrac{\partial \ddot{\mathbf{R}}_i}{\partial \mathbf{s}_i} = -\sum\limits_{\substack{j=0\\ j\neq i}}^{n} \mu_j \dfrac{\partial \mathbf{G}_{ji}}{\partial \mathbf{s}_i} + \left(\dfrac{\mu_i}{\mu_B} - 1\right) \sum\limits_{j=n+1}^{n+m} \mu_j \dfrac{\partial \mathbf{G}_{ji}}{\partial \mathbf{s}_i}, & k = i, \\ \dfrac{\partial \ddot{\mathbf{R}}_i}{\partial \mathbf{s}_k} = \mu_k \dfrac{\partial \mathbf{G}_{ik}}{\partial \mathbf{s}_k} + \frac{\mu_k}{\mu_B} \sum\limits_{j=n+1}^{n+m} \mu_j \dfrac{\partial \mathbf{G}_{jk}}{\partial \mathbf{s}_k}, & k \neq i, \end{cases} \qquad (2.257)$$

so we have to compute $\frac{\partial \mathbf{G}_{ij}}{\partial \mathbf{s}_j}$. Through equations (2.83) and (2.81) we have

$$\mathbf{G}_{ij} = \mathbf{C}_j^T \mathbf{G}_{ij}^{BF}. \qquad (2.258)$$

$$\frac{\partial \mathbf{G}_{ij}}{\partial \mathbf{s}_j} = \frac{\partial \mathbf{C}_j^T}{\partial \mathbf{s}_j}\mathbf{G}_{ij} + \mathbf{C}_j^T \frac{\partial \mathbf{G}_{ij}^{BF}}{\partial \mathbf{s}_j} = \frac{\partial \mathbf{C}_j^T}{\partial \mathbf{s}_j}\mathbf{G}_{ij} + \mathbf{C}_j^T \frac{\partial \mathbf{G}_{ij}^{BF}}{\partial \mathbf{r}_{ji}^{BF}} \frac{\partial \mathbf{r}_{ji}^{BF}}{\partial \mathbf{s}_j}, \qquad (2.259)$$

where $\frac{\partial \mathbf{G}_{ij}^{BF}}{\partial \mathbf{r}_{ji}^{BF}}$ are already been computed in section 2.6.4. Remain to compute $\frac{\partial \mathbf{C}_j^T}{\partial \mathbf{s}_j}$ and $\frac{\partial \mathbf{r}_{ji}^{BF}}{\partial \mathbf{s}_j}$.

It is possible to demonstrate that, for any orthogonal matrix $\mathbf{M}$ differentiable with respect to a parameter t is true that [48], [50]

$$\frac{d\mathbf{M}}{dt} = [\tilde{\omega}\times]\,\mathbf{M}, \qquad (2.260)$$

where $[\tilde{\omega}]$ indicate a vector of the form

$$\omega = \begin{pmatrix} \omega_1 \\ \omega_2 \\ \omega_3 \end{pmatrix}, \qquad (2.261)$$

corresponding to a symmetric matrix of the form

$$[\tilde{\omega}\times] = \Omega = \begin{pmatrix} 0 & -\omega_3 & \omega_2 \\ \omega_3 & 0 & -\omega_1 \\ -\omega_2 & \omega_1 & 0 \end{pmatrix}. \qquad (2.262)$$

Moreover is true that

$$[\tilde{\omega}\times]^T = -[\tilde{\omega}\times],$$

So, since the rotation matrix $\mathbf{C}$ is a matrix with the characteristics of $\mathbf{M}$ we have

$$\frac{\partial \mathbf{C}_j^T}{\partial \mathbf{s}_j} = [\tilde{\mathbf{s}}_j \times]\, \mathbf{C}_j^T \,, \tag{2.263}$$

and, recalling equations (2.81)

$$\frac{\partial \mathbf{r}_{ji}^{BF}}{\partial \mathbf{s}_j} = \frac{\partial}{\partial \mathbf{s}_j} \left[\mathbf{C}_j \left(\mathbf{R}_i - \mathbf{R}_j\right)\right] = \frac{\partial \mathbf{C}_j}{\partial \mathbf{s}_j} \left(\mathbf{R}_i - \mathbf{R}_j\right) \,. \tag{2.264}$$

Transposing equations (2.263) we have

$$\left(\frac{\partial \mathbf{C}_j^T}{\partial \mathbf{s}_j}\right)^T = \frac{\partial \mathbf{C}_j}{\partial \mathbf{s}_j} = \left([\tilde{\mathbf{s}}_j \times]\, \mathbf{C}_j^T\right)^T = \mathbf{C}_j \left[\tilde{\mathbf{s}}_j \times\right]^T = -\mathbf{C}_j \left[\tilde{\mathbf{s}}_j \times\right] \,, \tag{2.265}$$

so

$$\frac{\partial \mathbf{r}_{ji}^{BF}}{\partial \mathbf{s}_j} = -\mathbf{C}_j \left[\tilde{\mathbf{s}}_j \times\right] \left(\mathbf{R}_i - \mathbf{R}_j\right) \,. \tag{2.266}$$

So we have

$$\begin{aligned} \frac{\partial \mathbf{G}_{ji}}{\partial \mathbf{s}_j} &= \frac{\partial \mathbf{C}_j^T}{\partial \mathbf{s}_j} \mathbf{G}_{ij} + \mathbf{C}_j^T \frac{\partial \mathbf{G}_{ij}^{BF}}{\partial \mathbf{r}_{ji}^{BF}} \frac{\partial \mathbf{r}_{ji}^{BF}}{\partial \mathbf{s}_j} \\ &= [\tilde{\mathbf{s}}_j \times]\, \mathbf{G}_{ji} - \frac{\partial \mathbf{G}_{ij}^{BF}}{\partial \mathbf{r}_{ji}^{BF}} \mathbf{C}_j \left[\tilde{\mathbf{s}}_j \times\right] \left(\mathbf{R}_i - \mathbf{R}_j\right) \,, \end{aligned} \tag{2.267}$$

where

$$[\tilde{\mathbf{s}}_j \times] = \begin{pmatrix} 0 \\ 0 \\ 1 \end{pmatrix} \,, \tag{2.268}$$

for $\mathbf{s}_j = \alpha_j$,

$$[\tilde{\mathbf{s}}_j \times] = \begin{pmatrix} \sin \alpha_j \\ -\cos \alpha_j \\ 0 \end{pmatrix} \,, \tag{2.269}$$

for $\mathbf{s}_j = \delta_j$ and

$$[\tilde{\mathbf{s}}_j \times] = \begin{pmatrix} \cos \alpha_j \cos \delta_j \\ \cos \delta_j \sin \alpha_j \\ \sin \delta_j \end{pmatrix} \,, \tag{2.270}$$

for $\mathbf{s}_j = W_j$. Explicitly the matrices $\frac{\partial \mathbf{r}_{ji}^{BF}}{\partial \mathbf{s}_j}$ and $\frac{\partial \mathbf{C}_j^T}{\partial \mathbf{s}_j}$ are:

$$\frac{\partial \mathbf{r}_{ji}^{BF}}{\partial \mathbf{s}_j} = \frac{\partial}{\partial \mathbf{s}_j} \left[\mathbf{C}_j \left(\mathbf{R}_i - \mathbf{R}_j\right)\right] = \frac{\partial \mathbf{C}_j}{\partial \mathbf{s}_j} \left(\mathbf{R}_i - \mathbf{R}_j\right) \,, \tag{2.271}$$

so, suppressing the index j to ease the notation,

$$\frac{\partial \mathbf{C}}{\partial \alpha} = \begin{pmatrix} \sin\alpha \sin\delta \sin W - \cos\alpha \cos W & -\sin\alpha \cos W - \cos\alpha \sin\delta \sin W & 0 \\ \cos\alpha \sin W + \sin\alpha \sin\delta \cos W & \sin\alpha \sin W - \cos\alpha \sin\delta \cos W & 0 \\ -\cos\delta \sin\alpha & \cos\alpha \cos\delta & 0 \end{pmatrix} \,, \tag{2.272}$$

$$\frac{\partial \mathbf{C}}{\partial \delta} = \begin{pmatrix} -\cos\alpha \cos\delta \sin W & -\cos\delta \sin\alpha \sin W & -\sin\delta \sin W \\ -\cos\alpha \cos\delta \cos W & -\cos\delta \sin\alpha \cos W & -\sin\delta \cos W \\ -\cos\alpha \sin\delta & -\sin\alpha \sin\delta & \cos\delta \end{pmatrix} \,, \tag{2.273}$$

$$\frac{\partial \mathbf{C}}{\partial W} = \begin{pmatrix} \sin\alpha \sin W - \cos\alpha \sin\delta \cos W & -\cos\alpha \sin W - \sin\alpha \sin\delta \cos W & \cos\delta \cos W \\ \sin\alpha \cos W + \cos\alpha \sin\delta \sin W & \sin\alpha \sin\delta \sin W - \cos\alpha \cos W & -\cos\delta \sin W \\ 0 & 0 & 0 \end{pmatrix} \,, \tag{2.274}$$

while the partials $\frac{\partial \mathbf{C}_j^T}{\partial \mathbf{s}_j}$ are the transpose of the previous.

Case of an oblate body

In this case there is non dependence from W so $W = 0$ and the partials given into (2.272), (2.273) and (2.274) can be simplified as

$$\frac{\partial \mathbf{C}_{obl}}{\partial \alpha} = \begin{pmatrix} -\cos\alpha & -\sin\alpha & 0 \\ \sin\alpha\sin\delta & -\cos\alpha\sin\delta & 0 \\ -\cos\delta\sin\alpha & \cos\alpha\cos\delta & 0 \end{pmatrix}, \tag{2.275}$$

$$\frac{\partial \mathbf{C}_{obl}}{\partial \delta} = \begin{pmatrix} 0 & 0 & 0 \\ -\cos\alpha\cos\delta & -\cos\delta\sin\alpha & -\sin\delta \\ -\cos\alpha\sin\delta & -\sin\alpha\sin\delta & \cos\delta \end{pmatrix}, \tag{2.276}$$

$$\frac{\partial \mathbf{C}_{obl}}{\partial W} = \begin{pmatrix} -\cos\alpha\sin\delta & -\sin\alpha\sin\delta & \cos\delta \\ \sin\alpha & -\cos\alpha & 0 \\ 0 & 0 & 0 \end{pmatrix}. \tag{2.277}$$

2.7 Numerical integration of the satellites of Saturnian system

We have implemented the equations of motion and the variational equations developed in this chapter in an object-oriented, Fortran 95 code, named *SOSYA* (SOlar SYstem Astrometry). We have decided to adopt an object-oriented programming method because modern programming languages provide the programmers with three capabilities that improve and simplify the design of such programs. These are is encapsulation, inheritance and polymorphism. These new capabilities allow for better and safer programming design and, furthermore they make scientific programs easier to understand, share, explain and extend. We refer to Appendix D for a complete description of the software developed in this study.

We have used the numerical integrator DIVA [28], which is a variable order and variable step integrator for q-th order and mixed order problems. DIVA uses a PECE (predict, evaluate, correct, evaluate) scheme on the first step, a PEC (predict, evaluate, correct) scheme for the rest of the start phase and a PECE scheme thereafter. The predictor and corrector are orders k and $k+1$ respectively, $k \leq 19$, where k may differ from equation to equation [54]. DIVA increases the tolerance if the round-off noise is deemed to be too large.

2.7.1 Numerical ephemerides of the Saturnian System

By means of the *Orbit Simulation* capability of the *SOSYA* program, we have numerically integrated the equations of motion (2.72) in a reference frame centered in the Saturnian system barycenter. The perturbers are the Sun and Jupiter. We have considered also the zonal Stokes coefficients J_2, J_4, J_6, and J_8 of Saturn. The gravitational parameters of the Saturnian system and the other parameters we have used in our simulations are given in the Tables 2.4, 2.5, 2.6 and 2.7. The reference ephemerides for the Saturnian system, which we have used to compare with, are the JPL ephemerides **SAT132**, **SAT136**, **SAT143**, **SAT185**, **SAT199**, **SAT207**, **SAT243**, **SAT252**.

There are essentially two versions of these ephemerides files, both in binary format: an ODP version (ODP is the *Orbit Determination Program* of JPL [26]) and a SPICE version (SPICE toolkit is a NAIF, Navigation and Ancillary Information Facility at JPL, developed software system, [27]). Both these versions contain Chebyshev polynomial coefficients for the position and velocity of the body as a function of time. The ODP version contains, in addition, some information regarding the initial conditions of the satellites and the names and values pertaining to the dynamical constants associated with the ephemeris, e.g., the astronomical unit, the gravitational parameters, planetary zonal gravity harmonics, planetary pole orientation, and planetary prime meridian parameters.

The initial conditions of the satellites and the epoch of the initial conditions as well as the parameters mentioned above and used by JPL to generate the ephemerides have been accurately determined using

a utility application of the JPL *Orbit Determination Program*, which allows to extract these pieces of information directly from the ODP version of the JPL ephemeris files. In this sense the initial conditions of satellites and the epoch of initial conditions are crucial for the comparison between our ephemeris and JPL's ephemeris. The state of the perturbers is obtained using the SPICE toolkit (see [27] and Appendix D).

In Tables 2.1 and 2.2 we give the rms of the difference between our integration and the JPL ephemerides. The length of the integration is 5 years with an output step every hour. Figure 2.3 shows plots of the same rms values for differences in position of the JPL ephemeris with respect to the current integration. The y-axis is displayed on a logarithmic scale. Our numerical integration is in good agreement with the JPL ephemerides, particularly with the latest version of JPL ephemerides (**SAT243** and **SAT252**). In fact, in this case (see Table 2.2) the rms is on the order of 10 meters for Mimas and on the order of few meters for the other satellites.

To check the internal consistency of the integrator we have integrated a 12-body system perturbed by Jupiter and Sun for a period of 100 years. We have considered Saturn as an extended body with only three zonal harmonic, that is J_2, J_4, J_6. The parameters we have used are the same used in the case of comparison with the **SAT136**. We have integrated the equations of motion from 2004 Jan 2 $0^h0^m0^s.0$ to 2050 Jan 2 $0^h0^m0^s.0$ and from 2004 Jan 2 $0^h0^m0^s.0$ to 1950 Jan 2 $0^h0^m0^s.0$. In this way we have obtained two new sets of initial conditions for the 12 satellites, one at epoch 1950 and another at epoch 2050.

At this point we have started two 100-years integrations, one from 2050 to 1950 and the other from 1950 to 2050 with an output step of 1 day. Then we have compared the two integrations and computed the rms of their difference. From Table 2.3 we can see that the DIVA integrator maintains a good accuracy also over such long integrations. In fact the rms of the difference between the two integrations in position is smaller than 1 kilometer, except for Mimas. But the system of differential equations is correlated, because the satellites are mutually interacting, and a small tolerance error can bring the system to a very different evolution. Moreover Mimas, being the nearest satellite to Saturn (among those considered here), is strongly influenced by the zonal terms of Saturn. The more distant and more massive satellites are instead more stable. In Figure 2.4 we plot the difference in x, y and z between the two integrations for Titan and Mimas.

	SAT132		**SAT136**		**SAT143**		**SAT185**	
	$\Delta\lvert\mathbf{r}\rvert\,(m)$	$\Delta\lvert\mathbf{v}\rvert\,(m/s)$	$\Delta\lvert\mathbf{r}\rvert\,(m)$	$\Delta\lvert\mathbf{v}\rvert\,(m/s)$	$\Delta\lvert\mathbf{r}\rvert\,(m)$	$\Delta\lvert\mathbf{v}\rvert\,(m/s)$	$\Delta\lvert\mathbf{r}\rvert\,(m)$	$\Delta\lvert\mathbf{v}\rvert\,(m/s)$
Mimas	23.1	$1.1\cdot10^{-2}$	21.8	$1.9\cdot10^{-2}$	48.6	$1.1\cdot10^{-2}$	51.9	$2.5\cdot10^{-2}$
Enceladus	1.9	$7.7\cdot10^{-4}$	1.9	$7.7\cdot10^{-4}$	2.1	$7.8\cdot10^{-4}$	64.5	$1.6\cdot10^{-2}$
Tethys	1.8	$4.5\cdot10^{-4}$	1.8	$4.5\cdot10^{-4}$	1.9	$4.7\cdot10^{-4}$	25.9	$4.3\cdot10^{-3}$
Dione	8.6	$1.4\cdot10^{-3}$	8.6	$1.4\cdot10^{-3}$	8.7	$1.4\cdot10^{-3}$	51.0	$6.3\cdot10^{-3}$
Rhea	6.9	$8.4\cdot10^{-4}$	6.9	$8.4\cdot10^{-4}$	6.9	$8.4\cdot10^{-4}$	57.2	$4.7\cdot10^{-3}$
Titan	2.0	$6.6\cdot10^{-5}$	2.2	$6.7\cdot10^{-5}$	0.8	$6.6\cdot10^{-5}$	24.4	$9.9\cdot10^{-4}$
Hyperion	4.9	$1.7\cdot10^{-4}$	5.0	$1.7\cdot10^{-4}$	4.0	$1.7\cdot10^{-4}$	61.3	$2.6\cdot10^{-3}$
Iapetus	19.2	$4.1\cdot10^{-5}$	21.0	$4.2\cdot10^{-5}$	1.7	$3.7\cdot10^{-5}$	29.2	$6.1\cdot10^{-4}$
Phoebe	—	—	306.9	$1.6\cdot10^{-4}$	23.8	$1.6\cdot10^{-4}$	23.8	$1.6\cdot10^{-4}$
Helene	—	—	9.5	$1.6\cdot10^{-3}$	9.5	$1.6\cdot10^{-3}$	212.6	$2.7\cdot10^{-2}$
Telesto	—	—	1.8	$4.5\cdot10^{-4}$	1.9	$4.7\cdot10^{-4}$	26.2	$4.4\cdot10^{-3}$
Calypso	—	—	1.8	$4.4\cdot10^{-4}$	1.9	$4.6\cdot10^{-4}$	30.0	$5.0\cdot10^{-3}$

Table 2.1: Rms values for differences of **SAT132**, **SAT136**, **SAT143** and **SAT185** with respect to the current integration. The length of integration is 5 years with a time step of 1 hour.

	SAT199		**SAT207**		**SAT243**		**SAT252**	
	$\Delta\|\mathbf{r}\|\,(m)$	$\Delta\|\mathbf{v}\|\,(m/s)$	$\Delta\|\mathbf{r}\|\,(m)$	$\Delta\|\mathbf{v}\|\,(m/s)$	$\Delta\|\mathbf{r}\|\,(m)$	$\Delta\|\mathbf{v}\|\,(m/s)$	$\Delta\|\mathbf{r}\|\,(m)$	$\Delta\|\mathbf{v}\|\,(m/s)$
Mimas	51.5	$2.5 \cdot 10^{-2}$	51.6	$2.5 \cdot 10^{-2}$	13.5	$5.3 \cdot 10^{-3}$	10.5	$5.2 \cdot 10^{-3}$
Enceladus	64.5	$1.6 \cdot 10^{-2}$	64.5	$1.6 \cdot 10^{-2}$	1.9	$7.9 \cdot 10^{-4}$	1.9	$7.9 \cdot 10^{-4}$
Tethys	25.7	$4.3 \cdot 10^{-3}$	25.7	$4.3 \cdot 10^{-3}$	1.5	$3.5 \cdot 10^{-4}$	1.5	$3.5 \cdot 10^{-4}$
Dione	50.9	$6.3 \cdot 10^{-3}$	50.9	$6.3 \cdot 10^{-3}$	2.0	$4.1 \cdot 10^{-4}$	2.0	$4.1 \cdot 10^{-4}$
Rhea	57.1	$4.7 \cdot 10^{-3}$	57.1	$4.7 \cdot 10^{-3}$	2.1	$2.8 \cdot 10^{-4}$	2.1	$2.8 \cdot 10^{-4}$
Titan	0.8	$6.7 \cdot 10^{-5}$	0.8	$6.7 \cdot 10^{-5}$	0.9	$6.1 \cdot 10^{-5}$	0.9	$6.1 \cdot 10^{-5}$
Hyperion	61.3	$2.6 \cdot 10^{-3}$	61.3	$2.6 \cdot 10^{-3}$	3.9	$1.7 \cdot 10^{-4}$	3.9	$1.7 \cdot 10^{-4}$
Iapetus	29.2	$6.1 \cdot 10^{-4}$	29.2	$6.1 \cdot 10^{-4}$	1.7	$3.6 \cdot 10^{-5}$	1.7	$3.6 \cdot 10^{-5}$
Phoebe	23.8	$1.6 \cdot 10^{-4}$	23.8	$1.6 \cdot 10^{-4}$	6.9	$6.5 \cdot 10^{-5}$	6.9	$6.5 \cdot 10^{-5}$
Helene	212.6	$2.7 \cdot 10^{-2}$	212.7	$2.7 \cdot 10^{-2}$	5.1	$1.1 \cdot 10^{-3}$	5.2	$1.1 \cdot 10^{-3}$
Telesto	26.5	$4.4 \cdot 10^{-3}$	26.6	$4.5 \cdot 10^{-3}$	1.9	$4.7 \cdot 10^{-4}$	1.9	$4.7 \cdot 10^{-4}$
Calypso	31.5	$5.3 \cdot 10^{-3}$	31.6	$5.3 \cdot 10^{-3}$	1.9	$4.7 \cdot 10^{-4}$	1.9	$4.7 \cdot 10^{-4}$
Methon	—	—	—	—	9.3	$1.2 \cdot 10^{-3}$	2.6	$1.0 \cdot 10^{-3}$

Table 2.2: Rms values for differences of **SAT199**, **SAT207**, **SAT243** and **SAT252** with respect to the current integration. The length of integration is 5 years with a time step of 1 hour.

SAT136	$\Delta\|\mathbf{r}\|\,(km)$	$\Delta\|\mathbf{v}\|\,(km/s)$
Mimas	2.24	$1.73 \cdot 10^{-4}$
Enceladus	$5.36 \cdot 10^{-2}$	$2.84 \cdot 10^{-6}$
Tethys	$9.24 \cdot 10^{-1}$	$3.56 \cdot 10^{-5}$
Dione	$3.04 \cdot 10^{-1}$	$8.08 \cdot 10^{-6}$
Rhea	$4.02 \cdot 10^{-2}$	$6.47 \cdot 10^{-7}$
Titan	$5.42 \cdot 10^{-3}$	$2.47 \cdot 10^{-8}$
Hyperion	$4.90 \cdot 10^{-3}$	$1.70 \cdot 10^{-8}$
Iapetus	$5.56 \cdot 10^{-3}$	$5.17 \cdot 10^{-9}$
Phoebe	$2.21 \cdot 10^{-3}$	$3.05 \cdot 10^{-10}$
Helene	$3.04 \cdot 10^{-1}$	$8.08 \cdot 10^{-6}$
Telesto	$9.24 \cdot 10^{-1}$	$3.56 \cdot 10^{-5}$
Calypso	$9.24 \cdot 10^{-1}$	$3.56 \cdot 10^{-5}$

Satellite	$a(km)$	$T(day)$	$i(deg)$
Mimas	185520	0.9424	1.53
Enceladus	238020	1.3702	0.02
Tethys	294660	1.8878	1.09
Dione	377400	2.7369	0.02
Rhea	527040	4.5175	0.35
Titan	1221850	15.9454	0.33
Hyperion	1481100	21.2766	0.43
Iapetus	3561300	79.3301	7.52
Phoebe	12952000	550.48	175.3
Helene	377400	2.7369	0.2
Telesto	294660	1.8878	~ 0
Calypso	294660	1.8878	~ 0

Table 2.3: (Left) Rms values for differences between two integrations of 100 years, one from 1950 to 2050 and another from 2050 to 1950; the output time step is 1 day. (Right) Orbital parameters of the Saturnian satellites: a is the semimajor axis, T the sideral orbital period, i the orbital inclination [44].

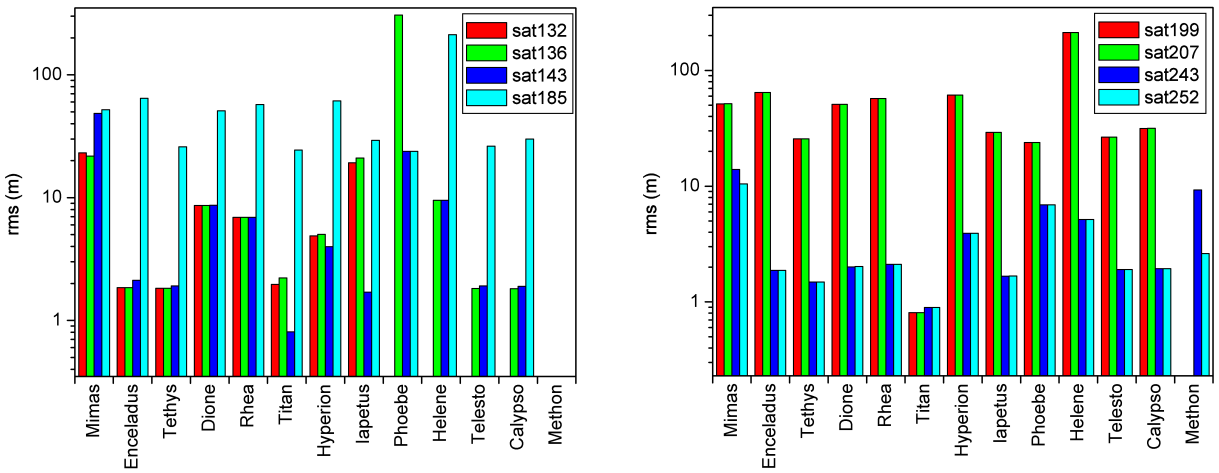

Figure 2.3: Plots of the rms values for differences in position of the JPL ephemeris with respect to current integration. The length of integration is 5 years with a time step of 1 hour. The y-axis is a logarithmic scale.

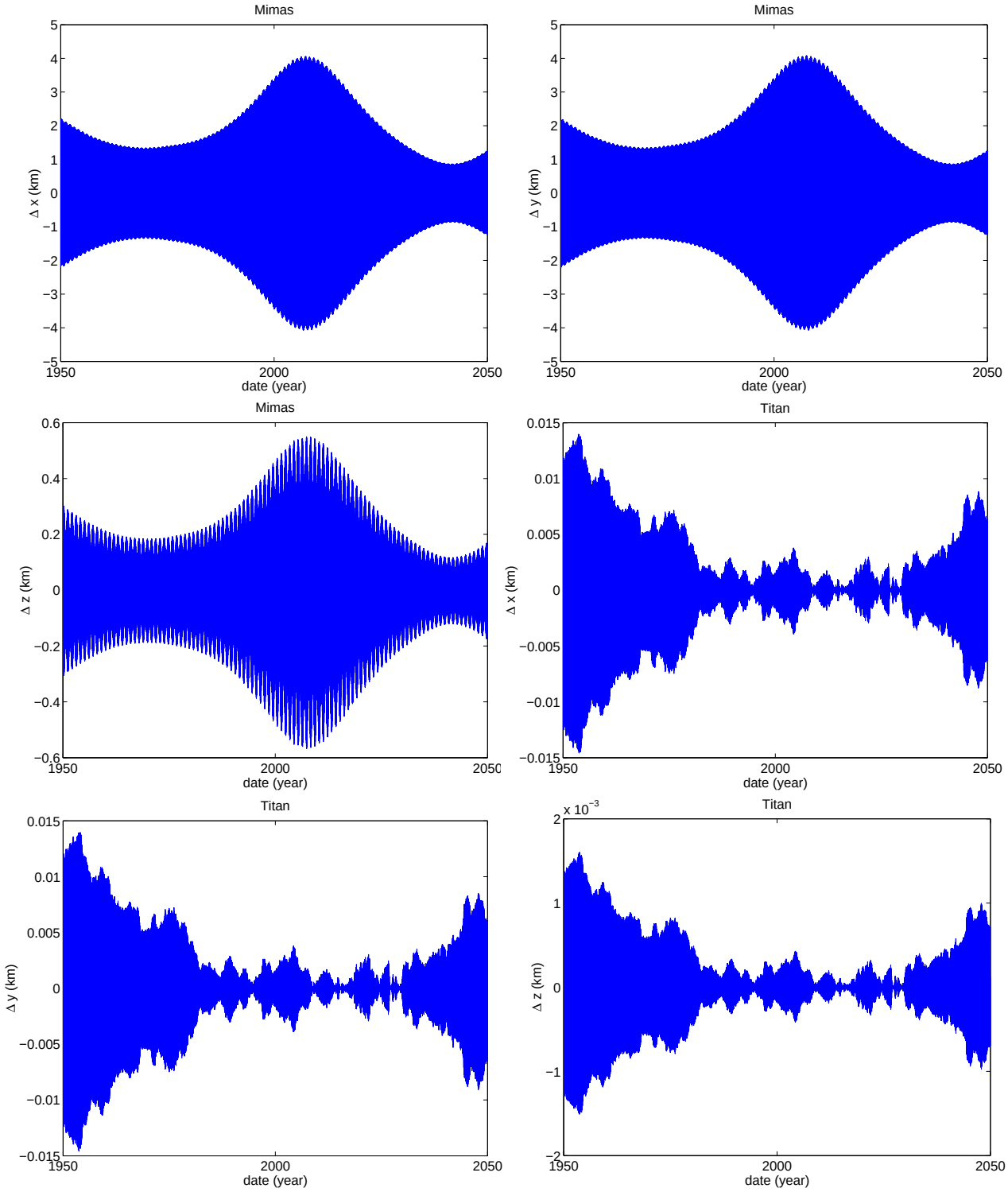

Figure 2.4: Difference in x, y and z (for Mimas and Titan) between two integration of 100 years, one from 1950 to 2050 and the other from 2050 to 1950.

GM (Km^3/s^2)	**SAT132**	**SAT136**	**SAT143**	**SAT185**
Mimas	2.562248694441524	2.560471922128287	2.5502	2.545348445855473
Enceladus	5.770493590875791	5.761920920729191	6.9495	7.935702533722493
Tethys	$4.120925828680387 \cdot 10^1$	$4.120708421715877 \cdot 10^1$	$4.1206 \cdot 10^1$	$4.121020211010504 \cdot 10^1$
Dione	$7.312857497096579 \cdot 10^1$	$7.312879579474816 \cdot 10^1$	$7.31221 \cdot 10^1$	$7.310964684397931 \cdot 10^1$
Rhea	$1.545888057352435 \cdot 10^2$	$1.545272868834633 \cdot 10^2$	$1.545897 \cdot 10^2$	$1.533039486680335 \cdot 10^2$
Titan	$8.978034767893490 \cdot 10^3$	$8.978086924687595 \cdot 10^3$	$8.9780817 \cdot 10^3$	$8.977888728363658 \cdot 10^3$
Hyperion	$7.2 \cdot 10^{-1}$	$7.2 \cdot 10^{-1}$	$7.2 \cdot 10^{-1}$	$7.2 \cdot 10^{-1}$
Iapetus	$1.317883630267206 \cdot 10^2$	$1.317353046042371 \cdot 10^2$	$1.296647 \cdot 10^2$	$1.207966650813797 \cdot 10^2$
Phoebe	—	$4.8 \cdot 10^{-1}$	$4.8 \cdot 10^{-1}$	$5.529118991291722 \cdot 10^{-1}$
Helene	—	0.0	0.0	0.0
Telesto	—	0.0	0.0	0.0
Calypso	—	0.0	0.0	0.0
Methon	—	—	—	—
Saturn	$3.793128449712308 \cdot 10^7$	$3.793129522215692 \cdot 10^7$	$3.79312841568 \cdot 10^7$	$3.79312226507585 \cdot 10^7$
Iupiter	$1.267127678577960 \cdot 10^8$	$1.267127678577960 \cdot 10^8$	$1.2671276376 \cdot 10^8$	$1.267127654543717 \cdot 10^8$
Sun	$1.327124400179870 \cdot 10^{11}$	$1.327124400179870 \cdot 10^{11}$	$1.327132332573103 \cdot 10^{11}$	$1.327132332573103 \cdot 10^{11}$

Table 2.4: Gravitational parameters of Saturnian system from **SAT132**, **SAT136**, **SAT143** and **SAT185** ephemerides.

GM (Km^3/s^2)	**SAT199**	**SAT207**	**SAT243**	**SAT252**
Mimas	2.540484103259363	2.541148617400836	2.50233349872229	2.503235302616387
Enceladus	7.205314063225305	7.206785177066757	7.209611958399121	7.205635156243085
Tethys	$4.120957262673035 \cdot 10^1$	$4.120820422245323 \cdot 10^1$	$4.120974833890971 \cdot 10^1$	$4.120916891851326 \cdot 10^1$
Dione	$7.311194675279130 \cdot 10^1$	$7.311245778258673 \cdot 10^1$	$7.311266327729938 \cdot 10^1$	$7.311254834628727 \cdot 10^1$
Rhea	$1.539007028508257 \cdot 10^2$	$1.540419354109296 \cdot 10^2$	$1.539416298366489 \cdot 10^2$	$1.539427760843498 \cdot 10^2$
Titan	$8.978126921030520 \cdot 10^3$	$8.978153726703011 \cdot 10^3$	$8.978135605052079 \cdot 10^3$	$8.978134878525367 \cdot 10^3$
Hyperion	$3.810909022584602 \cdot 10^{-1}$	$3.790313237358475 \cdot 10^{-1}$	$3.727176583878968 \cdot 10^{-1}$	$3.723680363576141 \cdot 10^{-1}$
Iapetus	$1.205237443791595 \cdot 10^2$	$1.205225639686346 \cdot 10^2$	$1.205117101205687 \cdot 10^2$	$1.205073273066122 \cdot 10^2$
Phoebe	$5.526908562645090 \cdot 10^{-1}$	$5.532451133127682 \cdot 10^{-1}$	$5.534373556730062 \cdot 10^{-1}$	$5.532743571682094 \cdot 10^{-1}$
Helene	0.0	0.0	0.0	0.0
Telesto	0.0	0.0	0.0	0.0
Calypso	0.0	0.0	0.0	0.0
Methon	—	—	0.0	0.0
Saturn	$3.79311226861876 \cdot 10^7$	$3.793115701725895 \cdot 10^7$	$3.793120767780971 \cdot 10^7$	$3.793120782046435 \cdot 10^7$
Iupiter	$1.267127654543717 \cdot 10^8$	$1.267127654543717 \cdot 10^8$	$1.267127648582231 \cdot 10^8$	$1.267127648582231 \cdot 10^8$
Sun	$1.327132332573103 \cdot 10^{11}$	$1.327132332573103 \cdot 10^{11}$	$1.327132332664355 \cdot 10^{11}$	$1.327132332664355 \cdot 10^{11}$

Table 2.5: Gravitational parameters of Saturnian system from **SAT199**, **SAT207**, **SAT243** and **SAT252** ephemerides.

parameter	SAT132	SAT136	SAT143	SAT185
r_{Saturn}	$6.033000000000000 \cdot 10^4$ km	$6.033000000000000 \cdot 10^4$ km	$6.033000000000000 \cdot 10^4$ km	$6.033000000000000 \cdot 10^4$ km
J_2	$1.629462560191289 \cdot 10^{-2}$	$1.629434522593014 \cdot 10^{-2}$	$1.62918579 \cdot 10^{-2}$	$1.628989636184908 \cdot 10^{-2}$
J_4	$-9.197277823946756 \cdot 10^{-4}$	$-9.208770012707456 \cdot 10^{-4}$	$-9.311922 \cdot 10^{-4}$	$-9.36318328862301 \cdot 10^{-4}$
J_6	$9.975895864684476 \cdot 10^{-5}$	$9.867314408762757 \cdot 10^{-5}$	$9.068679999999999 \cdot 10^{-5}$	$8.702006634709568 \cdot 10^{-5}$
J_8	A	A	$-1 \cdot 10^{-5}$	$-1 \cdot 10^{-5}$
pole time	JD 2444556.491238426	JD 2444556.491238426	JD 2444556.491238426	JD 2451545.0
α_0	40.5955°	40.5955°	40.5955°	40.587408445297°
$\dot{\alpha}$	$-4.229 \cdot 10^{-2}$°/century	$-4.229 \cdot 10^{-2}$°/century	$-4.229 \cdot 10^{-2}$°/century	$-4.229 \cdot 10^{-2}$°/century
δ_0	83.53812°	83.53812°	83.53812°	83.53727047285692°
$\dot{\delta}$	$-4.44 \cdot 10^{-3}$°/century	$-4.44 \cdot 10^{-3}$°/century	$-4.44 \cdot 10^{-3}$°/century	$-4.44 \cdot 10^{-3}$°/century
W_0	198.609246786157°	198.609246786157°	198.609246786157°	38.9°
$\dot{W}$	810.7939024°/century	810.7939024°/century	810.7939024°/century	810.7939024°/century
Planetary ephemerides	DE405	DE405	DE410	DE410

Table 2.6: Other parameters used for integration of **SAT132**, **SAT136**, **SAT143** and **SAT185** ephemerides.

parameter	SAT199	SAT207	SAT243	SAT252
r_{Saturn}	$6.033000000000000 \cdot 10^4$ km	$6.033000000000000 \cdot 10^4$ km	$6.033000000000000 \cdot 10^4$ km	$6.033000000000000 \cdot 10^4$ km
J_2	$1.629141514654057 \cdot 10^{-2}$	$1.629131266743793 \cdot 10^{-2}$	$1.62907093434601 \cdot 10^{-2}$	$1.629068765887807 \cdot 10^{-2}$
J_4	$-9.309661909573573 \cdot 10^{-4}$	$-9.301085515965242 \cdot 10^{-4}$	$-9.35832809584157 \cdot 10^{-4}$	$-9.358036984823224 \cdot 10^{-4}$
J_6	$9.113781633627933 \cdot 10^{-5}$	$9.247708761981535 \cdot 10^{-5}$	$8.614421902255098 \cdot 10^{-5}$	$8.630656493959520 \cdot 10^{-5}$
J_8	$-1 \cdot 10^{-5}$	$-1 \cdot 10^{-5}$	$-1 \cdot 10^{-5}$	$-1 \cdot 10^{-5}$
pole time	JD 2451545.0	JD 2451545.0	JD 2451545.0	JD 2451545.0
α_0	40.57607143792153°	40.57919510548007°	40.58278865638854°	40.58272557173299°
$\dot{\alpha}$	$-4.229 \cdot 10^{-2}$°/century	$-4.229 \cdot 10^{-2}$°/century	$-4.229 \cdot 10^{-2}$°/century	$-4.229 \cdot 10^{-2}$°/century
δ_0	83.53781486548286°	83.5380272417211°	83.53762527867866°	83.53762378765944°
$\dot{\delta}$	$-4.44 \cdot 10^{-3}$°/century	$-4.44 \cdot 10^{-3}$°/century	$-4.44 \cdot 10^{-3}$°/century	$-4.44 \cdot 10^{-3}$°/century
W_0	38.9°	38.9°	38.9°	38.9°
$\dot{W}$	810.7939024°/century	810.7939024°/century	810.7939024°/century	810.7939024°/century
Planetary ephemerides	DE410	DE410	DE414	DE414

Table 2.7: Other parameters used for integration of **SAT199**, **SAT207**, **SAT243** and **SAT252** ephemerides.

2.7.2 Numerical integration of variational equations

By means of the *Orbit Simulation* capability of the SOSYA program we have also numerically integrated the variational equations presented in section 2.5.

Hadjifotinou and Harper [17], as well as Hadjifotinou and Ichtiaroglou [16], have shown with the use of Floquet theory for the stability of periodic orbits that for two-body and three-body point-mass systems, all partial derivatives librate with an amplitude that increases linearly with time. In Hadjifotinou [18] it is shown that this linear behavior is not always preserved when oblateness perturbations and more bodies are included in the model. In particular, in non-resonant systems, regardless of the number of satellites, the behavior of all the partial derivatives exhibits a linear growth as shown in the two first plots of Figure 2.5. In resonant systems instead, and in the presence of oblateness perturbations, the behavior of the partial derivatives is considerably different, as shown in the rest of the plots of Figure 2.5, where long-period and short-period librations are observed. In Figure 2.6 we give some plots of the evolution of some partials with respect to the parameters of the system such as partials with respect to gravitational parameters of satellites and partials with respect to J_2 of Saturn. In this case, the behavior of the partials is similar to the case of resonant systems and long-period and short-period librations are observed. This behavior is not observed in the partials of Phoebe (fifth plot in Figure 2.6) due to the low ratio between the length of integration and the orbital period of Phoebe.

For the sake of completeness, and with the aim of validating the correctness of the integration of the partials, we have tried to investigate the behavior with time of a small variation $\Delta\mathbf{x}_0$ introduced in the initial conditions by means of the state propagation equation (1.9), that is

$$\Delta\mathbf{x}(t) = \mathbf{\Phi}(t, t_0)\Delta\mathbf{x}_0 \,. \tag{2.278}$$

To this purpose we have carried out two integrations. In the first one we have numerically integrated the equations of motion and the variational equations with the same set of initial conditions and dynamical parameters used in previous section and derived from **SAT136** ephemeris file. In the second integration we have changed the initial state of each satellite by 1 km in the three components of position and by 10^{-3} km/s in the three components of velocity. Then we have computed $\Delta\mathbf{x}_{true}$ obtained by the state difference between the two integrations. $\Delta\mathbf{x}_{true}$ shows a sinusoidal behavior as we can see in Figure 2.7 (left panel), where we plot the difference in the x component between the two numerically integrated orbits for Mimas. The evolution $\Delta\mathbf{x}(t)$ of the initial dynamical state difference $\Delta\mathbf{x}_0$ has also been obtained by means of equation (2.278), where the state transition matrix has been integrated numerically. It shows a linear growth with time due to the linear increase with time of the partial derivatives as noted above (Figure 2.7, right panel). This suggests that, in an orbit determination process, the arc length cannot be too long and must be limited to a length over which the linearity assumption is verified reasonably well. In fact, in the expansion in a Taylor series about the reference trajectory the orders higher than the first are normally neglected but in this case the problem is strongly not linear and over a long time period the first order assumption is not sufficient. This assertion warrants more accurate investigation, but the need to use of a multi-arc approach is clearly indicated.

The same procedure described previously has been applied by changing only the gravitational parameter of Titan by 1%. In this case the behavior of $\Delta\mathbf{x}_{true}$ and $\Delta\mathbf{x}$ (Figure 2.8 left panel and right panel respectively) for Dione are similar and both show a linear growth with time.

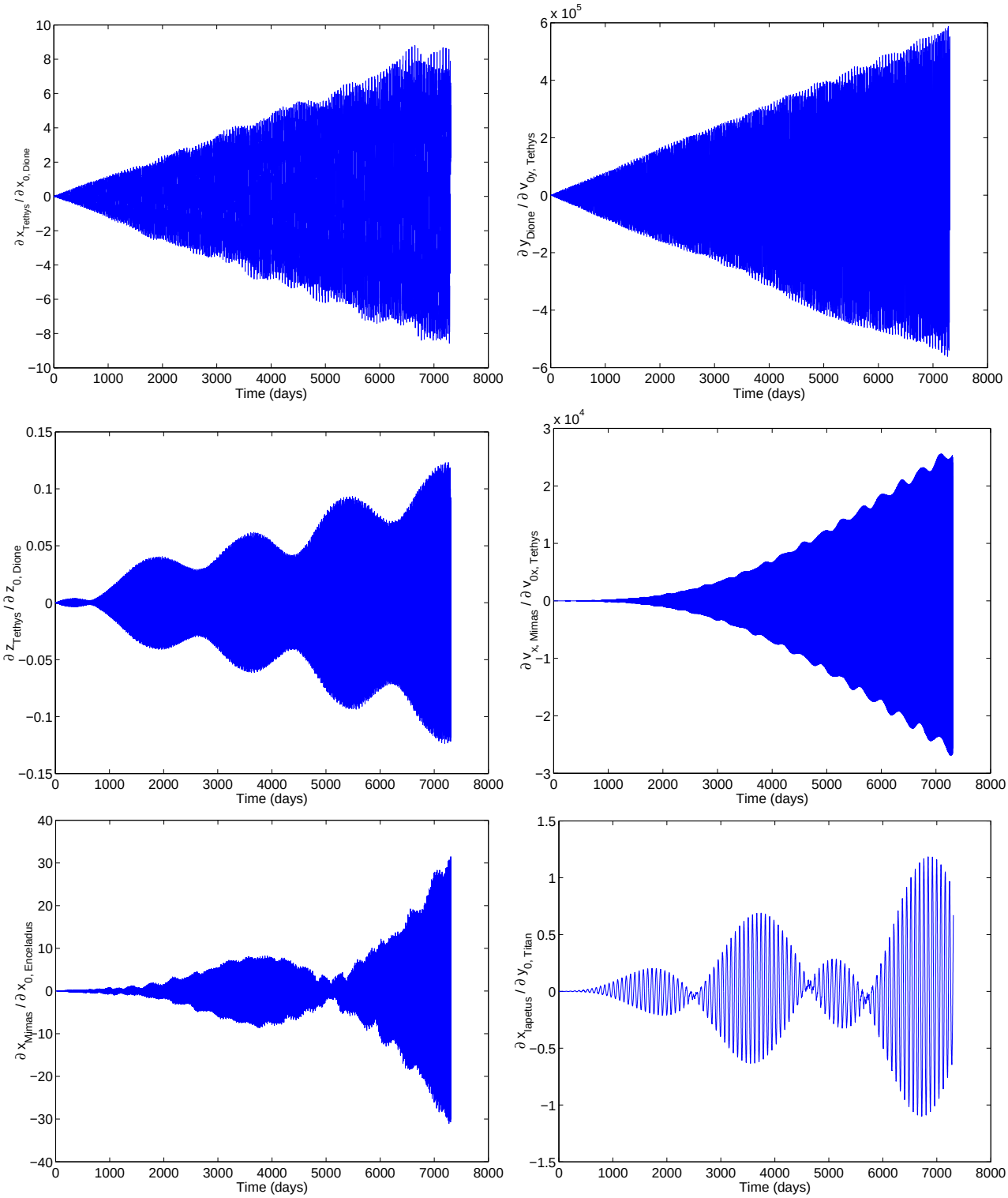

Figure 2.5: The evolution of the partial derivatives in the Saturnian system.

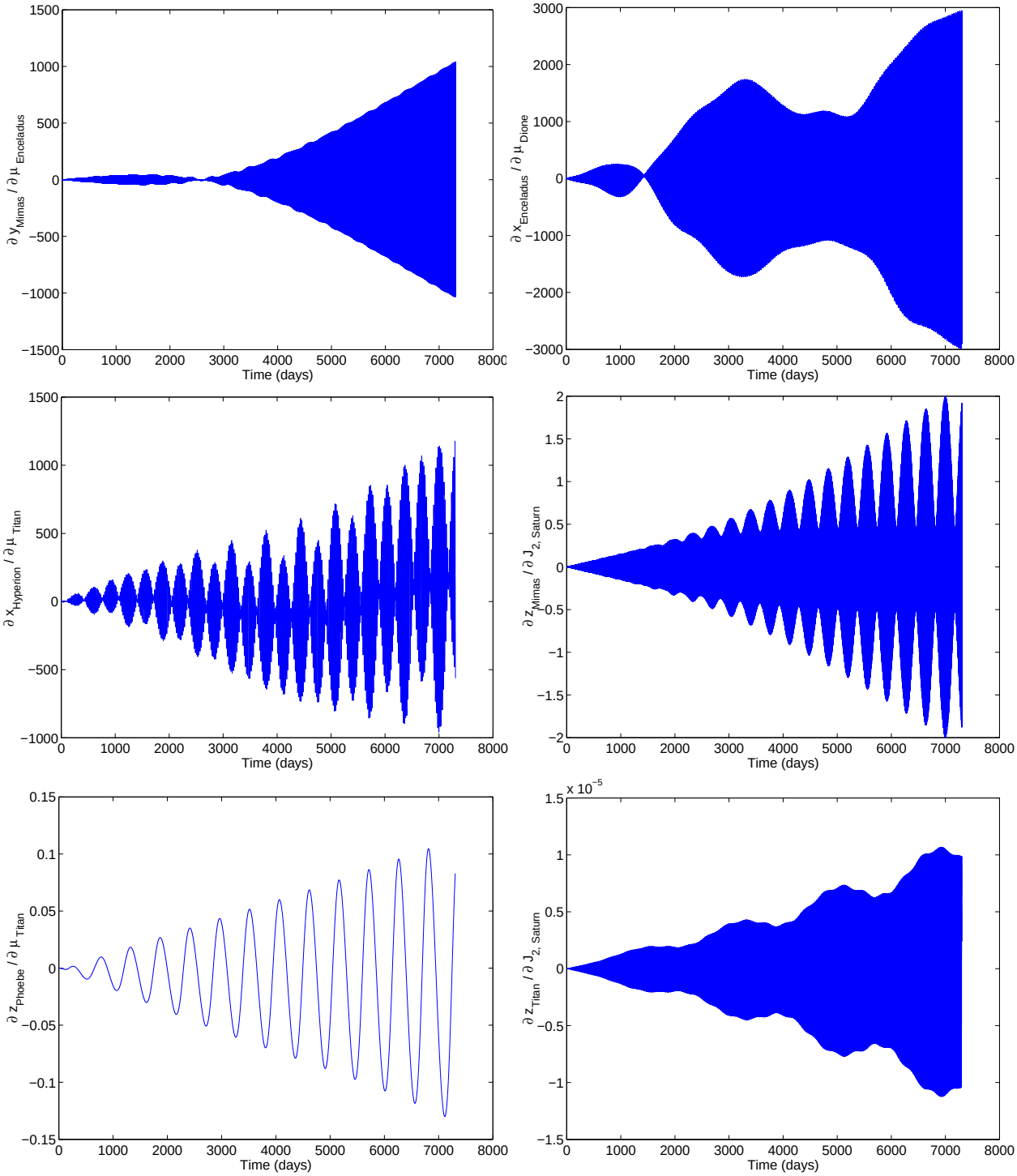

Figure 2.6: The evolution of the partial derivatives in the Saturnian system.

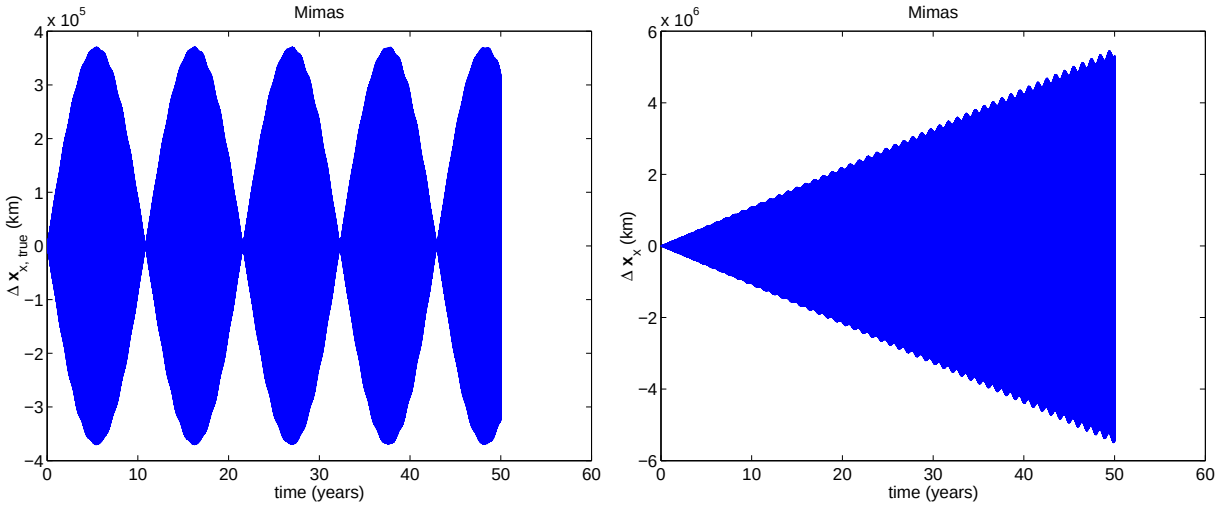

Figure 2.7: (Left) Difference in the x component between the two numerically integrated orbits for Mimas. (Right) Difference in the x component for Mimas obtained using the state propagation equation. The length of integration is 50 years. The variation in initial state of each satellite is by 1 km in the three components of position and by 10^{-3} km/s in the three components of velocity.

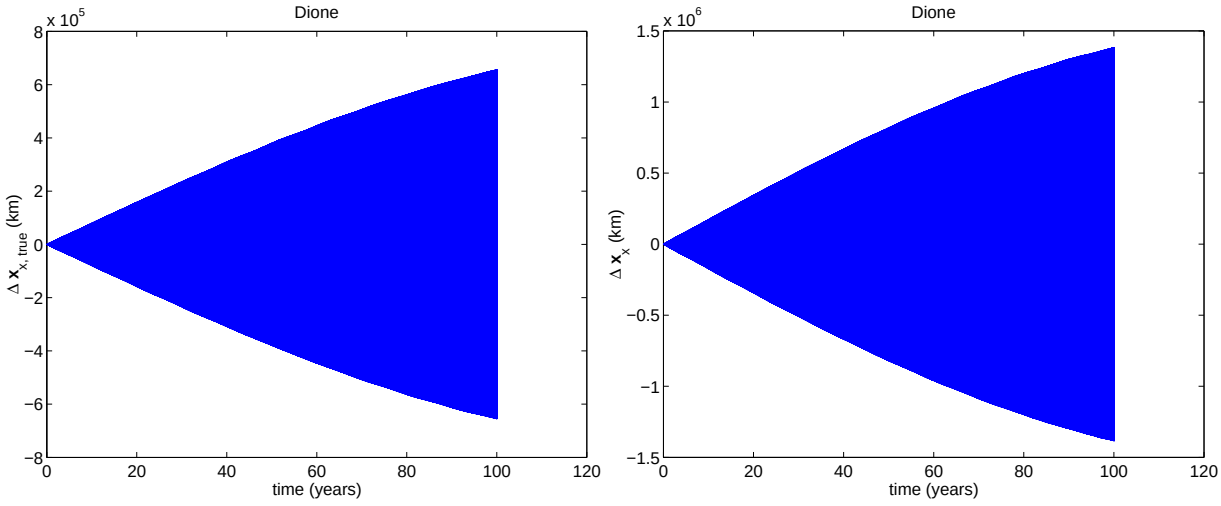

Figure 2.8: (Left) Difference in the x component between the two numerically integrated orbits for Dione. (Right) Difference in the x component for Dione obtained using the state propagation equation. The length of integration is 100 years. The variation of the gravitational parameter of Titan is by 1%.

Chapter 3

Optical Observations

3.1 Introduction

Optical observations are one of the most important sources of data for astrometry, the positional part of astronomy, which encompasses all that is necessary to provide positions and motions of the celestial objects. This includes observational techniques, instrumentation, processing and analysis of observational data, positions and motions of the bodies, reference frames, and the resulting astronomical phenomena. The practical side of astrometry is complemented by a number of theoretical aspects, which relate the observations to laws of physics and to the distribution of matter, or celestial bodies, in space. Among the most important are the celestial mechanics, optics, theory of time and space references (with regards to general relativity), astrophysics, and statistical inference theory.

However, the astrometric information which is sought is generally not the direction from which the light arrives, but a quantity more directly related to the geometric position of the celestial body. To achieve this, one must apply a certain number of corrections to the apparent direction in which the celestial body seems to lie.

3.2 Astronomical observations

The first technological advance in astronomical detectors was the photographic emulsion. Photographic emulsions can make a permanent record of astronomical objects imaged by telescopes. However, photographic emulsions are not a very good photometric devices for astronomy because of several drawbacks. Briefly, these are: photographic emulsions only record a small fraction, around 1%, of the photons that hit the emulsion. Because of the analog nature of the image record on an emulsion, it is difficult to make quantitative measurements of star brightness. Photographic emulsions are also nonlinear, twice the input light does not produce twice the output on the film. This feature is called reciprocity failure.

Modern detectors are digital. They detect individual photons and output a number which is directly and linearly related to the number of photons that were incident on the detector. The first modern detector in this sense is the photomultiplier tube (or PMT). A PMT consists of an evacuated glass tube, on one end of which is deposited a film of a material (such as indium antimonide) called a photocathode. This material has the property that when it is struck by a photon, an electron is often liberated from the material. Each electron liberated from the cathode is directed away from the cathode by an electric field, and is amplified into a pulse of electrons by a series of metal plates (called dynodes) and an accelerating electric field in the tube. Electronics coupled to the PMT counts these pulses. Thus, a single photon hitting the cathode results in an easily counted pulse of many electrons. The drawback of a PMT is that it is essentially a single channel device, meaning there is no positional information in the signal. The output signal does not depend on where on the cathode the photon hit, so we get only a measure of all

the light that fell on the photocathode. However, the PMT, unlike a photographic plate, has a digital output, meaning we can easily make quantitative measurements. The fraction of the photons which hit the cathode that are actually detected by the PMT is set by the fraction of photons that hit the cathode that liberate an electron. This fraction is typically 20% or so, so the efficiency of observing is much higher for a PMT than for the best photographic emulsion.

The detector of choice for optical astronomy is now the CCD (charge coupled device). The CCD has many advantages, it is a linear, photon counting device which records a large fraction of the photons that fall on it. It is far better than a PMT because it can record a two dimensional image, i.e. there is positional information.

For astronomical use, CCD is used as a device to measure how much light falls on each pixel. The output is a digital image, consisting of a matrix of numbers, one per pixel, each number being related to the amount of light that falls on that pixel. Of course, one of the advantages of the CCD is that the image, coming out in a digital form, is readily manipulated, measured, and analyzed by computer.

Ground-based observations of the satellites of Saturn can be classified according to the technique employed to make the observations [20]:

- *Visual micrometer measure.* These observations are made using a filar micrometer attached to the eyepiece of a telescope. The observer measures the position of the satellites relative to another object within the field of view, either the planet Saturn or another satellite. Almost all the observations made before 1966 are made in this form.
- *Photographic astrometric measures.* These observations are made by taking a photographic plate of Saturn and its satellites and a number of nearby reference stars, then using standard astrometric techniques to determine the right ascension and declination of each of the satellites. Most observation made since 1966 are in this form.
- *Automatic meridian circle measures.* These observations are made using automatic photoelectric meridian circles to determine the apparent right ascension and declination of the satellites at transit.
- *CCD image measures.* These observations are made by measuring the positions of the satellites from digital images obtained using a CCD device at prime focus of a telescope.
- *Photometry of mutual events.* At intervals approximately 15 years, the Earth and Sun pass through the ring-plane of Saturn. The orbits of the inner satellites lie very close to the ring-plane and it is possible to observe mutual eclipses and occultations during a period of roughly 18 around the time of ring-plane crossing. Analysis of the light-curves enables to determine the time of mid-event and the depth of the event, hence to derive corrections to the longitudes and inclinations of the satellites orbits [2].
- *Timings of elongation, opposition and conjunction.* There are a number of observations made in the late 18th and 19th centuries which give the estimated times of elongations, oppositions and conjunctions of the satellites.

3.3 Data Reduction

The apparent direction in the sky at which the celestial object appears is not the true direction from which the light was emitted. What is observed is the tangent direction of the light when it reaches the observer. For this reason the light path is not rectilinear and several corrections describing the effects of bending, or shift in direction, are to be applied to the direction from which the light is observed to determine the actual direction of the emission. We shall not deal with the various transformations undergone by the light within the observing instrument because they are particular to every used instruments. We shall consider only the direction from which the light came when it entered into the instrument. One has to consider the atmospheric refraction, the shift in direction due to the combination of the speed of light

with motion of the observer, called aberration, and the bending due to the presence of a gravitational field.

We deal these effects because some of them are to be considered not only in the data reduction but also in the computation of the observable.

3.3.1 Definitions

Mean place [15]: the mean coordinates (α_1, δ_1) of an object are its coordinates on the barycentric celestial sphere referred to the mean equator and equinox of date (the epoch of the equator and equinox is the same as the date of observation). The mean coordinates of an object only vary due to precession and proper motion, all other effects being excluded by definition. That is a mean place is determined by removing, from the directly observed position, the effects of refraction, geocentric and stellar parallax, and stellar aberration and by referring the coordinates to the mean equator and equinox of a standard epoch. In compiling star catalogs it has been the practice not to remove the secular part of stellar aberration.

True place [15]: the true coordinates (α_2, δ_2) of an object are its coordinates on the barycentric celestial sphere referred to the true equator and equinox of date. True coordinates introduce nutation.

Apparent place [15]: the apparent coordinates (α, δ) of an object are its coordinates on the geocentric celestial sphere referred to the true equator and equinox of date. The apparent place involves further corrections for annual aberration and parallax.

Standard mean place [15]: the standard mean coordinates (α_0, δ_0) of an object are its mean coordinates at the date of a standard epoch (B1950.0 or J2000.0).

Proper (or topocentric) place [29]: the apparent coordinates (α, δ) of an object are its coordinates as it would be seen by an observer on the surface of the Earth neglecting atmospheric refraction.

Astrometric place [43]: is directly comparable with the mean place; in fact it is computed from the geometric position corrected for the light travel time.

Standard coordinates [43] and [15]: the standard coordinates are defined as the tangential coordinates (ξ, η) referred to axes in the directions of increasing right ascension and declination respectively.

Virtual place (differential astrometry) [29]: the virtual place is the apparent place expressed in the coordinate system defined by the Earth's mean equator and equinox at the reference epoch.

Local place (differential astrometry) [29]: the local place is a topocentric place expressed in the coordinate system defined by the Earth's mean equator and equinox at the reference epoch.

3.3.2 Atmospheric refraction

The ground-based astronomical instruments are immersed in the atmosphere. The light coming from a body and reaching a ground instrument goes through a various atmospheric layers. This optically active element substantially affects the shape of the image and the apparent direction of the observed celestial body. The atmosphere deviates light because its refractive index is not equal to one. So for observational reduction the effect of atmospheric refraction must be included.

When the light crosses a surface which separates two gas layers with refractive indexes n and $n + dn$, it is deviated according to the Snell's law. If ξ is the angle of incidence in a medium characterized by the index of refraction n, the angle of refraction in the medium of refractive index $n + dn$ is $\xi + d\xi$ and obeys the relation

$$(n + dn) \sin(\xi + d\xi) = n \sin \xi \,. \tag{3.1}$$

The total bending of the light R is

$$R = z - z_0 \,, \tag{3.2}$$

where z_0 is the observed zenith distance of the object and z is the zenith distance it would have had without atmosphere and is referred to the zenith direction of the observer.

In theory the determination of R should imply the knowledge of n at all the point of the atmosphere crossed by the light path, and the angle of the local normals to iso-index layers with vertical V at the origin. It would be obtained by integrating equation (3.1) from the ground with a measured refractive index n_0 to space (an height of about 50 km is sufficient) from which one may consider that the vacuum is sufficient to assume $n = 1$. For practical applications in astrometry one is led to represent the atmosphere by a model that allows computation of R as a function only of conditions (temperature, pressure etc.) at the observatory.

The more precise algorithm for computation of atmospheric refraction uses numerical quadrature but the real accuracy is very dependent on the conditions, particularly for large zenith distances, and on the atmospheric model. The atmosphere is assumed to be spherically symmetric and in hydrostatic equilibrium, and to obey the perfect gas low for the combined mixture of dry air and water vapor, and also for the dry air and water vapor separately. The two layer of the atmosphere are the troposphere and the stratosphere. The numerical algorithm is given in [51] and calculates the total refraction as the sum of the refraction caused by the troposphere and the stratosphere.

Another approach is that uses an approximated formula, known as the Laplace formula [31], that gives the total bending of the light R as

$$R = A \tan z_0 - B \tan^3 z_0 \,, \tag{3.3}$$

where A and B depend upon physical conditions of the air at the place of observation.

Since atmospheric refraction depends on the atmospheric conditions at the observing site, usually this correction is applied directly into the data reduction procedure performed at the observing site. For a more detailed description of the atmospheric refraction see [31], [30], [51].

3.3.3 Aberration

The velocity of light is finite, and so the apparent direction of a moving celestial object from a moving observer is not the same as the geometric direction of the object from the observer at the same instant. This displacement of the apparent position from the geometric position may be attributed in part to the motion of the object, and in part to the motion of the observer, these motions being referred to an inertial frame of reference. The former part, independent of the motion of the observer, may be considered to be a correction for light-time; the latter part, independent of the motion or distance of the object, is referred to as stellar aberration, since for the stars the normal practice is to ignore the correction for the light-time. The sum of the two parts is called planetary aberration, since it is applicable to planets and other members of the Solar System.

We remark that, if the celestial coordinates of a Solar System body are determined with respect to stars of well-known coordinates, the stellar aberration are automatically eliminated [3]. In fact star catalog give the position of a star at an epoch referred to the mean equator and equinox at a chosen epoch, that is a mean place. Since the star positions a mean place, the coordinates are referred to the barycentric celestial sphere.

Light-Time

In Figure 3.1 E is a stationary observer at time t, and P is the position of a celestial object also at time t. The dotted curve represents the orbit of P. The light which is received at E at time t was emitted by the celestial object when it was at P' at time $(t - \tau)$, where τ is the light-time, i.e. the time taken for the light to travel from P' to E. The direction EP' is called the geometric direction of the object allowing for light-time.

Light-time is calculated iteratively, with a first approximation τ_1 calculated from the geometric distance between the object and the observer at time t, and the next approximation τ_2 calculated from the

distance between P' at $(t - \tau_1)$ and the observer at time t. No allowance has been made here for the relativistic delay caused by the Sun's gravitational field.

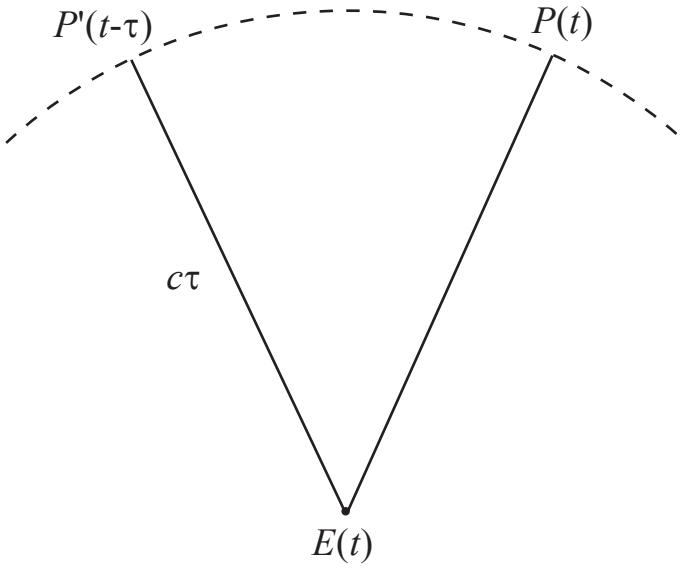

Figure 3.1: Light time aberration

Stellar aberration

In general, the observer at E will be moving with a velocity $\mathbf{V}$. The apparent change in the geometric direction of the celestial object at P' due to the orbital motion of the Earth about the barycenter of Solar System is called stellar aberration. In Figure 3.2, $\mathbf{p}$ is a unit vector in the geometric direction EP', i.e., in the direction of the body at time t allowing for light-time (but ignoring the effect of light deflection). The observer is moving with a velocity $\mathbf{V}$ relative to the stationary frame, and at time t will observe the body at P'' in the direction $\mathbf{p}_1$, where $P'EB = \theta$ is the angle between the direction of motion and $\mathbf{p}$ in the stationary frame, and $P'EP'' = \Delta\theta$ is the displacement due to aberration in the moving frame, which is always toward the direction of motion.

The classical Newtonian expression for the direction of the source as seen by the moving observer is obtained by vector addition of velocities as follows [51] [43]:

$$\mathbf{p}_1 = \frac{\mathbf{p} + \frac{\mathbf{V}}{c}}{|\mathbf{p} + \frac{\mathbf{V}}{c}|} \,. \tag{3.4}$$

Taking the scalar part of the vector cross product of $\mathbf{p}$ with equation (3.4), then

$$\sin\Delta\theta = \frac{\left(\frac{V}{c}\right)\sin\theta}{\sqrt{1 + 2\frac{V}{c} + (\frac{V}{c})^2}} = \frac{V}{c}\sin\theta - \frac{1}{2}\left(\frac{V}{c}\right)^2 \sin 2\theta + \ldots \,, \tag{3.5}$$

since $|\mathbf{p} \times \mathbf{p}_1| = \sin\Delta\theta$, $|\mathbf{p} \times \mathbf{p}| = 0$ and $|\mathbf{p} \times \frac{\mathbf{V}}{c}| = \frac{V}{c}\sin\theta$.

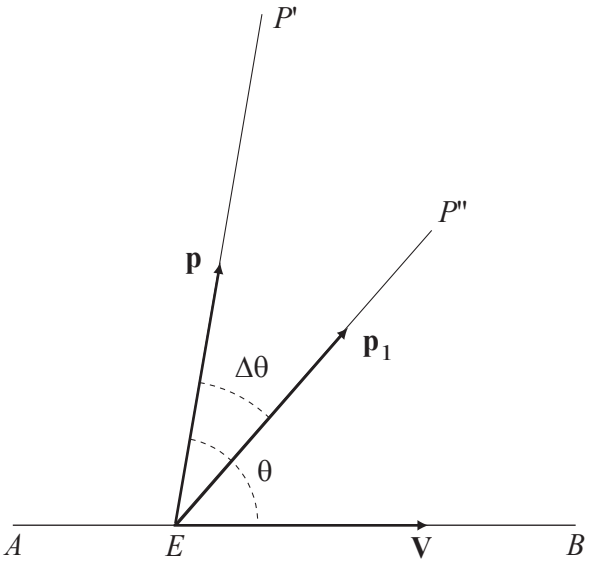

Figure 3.2: Stellar aberration

The term of order $\frac{V}{c}$ is about 0.0001 or $20''$; the term $(\frac{V}{c})^2$ has a maximum value of about $0''.001$.

In special relativity, the velocity of light is constant in the moving and stationary frame, and the Lorentz formula for the addition of velocities applies. Hence [51] [43]

$$\mathbf{p}_1 = \frac{\beta^{-1}\mathbf{p} + \frac{\mathbf{V}}{c} + \frac{(\mathbf{p}\cdot\frac{\mathbf{V}}{c})(\frac{\mathbf{V}}{c})}{1+\beta^{-1}}}{1 + \mathbf{p}\cdot\frac{\mathbf{V}}{c}}\,, \tag{3.6}$$

where $\beta^{-1} = \sqrt{1-(\frac{V}{c})^2}$, again taking the modulus of the vector cross products of equation (3.6) with $\mathbf{p}$, then [51]

$$\sin\Delta\theta = \frac{(\frac{V}{c})\sin\theta + \frac{\frac{1}{2}(\frac{V}{c})^2\sin 2\vartheta}{1+\beta^{-1}}}{1+\frac{V}{c}\cos\vartheta} = \frac{V}{c}\sin\theta - \frac{1}{4}\left(\frac{V}{c}\right)^2\sin 2\theta + \ldots\,, \tag{3.7}$$

which shows that special-relativistic aberration and classical Newtonian aberration agree to order $\frac{V}{c}$.

The motion of an observer on the Earth is the resultant of diurnal rotation of the Earth, the orbital motion of the Earth about the center of mass of the Solar System, and the motion of this center of mass in space. The stellar aberration is therefore made up of three components, which are referred to as diurnal aberration, annual aberration, and secular aberration. The stars and the center of mass of the Solar System may each be considered to be in uniform rectilinear motion. In this case the correction for light-time and the secular aberration are indistinguishable, and the aberrational displacement due to the relative motion is merely equal to the proper motion of the star multiplied by the light-time; it is constant for each star, and in general, is not known, and is therefore ignored.

Classical Annual Aberration

The annual aberration is calculated as from 1960 from the actual motion of the Earth, referred to an inertial frame of reference and to the center of mass of the Solar System. The resulting aberrational displacement $\Delta\theta$ may be resolved into corrections to the directional coordinates by standard methods [51] [3]. If, for example $\dot{X}$, $\dot{Y}$ and $\dot{Z}$ are the components of the Earth's velocity parallel to equatorial rectangular axes, the corrections to right ascension and declination, referred to the same equator and equinox, are, to second order in $\frac{V}{c}$,

$$\cos\delta\Delta\alpha = -\frac{\dot{X}}{c}\sin\alpha + \frac{\dot{Y}}{c}\cos\alpha + \frac{1}{c^2}(\dot{X}\sin\alpha - \dot{Y}\cos\alpha)(\dot{X}\cos\alpha - \dot{Y}\sin\alpha)\sec\delta + \dots\,, \tag{3.8}$$

$$\begin{aligned}\Delta\delta &= -\frac{\dot{X}}{c}\cos\alpha\sin\delta - \frac{\dot{Y}}{c}\sin\alpha\sin\delta + \frac{\dot{Z}}{c}\cos\delta - \frac{1}{2c^2}(\dot{X}\sin\alpha - \dot{Y}\cos\alpha)^2\tan\delta \\ &+ \frac{1}{c^2}(\dot{X}\cos\delta\cos\alpha + \dot{Y}\cos\delta\sin\alpha + \dot{Z}\sin\delta)(\dot{X}\sin\delta\cos\alpha + \dot{Y}\sin\delta\sin\alpha - \dot{Z}\cos\delta) + \dots\,,\end{aligned} \tag{3.9}$$

These equations are usually used to first order in $\frac{V}{c}$, and ignoring the $\dot{Z}$ term are expressed in terms of the Besselian day numbers C and D, which represent the classical annual aberration terms.

To a lower precision it is possible to use the expressions [51]

$$\dot{X} = +0.0172\sin\lambda\,, \qquad \dot{Y} = -0.0158\cos\lambda\,, \qquad \dot{Z} = -0.0068\cos\lambda\,, \tag{3.10}$$

for the barycentric velocity of the Earth with respect to the mean equator and equinox of J2000.0, where λ is the apparent longitude of the Sun.

Also to first order in $\frac{V}{c}$, we obtain for the aberration in right ascension and declination due to the unperturbed elliptic component of the orbital motion of the Earth with respect to the Sun, obtained as a correction to be applied to the geometric place α, δ in order to obtain the apparent place α_1, δ_1 [51]:

$$\begin{aligned}\alpha_1 - \alpha &= -(\kappa\sin\odot + \kappa e\sin\Pi)\sin\alpha\sec\delta - (\kappa\cos\odot\cos\epsilon + \kappa e\cos\Pi\cos\epsilon)\cos\alpha\sec\delta\,, \\ \delta_1 - \delta &= -(\kappa\sin\odot + \kappa e\sin\Pi)\cos\alpha\sin\delta \\ &- (\kappa\cos\odot\cos\epsilon + \kappa e\cos\Pi\cos\epsilon)(\tan\epsilon\cos\delta - \sin\alpha\sin\delta)\,,\end{aligned} \tag{3.11}$$

where $\odot$ is the true geometric latitude of the Sun, e and Π are the eccentricity and longitude of perigee of the solar orbit, ϵ is the mean obliquity of the ecliptic, and κ is the constant of aberration.

The second term in each factor in equation (3.11) depends explicitly on the eccentricity and represents the components of the displacement due to the departure of the elliptic orbital motion from a circle. The component of the aberration that depends on e is known as elliptic aberration.

The constant of aberration κ is the ratio of the mean orbital speed of the Earth to the speed of light, where perturbations and the motion of the Sun relative to the barycenter are neglected. It is derived from

$$\kappa = \frac{na}{c\sqrt{1-e^2}}\,, \tag{3.12}$$

where c is the speed of the light, a is the mean distance of the Earth from the Sun, n is the mean motion, and e is the eccentricity of the orbit.

The annual aberration due to the barycentric motion of the Sun or to the action of any particular planet may be obtained, when the ecliptic latitude of the planet is neglected, from [51]

$$\alpha_1 - \alpha = -\frac{nma}{c}(\sin\alpha\sin l + \cos\epsilon\cos\alpha\cos l)\sec\delta\,, \tag{3.13}$$

$$\delta_1 - \delta = -\frac{nma}{c}(\cos\alpha\sin\delta\sin l + \cos l(\sin\epsilon\cos\delta - \cos\epsilon\sin\alpha\sin\delta))\,, \tag{3.14}$$

where l is the heliocentric ecliptic longitude of the planet, m is the ratio of mass of the planet to Sun, a is the mean distance, and n is the mean motion. The coefficients to be used are given in Table 3.1.

The Sun's aberration in longitude, assuming unperturbed elliptical motion, can be given as

$$\Delta\lambda = -\kappa \sec\beta(1 + \epsilon\cos\nu) = \frac{\kappa a(1-e^2)}{R}\,, \tag{3.15}$$

where κ is the constant of aberration; a, e, and ν are the semi-major axis, eccentricity, and true anomaly of the Earth's orbit; and β and R are the Sun's latitude and true radius vector.

Planet	Coefficient $\frac{nma}{c}$
Venus	0".0001
Earth	0".0001
Jupiter	0".0086
Saturn	0".0019
Uranus	0".0002
Neptune	0".0002

Table 3.1: Coefficients $\frac{nma}{c}$ for the Major Planets [51]

Measurements of radial velocity may be reduced to a common origin at the barycenter by adding the component of the Earth's velocity in the direction of the object, that is, by adding

$$\dot{X}\cos\alpha\cos\delta + \dot{Y}\sin\alpha\cos\delta + \dot{Z}\sin\delta\,. \tag{3.16}$$

Diurnal Aberration

The rotation of the Earth on its axis carries the observer toward the east with a velocity $\omega\rho\cos\phi'$, where ω is the equatorial angular velocity of the Earth, and ρ and ϕ' are the geocentric distance and latitude of the observer, respectively. The corresponding constant of diurnal aberration is [51] [3] [15]

$$\frac{a\omega}{c}\frac{\rho}{a}\cos\phi' = 0''.3200\frac{\rho}{a}\cos\phi' = 0^s.02133\frac{\rho}{a}\cos\phi'\,. \tag{3.17}$$

The aberrational displacement may be resolved into corrections (apparent - mean) in right ascension and declination:

$$\Delta\alpha = 0^s.02133\frac{\rho}{a}\cos\phi'\cos h\sec\delta\,, \tag{3.18}$$

$$\Delta\delta = 0''.3200\frac{\rho}{a}\cos\phi'\sin h\sin\delta\,, \tag{3.19}$$

where h is the hour angle. The effect is small but is of importance in meridian observations. For a star at transit, $h = 0$ or 180°, so $\Delta\delta$ is zero, but

$$\Delta\alpha = \pm 0^s.02133\frac{\rho}{a}\cos\phi'\sec\delta\,, \tag{3.20}$$

where the plus and minus signs are used for upper and lower transits, respectively; this may be regarded as a correction to the time of transit.

Alternatively, the effect may be computed in rectangular coordinates using the following expression for the geocentric velocity ($\dot{\mathbf{r}}$) vector of the observer with respect to the celestial equatorial reference frame of date:

$$\dot{\mathbf{r}} = \begin{bmatrix} -\omega\rho\cos\phi'\sin(\vartheta+\lambda) \\ \omega\rho\cos\phi'\cos(\vartheta+\lambda) \\ 0 \end{bmatrix}\,, \tag{3.21}$$

where ϑ is the Greenwich sidereal time (mean or apparent as appropriate), and λ is the longitude (east longitudes are positive).

The geocentric velocity vector of the observer is added to the barycentric velocity of the Earth's center, to obtain the corresponding barycentric velocity vector of the observer.

Planetary Aberration

Planetary aberration is the apparent displacement of the observed position of a celestial body produced by both the motion of the body and the motion of the Earth. It is often calculated by adding the correction for stellar aberration to the geometric position corrected for light-time. On the other hand it may be calculated directly, either by using the barycentric positions of the body and the Earth at time $(t - \tau)$, or by using the barycentric positions and velocities of the body and the Earth at time t as described below. However, although these latter two methods are simple and widely used, the first method may be preferred, since it brings out the principle that aberration depends upon the relative velocity of observer and object.

If we denote the barycentric position of the Earth at time t by $\mathbf{E}_B(t)$ and the barycentric position of the planet at time t allowing for light-time is given by

$$\mathbf{P}(t) = \mathbf{u}_B(t - \tau) - \mathbf{E}_B(t)\,, \tag{3.22}$$

where $\tau = \frac{P}{c}$ is the light-time and $P = |\mathbf{P}|$. If $\mathbf{P}_1$ is the geocentric position of the planet allowing for planetary aberration, then using classical stellar aberration (3.4)

$$\mathbf{P}_1 = \mathbf{P} + \tau\dot{\mathbf{E}}_B(t)\,. \tag{3.23}$$

If we assume that the velocity of the Earth $\dot{\mathbf{E}}_B(t)$ and the velocity of the planet $\dot{\mathbf{u}}_B$ are constant during the light-time, then the equation (3.22) may be written as

$$\mathbf{P}_1 = \mathbf{u}_B(t - \tau) - \mathbf{E}_B(t - \tau)\,, \tag{3.24}$$

or

$$\mathbf{P}_1 = \mathbf{u}_B(t) - \mathbf{E}_B(t) - \tau(\dot{\mathbf{u}}_B(t) - \dot{\mathbf{E}}_B(t))\,. \tag{3.25}$$

Since Newtonian aberration and special-relativity aberration agree order $\frac{\mathbf{V}}{c}$, it is only when mas precision is required that it becomes necessary to use a rigorous formula (see equation 3.6).

Differential Annual Aberration

The differential coordinates of a moving object with respect to a fixed star will be affected by differential aberration. If $\Delta\alpha$, $\Delta\delta$ are the observed differences of the coordinates in the sense moving object minus star, then the corrections for differential annual aberration are

$$\Delta(\alpha_1 - \alpha) = (D\cos\alpha - C\sin\alpha)\sec\delta\Delta\alpha + (D\sin\alpha + C\cos\alpha)\sec\delta\tan\delta\Delta\delta\,, \tag{3.26}$$

$$\Delta(\delta_1 - \delta) = (D\cos\alpha - C\sin\alpha)\cos\delta\Delta\delta - (D\sin\alpha + C\cos\alpha)\sin\delta\Delta\alpha - C\tan\epsilon_0\sin\delta\Delta\delta\,, \tag{3.27}$$

where C and D are the aberration day numbers, and the units of each term are consistent. The corrections should be applied with those for differential precision and nutation to give mean positions referred to the same equator and equinox as those of the stars.

Differential Planetary Aberration

Aberration, because of its dependence on the relative motion and distances, sometimes has complex effects where two or more bodies are involved, as, e.g., in eclipses, transits, and the phenomena of satellite systems. The determination of these effects presents an intricate problem.

In a transit of a planet across the disk of the Sun, e.g., the external contacts occur when the observer is on the conical surface that circumscribes the Sun and the planet and has its vertex between the Sun and the planet. The internal contact occur when the observer is on the cone circumscribing the planet and the Sun having its vertex between the planet and the Earth. The observed contacts are at the instants when the apparent positions of a point on the limb of the planet and a point on the limb of the Sun are the same; i.e., the ray of light from the Sun that reaches the geometric position of the observer at the instant T of contact has grazed the planet on the way. This ray left the Sun at a previous time $T - \tau_2$ and reached the planet at time $(T - \tau_2) + \tau_1$. The circumscribing cones are formed by the grazing rays; hence, the points on the Earth and the planet that lie in the same straight line on one of the cones at the instant of a contact are the geometric position of the observer at the time T, and the geometric position of the point on the planet at time $T - \tau_2 + \tau_1$. Therefore, in the formulas of the theory of transits, for any value of the time T, all quantities depending on the time must be derived from the values of the geometric coordinates (r, l, b) of the planet at $T - \tau_2 + \tau_1$ and the geometric coordinates (r', l', b') of the Earth at t.

Similarly, in comparing observed positions of object in the Solar System with one another or with reference stars, in order to determine the coordinates of a body, great care is required in correcting the observations for aberration, according to the means of observation used, and the method of comparison.

In eclipsing binary systems, an apparent variation of the period may be produced by the variation in light-time with changing distance from the observer due to an orbital motion of the eclipsing pair with respect to a distant third component.

3.3.4 Gravitational light deflection

Predicted by Einstein and first confirmed at the eclipse of 1919 May, gravitational light deflection has been measured many times and most recent high precision measurements have been made with radio interferometers. The deflection increases the closer the light path is to the Sun; at heliocentric elongation of 90°, however the deflection has decreased to 0.004". The algorithm for the deflection of light [51] is that of Yallop (1984) as given in the *Astronomical Almanac 1984*, which is an adaptation of Murray's formulas. The isotropic metric has been assumed. Only the Sun's gravitational field has been included; each of the planets causes a similar effect that is smaller by a factor equal to the ratio of the planet's mass to that of the Sun ($\sim 1/1047$ for Jupiter). The gravitational field of Earth, also ignored, can deflect light for few tenth of a milliarcseconds for ground based observations.

In Figure 3.3, S is the Sun, P the observed body, E the Earth (ground based observation). The unit vectors $\mathbf{e}$ and $\mathbf{q}$ represent the heliocentric directions of the Earth and the body respectively. ψ is the heliocentric elongation of the Earth from P where

$$\cos\psi = \mathbf{q} \cdot \mathbf{e}\,. \tag{3.28}$$

The geocentric direction to the body P when the light left it is given by the versor $\mathbf{p}$. The arc AEB represents the light path as it passes the Earth. The tangent to the light path at E is XEY. As the light, which was emitted at P, travels along the path AB, it is always deflected towards the Sun. At E the direction between $\mathbf{p}$ and the tangent to the light path is $\Delta\phi$. Einstein's general relativity theory predicts that

$$\Delta\phi = \frac{2\mu}{c^2 d_E} \frac{\sin\psi}{1 + \cos\psi}\,, \tag{3.29}$$

where d_E is the distance of the Earth from the Sun, μ is the heliocentric gravitational constant and c is the speed of light. The apparent direction of P is along the tangent to the light path $\mathbf{p}_1$, and is [51]

$$\mathbf{p}_1 = \mathbf{p} + \frac{(\mathbf{q} \times \mathbf{e}) \times \mathbf{p}}{\sin\psi} \Delta\phi\,. \tag{3.30}$$

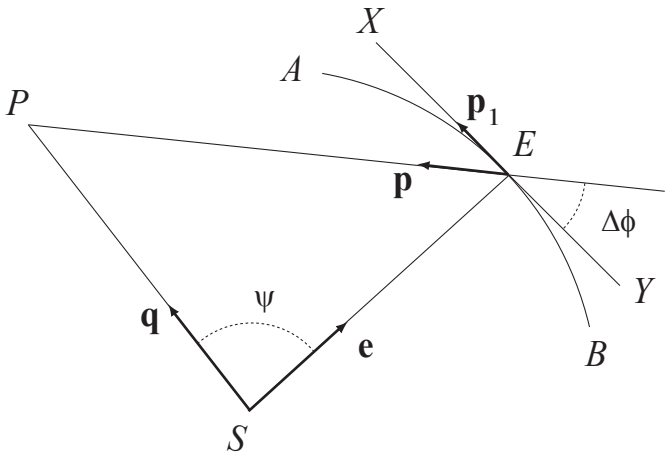

Figure 3.3: Gravitational light deflection

This equation can be written in a form that is more useful for computation,

$$\mathbf{p}_1 = \mathbf{p} + \frac{g_1}{g_2} \left[(\mathbf{p} \cdot \mathbf{q})\, \mathbf{e} - (\mathbf{e} \cdot \mathbf{p})\, \mathbf{q} \right] , \tag{3.31}$$

where g_1 and g_2 are dimensionless quantities

$$g_1 = \frac{2\mu}{c^2 d_E} , \qquad g_2 = 1 + \mathbf{q} \cdot \mathbf{e} . \tag{3.32}$$

For a more exhaustive treatment of the gravitational light deflection see [51] [31].

3.4 Observation modeling

In this section we give a series of algorithm for the computation of the position of a Solar System object as viewed from an observer according to the definitions given in Section 3.3.1. Depending on the observation type and on the data preprocessing some of the effects described in section 3.3 can be considered or neglected.

3.4.1 The apparent place for Earth-based observations

The coordinate system is defined by the Earth's mean equator and equinox of t_0, the reference epoch of J2000.0. For the definitions of the used reference frames and time systems, see Appendix A.

Given the ephemerides of a Solar System body with respect to the Solar System barycenter, its apparent place at a given epoch t' can be computed by [51], [29]

$$\mathbf{u}\,(t') = \mathbf{N}\,(t)\,\mathbf{P}\,(t)\;\; f_a \left\{ f_{gd} \left[\mathbf{u}_B\,(t-\tau) - \mathbf{E}_B\,(t) \right] \right\} , \tag{3.33}$$

where t' is the epoch of observation in the TDT timescale, t is the epoch of observation in the TDB timescale, τ is the light travel time from the body to the Earth in the TDB timescale for light arriving at the observation epoch t, $\mathbf{u}_B(t-\tau)$ is the position of the body with respect to the Solar System Barycenter at the epoch $t-\tau$ referred to the mean equator and equinox of t_0, $\mathbf{E}_B(t)$ is the position of the Earth with respect to the Solar System Barycenter at the epoch t referred to the mean equator and equinox of t_0, $f_{gd}[\ldots]$ is a function representing the gravitational deflection of light, $f_a[\ldots]$ is a function representing the aberration of light, $\mathbf{P}(t)$ is the precession matrix for the epoch t (a rotation from the mean equinox and equator of t_0 to the epoch of observation t), $\mathbf{N}(t)$ is the nutation matrix from the epoch t (a rotation from the mean equinox and equator of date to the true equinox and equator of date t) and $\mathbf{u}(t')$ is the apparent (geocentric) place of the body at the epoch of observation t' with origin at the center of mass of the Earth. The subscript $_B$ indicates that the subscripted quantity is computed in the Solar System Barycenter.

Below we give the step necessary to compute correctly the apparent place as give by formula 3.33. The algorithm take into account of some effects described in detail in section 3.3.

1. From the barycentric position and velocity of the Earth, $\mathbf{E}_B(t)$ and $\dot{\mathbf{E}}_B(t)$, and the barycentric position of the Sun $\mathbf{S}_B(t)$, both referred to the Earth mean equator and equinox of t_0, compute the vector $\mathbf{E}_H(t)$

$$\mathbf{E}_H(t) = \mathbf{E}_B(t) - \mathbf{S}_B(t)\ , \tag{3.34}$$

   which represents the heliocentric position of the Earth at the time t of observation.

2. From the barycentric position of the body $\mathbf{u}_B(t)$ referred to the Earth mean equator and equinox of t_0, compute d, the geometric distance between the centers of mass of the Earth and the planet at time t

$$d(t) = |\mathbf{u}_B(t) - \mathbf{E}_B(t)|\ . \tag{3.35}$$

3. Compute the geocentric position of body accounting for light time (see section 3.3.3):

   (a) Compute a first approximation to the light time travel between the body and the Earth as

$$\tau = \frac{d}{c}\,, \tag{3.36}$$

   where c is the speed of light (see [35] and [36] for IAU value).

   (b) From the barycentric position of the body $\mathbf{u}_B(t-\tau)$ and the Sun $\mathbf{S}_B(t-\tau)$ for the time $t-\tau$, compute

$$\mathbf{U}(t) = \mathbf{u}_B(t-\tau) - \mathbf{E}_B(t)\ , \tag{3.37}$$
$$\mathbf{Q}(t) = \mathbf{u}_B(t-\tau) - \mathbf{S}_B(t-\tau)\ , \tag{3.38}$$

   which represent a first approximation to the geocentric and heliocentric position of the center of mass of the body, respectively, at the epoch of observation t.

   (c) Compute a better approximation to light travel time between the body and the Earth as

$$c\tau' = |\mathbf{U}| + \frac{2\mu}{c^2}\ln\left(\frac{|\mathbf{E}_H| + |\mathbf{U}| + |\mathbf{Q}|}{|\mathbf{E}_H| - |\mathbf{U}| + |\mathbf{Q}|}\right)\ , \tag{3.39}$$

   where μ is the heliocentric gravitational constant (see [35] and [36] for IAU value). The second term in the previous equation (of the order of microarcsecond) takes into account the relativistic delay caused by the Sun's gravitational field (see [40], [31], [51]).

(d) Compare τ' with τ; if they are not equal within a certain tolerance replace the value of τ with the value of τ' and recompute $\mathbf{U}$ and $\mathbf{Q}$ until the light time converges to within the tolerance permitted (for a computational precision of one milliarcseconds, the tolerance must be about 10^{-8} days).

(e) Set

$$\mathbf{U}(t) = \mathbf{u}_B(t-\tau) - \mathbf{E}_B(t)\,, \tag{3.40}$$

$$\mathbf{Q}(t) = \mathbf{u}_B(t-\tau) - \mathbf{S}_B(t-\tau)\,, \tag{3.41}$$

where τ is the converged value of the light travel time.

4. Compute the effect of the relativistic deflection of light in the Sun's gravitational field (as seen in section 3.3.4):

(a) Compute the following unit vectors

$$\hat{\mathbf{U}} = \mathbf{U}/|\mathbf{U}|\,, \qquad \hat{\mathbf{Q}} = \mathbf{Q}/|\mathbf{Q}|\,, \qquad \hat{\mathbf{E}}_H = \mathbf{E}_H/|\mathbf{E}_H|\,, \tag{3.42}$$

and the scalar quantities

$$g_1 = \frac{2\mu}{c^2\,|\mathbf{E}_H|}\,, \qquad g_2 = 1 + \hat{\mathbf{Q}}\cdot\hat{\mathbf{E}}_H\,, \tag{3.43}$$

(b) Compute the deflected geocentric direction of the body (as from equation (3.31)) as

$$\mathbf{u}_g(t) = |\mathbf{U}|\left\{\hat{\mathbf{U}} + \frac{g_1}{g_2}\left[\left(\hat{\mathbf{U}}\cdot\hat{\mathbf{Q}}\right)\hat{\mathbf{E}}_H - \left(\hat{\mathbf{E}}_H\cdot\hat{\mathbf{U}}\right)\hat{\mathbf{Q}}\right]\right\}. \tag{3.44}$$

5. Compute the aberration of light contribution (see section 3.3.3):

(a) Compute the quantities

$$\hat{\mathbf{u}}_g = \frac{\mathbf{u}_g}{|\mathbf{u}_g|}\,, \qquad \mathbf{V} = \frac{\dot{\mathbf{E}}_B(t)}{c}\,, \qquad \beta^{-1} = \sqrt{1-|\mathbf{V}|^2}\,, \tag{3.45}$$

$$f_1 = \hat{\mathbf{u}}_g\cdot\mathbf{V}\,, \qquad f_2 = 1 + \frac{f_1}{1+\beta^{-1}}\,, \tag{3.46}$$

(b) Compute the aberrated geocentric direction of the body $\mathbf{u}_a$ (using equation (3.6))

$$\mathbf{u}_a = \frac{\left[\beta^{-1}\mathbf{u}_g + f_2\,|\mathbf{u}_g|\,\mathbf{V}\right]}{(1+f_1)}\,. \tag{3.47}$$

The previous formula includes relativistic terms which are of the order of one mas (see section 3.3.3 and [43]). If the requested accuracy is greater, it is possible to use the simplified classical formula

$$\mathbf{u}_a = \mathbf{u}_g + |\mathbf{u}_g|\,\mathbf{V}\,. \tag{3.48}$$

6. Apply precession to coordinate system; compute the three fundamental precession angles ς_A, z_A and θ_A (see Appendix A), and transform the coordinate system to that defined by the mean Earth equator and equinox at the epoch of observation by forming the precession rotation matrix $\mathbf{P}$ and applying it to the vector $\mathbf{u}_a$

$$\mathbf{u}_p = \mathbf{P}\mathbf{u}_a\,. \tag{3.49}$$

7. Apply nutation to coordinate system; compute the mean obliquity of the ecliptic, ϵ_0, the two fundamental nutation angles $\Delta\epsilon$, $\Delta\psi$ and the true obliquity of the ecliptic $\epsilon = \epsilon_0 + \Delta\epsilon$ and transform the coordinate system to that defined by true Earth equator and equinox at the epoch of observation, by forming the nutation rotation matrix $\mathbf{N}$ (see appendix A) and applying it to the vector $\mathbf{u}_p$

$$\mathbf{u} = \mathbf{N}\mathbf{u}_p\,, \tag{3.50}$$

where $\mathbf{u}$ is the final apparent position of the body as given by the formula (3.33).

3.4.2 The topocentric place

The topocentric place of a body is its apparent direction as it would be observed from the surface of the Earth, neglecting atmospheric refraction. The simplest way of computing a topocentric place is to compute an apparent place using the position and velocity vectors of the observer rather than the center of mass of the Earth. In fact the difference between the apparent and topocentric place is due to the different position and velocity of an observer on the Earth's surface compared with those of an observer on the Earth's barycenter. The direction's change of the observed body due to the different position of the observer is the *geocentric parallax* and is significant only for object in the Solar System. The direction's change due to the difference in velocity of the observer (Earth rotation) is the diurnal parallax: this effect is independent of the distance of the planet observed and is always less then $0''.32$ [51].

The algorithm for the computation of the topocentric place is similar to the algorithm for the apparent place. Below we give the steps necessary for the computation of the topocentric place and the common steps are indicated.

1. Compute the universal time of observation, that is the epoch of observation in the UT1 timescale (see Appendix A).

2. Get the vector $\mathbf{r}_o$ (in meters), that is the position vector of the observer in an Earth-fixed coordinate system centered in the Earth's center of mass. This coordinate system has the Earth's equator as xy-plane, the Greenwich meridian as the xz-plane and the z-axis toward the north terrestrial pole.

   (a) If ϕ, λ and h are the observer geodetic latitude, longitude and height above the Earth's reference ellipsoid respectively, then $\mathbf{r}_o$ is given by

   $$\mathbf{r}_o = \begin{bmatrix} (a_e C + h)\cos\phi\cos\lambda \\ (a_e C + h)\sin\phi\sin\lambda \\ (a_e S + h)\sin\phi \end{bmatrix}, \tag{3.51}$$

   where a_e is the equatorial radius of the Earth and

   $$C = \left(\cos^2\phi + \left(1-f^2\right)^2 \sin^2\phi\right)^{-1/2}, \tag{3.52}$$

   $$S = (1-f)^2 C, \tag{3.53}$$

   where f is the flattening of the Earth reference ellipsoid (see [35] and [36] for IAU value).

   (b) If ϕ', λ and r are the observer geocentric latitude, longitude and radius, then the computation of $\mathbf{r}_o$ is more simpler that is

   $$\mathbf{r}_o = \begin{bmatrix} r\cos\phi'\cos\lambda \\ r\sin\phi'\sin\lambda \\ r\sin\phi' \end{bmatrix}. \tag{3.54}$$

3. Compute the Greenwich Apparent Sidereal Time (GAST) at the epoch of observation (see Appendix A).

4. Compute the geocentric position and velocity vectors of the observer with respect to the true equator and equinox of date using

   $$\mathbf{g}(t) = \mathbf{R}_3(-\theta)\,\mathbf{R}_1(y_p)\,\mathbf{R}_2(x_p)\,\mathbf{r}_o, \tag{3.55}$$

   $$\dot{\mathbf{g}}(t) = w\hat{\mathbf{k}} \times \mathbf{g}(t), \tag{3.56}$$

   where $\mathbf{R}_i$ are rotation matrix (see Appendix B) , w is the rotational angular velocity of the Earth [51] (see [35] and [36] for IAU value), $\hat{\mathbf{k}}$ is the unit vector pointing toward the north Celestial Ephemeris

Pole of date and the angle x_p, y_p correspond to the coordinates of the Celestial Ephemeris Pole with respect to the terrestrial pole measured along the meridians at longitude 0° and 270° (see polar motion description in Appendix A). The polar motion affects the components of the observer's geocentric position at a level of 10 meters that corresponds to $0''.3$.

5. Transform the vector $\mathbf{g}(t)$ and $\dot{\mathbf{g}}(t)$ to the coordinate system defined by the Earth mean equator and equinox of t_0 (space fixed frame)

$$\mathbf{G}(t) = \mathbf{P}^{-1}\mathbf{N}^{-1}\mathbf{g}(t) = \mathbf{P}^{T}\mathbf{N}^{T}\mathbf{g}(t) , \tag{3.57}$$

$$\dot{\mathbf{G}}(t) = \mathbf{P}^{-1}\mathbf{N}^{-1}\dot{\mathbf{g}}(t) = \mathbf{P}^{T}\mathbf{N}^{T}\dot{\mathbf{g}}(t) . \tag{3.58}$$

This formulation neglects a Coriolis term due to the slow rotation of the two frames; the equivalent linear velocity of this rotation is of order 10^{-5} m/s for an observer on the surface of Earth and is comparable to the tracking velocity of a large telescope and so is negligible [51].

6. Compute the barycentric position and velocity of the observer with respect to the Solar System Barycenter as

$$\mathbf{o}_B = \mathbf{E}_B(t) + \mathbf{G}(t) , \tag{3.59}$$

$$\dot{\mathbf{o}}_B = \dot{\mathbf{E}}_B(t) + \dot{\mathbf{G}}(t) . \tag{3.60}$$

and continue from the beginning of section 3.4.1, that is from step 1 to the end. In this case we have to redefine the vector $\mathbf{E}_B$ and $\dot{\mathbf{E}}_B$ of section 3.4.1 with $\mathbf{o}_B$ and $\dot{\mathbf{o}}_B$ respectively.

3.4.3 The apparent place from spacecraft

Given the time of the end of the exposure t_{oe} and the time of exposure t_{ex} both in TDB scale, the time of observation t, corresponding to the center of the exposure, is given by

$$t = t_{oe} - \frac{1}{2}t_{ex} . \tag{3.61}$$

Given the ephemerides of a satellite of a planet, in order to compute the apparent position of the satellite at a given epoch t as seen from the spacecraft we proceed as follows. First of all we compute the true position of the satellite as seen from the spacecraft [22], [47]

$$\mathbf{T} = [\mathbf{s}(t-\tau) + \mathbf{b}(t-\tau)] - [\mathbf{r}(t) + \mathbf{b}(t)] , \tag{3.62}$$

where t is the observation time given by (3.61) in the TDB scale, τ is the light travel time from the satellite to the spacecraft, $\mathbf{s}$ is the satellite's position vector, $\mathbf{r}$ is the spacecraft position vector and $\mathbf{b}$ is position vector of the planet system barycenter (see Figure 3.4). The vectors $\mathbf{s}$ and $\mathbf{r}$ are relative to the planet system barycenter while the vector $\mathbf{b}$ is referred to the Solar System barycenter. Since

$$\tau = \frac{|\mathbf{T}|}{c} , \tag{3.63}$$

where c is the speed of light, the light travel time τ is computed by an iterative procedure involving the true relative distance between the spacecraft and the satellite (see section 3.4.1 step 3).

If the object is not in the Solar System like stars, the light time correction is never applied. In this case, given the right ascension α_0, the declination δ_0, the proper motion in right ascension μ_α and declination μ_δ at epoch t_α and t_δ respectively and the parallax p, the vector $\mathbf{s}$ (defining the direction of the star) in (3.62) relative to the Solar System barycenter is given by

$$\mathbf{s}(t-\tau) = \frac{1}{p}\begin{pmatrix} \cos\alpha(t)\cos\delta(t) \\ \sin\alpha(t)\cos\delta(t) \\ \sin\delta(t) \end{pmatrix} , \tag{3.64}$$

where

$$\alpha(t) = \alpha_0 + \mu_\alpha (t - t_\alpha) , \tag{3.65}$$

$$\delta(t) = \delta_0 + \mu_\delta (t - t_\delta) . \tag{3.66}$$

Because the observations include stellar aberration effects, the true position of the satellite (3.62) must be replaced by its apparent position, that is [23], [22], [47]

$$\mathbf{A} = \mathbf{T} + \tau \left[\dot{\mathbf{r}}(t) + \dot{\mathbf{b}}(t) \right] , \tag{3.67}$$

where the vectors $\dot{\mathbf{r}}$ and $\dot{\mathbf{b}}$ are the velocities of the spacecraft with respect to the planet system barycenter and of the planet system barycenter with respect to the Solar System barycenter respectively (see Figure 3.4).

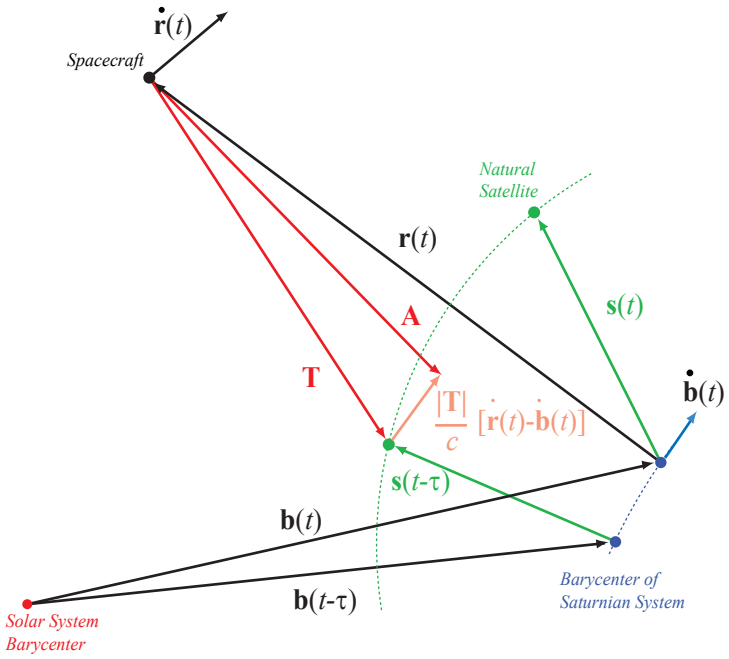

Figure 3.4: Apparent place from spacecraft

3.4.4 Differential astrometry model

In differential astrometry it is necessary to compute only the effect that can change the angles between the position vectors of the observed bodies. For the reduction of high precision differential observations it is not necessary to perform the final precession and nutation rotations. In fact, the orientation of the coordinate system is not considered of fundamental importance since in general the celestial and instrumental coordinate systems are coupled [29].

The positions commonly used in differential astrometry are three: the *virtual place*, the *local place* and the *astrometric place* (as defined in 3.3.1).

- The *virtual place* represents the position of the body as it would be seen from the center of mass of the Earth at some date in the coordinate system defined by the Earth's mean equator and equinox

of the reference epoch with the assumption that the Earth and its atmosphere were transparent and nonrefracting. As we have told in the computation of the virtual place it is not necessary to perform the final precession and nutation rotations. The expression (3.33) reduces to [29], [51]

$$\mathbf{u}_j(t') = f_a\left\{f_{gd}\left[\mathbf{u}_{jB}(t-\tau_j) - \mathbf{E}_B(t)\right]\right\} . \tag{3.68}$$

which represents the virtual place of body j. The algorithm is the same of the section 3.4.1.

- The *local place* represents the position of a body as it would be seen from a location on the Earth's surface at some date and time in the coordinate system defined by the Earth's mean equator and equinox of the reference epoch with the assumption that the Earth and its atmosphere were transparent and nonrefracting (so it is similar to topocentric place). The equation for computing it is the same of the equation (3.68) and the procedure is the same given for the computation the topocentric place algorithm given in section 3.4.2.
- The *astrometric place* is computed with the assumption that the aberration and the gravitational deflection of light can be neglected (besides the precession and nutation rotations). The expression, with the same definitions given in section 3.4.1, is [29], [51]

$$\mathbf{u}_j(t') = \mathbf{u}_{jB}(t-\tau_j) - \mathbf{E}_B(t) , \tag{3.69}$$

which represents the astrometric place of body j. Astrometric place is used only for the ephemerides of faint or fast-moving Solar System object such as minor planets.

Generally for differential astrometry the used positions are *virtual place* as given by equation (3.68). The differential measurement is given by the difference of two virtual places that is

$$\Delta\mathbf{u}_{ij}(t') = \mathbf{u}_j(t') - \mathbf{u}_i(t') , \tag{3.70}$$

with $\mathbf{u}_j$ and $\mathbf{u}_i$ given from the equation (3.68). As discussed by Vienne et al. [65], in the case of differential measurement, and particularly in the case of inter-satellites measurements, the measurements in CCD units are not directly comparable with ephemeris because they have been affected by some local effects. It is necessary to take into account of differential effects caused by refraction, stellar aberration, central projection, light travel time between satellites. The differential corrections can reach $1''$ for the refraction (at $z < 70°$), $0''.04$ for stellar aberration, $0''.03$ for central projection, $0''.025$ for light travel time between satellites (in the case of Saturnian satellites) [65].

3.5 Observation equations

The observations of the satellites generally do not provide cartesian coordinates but quantities related to geometrical configuration of satellites as seen from the Earth. The data types change in the course of time according to the instruments used. We can divide them into three fundamentals categories: absolute coordinates, differential coordinates and tangential coordinates.

3.5.1 Absolute coordinates

The absolute coordinates of a satellite, called right ascension α and declination δ correspond to the spherical angles of the observation reported to a terrestrial equatorial reference frame of fixed direction (J2000.0). These coordinates are computed comparing the position of the satellite with reference stars whose coordinates are well-known (catalog stars). From the cartesian state (x, y, z) of the satellite in a given reference frame at a given epoch the absolute coordinate are given by

$$\begin{cases} \alpha = \arctan\left(\dfrac{y}{x}\right) \\ \delta = \arctan\left[\dfrac{z}{\sqrt{x^2+y^2}}\right] \end{cases} . \tag{3.71}$$

According to the definition 3.3.1 and to Jacobson (private communication) the data types are:

- *Mean position*: right ascension α [(deg) or (hr,min,secs)] and declination δ [(deg) or (hr,min,secs)] with respect to the Solar System Barycenter.
- *Apparent position*: right ascension α [(deg) or (hr,min,secs)] and declination δ [(deg) or (hr,min,secs)] with respect to the Earth Barycenter.
- *Meridian circle position*: right ascension α [(deg) or (hr,min,secs)] and declination δ [(deg) or (hr,min,secs)] with respect to a topocentric observer.

3.5.2 Differential coordinates

The differential coordinates compare the coordinates of an object with the coordinates of another object. This type of coordinates is used in the case of observation of mutual phenomena. If we indicate with the subscript $_o$ the observed object and with the subscript $_r$ the reference object, the differential coordinates are essentially of three types, always expressed in terms of absolute coordinates, that is:

- differential right ascension $\Delta\alpha$ and differential declination $\Delta\delta$

$$\begin{cases} \Delta\alpha = \alpha_o - \alpha_r \\ \Delta\delta = \delta_o - \delta_r \end{cases}, \tag{3.72}$$

- differential right ascension $\Delta\alpha$ multiply by cosine of declination and differential declination

$$\begin{cases} \Delta\alpha\cos\delta_r = (\alpha_o - \alpha_r)\cos\delta_r \\ \Delta\delta = \delta_o - \delta_r \end{cases}, \tag{3.73}$$

- angular separation s (angular distance between the two objects) and position angle P (angle between the direction of the North and the direction of the object, counted positive towards East) [31], see Figure 3.5

$$\begin{cases} \cos s = \sin\delta_o \sin\delta_r + \cos\delta_o \cos\delta_r \cos\Delta\alpha \\ \tan P = \dfrac{\sin\Delta\alpha}{\cos\delta_r \tan\delta_o - \sin\delta_r \cos\Delta\alpha} \end{cases}, \tag{3.74}$$

  with $\Delta\alpha = \alpha_o - \alpha_r$.

According to the definition 3.3.1 and to Jacobson (private communication) the data types are

- *Micrometer relative apparent position*: differential right ascension $\Delta\alpha$ (hr,min,secs), differential declination $\Delta\delta$ (deg,min,secs) with respect to the Earth Barycenter.
- *Relative position*: differential right ascension $\Delta\alpha$ [(deg) or (hr,min,secs)] and differential declination $\Delta\delta$ [(deg) or (hr,min,secs)] with respect to a topocentric observer.
- *Relative position*: $\Delta\alpha\cos\delta$ [(deg) or (hr,min,secs)] and $\Delta\delta$ [(deg) or (hr,min,secs)] with respect to a topocentric observer.
- *Relative position*: separation s (secs), differential declination $\Delta\delta$ (deg,min,secs) with respect to a topocentric observer.
- *Astrometric micrometer*: position angle P (hr,min,secs) and separation s (secs) with respect to the Solar System Barycenter.
- *Apparent micrometer*: position angle P (deg) and separation s (secs) with respect to the Earth Barycenter.

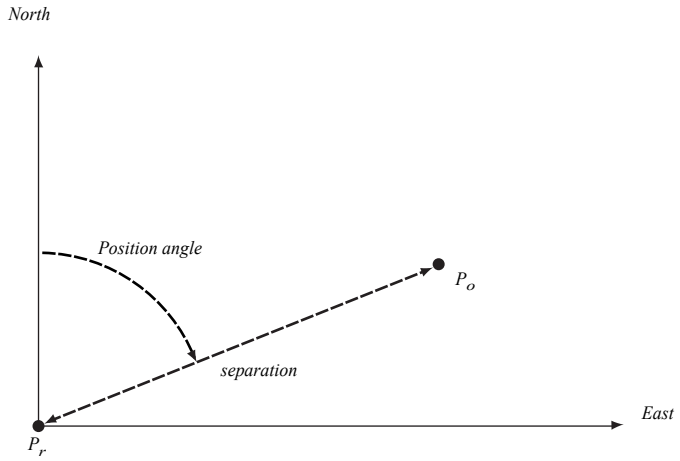

Figure 3.5: Differential coordinates: position angle and angular separation. P_o and P_r represent the observed object and the reference object respectively

3.5.3 Tangential coordinates

The tangential coordinates are a special set of differential coordinates. This type of coordinates is based on the correct determination of the tangential point on the celestial sphere, so the position of the satellites are projected on a plane tangent to celestial sphere in the point T with coordinates (α_T, δ_T) which may be chosen at the center of the planet when possible. The measurements from photographic plates or from CCD images are of this type. The tangential coordinates are measured in image unit: this implies the knowledge of the focal length of the telescope. Figure 3.6 gives a graphical representation of the tangential coordinates: Π is the tangent plane. The transformation from equatorial coordinates to tangential coordinates goes through the differential polar coordinates ρ and θ and makes use of spherical trigonometry. See [31] for derivation. If α_o and δ_o are the equatorial coordinates of the body the tangential coordinates X, Y are [31]:

$$\begin{cases} \mathsf{X}(\alpha_o, \delta_o) = \dfrac{\cos\delta_o \sin(\alpha_o - \alpha_T)}{\sin\delta_T \sin\delta_o + \cos\delta_T \cos\delta_o \cos(\alpha_o - \alpha_T)} \\ \mathsf{Y}(\alpha_o, \delta_o) = \dfrac{\cos\delta_T \sin\delta_o - \sin\delta_T \cos\delta_o \cos(\alpha_o - \alpha_T)}{\sin\delta_T \sin\delta_o + \cos\delta_T \cos\delta_o \cos(\alpha_o - \alpha_T)} \end{cases} . \tag{3.75}$$

According to the definition 3.3.1 and to Jacobson (private communication) the data types are:

- *Micrometer tangent plane apparent position*: X (hr,min,secs) and Y (secs) with respect to the Earth Barycenter.
- *Tangent plane position*: X (deg,min,secs) and Y (deg,min,secs) with respect to a topocentric observer.
- *Relative position in a rotated frame*: X (secs), rotation angle P (deg) with respect to a topocentric observer.
- *Relative position in a rotated frame*: rotation angle (deg), Y (secs) with respect to a topocentric observer.

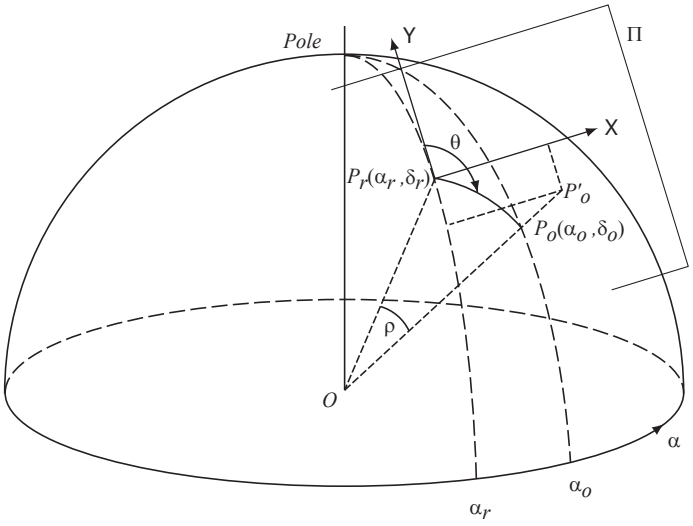

Figure 3.6: Standard tangential coordinates

Chapter 4

A Numerical Theory for the Main Satellites of Saturn

4.1 The observations

Our analysis is based on astrometric data of the main satellites of Saturn. The astrometric observations were acquired with the Flagstaff Astrometric Scanning Transit Telescope (FASTT), which is a fully automated, 20 cm (f/10), meridian refractor. The time period covered by the observations goes from 1998 to 2007. The Flagstaff telescope can be equipped with two different CCD: a Ford CRAF/*Cassini*, 1024^2 pixel, thick front-illuminated CCD with 12 μm pixel, or a Ford Loral 2048^2 pixel CCD with 15 μm pixel.

All data we have used can be obtained via anonymous file transfer protocol from the Naval Observatory Flagstaff Station (NOFS) site. The observations are in the form of absolute coordinates (α, δ) given in the International Celestial Reference Frame (ICRF) with no correction for light time. The observations have been reduced by the observers using the ACT (Astrographic Catalogue + Tycho) and the Tycho-2 catalogues, the accuracies ranging from $\pm 0''.08$ to $\pm 0''.25$ for single observations. The reduction procedure used by the observers is described in detail in the five papers of R. Stone [56] [57] [58] [59] [60]. All the observations were corrected for atmospheric refraction and diurnal aberration. The annual aberration is automatically corrected using the ACT catalogue for reduction.

All the available data are given in a table in ASCII format. The data are given for each planet or satellite in the format outlined in Table 4.1. The type of observation, as indicated in Table 4.1 at column 12, can be topocentric or geocentric. The set of data covering the periond 1998-1999 is topocentric. The rest of the data covering the period 2000-2007 is geocentric. The geocentric data have been computed by the observers from available ephemerides, so the resulting positions could be biased by earlier observations and by the ephemerides computed from them. The topocentric data are not biased. As a safety measure, we opted to use topocentric positions only.

To convert geocentric data to topocentric we simply subtract the value of the geocentric parallax in declination given in column 10 of Table 4.1 from the correspondig value of the declination given in column 8 of the same table. Since the Flagstaff refractor is a meridian telescope the geocentric parallax in right ascension is zero. The outlined procedure is approximate but, since the involved angular quantities are small, the error is smaller than the given accuracy. The exact procedure for the computation of the topocentric position given the geocentric position and the geocentric parallax is given in Appendix C.

The total number of available observations is 3153. The observed satellites of Saturn are Tethys, Dione, Rhea, Titan, Hyperion, Iapetus and Phoebe. The number of observations for each satellite is given in Table 4.2. There are no observations of Mimas or Enceladus. This is due to the fact that these two satellites were too close to Saturn for successful observations to be taken with the FASTT telescope.

Therefore satellites closer than 36" to Saturn are considered unmeasurable due to their close proximity [58]. In fact, the maximum elongation of Mimas and Enceladus with respect to Saturn are about 30" and 36" respectively.

Column	Quantity	Units
1	Planet identification	5-9
2	Satellite identification	0-9
3	Year of observation	yr
4	Month of observation	Jan-Dec
5	Day of observation	1-31
6	UTC of observation	(hr,m,s)
7	ICRF right ascension α	(hr,m,s)
8	ICRF declination δ	(deg,arcmin,arcsec)
9	Geocentric Parallax in α	arcsec
10	Geocentric parallax in δ	arcsec
11	Observation site code	689 (FASTT)
12	Type of observation	topo or geoc
13	Site/telescope/reduction catalogue	–
14	Proper name of planet/satellite	–

Table 4.1: Standard Naval Observatory Flagstaff Station (NOFS) format for FASTT positions of planets and planetary satellites [58].

Satellite	number of observations
Tethys	238
Dione	379
Rhea	621
Titan	615
Hyperion	434
Iapetus	654
Phobe	212
Total	3153

Table 4.2: Number of observations for each satellites acquired with FASTT in the period 1998-2007.

4.2 Orbit Determination - geometric partials

In our orbit determination process we adjust the model of the orbits of the main satellites of Saturn to obtain a weighted least squares fit to the observational data. The set of adjustable dynamical parameters is

- Position and velocity of the natural satellites at the epoch;
- The gravitational parameters of the entire Saturnian system and of each of the natural satellites;
- The zonal harmonics of Saturn J_2, J_4, J_6, J_8.

Following the notation used in Chapter 1 and Chapter 2, Section 2.5, equation (2.88), the state vector is

$$\mathbf{X} = \begin{pmatrix} \mathbf{X}_{ss} \\ \mathbf{p} \end{pmatrix}, \tag{4.1}$$

where $\mathbf{X}_{ss}$ is the state vector of the n natural satellites with n_{ss} components while $\mathbf{p}$ represents the set of dynamical parameters, that is

$$\mathbf{X}_{ss} = \begin{pmatrix} \mathbf{R}_1 & \cdots & \mathbf{R}_n & \mathbf{V}_1 & \cdots & \mathbf{V}_n \end{pmatrix}^T , \tag{4.2}$$

$$\mathbf{p} = \begin{pmatrix} \mu_1 & \cdots & \mu_n & \mu_B & J_{2i} \end{pmatrix}^T , \tag{4.3}$$

where the position $\mathbf{R}_j$ and velocity $\mathbf{V}_j$ of satellite j, with $j = 1, ...n$, are referred to the Saturnian System Barycenter.

As we mentioned, at the beginning of this chapter, the observational data are absolute coordinates in the form of right ascension and declination pairs (α, δ) of the observed satellite. Following the scheme given in Chapter 1 the function $\mathbf{G}_j\left(\mathbf{X}, t_j^e, t_j^r\right)$, representing the observation model, is given by

$$\mathbf{G}_j\left(\mathbf{X}, t_j^e, t_j^r\right) = \begin{pmatrix} \alpha_j \\ \delta_j \end{pmatrix} , \tag{4.4}$$

where α_j and δ_j are respectively the topocentric right ascension and declination of satellite j and t_j^e and t_j^r represent the emission time and the reception time of the light signal. The geometric relationship relating the observer-satellite j vector $\mathbf{u}_j = (u_{jx}, u_{jy}, u_{jz})^T$ to the observed (α_j, δ_j) coordinates is given by equation (3.71), that we rewrite here as

$$\begin{cases} \alpha_j = \arctan\left(\dfrac{u_{jy}}{u_{jx}}\right) , \\ \delta_j = \arctan\left(\dfrac{u_{jz}}{w_j}\right) , \end{cases} \tag{4.5}$$

where $w_j = \sqrt{u_{jx}^2 + u_{jy}^2}$.

The algorithm for the computation of the observer-satellite j vector $\mathbf{u}_j = (u_{jx}, u_{jy}, u_{jz})^T$ has been presented in Section 3.4.2 of Chapter 3. In this case, however, the algorithm can be simplified. As mentioned at the beginning of this chapter, in fact, all the Flagstaff observations were corrected for atmospheric refraction and diurnal aberration: moreover, the annual aberration is automatically corrected by the use of the ACT catalogue for reduction and the topocentric positions are mean positions referred to the mean equator and equinox of J2000.0. So the simplified algorithm, comprehensive of the light time correction, is:

- follow all the steps given in section 3.4.2; this procedure allows to compute the observer position at the time of observation t^r with respect to the Solar System Barycenter in the ICRF (J2000.0).
- follow the steps from 1 to 4 of section 3.4.1, i.e., do not apply the aberration correction and the precession and nutation rotations and compute only the effects of gravitational light deflection and light time correction.

4.2.1 Geometric partial derivatives

Now we have to compute the partial derivatives of the observation model (4.4) with respect to the state vector $\mathbf{X}$ expressed by equation (4.1). Recalling the notation given in Chapter 1, the matrix $\tilde{\mathbf{H}}_j$ representing the partials of the observation model of satellite j is given by

$$\tilde{\mathbf{H}}_j = \frac{\partial \mathbf{G}_j\left(\mathbf{X}, t_j^e, t_j^r\right)}{\partial \mathbf{X}} . \tag{4.6}$$

Using formula (4.1) we can split the previous equation into two elements, that is

$$\tilde{\mathbf{H}}_j = \begin{pmatrix} \dfrac{\partial \mathbf{G}_j\left(\mathbf{X}, t_j^e, t_j^r\right)}{\partial \mathbf{X}_{ss}} & \dfrac{\partial \mathbf{G}_j\left(\mathbf{X}, t_j^e, t_j^r\right)}{\partial \mathbf{p}} \end{pmatrix} . \tag{4.7}$$

Since the coordinates (α_j, δ_j) do not depend directly on the vector of parameters $\mathbf{p}$ given by (4.3), we have that

$$\frac{\partial \mathbf{G}_j\left(\mathbf{X}, t_j^e, t_j^r\right)}{\partial \mathbf{p}} = \mathbf{0}\,. \tag{4.8}$$

In the same manner (α_j, δ_j) do not depend on velocity. Therefore

$$\frac{\partial \mathbf{G}_j\left(\mathbf{X}, t_j^e, t_j^r\right)}{\partial \mathbf{V}_i} = \mathbf{0}, \qquad \forall i = 1, ..., n\,. \tag{4.9}$$

and $\frac{\partial \mathbf{G}_j\left(\mathbf{X}, t_j^e, t_j^r\right)}{\partial \mathbf{X}_{ss}}$ reduces to

$$\frac{\partial \mathbf{G}_j\left(\mathbf{X}, t_j^e, t_j^r\right)}{\partial \mathbf{X}_{ss}} = \delta_i^j \frac{\partial \mathbf{G}_j\left(\mathbf{X}, t_j^e, t_j^r\right)}{\partial \mathbf{R}_i}, \qquad i = 1, ..., n\,,\ j = 1, ..., n\,, \tag{4.10}$$

where δ_i^j is Kronecker's symbol, indicating that the partial is zero except for $i = j$. This condition is verified because (α_j, δ_j) are absolute coordinates and so they depend only on the position of satellite j. In the case of differential measurements, in particular in the case of inter-satellite measurements, we should apply the chain rule and should compute the partials also with respect to the other satellite.

The matrix $\tilde{\mathbf{H}}_j$ thus reduces to

$$\tilde{\mathbf{H}}_j = \left(\underbrace{\frac{\partial \mathbf{G}_j\left(\mathbf{X}, t_j^e, t_j^r\right)}{\partial \mathbf{R}_j}}_{\mathbf{R}} \quad \underbrace{\mathbf{0}}_{\mathbf{V}} \quad \underbrace{\mathbf{0}}_{\mathbf{p}} \right). \tag{4.11}$$

Using the chain rule the partials $\frac{\partial \mathbf{G}_j\left(\mathbf{X}, t_j^e, t_j^r\right)}{\partial \mathbf{R}_j}$ can be computed as

$$\frac{\partial \mathbf{G}_j\left(\mathbf{X}, t_j^e, t_j^r\right)}{\partial \mathbf{R}_j} = \frac{\partial \mathbf{G}_j}{\partial \mathbf{u}_j} \frac{\partial \mathbf{u}_j}{\partial \mathbf{R}_j}\,. \tag{4.12}$$

Computation of $\frac{\partial \mathbf{G}_j}{\partial \mathbf{u}_j}$

The geometric partials $\frac{\partial \mathbf{G}_j}{\partial \mathbf{u}_j}$ can be computed easily using formulas (4.5): removing the subscript j to lighten the notation, the relations (4.5) become

$$\begin{cases} \alpha = \arctan\left(\dfrac{u_y}{u_x}\right), \\ \delta = \arctan\left(\dfrac{u_z}{\sqrt{u_x^2 + u_y^2}}\right), \end{cases} \tag{4.13}$$

and the partials for each component are

$$\frac{\partial \alpha}{\partial u_x} = \frac{\partial}{\partial u_x} \arctan\left(\frac{u_y}{u_x}\right) = \frac{1}{1 + \left(\dfrac{u_y}{u_x}\right)^2} \left(-\frac{u_y}{u_x^2}\right) = -\frac{u_x^2}{u_x^2 + u_y^2} \frac{u_y}{u_x^2} = -\frac{u_y}{u_x^2 + u_y^2}\,, \tag{4.14}$$

$$\frac{\partial \alpha}{\partial u_y} = \frac{\partial}{\partial u_y} \arctan\left(\frac{u_y}{u_x}\right) = \frac{1}{u_x} \frac{1}{1 + \left(\dfrac{u_y}{u_x}\right)^2} = \frac{1}{u_x} \frac{u_x^2}{u_x^2 + u_y^2} = \frac{u_x}{u_x^2 + u_y^2}\,, \tag{4.15}$$

$$\frac{\partial \alpha}{\partial u_z} = \frac{\partial}{\partial u_z} \arctan\left(\frac{u_y}{u_x}\right) = 0\,, \tag{4.16}$$

$$\begin{aligned}\frac{\partial\delta}{\partial u_x} &= \frac{\partial}{\partial u_x}\arctan\left(\frac{u_z}{\sqrt{u_x^2+u_y^2}}\right) = \frac{1}{1+\left(\frac{u_z}{\sqrt{u_x^2+u_y^2}}\right)^2}\left(-\frac{u_z}{u_x^2+u_y^2}\frac{u_x}{\sqrt{u_x^2+u_y^2}}\right)\\ &= -\frac{u_x u_z}{u_x^2+u_y^2+u_z^2}\frac{1}{\sqrt{u_x^2+u_y^2}} = -\frac{u_x u_z}{w\ |\mathbf{u}|^2}\,, \end{aligned} \tag{4.17}$$

$$\begin{aligned}\frac{\partial\delta}{\partial u_y} &= \frac{\partial}{\partial u_y}\arctan\left(\frac{u_z}{\sqrt{u_x^2+u_y^2}}\right) = \frac{1}{1+\left(\frac{u_z}{\sqrt{u_x^2+u_y^2}}\right)^2}\left(-\frac{u_z}{u_x^2+u_y^2}\frac{u_y}{\sqrt{u_x^2+u_y^2}}\right)\\ &= -\frac{u_y u_z}{u_x^2+u_y^2+u_z^2}\frac{1}{\sqrt{u_x^2+u_y^2}} = -\frac{u_y u_z}{w\ |\mathbf{u}|^2}\,, \end{aligned} \tag{4.18}$$

$$\begin{aligned}\frac{\partial\delta}{\partial u_z} &= \frac{\partial}{\partial u_z}\arctan\left(\frac{u_z}{\sqrt{u_x^2+u_y^2}}\right) = \frac{1}{1+\left(\frac{u_z}{\sqrt{u_x^2+u_y^2}}\right)^2}\frac{1}{\sqrt{u_x^2+u_y^2}}\\ &= \frac{u_x^2+u_y^2}{u_x^2+u_y^2+u_z^2}\frac{1}{\sqrt{u_x^2+u_y^2}} = \frac{w}{|\mathbf{u}|^2}\,. \end{aligned} \tag{4.19}$$

Summarising the results we have that the geometric partials are

$$\begin{aligned} &\frac{\partial\alpha}{\partial u_x} = -\frac{u_y}{u_x^2+u_y^2}\,, && \frac{\partial\alpha}{\partial u_y} = \frac{u_x}{u_x^2+u_y^2}\,, && \frac{\partial\alpha}{\partial u_z} = 0\,,\\ &\frac{\partial\delta}{\partial u_x} = -\frac{u_x u_z}{w\ |\mathbf{u}|^2}\,, && \frac{\partial\delta}{\partial u_y} = -\frac{u_y u_z}{w\ |\mathbf{u}|^2}\,, && \frac{\partial\delta}{\partial u_z} = \frac{w}{|\mathbf{u}|^2}\,, \end{aligned} \tag{4.20}$$

where $w = \sqrt{u_x^2+u_y^2}$.

Computation of $\frac{\partial\mathbf{u}_j}{\partial\mathbf{R}_j}$

The geometric partials $\frac{\partial\mathbf{u}_j}{\partial\mathbf{R}_j}$ can be computed using formula (3.33) given in Chapter 3, Section 3.4.1. We remove the subscript j for ease of notation. The formula (3.33) that gives the apparent (geocentric) place for Earth-based observations is given by

$$\mathbf{u}(t') = \mathbf{N}(t)\,\mathbf{P}(t)\,f_a\left\{f_{gd}\left[\mathbf{u}_B(t-\tau) - \mathbf{E}_B(t)\right]\right\}\,, \tag{4.21}$$

where t' is the epoch of observation in the TDT timescale, t is the epoch of observation in the TDB timescale, τ is the light travel time from the body to the Earth in the TDB timescale for light arriving at the observation epoch t, $\mathbf{u}_B(t-\tau)$ is the position of the body with respect to the Solar System Barycenter at the epoch $t-\tau$ referred to the mean equator and equinox of t_0, $\mathbf{E}_B(t)$ is the position of the Earth with respect to the Solar System Barycenter at the epoch t referred to the mean equator and equinox of t_0, $f_{gd}[\ldots]$ is the function representing the gravitational deflection of light, $f_a[\ldots]$ is the function representing the aberration of light, $\mathbf{P}(t)$ is the precession matrix for the epoch t (a rotation from the mean equinox and equator of t_0 to the epoch of observation t), $\mathbf{N}(t)$ is the nutation matrix from the epoch t (a rotation from the mean equinox and equator of date to the true equinox and equator of date t) and $\mathbf{u}(t')$ is the apparent (geocentric) place of the body at the epoch of observation t' with origin at the center of mass of the Earth. The subscript $_B$ indicates that the subscripted quantity is computed in the Solar System Barycenter. In the case of topocentric observations the only difference is

in computation of the observer's position, as described in Section 3.4.2 of Chapter 3: in this case in fact we have to substitute $\mathbf{E}_B(t)$ with the position of the observer on the Earth's surface with respect to the Solar System Barycenter. The partials with respect to $\mathbf{R}$ are identical in both cases.

Given the position of the barycenter of Saturnian System $\mathbf{s}_B$ with respect to Solar System barycenter (from ephemerides), the relation involving $\mathbf{R}$ and $\mathbf{u}_B$ is

$$\mathbf{u}_B = \mathbf{R} + \mathbf{s}_B \,. \tag{4.22}$$

Using the formulas (3.44) and (3.47) of Section 3.4.1, we have that the partial derivatives of (4.21) are

$$\frac{\partial \mathbf{u}}{\partial \mathbf{R}} = \mathbf{N}(t)\,\mathbf{P}(t)\,\frac{\partial \mathbf{u}_a}{\partial \mathbf{u}_g}\frac{\partial \mathbf{u}_g}{\partial \mathbf{u}_B}\frac{\partial \mathbf{u}_B}{\partial \mathbf{R}}\,, \tag{4.23}$$

where $\mathbf{u}_a$ and $\mathbf{u}_g$ are given by (3.47) and (3.44) respectively. The matrices $\mathbf{N}(t)$ and $\mathbf{P}(t)$ do not need to be differentiated because they do not depend on the position of satellite.

Computation of $\frac{\partial \mathbf{u}_a}{\partial \mathbf{u}_g}$. The partials $\frac{\partial \mathbf{u}_a}{\partial \mathbf{u}_g}$ are computed using the formula (3.47), that is

$$\mathbf{u}_a = \frac{\left[\beta^{-1}\mathbf{u}_g + f_2\,|\mathbf{u}_g|\,\mathbf{V}\right]}{(1+f_1)}\,, \tag{4.24}$$

where, from the definitions (3.45) and (3.46),

$$\hat{\mathbf{u}}_g = \frac{\mathbf{u}_g}{|\mathbf{u}_g|}\,, \qquad \mathbf{V} = \frac{\dot{\mathbf{E}}_B(t)}{c}\,, \qquad \beta^{-1} = \sqrt{1-|\mathbf{V}|^2}\,, \tag{4.25}$$

$$f_1 = \hat{\mathbf{u}}_g \cdot \mathbf{V}\,, \qquad f_2 = 1 + \frac{f_1}{1+\beta^{-1}}\,. \tag{4.26}$$

So for the partials of (4.25) and (4.26) with respect to $\mathbf{u}_g$ we have

$$\begin{aligned}\frac{\partial \hat{\mathbf{u}}_g}{\partial \mathbf{u}_g} &= \frac{\partial}{\partial \mathbf{u}_g}\left(\frac{\mathbf{u}_g}{|\mathbf{u}_g|}\right) = \frac{1}{|\mathbf{u}_g|^2}\left(|\mathbf{u}_g|\;\mathbf{I}_{3\times 3} - \mathbf{u}_g\frac{\mathbf{u}_g^T}{|\mathbf{u}_g|}\right)\\ &= \frac{1}{|\mathbf{u}_g|}\mathbf{I}_{3\times 3} - \frac{\mathbf{u}_g\mathbf{u}_g^T}{|\mathbf{u}_g|^3}\,,\end{aligned} \tag{4.27}$$

$$\frac{\partial \mathbf{V}}{\partial \mathbf{u}_g} = \mathbf{0}_{3\times 3} = \frac{\partial \beta^{-1}}{\partial \mathbf{u}_g}\,, \tag{4.28}$$

$$\frac{\partial f_1}{\partial \mathbf{u}_g} = \mathbf{V}^T\frac{\partial \hat{\mathbf{u}}_g}{\partial \mathbf{u}_g}\,, \tag{4.29}$$

$$\frac{\partial f_2}{\partial \mathbf{u}_g} = \frac{1}{1+\beta^{-1}}\frac{\partial f_1}{\partial \mathbf{u}_g}\,, \tag{4.30}$$

and for $\frac{\partial \mathbf{u}_a}{\partial \mathbf{u}_g}$ we have

$$\begin{aligned}\frac{\partial \mathbf{u}_a}{\partial \mathbf{u}_g} &= \frac{\left[\beta^{-1}\mathbf{u}_g + f_2\,|\mathbf{u}_g|\,\mathbf{V}\right]}{(1+f_1)}\\ &= \frac{1}{(1+f_1)^2}\left[(1+f_1)\left(\beta^{-1} + |\mathbf{u}_g|\,\mathbf{V}\frac{\partial f_2}{\partial \mathbf{u}_g} + f_2\mathbf{V}\frac{\mathbf{u}_g^T}{|\mathbf{u}_g|}\right) - \left(\beta^{-1}\mathbf{u}_g + f_2\,|\mathbf{u}_g|\,\mathbf{V}\right)\frac{\partial f_1}{\partial \mathbf{u}_g}\right]\\ &= \frac{1}{(1+f_1)}\left(\beta^{-1} + |\mathbf{u}_g|\,\mathbf{V}\frac{\partial f_2}{\partial \mathbf{u}_g} + f_2\mathbf{V}\frac{\mathbf{u}_g^T}{|\mathbf{u}_g|}\right) - \frac{1}{(1+f_1)^2}\left(\beta^{-1}\mathbf{u}_g + f_2\,|\mathbf{u}_g|\,\mathbf{V}\right)\frac{\partial f_1}{\partial \mathbf{u}_g}\,.\end{aligned} \tag{4.31}$$

Computation of $\frac{\partial \mathbf{u}_g}{\partial \mathbf{u}_B}$. The partials $\frac{\partial \mathbf{u}_g}{\partial \mathbf{u}_B}$ are computed using the formula (3.44), that is

$$\mathbf{u}_g = |\mathbf{U}| \left\{ \hat{\mathbf{U}} + \frac{g_1}{g_2} \left[\left(\hat{\mathbf{U}} \cdot \hat{\mathbf{Q}} \right) \hat{\mathbf{E}}_H - \left(\hat{\mathbf{E}}_H \cdot \hat{\mathbf{U}} \right) \hat{\mathbf{Q}} \right] \right\} , \tag{4.32}$$

where, from definitions (3.40), (3.41), (3.42) and (3.43),

$$\begin{aligned} \mathbf{U}(t) &= \mathbf{u}_B(t-\tau) - \mathbf{E}_B(t) , \qquad \mathbf{Q}(t) = \mathbf{u}_B(t-\tau) - \mathbf{S}_B(t-\tau) , && (4.33) \\ \hat{\mathbf{U}} &= \mathbf{U}/|\mathbf{U}| , \qquad \hat{\mathbf{Q}} = \mathbf{Q}/|\mathbf{Q}| , \qquad \hat{\mathbf{E}}_H = \mathbf{E}_H/|\mathbf{E}_H| , && (4.34) \\ g_1 &= \frac{2\mu}{c^2 |\mathbf{E}_H|} , \qquad g_2 = 1 + \hat{\mathbf{Q}} \cdot \hat{\mathbf{E}}_H . && (4.35) \end{aligned}$$

Computing the partials with respect to $\mathbf{u}_B$ of (4.33), (4.34) and (4.35) we have

$$\begin{aligned} \frac{\partial \mathbf{U}}{\partial \mathbf{u}_B} &= \mathbf{I}_{3\times 3} = \frac{\partial \mathbf{Q}}{\partial \mathbf{u}_B} , && (4.36) \\ \frac{\partial |\mathbf{U}|}{\partial \mathbf{u}_B} &= \frac{\partial |\mathbf{U}|}{\partial \mathbf{U}} \frac{\partial \mathbf{U}}{\partial \mathbf{u}_B} = \frac{\mathbf{U}^T}{|\mathbf{U}|} , && (4.37) \\ \frac{\partial |\mathbf{Q}|}{\partial \mathbf{u}_B} &= \frac{\partial |\mathbf{Q}|}{\partial \mathbf{Q}} \frac{\partial \mathbf{Q}}{\partial \mathbf{u}_B} = \frac{\mathbf{Q}^T}{|\mathbf{Q}|} , && (4.38) \\ \frac{\partial \hat{\mathbf{E}}_H}{\partial \mathbf{u}_B} &= \mathbf{0}_{3\times 3} = \frac{\partial g_1}{\partial \mathbf{u}_B} , && (4.39) \end{aligned}$$

$$\begin{aligned} \frac{\partial \hat{\mathbf{U}}}{\partial \mathbf{u}_B} &= \frac{1}{|\mathbf{U}|^2} \left(|\mathbf{U}| \frac{\partial \mathbf{U}}{\partial \mathbf{u}_B} - \mathbf{U} \frac{\partial |\mathbf{U}|}{\partial \mathbf{u}_B} \right) = \frac{1}{|\mathbf{U}|} \mathbf{I}_{3\times 3} - \frac{1}{|\mathbf{U}|^3} \mathbf{U}\mathbf{U}^T , && (4.40) \\ \frac{\partial \hat{\mathbf{Q}}}{\partial \mathbf{u}_B} &= \frac{1}{|\mathbf{Q}|^2} \left(|\mathbf{Q}| \frac{\partial \mathbf{Q}}{\partial \mathbf{u}_B} - \mathbf{Q} \frac{\partial |\mathbf{Q}|}{\partial \mathbf{u}_B} \right) = \frac{1}{|\mathbf{Q}|} \mathbf{I}_{3\times 3} - \frac{\mathbf{Q}\mathbf{Q}^T}{|\mathbf{Q}|^3} , && (4.41) \\ \frac{\partial g_2}{\partial \mathbf{u}_B} &= \frac{\partial \hat{\mathbf{Q}} \cdot \hat{\mathbf{E}}_H}{\partial \mathbf{u}_B} = \hat{\mathbf{E}}_H^T \frac{\partial \hat{\mathbf{Q}}}{\partial \mathbf{u}_B} = \frac{\hat{\mathbf{E}}_H^T}{|\mathbf{Q}|} \left(\mathbf{I}_{3\times 3} - \hat{\mathbf{Q}} \hat{\mathbf{Q}}^T \right) , && (4.42) \end{aligned}$$

$$\begin{aligned} \frac{\partial}{\partial \mathbf{u}_B} \frac{g_1}{g_2} &= -\frac{g_1}{g_2^2} \frac{\partial g_2}{\partial \mathbf{u}_B} , && (4.43) \\ \frac{\partial \left(\hat{\mathbf{U}} \cdot \hat{\mathbf{Q}} \right)}{\partial \mathbf{u}_B} &= \hat{\mathbf{Q}}^T \frac{\partial \hat{\mathbf{U}}}{\partial \mathbf{u}_B} + \hat{\mathbf{U}}^T \frac{\partial \hat{\mathbf{Q}}}{\partial \mathbf{u}_B} , && (4.44) \\ \frac{\partial \left(\hat{\mathbf{E}}_H \cdot \hat{\mathbf{U}} \right)}{\partial \mathbf{u}_B} &= \hat{\mathbf{E}}_H^T \frac{\partial \hat{\mathbf{U}}}{\partial \mathbf{u}_B} . && (4.45) \end{aligned}$$

Then for $\frac{\partial \mathbf{u}_g}{\partial \mathbf{u}_B}$ we have

$$\begin{aligned} \frac{\partial \mathbf{u}_g}{\partial \mathbf{u}_B} &= \left\{ \hat{\mathbf{U}} + \frac{g_1}{g_2} \left[\left(\hat{\mathbf{U}} \cdot \hat{\mathbf{Q}} \right) \hat{\mathbf{E}}_H - \left(\hat{\mathbf{E}}_H \cdot \hat{\mathbf{U}} \right) \hat{\mathbf{Q}} \right] \right\} \frac{\partial |\mathbf{U}|}{\partial \mathbf{u}_B} && (4.46) \\ &\quad + |\mathbf{U}| \left\{ \frac{\partial \hat{\mathbf{U}}}{\partial \mathbf{u}_B} + \left[\left(\hat{\mathbf{U}} \cdot \hat{\mathbf{Q}} \right) \hat{\mathbf{E}}_H - \left(\hat{\mathbf{E}}_H \cdot \hat{\mathbf{U}} \right) \hat{\mathbf{Q}} \right] \frac{\partial}{\partial \mathbf{u}_B} \left(\frac{g_1}{g_2} \right) \right\} && (4.47) \\ &\quad + |\mathbf{U}| \left\{ \frac{g_1}{g_2} \left[\hat{\mathbf{E}}_H \frac{\partial \left(\hat{\mathbf{U}} \cdot \hat{\mathbf{Q}} \right)}{\partial \mathbf{u}_B} - \hat{\mathbf{Q}} \frac{\partial \left(\hat{\mathbf{E}}_H \cdot \hat{\mathbf{U}} \right)}{\partial \mathbf{u}_B} - \left(\hat{\mathbf{E}}_H \cdot \hat{\mathbf{U}} \right) \frac{\partial \hat{\mathbf{Q}}}{\partial \mathbf{u}_B} \right] \right\} . && (4.48) \end{aligned}$$

Computation of $\frac{\partial \mathbf{u}_B}{\partial \mathbf{R}}$. Finally, from formula (4.22), we have that $\frac{\partial \mathbf{u}_B}{\partial \mathbf{R}}$ is

$$\frac{\partial \mathbf{u}_B}{\partial \mathbf{R}} = \mathbf{I}_{3\times 3} . \tag{4.49}$$

4.3 Orbit solution and discussion

By means of the *Orbit Determination* capability of the SOSYA program we have tried to adjust the models of the orbits of the satellites of Saturn to obtain a weighted least squares fit to the observational data. The set of adjustable dynamical parameters contains only position and velocity at epoch of the observed satellites Tethys, Dione, Rhea, Titan, Hyperion, Iapetus and Phoebe. Mimas and Enceladus have also been included in the numerical integration, but their states have not been estimated because no observational data were available for these two satellites. It was nonetheless necessary to numerically integrate their orbits together with the other massive satellites of Saturn because Mimas's and Enceladus's gravitational interactions with the other satellites are not negligible.

The gravitational parameters of the satellites, Saturn's zonal harmonics and other system parameters we have used are the same as reported in Tables 2.4 and 2.6 of Chapter 2, Section 2.7.1 and have the same values used by JPL to produce the **SAT136** ephemeris. The epoch of the initial state of the nine satellites is 19 August 1998 $0^h0^m0^s.0000$ TDB (Barycentric Dynamical Time, see Appendix A for a brief description of time systems). The initial conditions of the satellites obtained from the **SAT136** ephemeris file are at epoch 2 January 2004 $0^h0^m0^s.0000$ TDB. Using the *Orbit Simulation* capability of SOSYA we have numerically integrated the equations of motion starting at epoch 2 January 2004 $0^h0^m0^s.0000$ and finishing at epoch 19 August 1998 $0^h0^m0^s.0000$. In this way we have determined a new set of initial conditions that we have used as the initial states in the orbit determination process.

The geocentric coordinates of the FASTT telescope are $\rho\cos\phi' = 0.81851$, $\rho\sin\phi' = 0.57319$ and $\lambda = 248^\circ.2601$, where ρ is the distance of the observing site from the center of the Earth in units of the Earth's equatorial radius, ϕ' is the geocentric latitude of the observing site and finally λ is its geocentric longitude. We have obtained these values of the geocentric coordinates from the site *http://www.cfa.harvard.edu/iau/lists/ObsCodes.html*. The value of the Earth's equatorial radius we have used is that recomended by the IERS conventions [36] as $R_e = 6378.1366\,\mathrm{km}$.

We have used a uniform weight of $0''.1$ for all the observations. This weight is close to the best accuracy achievable with the FASTT telescope. To invert the normal equations and fit the data we have applied a Cholesky decomposition. We have verified that the covariance matrix was positive definite.

Tables 4.3 contain the rms of the pre-fit (left panel) and post-fit (right panel) residuals for the astrometric observations, grouped by satellite. In the same tables we also give some statistical information like the mean and the standard deviation. Let us recall that the accuracies of the Flagstaff observational data ranges from $\pm0''.08$ to $\pm0''.25$ for single observation but a specific value is not associated with any single observation. The value $\pm0''.08$ is equivalent to about 500 km at Saturn's distance. From Tables 4.3 we note that the rms of the post-fit residuals, both in right ascension and declination, is the mean between the best and the worst accuracy of Flagstaff observations. Only the rms in α improves by about $0''.02$ from the first to the last interation while the rms in δ is unchanged. Moreover we note that the observational residuals show a bias in both coordinates. Nontheless, the bias is lower than the accuracy of observations. The source of the bias is not clear and needs to be investigated. If the bias is due to errors in the data reduction performed by the observers, a possible method to remove the bias is to use differential observations such as ($\Delta\alpha$,$\Delta\delta$). These differential observations can be constructed by explicit differencing of published (α,δ) observations. Other approaches are to reject the measurements outside 3 times the weighted residuals, or alternatively, solve for the biases. These two methods have yet to be implemented in the SOSYA program.

Table 4.4 provides the converged state vector of the satellites at epoch with the standard deviation representing an assessment of the state uncertainty. Extra digits are included in the values of the state to facilitate the reproduction of the integration of the orbits. The standard deviations in position are within the measurement errors. Moreover, by comparing Table 4.2 with Table 4.4 we realize that the larger errors correspond to the less observed satellites.

In Table 4.5 we give the converged orbital elements of the satellites at epoch and their corrections with respect to the osculating orbital elements corresponding to the initial conditions.

Tables 4.6 give the complete set of correlation coefficients between the various components of the states of the satellites. The two tables show a strong correlation between the position and the velocity components of the same satellites. This behaviour can be ascribed to the approximate conservation of the angular momentum for each satellite. Instead, the correlation between the initial conditions (position-position and velocity-velocity) of the same satellite is due to the fact that the observations are measurements on the sky-plane and do not provide any direct information on the radial position of the satellites. In the same tables we can observe some weak correlation between the state of Titan and the state of Hyperion which may be explained by the well-known 4:3 mean motion resonance between these two satellites. The other satellites are uncorrelated. Unfortunately, the lack of observations of Mimas and Enceladus has made it impossible to observe correlations due to the Mimas-Tethys and Enceladus-Dione resonances.

The post-fit measurement residuals for Tethys, Dione, Rhea, Titan, Hyperion, Iapetus and Phoebe are presented in Figures 4.1, 4.2, 4.3, 4.4, 4.5, 4.6 and 4.7.

The robustness of the solution has been checked by changing the initial guess of the state vector by 1 km in each components of position and the solution converged to the same values with the same accuracy. Changing the initial guess in position by more than 10 km makes the solution diverge. This is due to the fact that a small variation in the initial conditions leads the system to a widely different evolution because the satellites are gravitationally interacting. In fact, using a shorter data arc, e.g. a 1 year long arc, the solution converges also if the initial guess in position is changed by 50 km.

As well as the satellites states we have tried to solve for the gravitational parameters of the satellites but the attempts were unsuccessful. In fact, the correction to the gravitational parameters were excessively large. We can say that the gravitational parameters of the satellites are not estimable because the length of the observational arc is too short. The solution for the masses will only be achievable if the number of observations toghether with the number of observing sites is increased. Nontheless, extending the time interval of observations brings about the previously mentioned problem of the linear growth of the state transition matrix (as seen in Chapter 2 Section 2.7.2). The appropriate methodology will be to adopt a multi-arc technique.

first	α (arcsec)			δ (arcsec)		
iteration	**mean**	σ	**rms**	**mean**	σ	**rms**
Tethys	0.041	0.218	0.222	-0.017	0.207	0.207
Dione	0.074	0.151	0.168	-0.033	0.168	0.171
Rhea	0.070	0.121	0.140	-0.050	0.122	0.132
Titan	0.084	0.130	0.155	-0.052	0.131	0.141
Hyperion	0.085	0.204	0.221	-0.030	0.214	0.216
Iapetus	0.074	0.115	0.137	-0.059	0.112	0.127
Phoebe	0.034	0.292	0.294	-0.053	0.334	0.338
Total	0.072	0.164	0.179	-0.045	0.172	0.177

last	α (arcsec)			δ (arcsec)		
iteration	**mean**	σ	**rms**	**mean**	σ	**rms**
Tethys	0.040	0.216	0.220	-0.016	0.202	0.203
Dione	0.026	0.146	0.148	-0.013	0.172	0.173
Rhea	0.004	0.125	0.125	-0.036	0.122	0.127
Titan	0.013	0.126	0.127	-0.059	0.130	0.143
Hyperion	0.008	0.190	0.190	-0.040	0.213	0.216
Iapetus	0.024	0.110	0.112	-0.077	0.110	0.134
Phoebe	0.017	0.291	0.291	-0.026	0.329	0.329
Total	0.017	0.160	0.161	-0.045	0.171	0.177

Table 4.3: Astrometric observation residuals, mean and standard deviation for the first iteration (left table) and for the last iteration (right table).

		position (km)		**velocity** (km/s)	
		value	$\boldsymbol{\sigma}$	**value**	$\boldsymbol{\sigma}$ $(\cdot 10^{-3})$
Tethys	x	16752.358510361661	145	11.277682754977867	1.53
	y	-293225.97652607993	39	0.55968862638984063	5.18
	z	23372.984302153502	60	-1.1750782845165255	2.41
Dione	x	374003.33724476525	32	0.93722951421086775	2.45
	y	-36877.559845038813	102	9.9544832140012236	0.84
	z	-29556.957414090368	48	-0.81048175549334933	1.34
Rhea	x	-109604.46640519341	80	8.2729052584209235	0.54
	y	-512842.24820120819	27	-1.8131173435759194	1.07
	z	49544.441228215212	39	-0.60451652869482708	0.59
Titan	x	1184999.8959414011	15	0.07725801110289536 0	0.28
	y	-8699.7842015980732	67	5.7055732136150983	0.07
	z	-102704.99272881061	37	-0.39331812556531648	0.18
Hyperion	x	-1172590.0521899730	96	3.3318843377162621	0.23
	y	-1146225.0446823197	90	-3.0608411952937216	0.22
	z	175947.33675307164	53	-0.13224027006120737	0.13
Iapetus	x	-1241777.1703393147	64	-3.0140691855666382	0.02
	y	3251382.2880002125	36	-1.1490417646178186	0.05
	z	824230.02824057371	34	0.39315165316213546	0.03
Phoebe	x	-12349597.193654286	45	0.32803691385316752	0.02
	y	3834500.1431604321	140	1.4966074287232678	0.01
	z	3327793.5937733576	79	0.63236651665801824	0.01

Table 4.4: Solved-for barycentric satellite state vectors at 19 August 1998 $0^h0^m0^s.0000$ TDB referred to the ICRF. The errors represent an assessment of the states uncertainties.

		final value	**correction to initial value**		**final value**	**correction to initial value**
Tethys	a (km)	294951.313	0.549	ω (°)	178.843	-6.304
	e	0.001340	-0.000061	Ω (°)	130.517	0.092
	i (°)	7.490	-0.059	f (°)	323.673	6.149
Dione	a (km)	377004.935	0.936	ω (°)	136.213	-31.801
	e	0.0019543	0.0000025	Ω (°)	130.357	-0.097
	i (°)	6.458	-0.024	f (°)	87.981	31.985
Rhea	a (km)	527379.026	0.453	ω (°)	179.660	-13.518
	e	0.001932	0.000462	Ω (°)	130.675	0.0497
	i (°)	6.770	-0.006	f (°)	307.408	13.451
Titan	a (km)	1220764.031	-0.607	ω (°)	205.928	0.237
	e	0.028342	0.000241	Ω (°)	127.858	0.070
	i (°)	6.300	-0.005	f (°)	25.967	-0.314
Hyperion	a (km)	1486754.328	-1.016	ω (°)	258.132	-0.126
	e	0.122834	0.000212	Ω (°)	121.996	0.140
	i (°)	6.268	-0.002	f (°)	204.148	-0.001
Iapetus	a (km)	3561383.267	-0.136	ω (°)	323.360	0.010
	e	0.028791	0.000082	Ω (°)	48.109	-0.003
	i (°)	14.910	-0.003	f (°)	100.224	0.003
Phoebe	a (km)	12927376.987	-0.146	ω (°)	285.357	-0.007
	e	0.174373	-0.000031	Ω (°)	196.019	-0.004
	i (°)	154.868	0.001	f (°)	110.574	-0.001

Table 4.5: Values of the osculating orbital elements for the converged solution. We give also the correction to the osculating orbital elements for the converged solution with respet to the osculating element corresponding to the initial guess of the state vector.

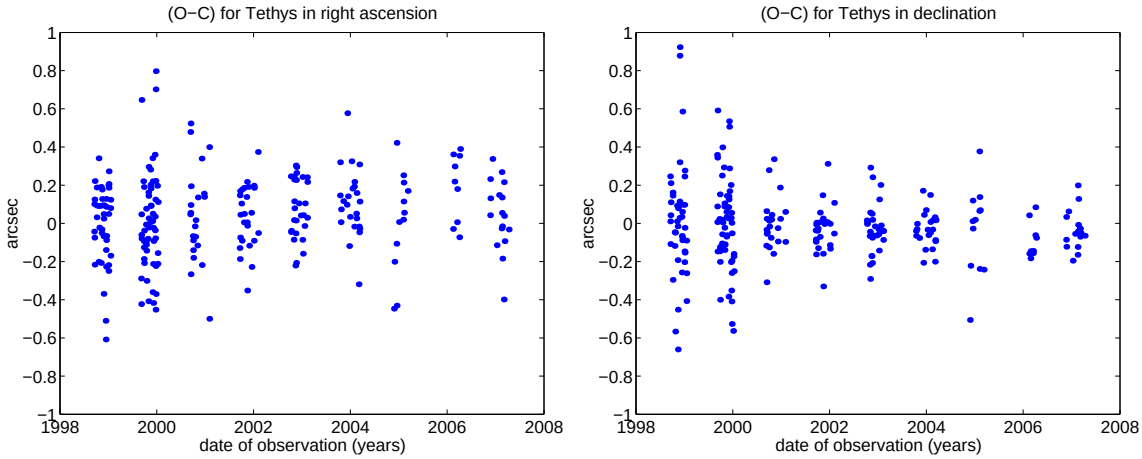

Figure 4.1: Post-fit measurement residuals for Tethys in α and δ.

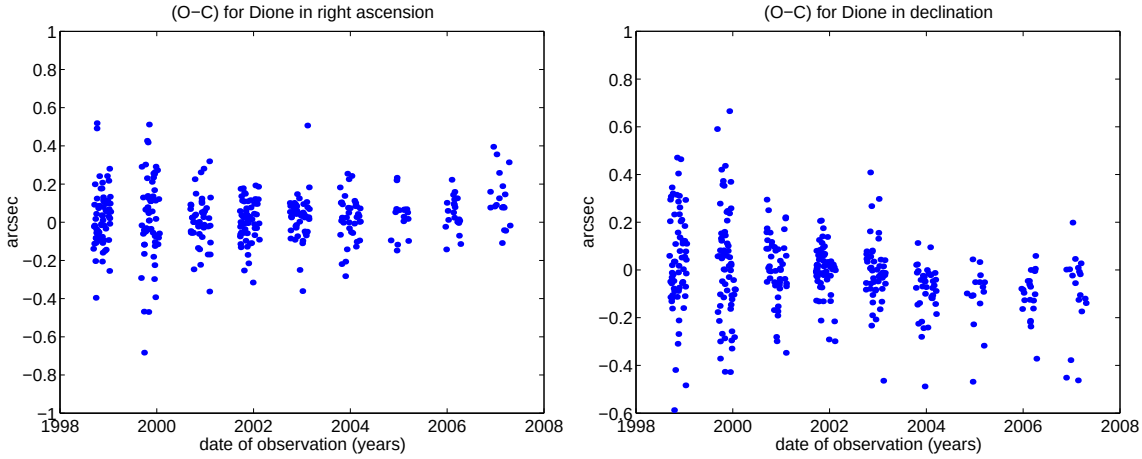

Figure 4.2: Post-fit measurement residuals for Dione in α and δ.

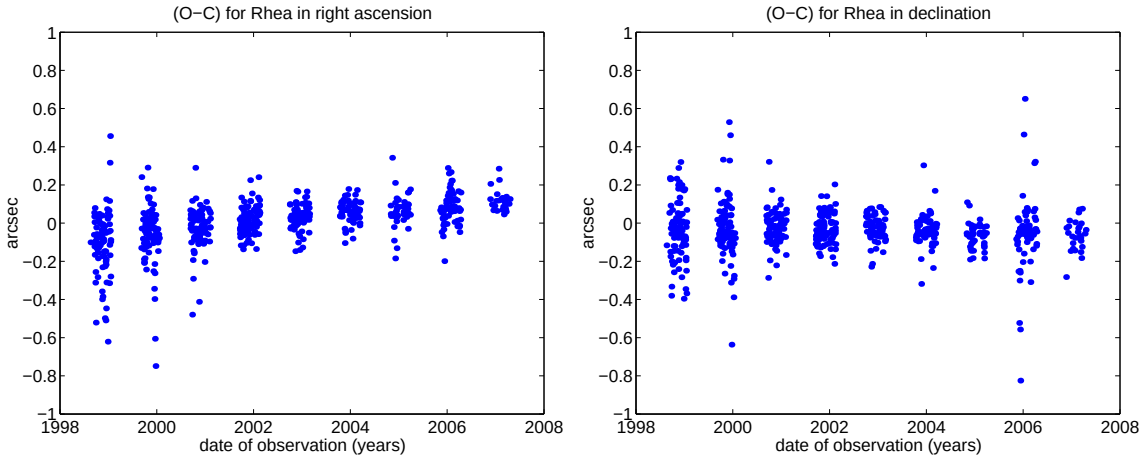

Figure 4.3: Post-fit measurement residuals for Rhea in α and δ.

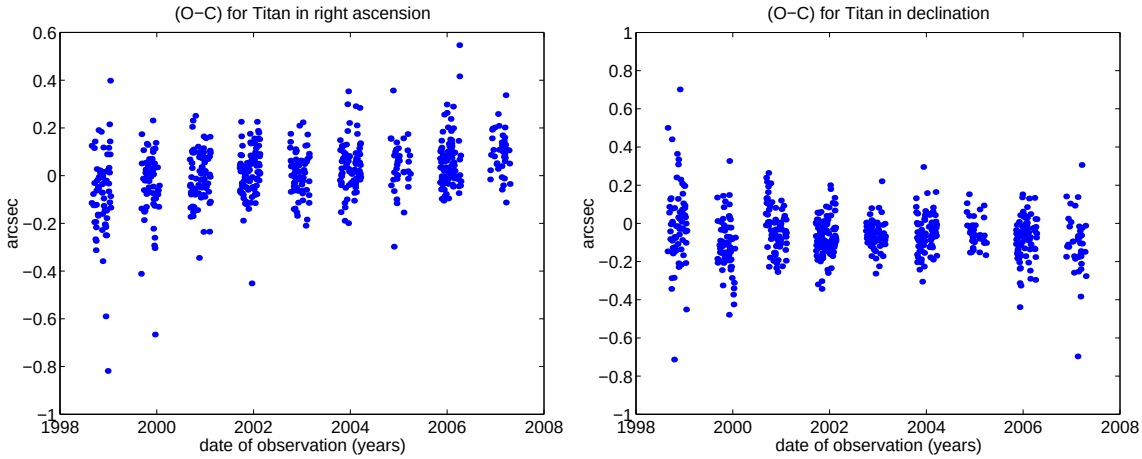

Figure 4.4: Post-fit measurement residuals for Titan in α and δ.

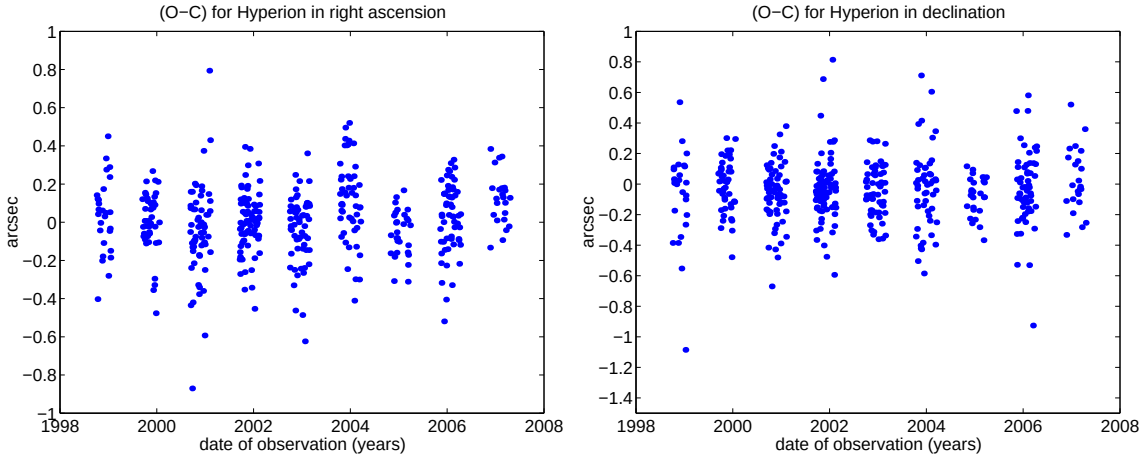

Figure 4.5: Post-fit measurement residuals for Hyperion in α and δ.

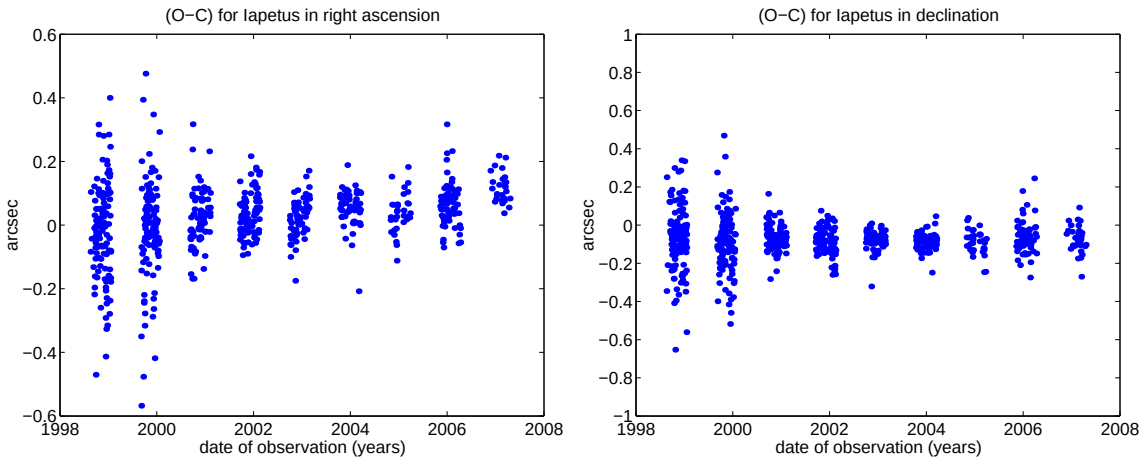

Figure 4.6: Post-fit measurement residuals for Iapetus in α and δ.

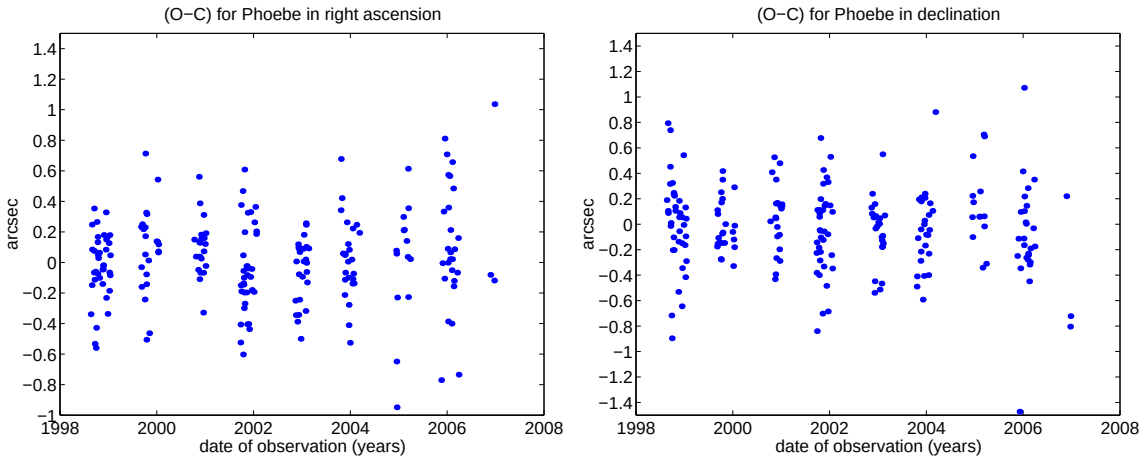

Figure 4.7: Post-fit measurement residuals for Phoebe in α and δ.

	x_3	y_3	z_3	x_4	y_4	z_4	x_5	y_5	z_5	x_6	y_6	z_6	x_7	y_7	z_7	x_8	y_8	z_8	x_9	y_9	z_9
x_3	**1.00**	0.12	-0.26	0.00	0.00	0.00	0.00	0.00	0.00	0.00	0.01	0.00	0.00	0.00	0.00	0.00	0.00	0.00	0.00	0.00	0.00
y_3		**1.00**	0.06	0.00	0.00	0.00	0.00	0.00	0.00	0.00	0.00	0.00	0.00	0.00	0.00	0.00	0.00	0.00	0.00	0.00	0.00
z_3			**1.00**	0.00	0.00	0.00	0.00	0.00	0.00	0.00	0.00	0.00	0.00	0.00	0.00	0.00	0.00	0.00	0.00	0.00	0.00
x_4				**1.00**	0.28	0.10	0.00	0.01	0.00	0.00	0.01	0.00	0.00	0.00	0.00	0.00	0.00	0.00	0.00	0.00	0.00
y_4					**1.00**	0.07	0.00	0.00	0.00	0.01	0.02	0.00	0.00	0.00	0.00	0.00	0.00	0.00	0.00	0.00	0.00
z_4						**1.00**	0.00	0.00	0.00	0.00	0.00	0.00	0.00	0.00	0.00	0.00	0.00	0.00	0.00	0.00	0.00
x_5							**1.00**	-0.22	-0.07	0.00	0.00	0.00	0.00	0.00	0.00	0.00	0.00	0.00	0.00	0.00	0.00
y_5								**1.00**	0.07	0.00	0.00	0.00	0.00	0.00	0.00	0.00	0.00	0.00	0.00	0.00	0.00
z_5									**1.00**	0.00	0.00	0.01	0.00	0.00	0.00	0.00	0.00	0.00	0.00	0.00	0.00
x_6										**1.00**	0.13	0.12	0.09	0.04	-0.05	0.00	0.00	0.00	0.00	0.00	0.00
y_6											**1.00**	-0.01	0.05	0.08	0.01	0.00	0.00	0.00	0.00	0.00	0.00
z_6												**1.00**	-0.03	0.01	0.14	0.00	0.00	-0.01	0.00	0.00	0.00
x_7													**1.00**	-0.96	-0.04	0.00	0.00	0.00	0.00	0.00	0.00
y_7														**1.00**	0.12	0.00	0.00	0.00	0.00	0.00	0.00
z_7															**1.00**	0.00	0.00	0.00	0.00	0.00	0.00
x_8																**1.00**	0.72	-0.03	0.00	0.00	0.00
y_8																	**1.00**	-0.21	0.00	0.00	0.00
z_8																		**1.00**	0.00	0.00	0.00
x_9																			**1.00**	0.69	0.62
y_9																				**1.00**	0.64
z_9																					**1.00**
$\dot{x}_3$																					
$\dot{y}_3$																					
$\dot{z}_3$																					
$\dot{x}_4$																					
$\dot{y}_4$																					
$\dot{z}_4$																					
$\dot{x}_5$																					
$\dot{y}_5$																					
$\dot{z}_5$																					
$\dot{x}_6$																					
$\dot{y}_6$																					
$\dot{z}_6$																					
$\dot{x}_7$																					
$\dot{y}_7$																					
$\dot{z}_7$																					
$\dot{x}_8$																					
$\dot{y}_8$																					
$\dot{z}_8$																					
$\dot{x}_9$																					
$\dot{y}_9$																					
$\dot{z}_9$																					

	$\dot{x}_3$	$\dot{y}_3$	$\dot{z}_3$	$\dot{x}_4$	$\dot{y}_4$	$\dot{z}_4$	$\dot{x}_5$	$\dot{y}_5$	$\dot{z}_5$	$\dot{x}_6$	$\dot{y}_6$	$\dot{z}_6$	$\dot{x}_7$	$\dot{y}_7$	$\dot{z}_7$	$\dot{x}_8$	$\dot{y}_8$	$\dot{z}_8$	$\dot{x}_9$	$\dot{y}_9$	$\dot{z}_9$
x_3	-0.22	0.96	0.03	0.00	0.00	0.00	0.00	0.00	0.00	-0.01	0.00	0.00	0.00	0.00	0.00	0.00	0.00	0.00	0.00	0.00	0.00
y_3	0.92	0.16	-0.04	0.00	0.00	0.00	0.00	0.00	0.00	0.00	0.00	0.00	0.00	0.00	0.00	0.00	0.00	0.00	0.00	0.00	0.00
z_3	0.03	-0.28	-0.05	0.00	0.00	0.00	0.00	0.00	0.00	0.00	0.00	0.00	0.00	0.00	0.00	0.00	0.00	0.00	0.00	0.00	0.00
x_4	0.00	0.00	0.00	-0.35	-0.79	0.15	0.00	0.00	0.00	-0.01	0.00	0.00	0.00	0.00	0.00	0.00	0.00	0.00	0.00	0.00	0.00
y_4	0.00	0.00	0.00	-0.97	0.34	0.20	0.00	0.00	0.00	-0.01	0.00	0.00	0.00	0.00	0.00	0.00	0.00	0.00	0.00	0.00	0.00
z_4	0.00	0.00	0.00	-0.05	0.08	0.20	0.00	0.00	0.00	0.00	0.00	0.00	0.00	0.00	0.00	0.00	0.00	0.00	0.00	0.00	0.00
x_5	0.00	0.00	0.00	0.00	0.00	0.00	0.75	0.92	0.01	0.00	0.00	0.00	0.00	0.00	0.00	0.00	0.00	0.00	0.00	0.00	0.00
y_5	0.00	0.00	0.00	0.00	-0.01	0.00	0.45	-0.49	-0.13	0.00	0.00	0.00	0.00	0.00	0.00	0.00	0.00	0.00	0.00	0.00	0.00
z_5	0.00	0.00	0.00	0.00	0.00	0.00	-0.13	-0.08	-0.08	0.00	0.00	-0.01	0.00	0.00	0.00	0.00	0.00	0.00	0.00	0.00	0.00
x_6	0.00	0.00	0.00	-0.01	0.00	0.00	0.00	0.00	0.00	-0.13	-0.96	0.01	0.09	-0.08	0.01	0.00	0.00	0.00	0.00	0.00	0.00
y_6	0.00	0.01	0.00	-0.02	0.00	0.00	0.00	0.00	0.00	-0.96	-0.04	0.02	0.19	0.04	0.00	0.00	0.00	0.00	0.00	0.00	0.00
z_6	0.00	0.00	0.00	0.00	0.00	0.00	0.00	0.00	0.01	0.01	0.09	-0.01	-0.03	0.01	0.14	0.00	0.00	0.00	0.00	0.00	0.00
x_7	0.00	0.00	0.00	0.00	0.00	0.00	0.00	0.00	0.00	0.02	-0.09	0.06	0.98	0.94	-0.04	0.00	0.00	0.00	0.00	0.00	0.00
y_7	0.00	0.00	0.00	0.00	0.00	0.00	0.00	0.00	0.00	-0.09	-0.03	-0.05	-0.93	-0.98	0.02	0.00	0.00	0.00	0.00	0.00	0.00
z_7	0.00	0.00	0.00	0.00	0.00	0.00	0.00	0.00	0.00	-0.03	0.06	-0.12	-0.08	-0.07	-0.08	0.00	0.00	0.00	0.00	0.00	0.00
x_8	0.00	0.00	0.00	0.00	0.00	0.00	0.00	0.00	0.00	0.00	0.00	0.00	0.00	0.00	0.00	-0.62	0.94	0.40	0.00	0.00	0.00
y_8	0.00	0.00	0.00	0.00	0.00	0.00	0.00	0.00	0.00	0.00	0.00	0.00	0.00	0.00	0.00	0.01	0.81	0.24	0.00	0.00	0.00
z_8	0.00	0.00	0.00	0.00	0.00	0.00	0.00	0.00	0.00	0.00	0.00	0.00	0.00	0.00	0.00	0.14	-0.09	0.00	0.00	0.00	0.00
x_9	0.00	0.00	0.00	0.00	0.00	0.00	0.00	0.00	0.00	0.00	0.00	0.00	0.00	0.00	0.00	0.00	0.00	0.00	0.74	-0.19	-0.25
y_9	0.00	0.00	0.00	0.00	0.00	0.00	0.00	0.00	0.00	0.00	0.00	0.00	0.00	0.00	0.00	0.00	0.00	0.00	0.92	-0.71	-0.49
z_9	0.00	0.00	0.00	0.00	0.00	0.00	0.00	0.00	0.00	0.00	0.00	0.00	0.00	0.00	0.00	0.00	0.00	0.00	0.71	-0.58	-0.36
$\dot{x}_3$	**1.00**	-0.17	0.11	0.00	0.00	0.00	0.00	0.00	0.00	0.00	0.00	0.00	0.00	0.00	0.00	0.00	0.00	0.00	0.00	0.00	0.00
$\dot{y}_3$		**1.00**	0.09	0.00	0.00	0.00	0.00	0.00	0.00	-0.01	0.00	0.00	0.00	0.00	0.00	0.00	0.00	0.00	0.00	0.00	0.00
$\dot{z}_3$			**1.00**	0.00	0.00	0.00	0.00	0.00	0.00	0.00	0.00	0.00	0.00	0.00	0.00	0.00	0.00	0.00	0.00	0.00	0.00
$\dot{x}_4$				**1.00**	-0.26	-0.16	0.00	0.00	0.00	0.02	0.01	0.00	0.00	0.00	0.00	0.00	0.00	0.00	0.00	0.00	0.00
$\dot{y}_4$					**1.00**	0.11	0.00	0.00	0.00	0.00	0.00	0.00	0.00	0.00	0.00	0.00	0.00	0.00	0.00	0.00	0.00
$\dot{z}_4$						**1.00**	0.00	0.00	0.00	0.00	0.00	0.00	0.00	0.00	0.00	0.00	0.00	0.00	0.00	0.00	0.00
$\dot{x}_5$							**1.00**	0.54	0.04	0.00	0.00	0.00	0.00	0.00	0.00	0.00	0.00	0.00	0.00	0.00	0.00
$\dot{y}_5$								**1.00**	0.11	0.00	0.00	0.00	0.00	0.00	0.00	0.00	0.00	0.00	0.00	0.00	0.00
$\dot{z}_5$									**1.00**	0.00	0.00	0.01	0.00	0.00	0.00	0.00	0.00	0.00	0.00	0.00	0.00
$\dot{x}_6$										**1.00**	0.05	0.05	-0.12	-0.04	-0.01	0.00	0.00	0.00	0.00	0.00	0.00
$\dot{y}_6$											**1.00**	0.16	-0.07	0.10	0.03	0.00	0.00	0.00	0.00	0.00	0.00
$\dot{z}_6$												**1.00**	0.08	0.05	0.05	0.00	0.00	-0.01	0.00	0.00	0.00
$\dot{x}_7$													**1.00**	0.94	0.01	0.00	0.00	0.00	0.00	0.00	0.00
$\dot{y}_7$														**1.00**	0.01	0.00	0.00	0.00	0.00	0.00	0.00
$\dot{z}_7$															**1.00**	0.00	0.00	0.00	0.00	0.00	0.00
$\dot{x}_8$																**1.00**	-0.53	-0.09	0.00	0.00	0.00
$\dot{y}_8$																	**1.00**	0.30	0.00	0.00	0.00
$\dot{z}_8$																		**1.00**	0.00	0.00	0.00
$\dot{x}_9$																			**1.00**	-0.69	-0.43
$\dot{y}_9$																				**1.00**	0.03
$\dot{z}_9$																					**1.00**

Table 4.6: Correlation coefficients of the last iteration. The subscripts indicates: 3 = Tethys, 4 = Dione, 5 = Rhea, 6 = Titan, 7 = Hyperion, 8 = Iapetus, 9 = Phoebe.

Chapter 5

Conclusion and Future Work

The research presented in this thesis has dealt with the determination of the orbits of the main satellites of the Saturnian system from optical, ground-based observations. The main purpose of the present work, that is the development of a software tool for numerical orbit determination and estimation of the parameters that characterize the dynamic of the Saturnian system, has been successfully achieved. The developed software, named SOSYA (*SOlar SYstem Astrometry*), has been coded in Fortran95 adopting an object-oriented programming methodology, since this allows for better and safer programming.

The research carried out has moved essentially into two directions. The first has been the development of a dynamical model of the Saturnian system capable of describing in a sufficiently accurate and realistic manner the motion of the natural satellites of Saturn. The second has been the definition of the algorithms for the computation of the position of a Solar System object as viewed by an observer, both in the case of ground-based observations and spacecraft based-observations.

As regards the dynamical model of the Saturnian system we have adoped the model developed by Peters with the difference that we compute the gravitational potential of extended bodies using a spherical harmonics expansion. This model has been implemented in the SOSYA software. By means of the *Orbit Simulation* capability of SOSYA, we have numerically integrated the equations of motion and the variational equations of the main natural satellites of Saturn in a reference frame centered in the barycenter of the Saturnian system. The comparison between our numerically integrated ephemeris and the JPL ephemeris is good, particularly with the latest versions of the JPL ephemerides. In fact, in this case the rms over a period of 5 years is on the order of 10 meters and 7 meters respectively for Mimas and Phoebe and on the order of 2-3 meters for the other satellites. With regard to the integration of the variational equations we have verified that the partial derivatives exhibit the behaviour described by Hadjifotinou and Harper [17] and Hadjifotinou and Ichtiaroglou [16]. Some partials librate with an amplitude that increases linearly with time, while some others show long-period and short-period librations due to the oblateness perturbations and to the presence of resonances in the satellite system. The state transition matrix obtained by numerical integration shows a linear growth with time due to the linear increase with time of the partials. This suggests that, in an orbit determination process, the arc length cannot be too long and must be limited to a length over which the linearity assumption is verified reasonably well. In fact, in the expansion in a Taylor series about the reference trajectory the orders higher than the first are normally neglected but in this case the problem is strongly not linear and over a long time period the first order assumption is not sufficient. This assertion warrants more accurate investigation, but the need to use of a multi-arc approach is clearly indicated.

With reference to the definition of the algorithms for the computation of the position of a Solar System object as viewed by an observer, we have examined the corrections that must be applied to Earth-based observations. These corrections list includes atmospheric refraction, aberration, light-time and gravitational light deflection corrections. Additionally, algorithms for computing the apparent place

of Earth-based observations and spacecraft-based observations, as well as for computing the topocentric and the apparent places in the case of differential astrometric observations have been given.

The correct development and implementation of both the equations of motion and the variational equations, in conjunction with the study of the algorithm for the computation of the ground-based observables, played a key role in the determination of the orbit of the main natural satellites of Saturn.

The *Orbit Determination* capability of SOSYA has enabled us to adjust the models of the orbits of Tethys, Dione, Rhea, Titan, Hyperion, Iapetus, Phoebe. Our model has been adjusted to a total of 3153 observations covering a period between 1998 and 2007 and acquired with the Flagstaff Astrometric Scanning Transit Telescope (FASTT). Mimas and Enceladus have been included in the numerical integration, but their states have not been estimated because no observational data were available for these two satellites. The rms of the post-fit residuals is $0''.161$ and $0''.177$ respectively in α and δ. It is clearly limited by the intrinsic accuracy of the observational data.

The analytical formulations and numerical tools developed in this study were designed in a very general way, making them applicable to other satellite systems consisting of a primary and its natural satellites.

There are many areas where our research could move forward. With the goal of a numerical theory of the main satellites of Saturn in mind we have surely to increase the time span of the observations and use observations from more observing sites. Ideally, the increase of the time period of the observations could extend back to 1874, i.e., back to when the first visual micrometer measurements were taken with an accuracy lower than $0''.5$. Moreover new data types such as differential measurements and inter-satellites distances have to be considered, as well as photometric observations. In this regard the photometric observations of mutual events performed by Aksnes [2] during the opposition of 1979-1980 are one of the most accurate ground-based observations reaching an accuracy of $0''.02$. Since the accuracy of optical ground-based observations is seldom better than $0.''08$ (corresponding to about 500 km at Saturn) the goal of more accurate numerical theories can only be achieved through the use of the more accurate space-based observations, such as HST and, more importantly, spacecraft-based data. In fact, the accuracy of HST observations varies between $0''.014$ and $0''.02$, correspondig respectively to 80 km and 120 km at Saturn. These are among the most accurate Earth-based observations of Saturn's satellites. The accuracy of the observations of Cassini, the spacecraft currently orbiting the Saturnian system varies between 5 and 200 km, depending on the spacecraft-satellite range [13].

The use of more observations and more data types could help us remove the bias we have found in our solution, both when the bias is due to errors of observation and when it is due to errors in the model. Furthermore, extending the time period of observational data could enable us to solve for the gravitational parameters of the satellites.

Appendix A

Time and Reference Systems

A.1 Introduction

Time and coordinate systems are an inherent component of the orbit determination problem. Any measurement of some aspect of a satellite's position or motion must be indexed in time. The time index of the observations must be related to the time used in the equations of motion, but different time systems are used.

Measurements collected by some instrumentation located on the Earth's surface suggest the use of coordinate systems attached to the Earth at the position of the instrument. These coordinate systems (topocentric) rotate since they are fixed to the Earth's surface. On the other hand, the equations of motion are related to an inertial system. So we have to know the transformations between the various coordinate systems.

For computational purposes exists a collection of Fortran 77 subprograms that implement official International Astronomical Union algorithm for fundamental astronomy. This free collection goes under the name of Standards of Fundamentals Astronomy (SOFA).

A.2 Time systems

There are two widely used types of time standards [10] [51]. Those related with the rotation of the Earth, and those related with the frequency of atomic oscillations (mainly the cesium-133 atom). The Earth rotation is not uniform, therefore the rate of the clocks referenced to the rotation exhibits both periodic changes and long term drifts of the order of a second per year. Atomic standards are the closest approximations we currently have to a uniform time with accuracy on the order of microseconds per year.

A.2.1 International Atomic Time - TAI

TAI is a uniform and stable scale established by the Bureau International des Poids et Measures (BIPM) on the basis of atomic clock data. This is result of statistically combining the input of many clocks around the world, each corrected for known environmental and relativistic effects. These clocks have different weighting factors in the TAI.

TAI is a scale that does not keep in step with the slightly irregular rotation of the Earth, therefore for public and practical purposes it is necessary to have another scale that, in long term, does. In relativistic terms TAI is an Earth-based time since it is defined for a gravitational potential and inertial reference on the surface of the earth, i.e. in another reference frame TAI would be different. TAI is the standard for the SI second defined as the duration of 9,192,631,770 cycles of radiation corresponding to the transition between two hyperfine levels of the ground state of cesium 133.

Although TAI was officially introduced in January 1972, it has been available since July 1955. Its epoch was set so that TAI was in approximate agreement with UT1 on 1st January 1958.

A.2.2 Coordinate Universal Time - UTC

UTC is the time scale based on the second SI and maintained by the BIPM. It follows TAI exactly except for an integer number of seconds, called leap seconds since 1st January 1972, which have been introduced to keep solar noon at the same UTC (averaged over the year) even though the rotation of the Earth is slowing down. Before 1972, UTC was also adjusted, but following a different and more complicated protocol that was changed to the actual one. The offset is changed as needed to keep UTC within about 0.9 seconds of Earth rotation time or UT1. Leap seconds are typically added once per year at the last second of December 31 or June 30, but they can be added (or subtracted) at other designated times throughout the year, on the advice of the International Earth Rotation Service (IERS) so

$$\mathrm{UTC} = \mathrm{TAI} - (\text{number of leap seconds})\,. \tag{A.1}$$

The offset between UTC and TAI is currently 33 seconds.

UTC is the standard time common to every place in the world. Formerly and still widely known as GMT (Greenwich Mean Time), UTC nominally reflects the mean solar time along the Earth's prime meridian. UTC forms the basis of a coordinated dissemination of standard frequencies and time signals.

A.2.3 Dynamical Time

Dynamical time is the independent variable in the theories that describe the motion of the bodies in the Solar System. This concept corresponds to the concept of the inertial time, i.e. the time scale that fulfills exactly the equations of motion of celestial bodies. Therefore, every time that an ephemeris is used, the date and time must be in terms of one of the dynamical times.

These time scales are necessary because no other time scales satisfy the objectives of the dynamical ones. UTC would clearly be unsuitable as the argument of an ephemeris because of leap seconds. A Solar System ephemeris based on an Earth rotation based time scale would somehow have to include the unpredictable variations of the Earth's rotation. TAI would work, but eventually the ephemeris and the ensemble of atomic clocks would drift apart. Only two of the dynamical time scales are of any great importance for planetary missions, TDT and TDB.

Terrestrial Dynamical Time - TT or TDT

TDT is the independent argument for apparent geocentric ephemeris of Solar System bodies, defining a theoretical time scale. In principle, it applies to an earthbound clock at sea level, and for practical purposes it is tied to TAI, and its unit of duration is a day of 86400 SI seconds on the geoid.

TDT is used as the time scale of ephemeris for observations from Earth's surface. TDT replaced ET when the IAU 1976 System of Astronomical Constants was implemented in the Astronomical Almanac in 1984. This time, as it is referred to the geocenter, is the Proper Time with periodic variations up to 1.6 milliseconds, but common between Earth and objects within the Earth's gravity field.

TDT was renamed simply Terrestrial Time (TT) in 1991, when it acquired the actual time unit, the SI second at mean sea level. That is important for precise time keeping because, according to general relativity, the rate of passage of time depends on the gravitational potential.

The difference between TAI and TDT in seconds is defined by

$$\mathrm{TDT} = \mathrm{TAI} + 32.184\,s\,. \tag{A.2}$$

Barycentric Dynamical Time - TB or TDB

TDB is the independent argument for orbital motions referenced to the center of mass of the Solar System, the origin of this reference frame. It is as close as possible to an inertial reference frame in the gravitational theory, thus it fulfills exactly the equations of motion of the celestial bodies. TDB is derived from orbital motions referred to the barycenter of the Solar System. This time is the coordinated time in terminology of General Relativity.

TDB differs from TDT by an amount that cycles back and forth by a millisecond or two due to relativistic effects, related with variations in the gravitational potential around the Earth's orbit combined with velocity terms. The maximum of these variations is about 1.6 milliseconds and they are periodic with an average of zero. The variation is negligible for most purposes, but unless taken into account would swamp long term analysis of pulse arrival times from the millisecond pulsars. It is a consequence of the TDT clock being on the Earth rather than in empty space. The ellipticity of the Earth's orbit means that the TDT clock's speed and gravitational potential vary slightly during the course of the year, and as a consequence its rate as seen from an outside observer varies due to transverse Doppler effect and gravitational redshift.

TDB is used as a time scale of ephemeris referred to the barycenter of the Solar System that employs the fundamental equations of motion, and therefore it is subject to the inadequacies of those analytical theories. TDB replaced ET when the IAU 1976 System of Astronomical Constants was implemented in the Astronomical Almanac in 1984, to use in this type of ephemeris.

The difference between TDT and TDB are due to relativistic correction to move the origin to the Solar System Barycenter. The relationship between them is given by the following formula (in seconds)

$$\mathrm{TDB} = \mathrm{TDT} + 0.001658 \sin g + 0.000014 \sin 2g \,, \tag{A.3}$$

where

$$g = 357^\circ.53 + 0^\circ.9856003\,(\mathrm{JD} - 2451545.0) \,, \tag{A.4}$$

and JD is the Julian Date (see Section A.2.5). A more accurate formula, with adds terms smaller than $20\,\mu s$, is given in [51] and [42].

A.2.4 Earth Rotation Time Standards

Several important time scales still follow the rotation of the Earth, most notably civil times, but some of these are now derived from atomic time through a combination of Earth rotation theory and actual measurements of the Earth's rotation and orientation.

Universal Time - UT

The atomic times give us the interval of time between two different events, but they do not give us the hour angle of the Sun, i.e. the position of the Sun in the sky. The required time scale for this purpose is the UT, and is for most purposes, the same as UTC.

However, for very precise work there are several subtly different varieties of UT. When a precision of a second or better is needed, it is necessary to be more specific about the variety of UT that is being used.

Normally, the instant of time at which events are observed should be recorded and reported in UTC. Of course, if observation is not made with a precision better than a second, it is not possible to distinguish between the various versions of UT, and the time recorded should be UT.

UT1

UT1 is a measurement of the actual rotation of the Earth, independent of observing location. It is the observed rotation of the Earth with respect to the mean Sun corrected for the observer's longitude with

respect to the Greenwich Meridian and for the observer's small shift in longitude due to polar motion (see Section A.3.3).

Since the Earth's rotation is not uniform, the rate of UT1 is not constant, and its offset from atomic time is continually changing in a not completely predictable way. This variation in UT1 is dominated by seasonal oscillations due primarily to the exchange of angular momentum between the atmosphere and the solid Earth and seasonal tides.

Since UTC is intentionally incremented by integer seconds (leap seconds) to stay within 0.9 seconds of UT1, the difference between UT1 and UTC is never greater than this. The difference DUT1 = UT1−UTC, is monitored by the IERS and published weekly in IERS Bulletin A along with predictions for a number of month into the future so

$$\mathrm{UT1} = \mathrm{UTC} + \mathrm{DUT1}\,. \tag{A.5}$$

UT0

UT0 (Universal Time Observed) is an observatory specific version of UT1 in the sense that UT0 contains the effect of polar motion (see Section A.3.3) on the observed rotation of the Earth. Since UT1 is now determined from observations from an ensemble of observatories, the practical use of UT0 has dwindled. The conversion from UT1 to a local observatory time with respect to the mean Sun or stars is now done as a set of coordinate rotations that do not explicitly use UT0 as an intermediate step, as before. The difference, involving corrections for the latitude and longitude of observatory's points on the Earth's surface with respect to the Earth's instantaneous rotation axis, is based on the following formula (in seconds):

$$\mathrm{UT0} = \mathrm{UT1} + \tan\varphi\ (x\sin\lambda + y\cos\lambda)\ , \tag{A.6}$$

where x and y are the pole offset published in IERS Bulletin A and φ and λ are the observatory's nominal station coordinates.

UT2

UT2 is UT1 with annual and semiannual variations in the Earth's rotation removed. UT2 is obtained by applying an adopted formula that approximates the seasonal oscillations in the Earth's rotation. However, due to other variations including those associated with the secular effects of tidal friction (the Earth's spin is continually but gradually slowing down), high frequency tides and winds, and the exchange of angular momentum between the Earth's core and its shell, UT2 is also not a uniform time scale. The difference between UT1 and UT2 is based on the following formula (in seconds):

$$\mathrm{UT2} = \mathrm{UT1} + 0.022\sin 2\pi t - 0.012\cos 2\pi t - 0.006\sin 4\pi t + 0.007\cos 4\pi t\,, \tag{A.7}$$

where

$$t = 2000.0 + \frac{\mathrm{MJD} - 51544.03}{365.2425}\,, \tag{A.8}$$

is the Besselian day fraction and MJD is defined in section (A.2.5).

Ephemeris Time - ET

For much of the twentieth century, ET was the time scale used for theoretical ephemeris calculations. The first time scales were based on the rotation of the Earth. However, as clocks became more precise, it became clear that the rotation of the Earth was not constant, explaining the errors in the calculation of the celestial positions of planets. ET was based not on the irregularly rotating Earth, but in principle on the motion of Earth in its orbit around the Sun, which was presumed to be uniform. In practice, ET was calculated from observations of occultation of stars by the Moon, the motion of the Moon in its orbit being supposed to be calculated using a uniformly flowing ET. ET, however, did not include

relativistic effects, such as corrections for the gravitational potential and velocity, required by advances in the accuracy, and therefore, in 1984 it was replaced by TDT/TDB.

Greenwich Mean Time - GMT

GMT is a time scale based on the apparent motion of the mean Sun with respect to the meridian through the Old Greenwich Observatory. The mean Sun is used because time based on the actual or true apparent motion of the Sun does not tick a constant rate, hence at different times of the year the Sun appears to move faster or slower in the sky. So if the mean Sun is directly over the Greenwich meridian, it is exactly 12:00 GMT.

GMT is formerly used as a basis for every world time zone that sets the time of day and is at the center of the time zone map. GMT is the average time that the Earth takes to rotate from noon-to-noon. GMT is fixed all year and does not switch to daylight saving times. GMT is essentially the same as the UT1.

Greenwich Mean Sideral Time - GMST

GMST, also known as Greenwich Hour Angle, denotes the angle between the mean vernal equinox of date and the Greenwich meridian. It is a direct measure of the Earth's rotation an may jointly be expressed in angular units. In terms of SI seconds, the length of a sideral day (i.e. the Earth spin period) amounts to $23^h56^m04.091^s \pm 0.005^s$, making it about four minutes shorter than a 24^h solar day. Due to length of day variations with an amplitude of several milliseconds, sideral time cannot be computed from other time scales with sufficient precision but must be derived from astronomical and geodetic observations. In conformance with IAU conventions for the motion of the Earth's equator and equinox GMST is linked directly to UT1 through equation:

$$\text{GMST (in seconds at UT1} = 0) = 24110.54841 + 8640184.812866\,t + 0.093104\,t^2 - 0.0000062\,t^3\,, \quad \text{(A.9)}$$

where t is in Julian centuries from 2000 Jan. 1^{st} 12h UT1, i.e.

$$t = \frac{d}{36525}\,, \quad \text{(A.10)}$$

$$d = \text{JD} - 2451545.0\,. \quad \text{(A.11)}$$

Greenwich Apparent Sideral Time - GAST

GAST is Greenwich Mean Sidereal Time (GMST) corrected for the shift in the position of the vernal equinox due to nutation (see Section A.3.3). Nutation is the mathematically predictable change in the direction of the Earth's axis of rotation due to changing external torques from the Sun, Moon and planets. The smoothly varying part of the change in the Earth's orientation (precession) is already accounted for in GMST. The relation between GAST and GMST is given by:

$$\text{GAST} = \text{GMST} + \text{EE}\,, \quad \text{(A.12)}$$

where EE is the equation of the equinox (see Section A.3.3).

A.2.5 Standard dating methods

Julian Date - JD

Julian Day or Julian Date is a continuous count of days and fractions, started in January 1^{st} , 4713 BC (-4712 in the Astronomical Almanac) at Greenwich mean noon (12 h UT). Astronomers use this method in order to avoid the complexity of the other calendars.

Julian dates assign a unique number to each calendar day. Hours, minutes and seconds are counted as fractions of a day since the last noon. Note that the JD is always determined from an universal time standard (i.e. UTC, TDT, TAI, ...) but never Local Time.

JD is very useful because it makes easy to determine the number of days between two events by simply subtracting their JD numbers. Such a calculation is difficult for the standard (Gregorian) calendar, because days are grouped into months, which can contain a variable number of days, and there is the added complication of Leap Years. Astronomers use certain JD values as important reference points, such as J2000, that is the JD for 1st January 2000 at 12:00 UTC.

Modified Julian Date - MJD

MJD is an abbreviated version of the JD dating methods. It was introduced by space scientists in the late 50's. It is based on a shift of the JD so its origin occurs at midnight on 17th November 1858. The MJD differs from the JD by exactly 2400000.5, therefore the computation of the MJD is easily done from the JD using the following formula:

$$\mathrm{MJD} = \mathrm{JD} - 2400000.5\,. \tag{A.13}$$

The half-day is subtracted so that the day starts at midnight in conformance with civil time reckoning. Various international commissions (such as IAU, International Astronomical Union) have sanctioned this MJD, because they recommend it as a decimal day count, which is independent of the civil calendar in use.

The MJD is always referred to as a time reckoned in UT, or UTC, TAI or TDT.

MJD is a convenient dating system with only 5 digits, sufficient for most modern computational purposes. The days of the week can easily be computed because the same weekday is obtained for the same remainder of the MJD after division by 7.

A.3 Coordinate Systems

In astronomy it is necessary and convenient to represent the position of an object, such as planet, star or spacecraft, in several different coordinate systems according to the context in which position is to be used. Each coordinate system corresponds to a particular way of expressing the position of a point with respect to a coordinate frame. In many cases the coordinate frames with respect to which observations are made differ from the coordinate frames that are most convenient for the comparison of observational data with theory. In this section we explore the two most important reference frames: the celestial reference frame (linked to the fixed stars) and the terrestrial reference frame (dependent on the Earth's rotation) and the transformation between the two systems.

A.3.1 International Celestial Reference System

The celestial reference system is based on a kinematical definition, making the axis directions fixed with respect to the distant matter of universe. The International Astronomical Union recommends that the origin is to be at the barycenter of the Solar System and the directions of the axes should be fixed with respect to quasars. Also the celestial reference system should have its principal plane as close as possible to the mean equator at J2000.0 and that the origin of this principal plane should be as close as possible to the dynamical equinox of J2000.0. This system was prepared by the IERS and has been adopted by the IAU General Assembly of 1997 under the name of the International Celestial Reference System (ICRS).

The ICRS is materialized by the International Celestial Reference Frame (ICRF). A realization of the ICRF consists of a set of precise coordinates of extragalactic radio sources.

The planetary and lunar ephemerides recommended for the IERS standards are the JPL Development Ephemeris DE405 and the Lunar Ephemeris. The reference frame of DE405 is that of the International Celestial Reference Frame (ICRF).

A.3.2 International Terrestrial Reference System

A Terrestrial Reference System (TRS) is a spatial reference system corotating with the Earth in its diurnal motion in space. In such a system, positions of points attached to the solid surface of the Earth have coordinates which undergo only small variations with time, due to geophysical effects (tectonic or tidal deformations). The Conventional Terrestrial Reference System (CTRS) monitored by IERS is the International Terrestrial Reference System (ITRS). Realizations of the ITRS are produced by IERS under the name of International Terrestrial Reference Frame (ITRF), which consist of list of coordinates and velocities for a selection of IERS site (see [35] and [36]).

A.3.3 Transformation Between the Celestial and Terrestrial Systems

To convert from ICRS to ITRS a set of rotations must be employed. At the date t, the transformation can be written as [35] [36]:

$$[\text{ITRS}] = \mathbf{W}(t)\,\mathbf{R}(t)\,\mathbf{N}(t)\,\mathbf{P}(t)\,[\text{ICRS}]\ , \tag{A.14}$$

where $\mathbf{N}(t)\,\mathbf{P}(t)$, $\mathbf{R}(t)$ and $\mathbf{W}(t)$ are the transformations arising from the motion of the Celestial Ephemeris Pole (CEP) in the ICRS, from the rotation of the Earth around the axis of (CEP) and from the polar motion respectively.

Precession

Neither the plane of the Earth's orbit, the ecliptic, nor the plane of the Earth's equator are fixed with respect to distant objects.

The motion of the ecliptic is due to the gravitational attraction of the planets on the Earth's orbit and makes a contribution to precession known as planetary precession. If the equator were fixed, this motion would produce a precession of the equinox of about $12''$ per century [51] and a decrease in the obliquity of the ecliptic of about $47''$ per century.

The motion of the equator is due to the torque of the Sun, Moon and planets on the dynamical figure of the Earth. It can be separated into two parts, the lunisolar precession, which is the smooth and long period motion of the mean pole of the equator about the pole of the ecliptic, with a period of 26000 years, and nutation which is the short period motion of the true pole around the mean pole with an amplitude of about $9''$ per century. The combination of lunisolar and planetary precession is called general precession.

The precession matrix $\mathbf{P}$ precesses equatorial rectangular coordinates from an arbitrary mean equator and equinox of a fixed epoch ε_F (J2000.0) to a mean equator and equinox of date ε_D and is given by

$$\mathbf{P}[\varepsilon_F, \varepsilon_D] = \mathbf{R}_3(-z_A)\,\mathbf{R}_2(\theta_A)\,\mathbf{R}_3(-\varsigma_A)\ , \tag{A.15}$$

where $\mathbf{R}_3$ and $\mathbf{R}_2$ are rotation matrix (see Appendix B) and standard values for z_A, θ_A and ς_A quantities are given as a series of functions of two parameters t and T (the last parameter representing the Julian centuries from J2000.0 to an arbitrary epoch and are part of the 1976 IAU Theory of Precession [32].

Nutation

The long period motion of the Earth's rotation axis with respect to the axis of the ecliptic caused by lunisolar torque is called lunisolar precession. The short period motion of the Earth's rotation axis with respect to a space fixed coordinate system is called nutation. It is strictly connected with polar motion,

which is the movement of the Earth's rotation axis with respect to an Earth's fixed coordinate system. The reference pole for nutation and polar motion is called the Celestial Ephemeris Pole (CEP).

The 1980 IAU Theory of Nutation [52] describes the motion of the true pole relative to the mean pole and may be resolved into the components $\Delta\psi$ in longitude and $\Delta\epsilon$ in obliquity. The nutation matrix $\mathbf{N}$ is a sequence of three rotations which uses these angles and the mean obliquity of the ecliptic, ϵ_0, to transform equatorial coordinates referred to the mean equator and equinox of date to the true equator and equinox of date and is expressed as

$$\mathbf{N} = \mathbf{R}_1\left(-\epsilon\right)\mathbf{R}_3\left(-\Delta\psi\right)\mathbf{R}_1\left(\epsilon_0\right) , \tag{A.16}$$

where $\epsilon = \epsilon_0 + \Delta\epsilon$.

Polar Motion

The rotation of the Earth is represented by a diurnal rotation around a reference axis whose motion with respect to the inertial reference frame is represented by the theories of precession and nutation. The reference axis doesn't coincide with the axis of figure (maximum moment of inertia) of the Earth, but moves slowly (in a terrestrial reference frame) in a quasi-circular path around it. The reference axis is the Celestial Ephemeris Pole.

The position of the terrestrial reference frame with respect to the true equator and equinox of date is defined by successive rotations through two small angle x and y and the Greenwich apparent sideral time (GAST) θ. The angles x and y correspond to the coordinates of the CEP with respect to the terrestrial pole measured along meridians at longitude 0° and 270°. Time series for polar motion can be retrieved from the IERS Bulletin B.

The rigorous transformation from the frame of true equator and equinox of date to the terrestrial frame is given by the matrices' composition $\mathbf{W}\left(t\right)\mathbf{R}\left(t\right)$ where

$$\begin{aligned} \mathbf{W}\left(t\right) &= \mathbf{R}_2\left(-x\right)\mathbf{R}_1\left(-y\right)\mathbf{R}_3\left(\theta\right) , \\ \mathbf{R}\left(t\right) &= \mathbf{R}_3\left(\theta\right) . \end{aligned} \tag{A.17}$$

Appendix B

Elementary Rotation Matrices

In $\mathbb{R}^3$, coordinate system rotations of the x, y, and z axes in a counterclockwise direction of an angle α when looking towards the origin give respectively the matrices

$$\mathbf{R}_x(\alpha) = \begin{pmatrix} 1 & 0 & 0 \\ 0 & \cos\alpha & \sin\alpha \\ 0 & -\sin\alpha & \cos\alpha \end{pmatrix}, \tag{B.1}$$

$$\mathbf{R}_y(\alpha) = \begin{pmatrix} \cos\alpha & 0 & -\sin\alpha \\ 0 & 1 & 0 \\ \sin\alpha & 0 & \cos\alpha \end{pmatrix}, \tag{B.2}$$

$$\mathbf{R}_z(\alpha) = \begin{pmatrix} \cos\alpha & \sin\alpha & 0 \\ -\sin\alpha & \cos\alpha & 0 \\ 0 & 0 & 1 \end{pmatrix}. \tag{B.3}$$

Appendix C

Geocentric to topocentric transformation

Given the geocentric coordinates (α, δ) of an object in the Solar System and its geocentric parallax p we want to compute the topocentric coordinates (α', δ') of the same object. In the following the apex indicates that the quantity is topocentric. The trasformation is given by (see [3] and [15])

$$\begin{cases} \tan\delta' = \dfrac{\tan\delta - \rho\sin\pi\sin\varphi_g\sec\delta\cos\Delta\alpha}{1 - \rho\sin\pi\cos\varphi_g\sec\delta\cos HA} \\ \sin p = \sin\pi\dfrac{\sin HA'\cos\delta'}{\sin HA\cos\delta} \end{cases} , \tag{C.1}$$

where ρ is the geocentric distance of the observing site from the center of the Earth in units of the Earth equatorial radius, φ_g is the geocentric latitude of the observing site, $\Delta\alpha$ is the correction into α, p is the geocentric parallax, π is the horizontal parallax, and HA and HA' are the geocentric and topocentric hour angle respectively. These rigorous formulas can be developed to first order giving the corrections $\Delta\alpha$ and $\Delta\delta$

$$\begin{cases} \Delta\alpha = -\rho\sin\pi\dfrac{\sin HA\cos\varphi_g}{\cos\delta} \\ \Delta\delta = -\rho\sin\pi\sin\left(\varphi_g - \delta\right) \end{cases} , \tag{C.2}$$

and so

$$\begin{cases} \alpha' = \alpha + \Delta\alpha \\ \delta' = \delta + \Delta\delta \end{cases} . \tag{C.3}$$

Remain to compute the horizontal parallax π from the geocentric parallax p. The correct formula involving known quantity is (see [3])

$$\tan p = \rho\sin\pi\frac{\sin z}{(1 - \rho\sin\pi\cos z)} , \tag{C.4}$$

where z is the geocentric zenith distance and is given by

$$z = \varphi_g - \delta .$$

The equation (C.4) is an non linear equation that can be solved using Newton-Rhapson's method. If we set $x = \sin\pi$, our function is

$$f(x) = \tan p - \frac{x\rho\sin z}{(1 - x\rho\cos z)} = 0 , \tag{C.5}$$

and its derivative is

$$\begin{aligned}\frac{df}{dx} &= -\frac{\rho\sin z\,(1-\rho x\cos z)+x\rho\sin z\rho\cos z}{(1-x\rho\cos z)^2}\\ &= -\frac{\rho\sin z-x\rho^2\sin z\cos z+x\rho^2\sin z\cos z}{(1-x\rho\cos z)^2}\\ &= -\frac{\rho\sin z}{(1-x\rho\cos z)^2}\,. \end{aligned} \tag{C.6}$$

Assigning the initial value $x^{(0)}$ to x the Newton's method is given by (see [67], [50])

$$x^{(k+1)} = x^{(k)} - \frac{f\left(x^{(k)}\right)}{\left(\frac{df}{dx}\right)_{x^{(k)}}}\,. \tag{C.7}$$

Appendix D

SOSYA Software Description

The aim of the SOlar SYstem Astrometry (SOSYA) software is the orbit determination of the natural satellites of Saturn. In order to reach this scope, the software processes optical Earth-based observations. Moreover, the software provides orbit and data simulations by means of a complete dynamical and observation models implementation. In addition, the software performs covariance analysis and sensitivity studies of the spacecraft orbit and natural satellites (at the present not implemented).

D.1 Function and purpose of the software

The technical objectives of the software are summarized as follows:

- **Orbit Simulation**: natural satellites orbit propagation by numerical integration of the equations of motion using a full set of acceleration models; implementation of a dynamical model of the Solar System for application to different bodies of Solar System;
- **Measurement Simulation**: optical Earth-based data simulation;
- **Orbit Determination and Parameters Estimation**: orbit determination of the natural satellites; geophysical (gravitational parameters, Stokes coefficients) parameters estimation;
- **Covariance Analysis** (not implemented): sensitivity study of orbits of natural satellites; a priori observation errors covariance matrix and a priori covariance matrix of consider parameters.

The software is coded using as programming language the Fortran95 standard (see [9] and [37]) and adopting object-orienting programming methodology [1].

D.2 Relation to other systems

The software interacts with three external systems precompiled into three separated library and linked to the software:

- SPICE [27], a NAIF (Navigation and Ancillary Information Facility at JPL) developed software system that provides the capability to easily combine accurate space geometry and event data with mission analysis, observation planning, or science data processing software. SOSYA uses SPICE toolkit to read the JPL ephemeris files.
- SOFA (Standards of Fundamental Astronomy), a collection of Fortran 77 subprograms that implement official IAU algorithm for fundamental astronomy computations. SOSYA uses SOFA library to determine the Earth attitude.
- DIVA [28], a variable order integrator for ordinary differential equations: this integrator is based on the predictor-corrector scheme of Adams-Bashforth and Adams-Moulton.

D.3 Modular description

In Figure D.1 we give the modular view of the SOSYA program. In Figures D.3 and D.2 we give the flowchart diagrams of the SOSYA program and of the orbit simulation module of SOSYA respectively.

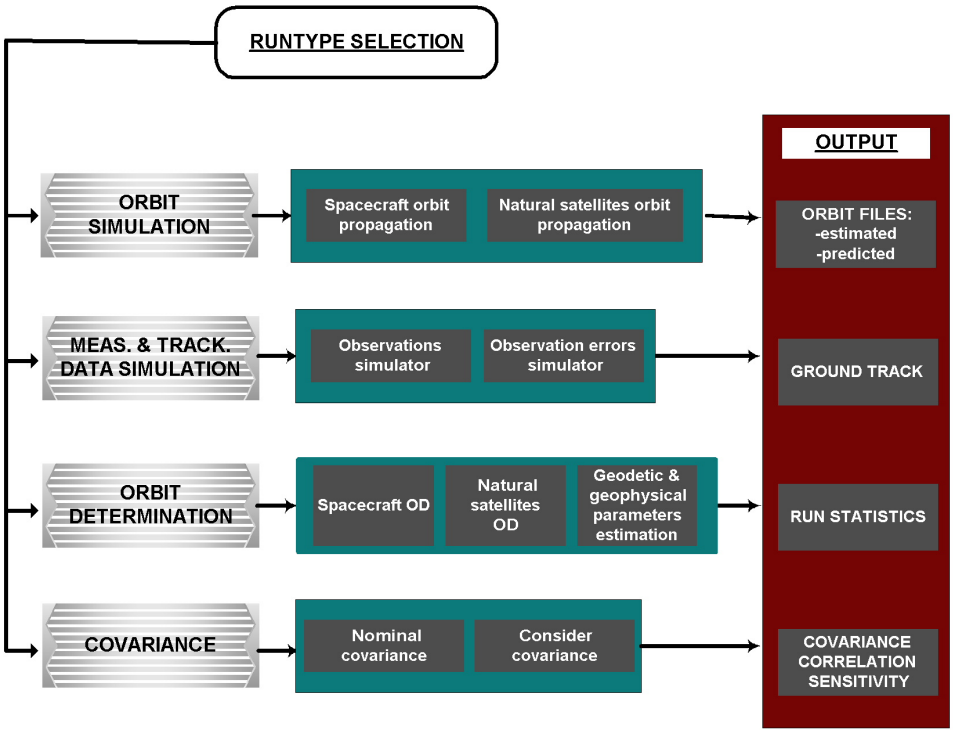

Figure D.1: Modular view of SOSYA.

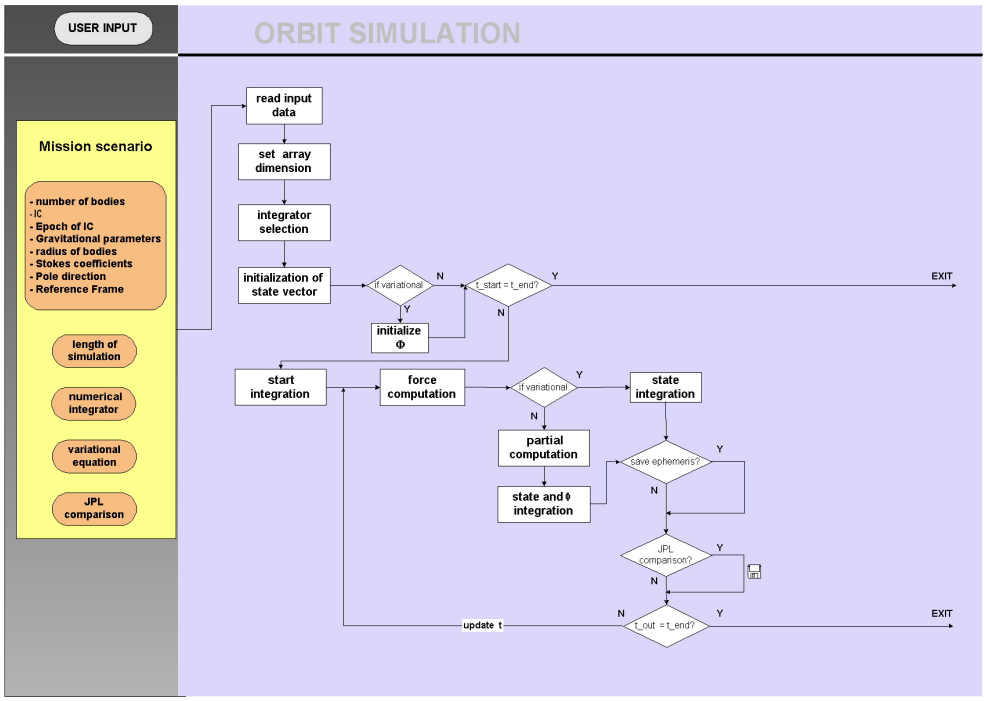

Figure D.2: Flow chart diagram of SOSYA orbit simulation module.

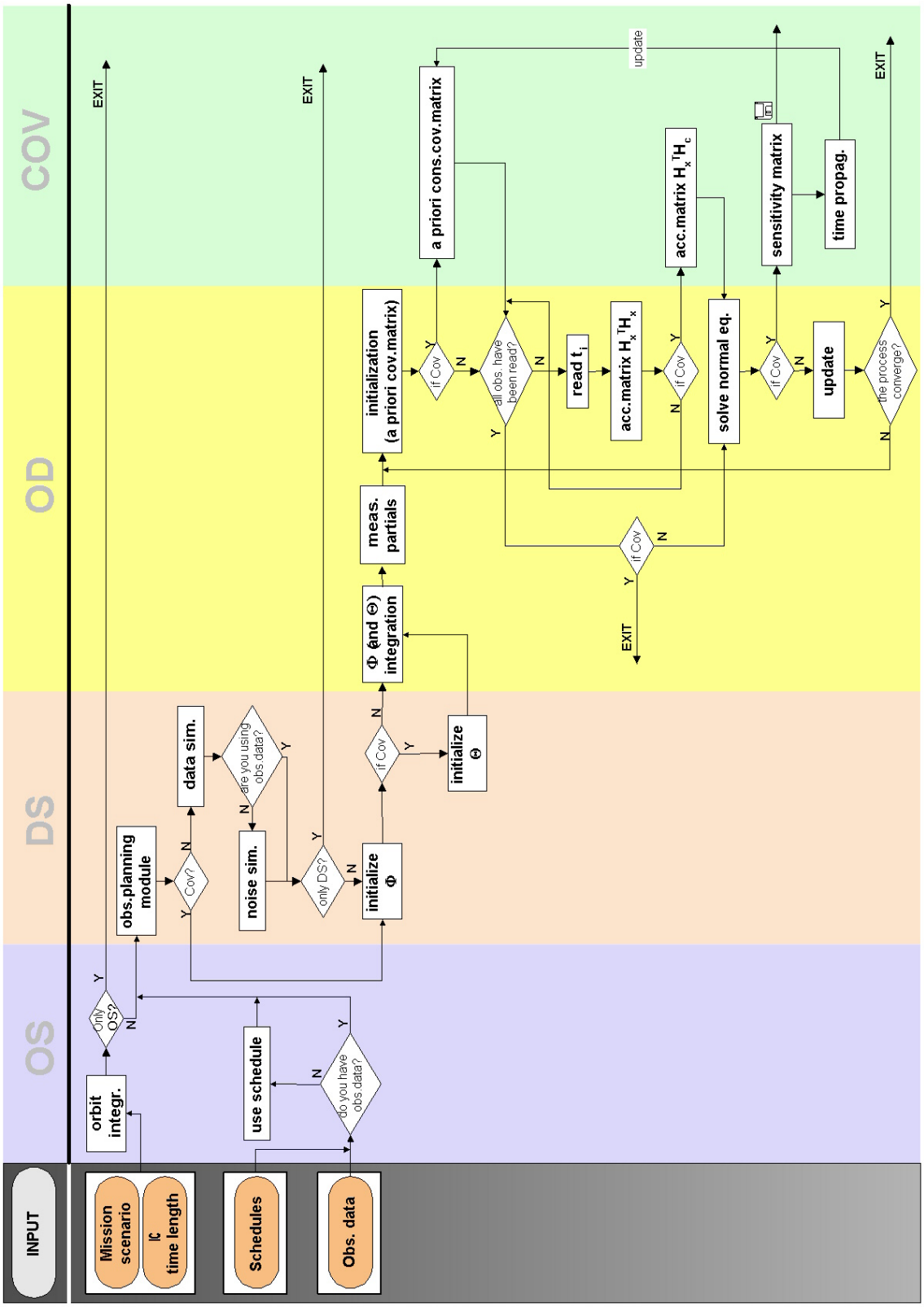

Figure D.3: Flow chart diagram of SOSYA.

D.4 Component description

This section describes the components of the SOSYA software.

D.4.1 Classes

In the following tables a brief description of all the classes contained in the SOSYA software is given.

Class	Description
angle_class	manages angles as [deg, arcmin, arcsec]
body_class	manages all the bodies, that is primary planet, satellites, perturbers
diff_table_class	manages differences tables for interpolation using DIVA
diva_diff_table_class	manages differences tables and integration order for interpolation using DIVA
dynamical_par1_class	manages gravitational parameters as dynamical parameters
dynamical_par2_class	manages Stokes coefficients as dynamical parameters
dynamical_state_class	manages the dynamical estimable state
earth_rotation_params_class	manages the Earth orientation parameters readed from IERS Bulletin B
estimation_class	manages all the estimable parameters
integrated_orbit_class	manages the orbits of integrated satellites saved into memory
integration_class	manages the integrator settings
observation_class	manages the available observations
observatory_class	manages the list of the observatory with their coordinates
state_transition_matrix_class	manages the state integrated transition matrix saved into memory
user_input_class	manages the user choices

angle_class

Variables		
Name	**Type**	**Description**
hd	integer	hours or degrees
min	integer	minutes of hours or degrees
sec	real	seconds of hours or degrees

Methods	
Name	**Description**
init_angle_class	initializes variables of angle_class
set_angle_type	sets values of angle_class

diff_table_class

Variables		
Name	**Type**	**Description**
KQMAXI	integer	maximum integration order used for equations which are not stiff
KORD	integer(:)	store integration orders and user flags
TN	real	base value of independent variable
XI	real(20)	store values of TN k step back ($k \leq 20$)
F	real(:)	store derivative values, options and difference tables
Y	real(:)	vector of dependent variable

Methods	
Name	**Description**
init_diff_table	allocates and initialize variables of diff_table_class
deallocate_diff_table	deallocates diff_table_class
set_diff_table	sets diff_table_class
get_diff_table_TN	gets value of TN
get_diff_table	gets diff_table_class

body_class

Variables		
Name	**Type**	**Description**
name	character(6)	body's name, JPL nomenclature
obj	character(2)	body's type (planet, natural satellite, artificial satellite)
objtp	character(2)	body's type (primary, integrated satellite, perturber
id	integer	body's identification number, JPL nomenclature
gm	real	body's gravitational parameter
stokes	real(:,:)	stokes coefficients
radius	real(3)	body's radius as triaxial ellipsoid (a,b,c)
ic	type	information on initial conditions
poltim	real	pole epoch
pole	real(3,2)	pole coordinates
ic%epoch	real	Julian Date of initial conditions
ic%init_cond	real(6)	initial conditions
ic%frame	character(10)	Reference frame of initial conditions
ic%rf_center	integer	Center of the reference frame

Methods	
Name	**Description**
init_body	initializes variables of body_class
set_body_name	sets name
set_body_obj	sets type
set_body_objtp	sets type
set_body_id	sets identification number
set_body_GM	sets gravitational parameters
set_body_GM_single	sets gravitational parameter
set_body_ic_epoch	sets epoch of initial conditions
set_body_radius	sets radius of extended body
set_body_pole	sets pole orientation values
set_body_stokes	sets values of stokes coefficients
set_body_ic_single	sets value of initial conditions
set_body_ic_all	sets values of initial conditions
set_frame_center	sets reference frame
order_body	orders bodies (primary, satellites, perturbers)
get_body_name	gets name
get_body_id	gets identification number
get_body_objtp	gets type
get_frame_center	gets reference frame
get_body_rv	gets position and velocity
get_body_IC	gets initial conditions
get_id_per_objtp	gets identification number from type
get_body_GM	gets gravitational parameter
get_body_pole	gets pole orientation
inquire_if_body_extended	checks if body is extended
get_Stokes_coefficients	gets Stokes coefficients
get_body_radius	gets radius of extended body
get_body_ic_epoch	gets epoch of initial conditions
get_index_from_body_id	gets memory index from identification number
get_body_name_from_id	gets name from identification number
get_body_gm_from_id	gets gravitational parameter from identification number

user_input_class

Variables		
Name	**Type**	**Description**
file_new_IC	character(50)	name of file with new initial conditions
save_ephemeris	logical	ephemeris generated during integration
save_difference	logical	flag to save the difference wrt JPL ephemeris
save_incre_rms	logical	flag to save the incremental rms wrt JPL ephemeris
save_total_rms	logical	flag to save the total rms wrt JPL ephemeris
phi	logical	flag to write the computed state transition matrix
phi_test	logical	flag to test the computed state transition matrix
run_type	character(2)	run type selector

Methods	
Name	**Description**
set_user_file_new_IC	sets the name of file with new initial conditions
set_user_save	sets the values of the saving variables
set_user_phi_test	sets value of phi test
set_user_run_type	sets the value of run type selector
get_user_file_new_IC	gets the name of file with new initial conditions
get_user_save	gets values of the saving variables
get_user_phi_test	gets value of phi test
get_user_run_type	gets the value of run type selector

diva_diff_table_class

Variables		
Name	**Type**	**Description**
IOPST	integer	variable used in case of stiff equations
KORDI	integer	order of diff. eqs. in the case that all diff eqs. have same order
KQMAXD	integer	maximum integration order used for stiff equations
LDT	integer	flag giving current state of difference tables
MAXDIF	integer	maximum order derivative of F to be computed
MAXINT	integer	maximum number of integration to be performed
NKDKO	integer	starting index for storing orders in KORD
NTE	integer	total number of differential equations being integrated
NYNY	integer	starting index for storing the base values in Y
NDTF	integer	starting index for storing difference tables in F
NUMDT	integer	number of difference for each equations
diff_table	type(:,:)	store values of difference tables (diff_table_class)

Methods	
Name	**Description**
set_diva_diff_table_fix	sets values of variables of diff. tables that not change during integration
allocate_diva_diff_table	allocates and initialize variables of diva_diff_table_class
deallocate_diva_diff_table	deallocates diva_diff_table_class
set_diva_diff_table_var	sets values of variables of diff. table that change during integration
get_diva_diff_table_fix	gets values of variables of diff. tables that not change during integration
get_diva_diff_table_tobs	gets values of variables of diff. table that change during integration

dynamical_par1_class

Variables		
Name	**Type**	**Description**
value	real	value of gravitational parameter
correction	real	correction to gravitational parameter computed in estimation process
flag	character(1)	flag characterizing the variable (fixed, considered, estimated)

Methods	
Name	**Description**
init_dynamical_parameter_1	initializes variables of the class
set_dynamical_parameter_1_flag	sets value of flag
set_dynamical_parameter_1_value	sets value of gravitational parameters
set_dynamical_parameter_1_corr	sets value of correction to gravitational parameter
check_dynamical_par_1_flag_e	checks if the gravitational parameter is estimated
get_dynamical_parameter_1_flag	gets value of flag
get_dynamical_parameter_1_value	gets value of gravitational parameter

Interfaces	
Private name	**Public name**
init_dynamical_parameter_1	init_dynpar
set_dynamical_parameter_1_flag	set_dynpar_flag
set_dynamical_parameter_1_value	set_dynpar_value
set_dynamical_parameter_1_corr	set_dynpar_correction
check_dynamical_par_1_flag_e	check_flag_e
get_dynamical_parameter_1_flag	get_dynpar_flag
get_dynamical_parameter_1_value	get_dynpar_value

dynamical_par2_class

Variables		
Name	**Type**	**Description**
value	real(:,:)	value of Stokes coefficients
correction	real(:,:)	correction to Stokes coefficients computed in estimation process
flag	character(1)(:,:)	flag characterizing the variables (fixed, considered, estimated)

Methods	
Name	**Description**
init_dynamical_parameter_2	initializes variables of the class
set_dynamical_parameter_2_flag	sets value of flag
set_dynamical_parameter_2_value	sets value of Stokes coefficients
set_dynamical_parameter_2_corr	sets value of correction to Stokes coefficients
check_dynamical_par_2_flag_e	checks if the Stokes coefficients are estimated
get_dynamical_parameter_2_flag	gets value of flag
get_dynamical_parameter_2_value	gets value of Stokes coefficients

Interfaces	
Private name	**Public name**
init_dynamical_parameter_2	init_dynpar
set_dynamical_parameter_2_flag	set_dynpar_flag
set_dynamical_parameter_2_value	set_dynpar_value
set_dynamical_parameter_2_corr	set_dynpar_correction
check_dynamical_par_2_flag_e	check_flag_e
get_dynamical_parameter_2_flag	get_dynpar_flag
get_dynamical_parameter_2_value	get_dynpar_value

dynamical_state_class

Variables		
Name	**Type**	**Description**
value	real(6)	value of state
correction	real(6)	correction to state computed in estimation process
flag	character(1)(6)	flag characterizing the variables (fixed, considered, estimated)

Methods	
Name	**Description**
init_dynamical_state	initializes variables of the class
set_dynamical_state_flag	sets value of flag
set_dynamical_state_value	sets value of state
set_dynamical_state_corr	sets value of correction to state
check_dynamical_state_flag_e	checks if the state is estimated
get_dynamical_state_flag	gets value of flag
get_dynamical_state_value	gets value of state
check_position_flag_e	counts number of estimated coordinates of position

Interfaces	
Private name	**Public name**
init_dynamical_state	init_dynpar
set_dynamical_state_flag	set_dynpar_flag
set_dynamical_state_value	set_dynpar_value
set_dynamical_state_corr	set_dynpar_correction
check_dynamical_state_flag_e	check_flag_e
get_dynamical_state_flag	get_dynpar_flag
get_dynamical_state_value	get_dynpar_value

estimation_class

Variables		
Name	**Type**	**Description**
name	character(6)	body's name, JPL nomenclature
id	integer	body's identification number, JPL nomenclature
state	type	value of state, inherits property of dynamical_state_class
gm	type	value of Gm, inherits property of dynamical_par1_class
stokes	type	value of Stokes coefficients, inherits property of dynamical_par2_class

Methods	
Name	**Description**
init_estimable_state	initializes variables of the class
set_estimable_name_id	sets the body's name and the identification number
set_estimable_dynpar_flag	sets value of flag
set_estimable_dynpar_value	sets value
set_estimable_dynpar_corr	sets value of correction
count_est_par_flag_e	counts the number of dynamical parameters that have to be estimated
count_est_state_flag_e	counts the number of state that have to be estimated
count_est_position_flag_e	counts the number of position that have to be estimated
check_est_par_flag_e	checks if some gm or stokes have to be estimated
check_estimation_state_flag_e	checks if some state have to be estimated
get_estimable_id	gets identification number
get_estimable_dynpar_flag	gets value of flag
get_estimable_dynpar_value	gets value
order_estimable_as_body	orders the name variable of class with same order of name of body_class

earth_rotation_params_class

Variables		
Name	**Type**	**Description**
mjd	integer	modified julian date
xp	real	x pole offset (in arcsec)
yp	real	y pole offset (in arcsec)
ut1_utc	real	UT1-UTC (in seconds)
ut1_ut1r	real	UT1-UT1R (in seconds)
dpsi	real	nutation in longitude (in arcsec)
deps	real	nutation in obliquity (in arcsec)

Methods	
Name	**Description**
init_erp_data_class	initializes variables of the class
set_erp_data	sets the value of the Earth rotation parameters
get_interpolated_erp_data	interpolates linearly the Earth rotation parameters
search_mjd_index	searches the index of mjd closer to the given mjd

integrated_orbit_class

Variables		
Name	**Type**	**Description**
name	character(6)	body's name, JPL nomenclature
id	integer	body's identification number, JPL nomenclature
epoch	real(:)	epoch of state in ET
state	real(:,:)	body's state

Methods	
Name	**Description**
init_integrated_orbit_type	initializes variables of the class
allocate_epoch_and_state	allocates the variables epoch and state of this class
copy_body_names_and_id	copies name and identification number from body class
set_epoch_and_states	sets value of epoch and state to memorize during integration
get_integrated_orbit	gets value of epoch and state memorized during integration
get_state	gets value of state
copy_integrated_orbit_type	copies values of the variables of this class in another class of same type

observatory_class

Variables		
Name	**Type**	**Description**
observatory_code	character(3)	observatory code
coordinates	real(3)	geocentric coordinates of observatory
name	character(50)	name of observatory

Methods	
Name	**Description**
init_observatory_class	initializes the variables of the class
set_code_observatory	sets observatory code
set_name_observatory	sets observatory name
set_coord_observatory	sets observatory coordinates
get_coord_observatory	gets observatory coordinates

state_transition_matrix_class

Variables		
Name	**Type**	**Description**
epoch	real	epoch of state transition matrix (TDB)
transition_matrix	real(:,:)	state transition matrix

Methods	
Name	**Description**
init_rectangular_matrix	initializes a rectangular state transition matrix
init_square_matrix	initializes a square state transition matrix
set_epoch_and_phi	sets values of epoch and state transition matrix
get_phi	gets state transition matrix
copy_state_transition_type	copies values of the variables of this class in another class of same type
get_trans_matrix_shape	gets shape of state transition matrix

Interfaces	
Private name	**Public name**
init_square_matrix	init_state_trans_mat_type
init_rectangular_matrix	init_state_trans_mat_type

integration_class

Variables		
Name	**Type**	**Description**
t_start_JD	character(50)	integration start epoch (Julian Date)
t_end_JD	character(50)	integration end epoch (Julian Date)
t_start_ET	real	integration start epoch (TDB)
t_end_ET	real	integration end epoch (TDB)
t_IC_ET	real	epoch of initial conditions (TDB)
t_IC_JD	real	epoch of initial conditions (Julian Date)
deltat	real	time increment for saving solution (in seconds)
integrator	character(10)	integrator selector

Methods	
Name	**Description**
set_integration_tstart	sets integration start epoch
set_integration_tend	sets integration end epoch
set_integration_deltat	sets time increment for saving solution
set_integration_t_IC	sets epoch of initial conditions
set_integration_integrator	sets integrator selector
get_t_start_ET	gets integration start epoch
get_t_end_ET	gets integration end epoch
get_deltat	gets time increment for saving solution
get_t_IC_ET	gets epoch of initial conditions
get_integrator	gets integrator selector
update_t	updates time from integration start

observation_class

Variables		
Name	**Type**	**Description**
time_string	character(30)	UTC time of observation
time_ET	real	TDB time of observation
alfa_h	type	right ascension value, inherits property of angle_class
alfa_r	real	right ascension value, in radians
delta_d	type	declination value, inherits property of angle_class
delta_r	real	declination value, in radians
sigma_alfa	real	error in right ascension, in radians
sigma_delta	real	error in declination, in radians
keep	logical	rejection flag, .true. = used, .false. = reject
observatory_code	character(3)	code of observatory that made the observation
observation__type	character(4)	observation type, 'topo'=topocentric, 'geoc'=geocentric
frame	character(5)	reference frame of observation, 'ICRF' =J2000
id_sat	integer	identification number of the observed satellite
res_alfa	real	observed minus computed, in radians
res_delta	real	observed minus computed, in radians

Methods	
Name	**Description**
init_observation_class	initializes variables of observation_class
set_idsat_observation	sets value of identification number of observed satellite
set_frame_observation	sets the frame of observation
set_time_string_observation	sets the UTC time of observation
set_time_ET_observation	sets the TDB time of observation
set_alfa_h_observation	sets value of right ascension
set_delta_d_observation	sets value of declination
set_alfadelta_rad_observation	sets value of right ascension and declination
set_observation_sigma	sets value of errors in right ascension and declination
set_obsy_code_observation	sets observatory code
set_obs_type_observation	sets observation type
set_keep_observation	sets rejection flag
set_residuals_observation	sets the values of observed minus computed
order_observation_class	orders the value of observation time in increasing order
count_n_observation_time	counts the number of observation time
get_not_repeated_obs_time	gets an array of values of not repeated observation time
get_observation_time_ET	gets the TDB time of observation
get_observation_time_UTC	gets the UTC time of observation
get_obsy_code_observation	gets observatory code
get_obs_type_observation	gets observation type
get_keep_observation	gets rejection flag
get_observation_coord_R	gets right ascension and declination of observation (in radians)
get_observation_sigma	gets value of errors in right ascension and declination
get_idsat_observation	gets value of identification number of observed satellite
get_observation_frame	gets the frame of observation
count_notrej_observations	counts the number of observation not rejected
count_nobs_idsat_observation	counts number of observation for each satellite
satellites_statistics	computes statistics (mean and standard deviation) for each satellite
satellite_alfa_delta_statistic	computes residuals for each satellite
alfa_delta_statistics	computes global statistic in right ascension and declinaton
global_statistics	computes residuals in right ascension and declination
rms_statistics	computes global residuals

Interfaces	
Private name	**Public name**
satellites_statistics	statistic_on_resid_observation
alfa_delta_statistics	statistic_on_resid_observation
global_statistics	statistic_on_resid_observation
rms_statistics	statistic_on_resid_observation
satellite_alfa_delta_statistic	statistic_on_resid_observation

D.4.2 Modules

In the following tables a brief description of all the modules contained in the SOSYA software is given.

Diva_module

It contains the setting necessary to use the DIVA integrator.

Subroutine	Description
diva_integration_driver	setting routine for DIVA
divaf	derivative subroutine for use with DIVA
divao	output subroutine for use with DIVA
set_state_vector	sets the vector of initials condition for integration
set_diva_param_for_array_dim	DIVA parameters set up

EoM_and_partials_allocation

It contains and allocates the variables used by the *EoM__variational_module*.

Subroutine	Description
set_up_equation_of_motion	allocates the variable for equations of motion
set_up_variational_partials	allocates the variables for the partials
deallocation_Eom_and_partials	deallocates the variables allocated (at the end of integration)

EoM__variational_module

It contains the equations of motion and the variational equations.

Subroutine	Description
equation_of_motion	computes the right member of the equations of motions
variational_equation_comput	computes the variational equations
compute_phi_dot	forms the derivative of state transition matrix
gm_partials_computation	computes the partials with respect to the gravitational parameters
stokes_partials_computation	computes the partials with respect to the Stokes coefficients
compute_delta_R	computes $\mathbf{R}_{ij}$, $\lvert\mathbf{R}_{ij}\rvert$, $\lvert\mathbf{R}_{ij}^{-3}\rvert$, $\lvert\mathbf{R}_{ij}^{-5}\rvert$
reshape_vector_to_matrix	reshapes the state vector to a 2-dimensional matrix
reshape_vector_for_EOM	reshapes the 2-dimensional matrix to a state vector

G_functions_module

It contains the subroutine that computes the oblateness functions.

Subroutine	Description
compute_G_function	computes the $\mathbf{G}_{ij}$ functions
potential_computation_interface	interface for the call to the subroutine that computes the gravitational potential of extended bodies

Interpolation_module

It contains the subroutine that interpolates the satellites state.

Subroutine	Description
interpolate_satellite_state	interpolates satellite state using the save difference tables and DIVAIN

Associated_Legendre_functions

It contains the routine for the associated Legendre functions.

Subroutine	Description
LegendrePr	Computes the associated Legendre functions of the first kind of real argument

queue

It implements a queue container.

Subroutine	Description
init_queue	initializes the queue
put_in_rear	puts in rear of queue the new entry
take_from_front	takes the first entry from the queue
is_queue_empty	checks if the queue is empty
count_queue_elements	counts the number of elements of the queue

oblate_gravity_module

Computes the gravitational potential of an extended body and its derivatives.

Subroutine	Description
oblate_acceleration	computes the oblateness functions in a body-fixed reference frame
grad_pot	computes the gradient of the gravitational potential
jacobian_pc	computes the jacobian from polar to cartesian coordinates
cartesian_to_equatorial	computes the transformation from cartesian to polar coordinates

observation_module

It contains implementation of the observational model.

Subroutine	Description
obs_residuals_and_partials	computes the observation residuals and partials
observer_and_sun_state	computes the state of observer and state of Sun
iau_1976_1980_sofa	computes Earth attitude using SOFA routines
observer_state_SSB	computes observer state wrt the Solar System Barycenter
light_time_correction	computes light time correction
sun_field_deflection	computes gravitational light deflection
light_aberration	computes the aberration of light
geometric_partials	computes the geometric partials
compute_residuals	computes observation residuals

orbit_determination_module

It controls orbit determination.

Subroutine	Description
Orbit_determination	driver for orbit determination
normal_equations	forms the normal equations
open_files_for_residuals	opens files to write residuals
close_files_for_residuals	closes files to write residuals
update_state_estimate	updates state estimate
form_mask_for_cutting	mask used to reformat $\mathbf{H}^T\mathbf{WH}$ and $\mathbf{H}^T\mathbf{Wy}$ matrices
reshaping_normal_matrix	reshapes the $\mathbf{H}^T\mathbf{WH}$ and $\mathbf{H}^T\mathbf{Wy}$ matrices
count_nobs_per_satellites	counts the number of observations for each satellite
compute_statistics_on_residuals	computes statistics on residuals
minvch	inverts a symmetric matrix using choleski algorithm

Integration_module

It controls orbit integration.

Subroutine	Description
Orbit_Integration	set up for orbit integration
write_LOG_execution	write the log file

Read_input

It reads the input files supplied by the user.

Subroutine	Description
Read_Input_Data	reads a file with the paths of each input file
Read_Bodies_Input_Data	reads the number of bodies and its gravitational parameters
Read_Parameters_Input_Data	reads other parameters related to the input bodies
Read_IC_Input_Data	reads the initial conditions
Read_User_Input	reads user choices
copy_IC_and_GM	copies initial conditions and μ from body class to estimation class
Read_Observation_Input_Data	reads observational data
Read_Observatory_Code	reads observatory codes
Read_Erp_input_data	reads Earth rotation parameters
check_not_consistent_flag	checks that user choices are consistent for execution
inquire_if_file_exixts	inquires the existence of an input file

rotation

It implements the rotation matrix from inertial to body-fixed.

Subroutine	Description
rotation_I2BF_oblate	Computes the rotation matrix from inertial to body fixed reference frame

state_transition_matrix_test

It tests the computation of state transition matrix.

Subroutine	Description
state_transition_check	tests the computation of the state transition matrix
reshape_state	reshapes a 2-dimensional matrix to a state vector
reshape_1D_vector_to_2D	reshapes a state vector to a 2-dimensional matrix
symplectic_test	verifies the symplectic property of state transition matrix

write_output

It manages the files writing .

Subroutine	Description
write_integration_output	writes ephemerides
write_new_file_of_IC	writes a new file of converged initial conditions
compute_module_of_vector	computes the module of a 3-dimensional vector
write_estimation_output_state	writes the estimated state
write_estimation_output_gm	writes the estimated gravitational parameter
write_output_correlation	writes correlations
write_estimation_output_elorb	writes the estimated orbital elements
vecels	calculates the classical orbital elements from a state vector

precision

It specifies the arithmetic precision used by the program.

input_parameters

It specifies the common variables.

constants

It defines some constants used by SOSYA.

In Figures D.4, D.5, D.6, D.7, D.8, D.9, D.10, D.11, D.12, D.13, D.14 and D.15 we give the call trees of the SOSYA program. The dashed routine are subroutine contained in the precompiled library and linked to SOSYA (SPICE, SOFA, DIVA) except *divaf* and *divao* that contains the interface to comunicate with the numerical integrator. *divaf* contains the equation of motion while *divao* allows to manage the output of the integrator.

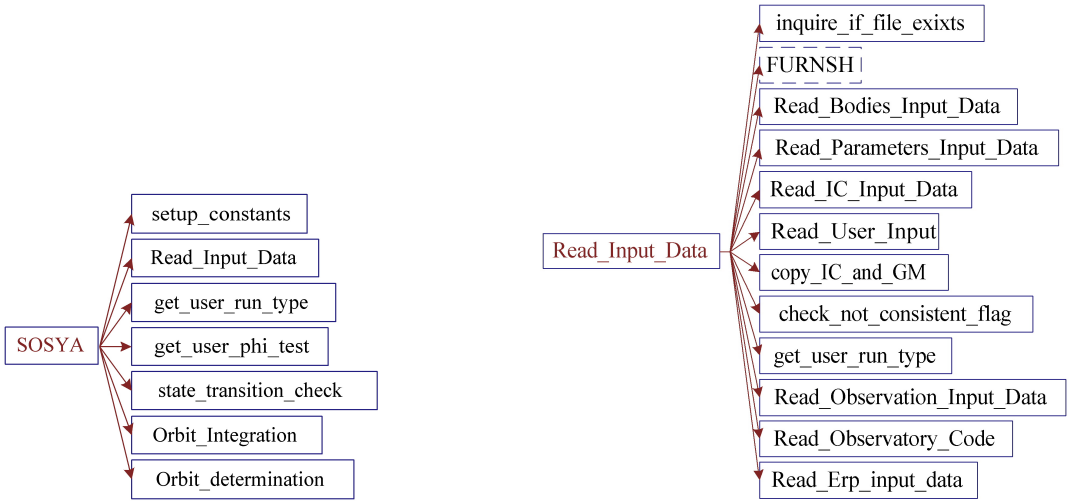

Figure D.4: SOSYA call tree.

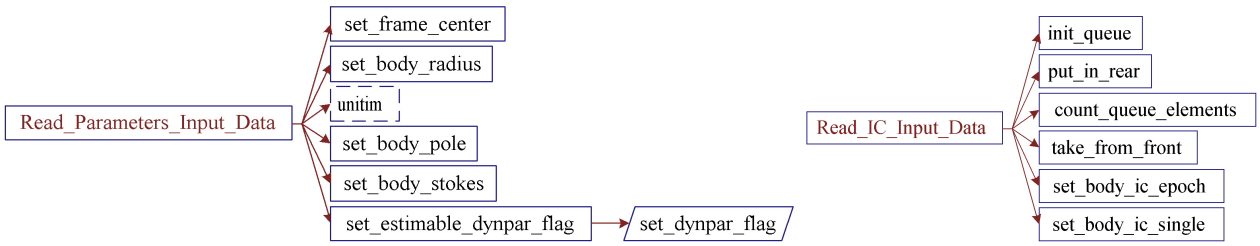

Figure D.5: SOSYA call tree.

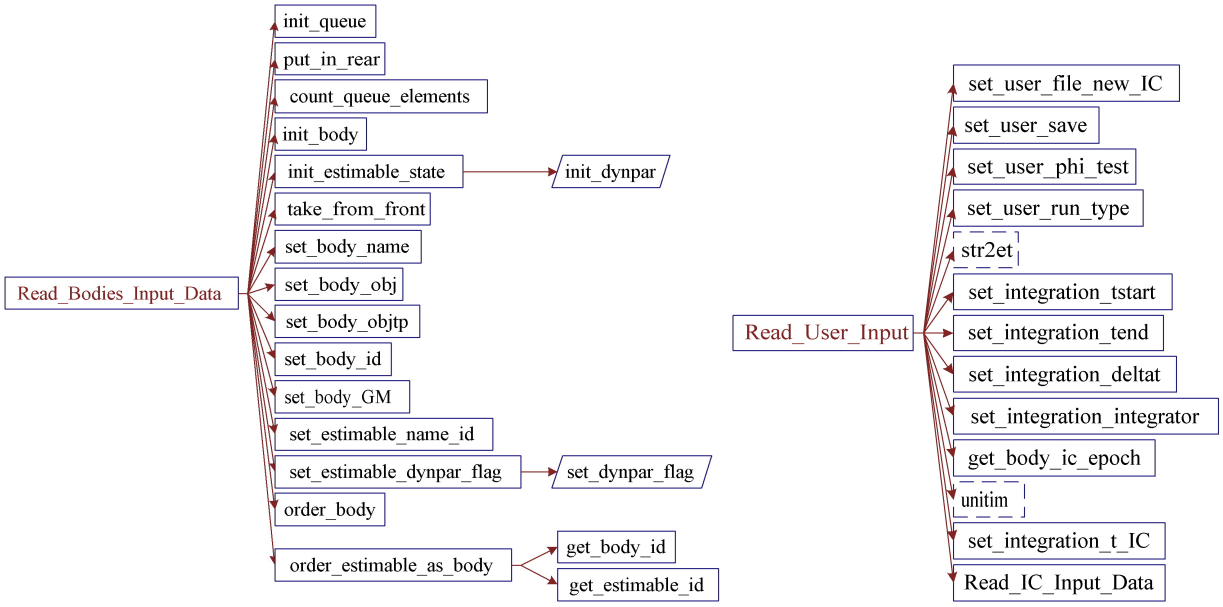

Figure D.6: SOSYA call tree.

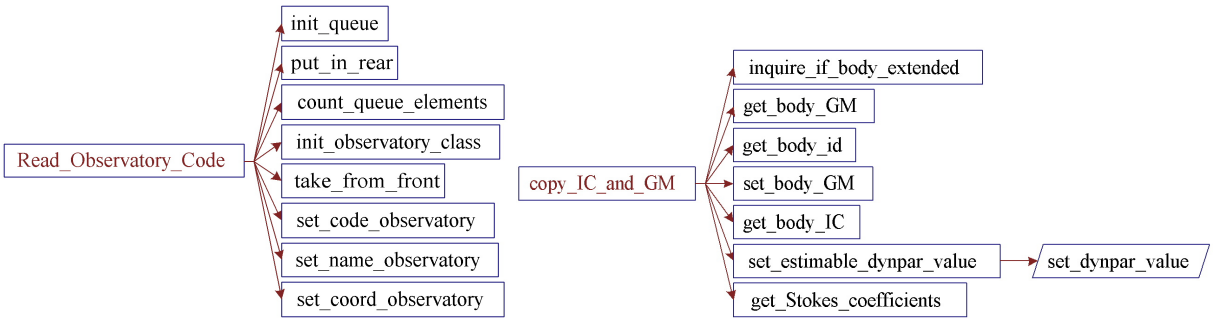

Figure D.7: SOSYA call tree.

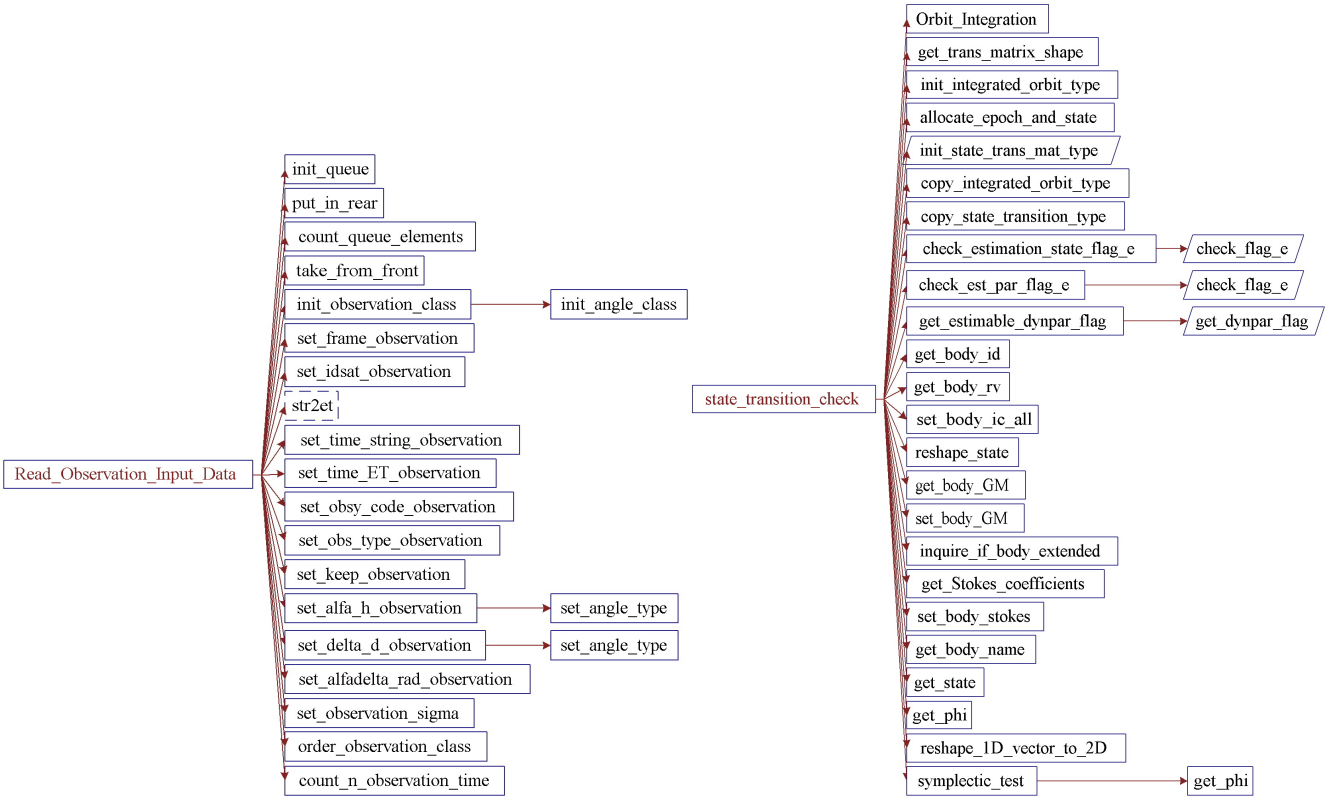

Figure D.8: SOSYA call tree.

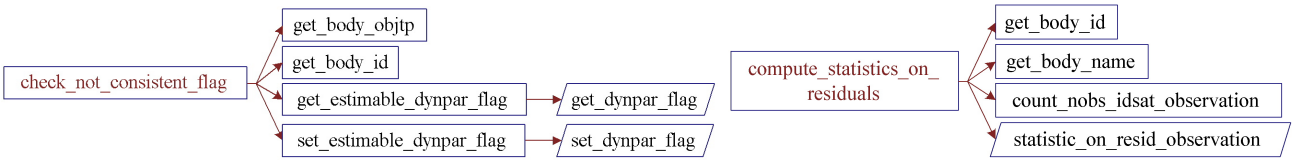

Figure D.9: SOSYA call tree.

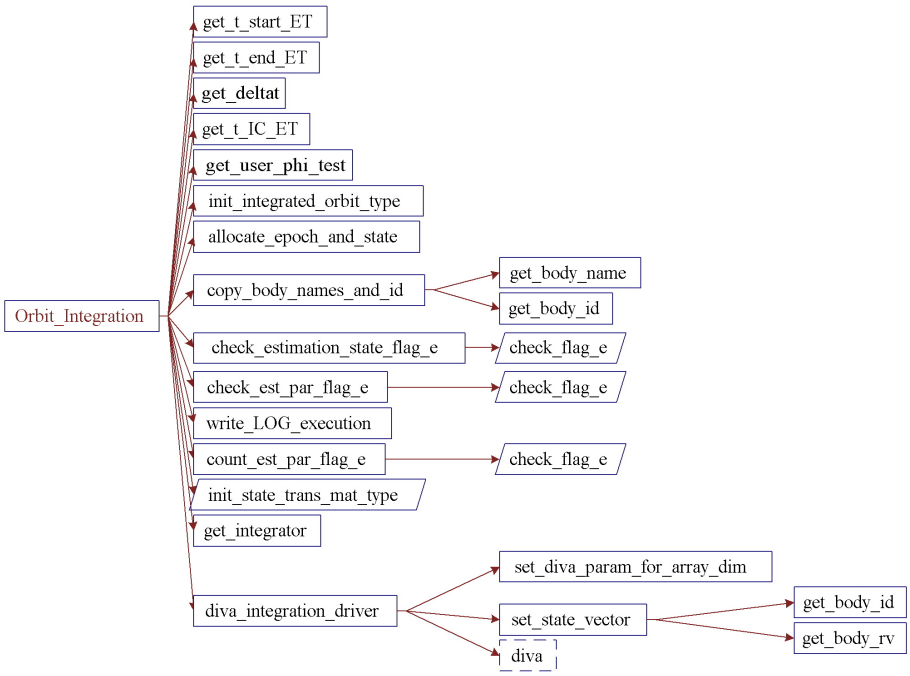

Figure D.10: SOSYA call tree.

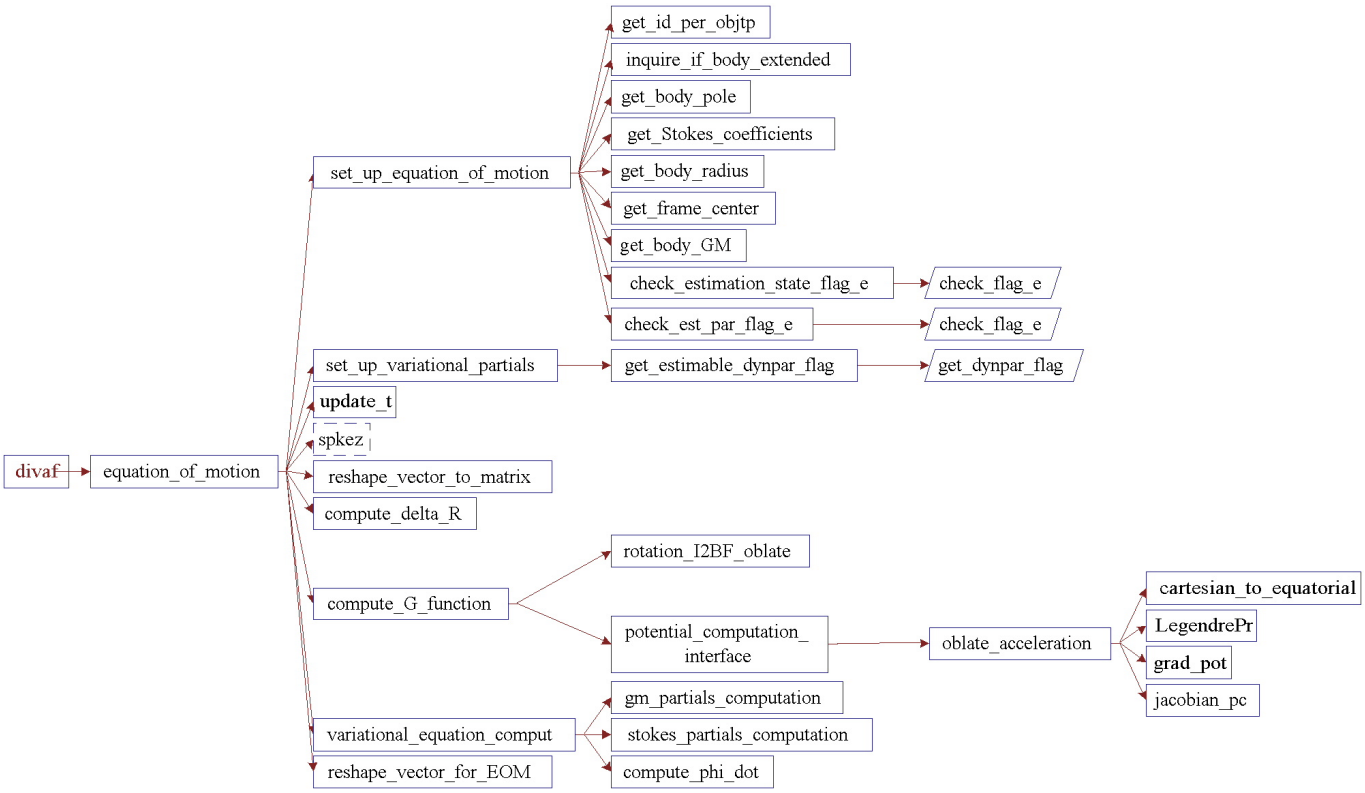

Figure D.11: SOSYA call tree.

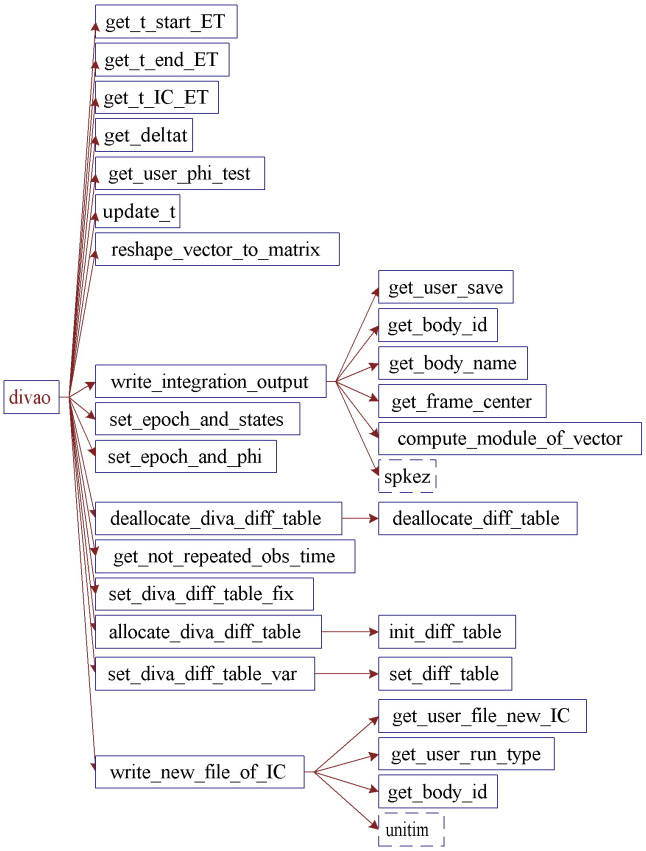

Figure D.12: SOSYA call tree.

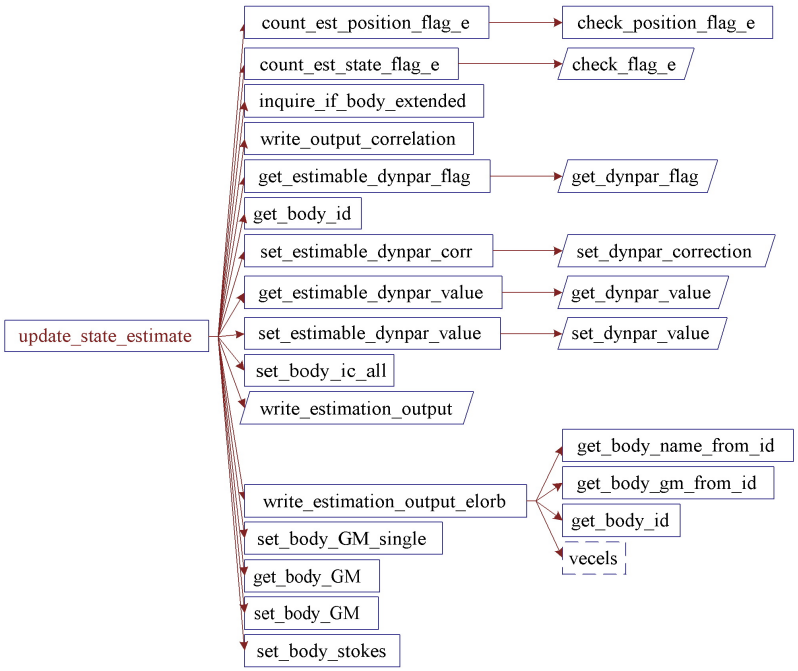

Figure D.13: SOSYA call tree.

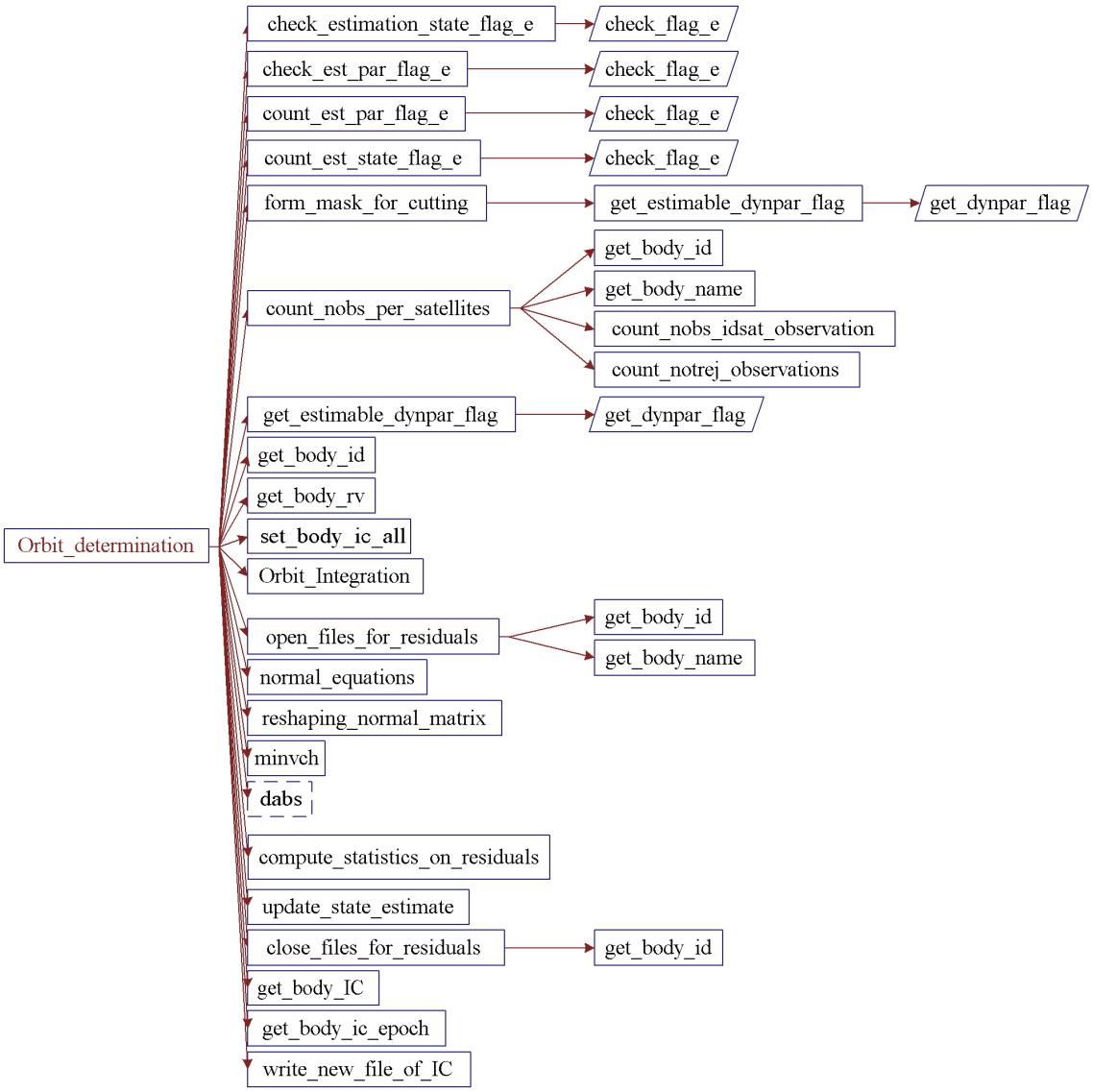

Figure D.14: SOSYA call tree.

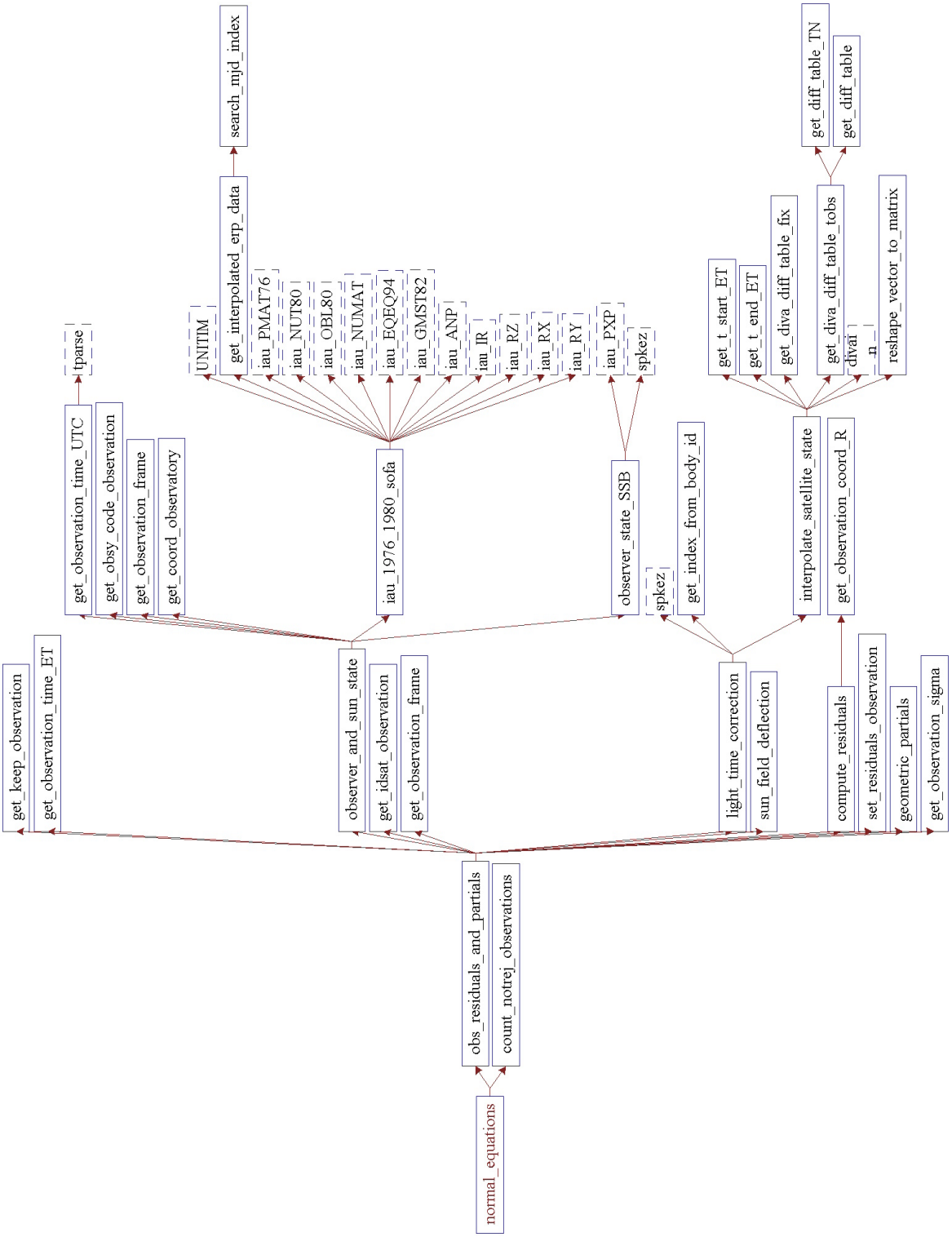

Figure D.15: SOSYA call tree.

Bibliography

[1] Akin, E., *Object Oriented Programming via Fortran 90/95*, Cambridge University Press, New York, 2003.

[2] Aksnes, K., et al., "Mutual phenomena of the Galilean and Saturnian satellites in 1973 and 1979/1980", *Astronomical Journal*, **89**, 1984.

[3] Barbieri, C., *Lezioni di Astronomia*, Zanichelli, Bologna, 1999.

[4] Bierman, G.J., *Factorization Method for Discrete Sequential Estimation*, Mathematics in Science Engineering Vol. 128, Academic Press, New York, 1977.

[5] Brouwer, D., Clemence, G.M., *Methods of Celestial Mechanics*, Academic Press, New York, 1961.

[6] Davenport, W.B.Jr., *Probability and Random Process - An introduction for Applied Scientist and Engineers*, Mc Grawn-Hill Book Company, 1970.

[7] Dourneau, G., "Orbital elements of the eight major satellites of Saturn determined from a fit of their theories of motion to observations from 1886 to 1985", *Astronomy and Astrophysics*, **267**, 1993.

[8] Eddy, W.F., McCarthy, J.J., Pavlis, D.E., Marshall, J.A., Luthcke, S.B., Tsaoussi, L.S., Leung, G., Williams, D.A., "GEODYN II - Vol. 1, Systems Description", STX System Corporation, Philadelphia, 1990.

[9] Ellis, T.M.R., Philips, I.R., Lahey, T.M., *Fortran 90 Programming*, Addison-Wesley, Norwich, 1994.

[10] ESA, "Time Standards Overview", Prepared by J. Diaz del Rio, SOP-RSSD-TN-014, 2003.

[11] ESA, "Software Engineering Standards", PSS-05-00, Issue 2, ESA, 1991.

[12] Fränz, M., Harper, D., "Heliospheric coordinate Systems", *Planetary and Space Science*, **50**, 2002.

[13] French, R.G., et al., "Astrometry of Saturn's Satellites from the Hubble Space Telescope WFPC2", *Publications of the Astronomical Society of the Pacific*, **118**, 2006.

[14] Gelb, A., *Applied Optimal Estimation*, written by Technical Staff, The Analytic Science Corporation, edited by A. Gelb, MIT Press, London, 1974.

[15] Green, R.M., *Spherical Astronomy*, Cambridge University Press, Cambridge, 1985.

[16] Hadjifotinou, K.G. "Numerical Integration of the Variational Equations of Satellite Orbits", *Planetary and Space Science*, **50**, 2002.

[17] Hadjifotinou, K.G., Harper, D., "Numerical integration of orbits of planetary satellites", *Astronomy and Astrophysics*, **303**, 1995.

[18] Hadjifotinou, K.G., Ichtiaroglou, S., "Theoretical Study of the Partial Derivatives produced by Numerical Integration of Satellite Orbits", *Astronomy and Astrophysics*, **322**, 1997.

[19] Harper, D., Taylor, D.B., "The orbits of the major satellites of Saturn", *Astronomy and Astrophysics*, **268**, 1993.

[20] Harper, D., Taylor, D.B., "Analysis of ground-based observations of the satellites of Saturn 1874-1988", *Astronomy and Astrophysics*, **284**, 1994.

[21] Hwei, P. Hsu, *Theory and Problems of Probability, Random Variables, and Random Process*, Schaum's Outline Series, Mc Grawn-Hill, 1997.

[22] Jacobson, R.A., "Triton and Nereid astrographic observations from Voyager 2", *Astronomy and Astrophysics Supplement Series*, **90**, 541-563, 1991.

[23] Jacobson, R.A., "The orbit of Phoebe from Earthbased and Voyager observations", *Astronomy and Astrophysics Supplement Series*, **128**, 7-17, 1998.

[24] Jacobson, R.A., "Numerical Integration of Planetary Satellites", JPL Interoffice Memorandum, 312.F-98-018, 1999.

[25] Jacobson, R.A., "The Orbits of the Major Saturnian Satellites and the Gravity Field of Saturn from Spacecraft and Earth-Based Observations", *The Astronomical Journal*, **128**, 492, 2004.

[26] JPL, Navigation Software Group, "DPTRAJ-ODP User's Reference Manual", Volume 1, Volume 2, Volume 3, Volume 4, 1996.

[27] JPL, NAIF (The Navigation and Ancillary Information Facility at JPL), "Most Useful SPICELIB subroutines", NAIF, 2001.

[28] JPL, *Variable Order Adams Method for Ordinary Differential Equations*, California Institute Of Technology, Math à la Carte, 2006.

[29] Kaplan, G.H., Hughes, J.A., Seidelmann, P.K., Smith, C.A., Yallop, B.D., "Mean and Apparent Place Computations in the new IAU System. III. Apparent, Topocentric, and Astrometric Places of Planets and Stars", *The Astronomical Journal*, **97** (4), 1989.

[30] Kovalevsky, J., *Modern Astrometry*, Springer Verlag Berlin Heidelberg, 1995.

[31] Kovalevsky, J., Seidelmann, P.K., "Fundamentals Of Astrometry", Cambridge University Press, Cambridge, 2004.

[32] Lieske, J. H., et al. "Expressions for the Precession Quantities Based upon IAU (1976) System of Astronomical Constants", *Astronomy and Astrophysics*, **58**, 1977.

[33] Long, A.C., Cappellari Jr., J.O., Velez, C.E., Fuchs, A.J., "Goddard Trajectory Determination System (GTDS) - Mathematical Theory (Rev. 1)", Document X5827677, Goddard Space Flight Center, 1989.

[34] Maybeck, P., *Stochastic models, estimation, and control*, Volumes 1-2-3, Mathematics in Science Engineering Vol. 141, Navtech Book and Software Store, 1994.

[35] McCarthy, D.D., IERS conventions, Technical Note 21, International Earth Rotation Service (IERS), Observatoire de Paris, July 1996.

[36] McCarthy, D. D., Petit, G., IERS Conventions, Technical Note 32, International Earth Rotation Service (IERS), Observatoire de Paris, 2003.

[37] Metcalf, M., Reid, J., *Fortran 90/95 explained*, second edition, Oxford University Press, New York, 1999.

[38] Miller, K.S., Leskiw, D.M., *An Introduction to Kalman Filtering with Application*, Robert E. Krieger Publishing Company, Malabar, Florida, 1987.

[39] Montenbruck, O., Gill, E., *Satellie Orbits*, Springer-Verlag Berlin Heidelberg, 2000.

[40] Moyer, T.D., *Mathematical Formulation of the Double-Precision Orbit Determination Program DPODP*, Technical Report 32-1527, National Aeronautics and Space Administration, JPL, California Institute of Technology, Pasadena, California, 1971.

[41] Moyer, T.D., *Formulation for Observed and Computed Values of Deep Space Network Data Types for Navigation*, Monograph 2, Deep Space Comunication and Navigation Series, JPL Publication 00-7, 2000.

[42] Moyer, T.D., "Transformation from Proper Time on Earth to Coordinate Time in Solar System Barycenter Space-Time Frame of Reference", *Celestial Mechanics*, **23**, 1, 1981.

[43] Murray, C.A., *Vectorial Astrometry*, Adam Hilger Ltd, Bristol, 1983.

[44] Muray, C.D., Dermott, S.F., *Solar System Dynamics*, Cambridge University Press, Cambridge, 1999.

[45] Newhall, X.X., Standish, E.M., Williams, J.G., "DE 102: a numerically integrated ephemeris of the Moon and planets spanning forty-four centuries", *Astronomy and Astrophysics*, **125**, 150-167, 1983.

[46] Oesterwinter, C., Cohen, C.J., "New Orbital Elements for Moon and Planets", *Celestial Mechanics*, **5**, 1972.

[47] Owen, W.M., Vaugham, R.M., "Optical Navigation Program Mathematical Model", Jet Propulsion Laboratory, Engineering Memorandum 314-512, Pasadena, 1991.

[48] Peters, C.F., "Numerical Integration of the Satellites of the Outer Planets", *Astronomy and Astrophysics*, **104**, 37-41, 1981.

[49] Pines, S., "Uniform Representation of the Gravitational Potential and its Derivatives", *AIAA Journal*, **11**, n.11, 1973.

[50] Quarteroni, A., Sacco, R., Saleri, F., *Numerical Mathematics*, Springer Verlag, New York, 2000.

[51] Seidelmann, P.K. (Editor), *Explanatory Supplement to the Astronomical Almanac*, University Science Books, Mill Valley, California, 1992.

[52] Seidelmann, K., "1980 IAU Nutation: the Final Report of the IAU Working Group on Nutation", *Celestial Mechanics*, **27**, 1982.

[53] Seidelmann, K. et al., "Report of the IAU/IAG Working Group on Cartographic Coordinates and Rotational Elements of the Planets and Satellites: 2000", *Celestial Mechanics and Dynamical Astronomy*, **82**, 2002.

[54] Sharp, P.W., "Comparison of integrators on a diverse collection of restricted three-body test problems", *IMA Journal of Numerical Analysis*, **24**, 557, 2004.

[55] Spier, G.W., "Design and Implementation of Models for the Double Precision Trajectory Program (DPTRAJ)", Technical Memorandum 33-451, National Aeronautics and Space Administration, Jet Propulsion Laboratory, California Institute of Technology, Pasadena, California, 1971.

[56] Stone, R.C., "CCD Positions for the outer Planets in 1995 determined in the Extragalactic Reference Frame", *The Astronomical Journal*, **112**, 781, 1996.

[57] Stone, R.C., "CCD Positions for the outer Planets in 1996-1997 determined in the Extragalactic Reference Frame", *The Astronomical Journal*, **166**, 1461, 1998.

[58] Stone, R.C., Harris, F.H., "CCD Positions determined in the International Celestial Reference Frame for the outer Planets and many of their Satellites in 1995-1999", *The Astronomical Journal*, **119**, 1985, 2000.

[59] Stone, R.C., "Positions for the outer Planets and many of their Satellites. IV. FASTT Observations taken in 1999-2000 ", *The Astronomical Journal*, **120**, 2124, 2000.

[60] Stone, R.C., "Positions for the outer Planets and many of their Satellites. V. FASTT Observations taken in 2000-2001 ", *The Astronomical Journal*, **122**, 2723, 2001.

[61] Tapley, B., Schutz, B., Born, G.H., *Statistical Orbit Determination*, Elsevier Academic Press, 2004.

[62] Thomasian, A.J., *The Structure of Probability Theory with Appllications*, Mc Grawn-Hill Book Company, 1969.

[63] Tragesser, S.G., Longuski, J.M., "Modeling issues concerning motion of the Saturnian satellites", Conference Paper, AAS Paper 97-670, 1997.

[64] Vallado, D.A., *Fundamentals of Astrodynamics and Application*, 2nd edition, Space Technology Library, 2001.

[65] Vienne, A., Thuillot, W., Veiga, C.M., Arlot, J.E., Viera Martins, R., "Saturnian Satellite Observations made in Brazil during the 1995 Opposition with an Astrometric Analysis", *Astronomy and Astrophysics*, **380**, 727, 2001.

[66] Vienne, A., Duriez, L., "TASS1.6: Ephemerides of the major Saturnian satellites", *Astronomy and Astrophysics*, **297**, 1995.

[67] Zilli, G., *Lezioni di Calcolo Numerico*, Edizioni Libreria Progetto Padova, 2003.